Hydrological, vegetation, greenhouse gas and GEST monitoring in project sites in Latvia

3rd Monitoring Report

Melnais Lake Mire. Image: © M.Pakalne

2025

Hydrological, vegetation, greenhouse gas and GEST monitoring in project sites in Latvia.
3nd Monitoring report

Prepared by:

Andis Kalvāns[1], Konrāds Popovs[1], Māra Pakalne[2], Līga Strazdiņa[2], Andis Lazdiņš[3], Arta Bārdule[3], Dana Purviņa[3] Rūta Abaja[4], Jevgēnijs Fiļipovs[4], Dainis Jakovels[4], Uldis Bethers[5] , Andrejs Timuhins[5], Juris Seņņikovs[5]

1. University of Latvia, Faculty of Geography and Earth Sciences
2. University of Latvia, Botanical Garden
3. Latvian State Forest Research Institute "Silava"
4. Institute for Environmental Solutions
5. University of Latvia, Institute of Numerical Modeling

Riga, Latvia, 2025

LIFE21 - CCM - LV - LIFE – PeatCarbon

Peatland restoration for greenhouse gas emission reduction and carbon sequestration in the Baltic Sea region

Content

1. Project Sites

The aim of the LIFE PeatCarbon project monitoring program is to assess the cumulative effect of hydrological regime stabilization on the water level of the project sites, plant communities and GHG gas emissions. Therefore, territories were selected: (a) in which restoration has been carried out earlier before 6 to 15 years, in order to follow the vegetation succession and capture the moment after how long the effect is achieved also in other indicative parameters like increased groundwater level; (b) where restoration will only be carried out during the project and serves as the starting situation or the worst state of the degraded peatland.

In Latvia, within the framework of LIFE PeatCarbon project, monitoring is carried out in four territories - in two of them, stabilization of the hydrological regime will also be implemented, and in two - only the monitoring (**Figure 1.1, Table 1.1**). Several project sites have already undergone restoration as well as vegetation, hydrological and GEST monitoring and the results will serve as a reference, but some are monitored for the first time; GHG flux monitoring was performed for the first time in all locations. Cena Mire was restored in 2006 in LIFE “MIRES” project, the Melnais Lake Mire was restored in 2012 in LIFE “Raised bogs” project, but Sudas-Zviedru Mire was restored in 2017 in the LIFE “Wetlands” project.

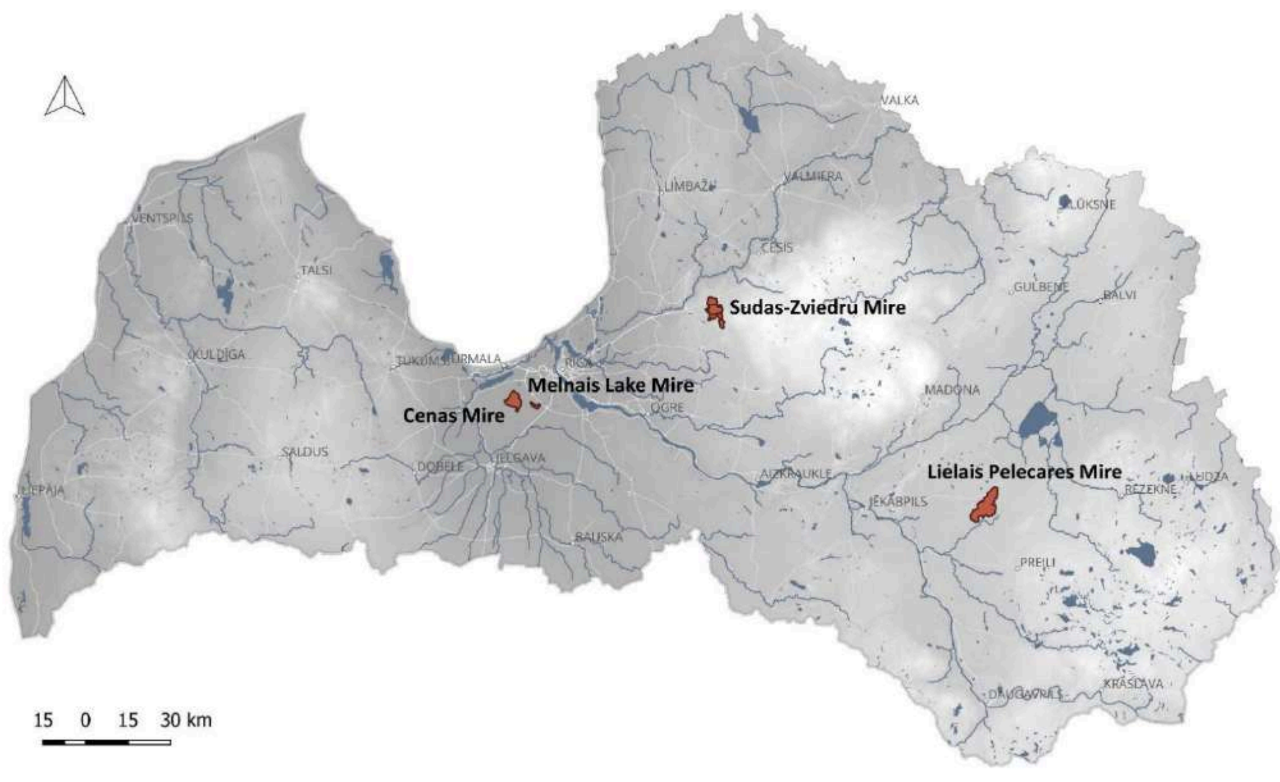

Figure 1.1. *Location of the LIFE PeatCarbon project sites in Latvia. Image: © L. Strazdiņa*

All project sites correspond to the Natura 2000 territory and nature reserve status, their total area reaching 11,838 ha. All sites are active raised bogs and have been affected by peat extraction and drainage. Large scale peat mining has never been initiated in Sudas-Zviedru Mire and Lielais Pelečāre Mire but is still taking place in the immediate vicinity of Cena Mire and

Melnais Lake Mire. Accordingly, the first two sites are in relatively better condition, however, all sites have degraded areas that are either open drained or irrigated peat fields or overgrown with shrubs and trees along drainage ditches. In all places, except for Sudas-Zviedru Mire, the issue of fire safety is relevant, and several cases of burning have been recorded in them.

Table 1.1. *Status of the project sites in Latvia regarding previously completed and/or newly planned restoration and monitoring within this LIFE PeatCarbon project (abbr. "LIFE" in the table).*

Project site	Hydrological regime stabilization		Monitoring							
			Hydrological		Vegetation		GHG flux		GEST	
	before	LIFE	before	LIFE	before	LIFE	before	LIFE	before	LIFE
Cenas Mire	✓	✓	✓	✓	✓	✓	-	✓	-	✓
Melnais Lake Mire	✓	-	✓	✓	✓	✓	-	✓	-	✓
Lielais Pelečāres Mire	-	✓	-	✓	-	✓	-	✓	-	✓
Sudas-Zviedru Mire	✓	-	✓	✓	✓	✓	-	✓	✓	-

Hydrological and vegetation monitoring is carried out by the University of Latvia; GHG flux monitoring is implemented by the Latvian State Forest Research Institute "Silava"; GEST mapping and monitoring is performed by the Institute for Environmental Solutions with assistance from the University of Latvia.

1.1. Cena Mire Nature Reserve

1.1.1. Protection status

- Protected area since 1999
- Total area 2295.79 ha
- Natura 2000 site since 2004, site code LV0519800
- Site-centre location [decimal degrees]: 23.849200, 56.857300.

1.1.2. Nature values

Cena Mire Nature Reserve consists of a complex of wetland habitats, namely intact raised bog, transition mire, dystrophic lakes, pine dominated bog woodland. Hummock-hollow complexes and bog pools characterize the bog.

It is one of few bogs in Latvia that supports *Trichophorum caespitosum* as a species of western distribution and *Betula nana* and *Chamaedaphne calyculata* as species of eastern and northern distribution. The site is used as a trespassing area by wolves. Highly important for conservation of bird species breeding and staging on raised bogs, e.g. Black Grouse, Golden Plover, Wood Sandpiper and Common Crane.

1.1.3. Habitats of EU importance

In total, seven different types of habitats of EU importance were identified in the Cena Mire, and their total cover occupies 88% of the Nature Reserve (Appendix 6.1, 6.2). Most of it belongs to Active raised bogs (7110*) (1769 ha). Other mire habitats at the site include Degraded raised bogs (7120) (50 ha) and Transition mires and quacking bogs (7140) (17 ha). The total coverage of Degraded raised bogs (7120) is probably even greater after the extension of the boundary of the Nature Reserve and the inclusion of an additional drained area of the bog. The other habitats belong to two forest types (Western Taiga (9010*) and Bog woodland (91D0*), total 112 ha) and Natural dystrophic lakes (3160) (67 ha).
Drainage has affected almost all habitat types, apart from Transition mire (7140), which is in the central part of the Nature Reserve. In addition, most of the Natural dystrophic lakes (3160) are in good to excellent condition.

Figure 1.1.1. *Success of previous hydrological regime restoration around Lake Skaista is indicated by pine decay. Situation in 2006 short before activities (left) and in 2024 (right). Images: © M. Pakalne*

1.1.4. Drainage impact in the area

The territory of the Cenas Mire Nature Reserve has changed little in the period from the middle of the 19th century to the middle of the 20th century. Later, the entire territory of the Nature Reserve and the adjacent mire massifs were little affected because of human economic activity. Change begins after World War 2. Around 1962, peat extraction was started in the areas adjacent to the SE of the Nature Reserve. Ditches have also been created near Skaista Lake (**Figure 1.1.1**). Around 1967, the peat extraction fields were further expanded, reaching the S and W border of the Nature Reserve. Later, even more ditches have been installed in the S part of the mire (**Figure 1.1.2**).

Figure 1.1.2. *Peat dams built in 2006 (left) and in 2025 (right) that was established during LIFE PeatCarbon project in the SE part of Cena Mire. Images: © M. Pakalne, L. Strazdiņa*

In following years, peat extraction fields were established along entire E border of Nature Reserve, and the situation did not change significantly until the 1990s. In the second half of the 90s, in the 2000s, no new peat fields are developed or are created only irregularly, including the territory adjacent to NE part of mire where restoration of the hydrological regime is planned.
In the autumn and winter of 2025, peat dams were built on drainage ditches in the Cena Mire as outlined in the Hydrological Regime Stabilization Plan (**Figure 1.1.2, 1.1.3**). Since the vegetation season had already ended by that time, the monitoring will be repeated in the summer of 2026, seven to ten months after the restoration activities.

Figure 1.1.3. *On the left: dam building in Cena Mire in autumn 2025. On the right: participants of a demonstration seminar stand on a newly completed dam after observing the dam-building process. Images: © L. Strazdiņa, R. Gorodko*

1.2. Melnais Lake Mire Nature Reserve

1.2.1. Protection status

- Protected area since 2004
- Total area 342.89 ha

- Natura 2000 site since 2004, site code LV0528700
- Site-centre location [decimal degrees]: 23.986300, 56.836500.

1.2.2. Nature values

The site includes raised bog vegetation with bog lakes. It is surrounded by peat cutting fields located outside the site.

Main qualifying features are Active raised bogs (7110*) and Natural dystrophic lakes (3160). A relatively high diversity and abundance of rare bird species for a small area. 12 Annex I bird species recorded in 2002. The most important are Wood Sandpiper, Spotted Crake and Whooper Swan (one of the few breeding sites for the latter in the central region of Latvia). Bean and White-fronted Geese use the site as a roosting place during the autumn passage.

1.2.3. Habitats of EU importance

In total, four types of habitats of EU importance have been identified in the Melnais Lake Mire. The total cover of all habitats takes 87% of the Nature Reserve (Appendix 6.1, 6.2). Most of it belongs to Active raised bogs (7110*) (186 ha), and about a half of that cover belong to Degraded raised bogs (7120) (88 ha). The habitat Natural dystrophic lakes (3160) take 18 ha, while only 3 ha belong to Western Taiga (9010*). About 25 ha of the Nature Reserve is taken by irrigated open peat mining field.

Figure 1.2.1. *Species poor (left) and fen (right) vegetation in overflooded peat-mining fields in Melnais Lake Mire in 2024 after completed hydrology stabilization in 2012. Images: © M.Pakalne*

1.2.4. Drainage impact in the area

Melnais Lake Mire has a dome formed from the accumulation of peat over thousands of years. In the centre of the dome is Melnais Lake. It collects water from the immediate surroundings, but in the previous century a ditch was dug to connect the lake to a drainage system. In general, the hydrological conditions of Melnais Lake Mire have been significantly changed by human activity, 84% of the territory is surrounded by drainage ditches. Peat mining was started in the 1930s in the vicinity of the Nature Reserve and continues to this day.

After peat extraction, it is not possible to fully restore the natural vegetation of the raised bog. However, the impact of drainage can be reduced, and the hydrological situation stabilized. To raise the groundwater level and reduce seasonal fluctuations, dam building on ditches was finished in 2012 (**Figure 1.2.1**).

1.3. Lielais Pelečāre Mire Nature Reserve

1.3.1. Protection status

- Protected area since 1977
- Total area 5683.26 ha
- Natura 2000 site since 2004, site code LV0512200
- RAMSAR site together with Teiču Mire Strict Nature Reserve
- Site-centre location [decimal degrees]: 26.556500, 56.497200.

1.3.2. Nature values

Site includes a raised bog surrounded by bog woodland. In the site periphery transition mires are found.
Qualifying features are Active raised bogs (7110*), Transition mires and quaking bogs (7140) and Bog woodland (91D0*). Qualifying species is butterfly Large Copper. Apart from the vast area of open peatland (raised bog and transition mire) that is important for breeding waders etc, surrounding forests also important for woodpeckers and owls. Up to 5 estimated pairs of Ural Owl and perhaps 5 to 10 pairs of Tengmalm's Owl occur within the site.

Figure 1.3.1. *Hollow-bog pool-ridge relief in the natural active raised bog (left) strongly contrasts with the almost square-shaped drained area that has overgrown by birches and pines (right) in Lielais Pelečāre Mire. Drone image: © J. Matuko*

1.3.3. Habitats of EU importance

Ten habitats of EU importance with a total area of 5177 ha or 91.1% from the Nature Reserve have been found throughout the project site (Appendix 6.1, 6.2). The remaining 9% of the area belong to forest stands of various ages, mainly on the periphery of the Nature Reserve, which do not meet the quality requirements of protected habitats.
Of all habitats of EU importance, the largest area is occupied by Active raised bogs (7110*), which takes around 67% of the entire Nature Reserve. The habitat is in the central part of the

Lielais Pelečāre Mire and around Lake Deguma, as well as small, isolated fragments are separated by forest areas on the periphery of the mire. During the 1960s and 1970s, preparatory works for peat extraction were started in the area to the SW from Lake Deguma. Here, the habitat Degraded raised bogs (7120), with a total area of 25 ha has developed. A dense network of draining ditches was installed, and the top layer of vegetation has been partially removed, however, peat extraction has not taken place (**Figure 1.3.1**). The habitat Transition mires and quacking bogs (7140) takes a small area, in only two places – in a narrow strip around the Lake Deguma and in the NW part of the territory around bog pools. In the nature reserve, freshwater habitats are represented by Natural dystrophic lakes (3160) – both the largest lake in the mire, Lake Deguma, and bog pools with the area over 0.1 ha. Five different protected forest habitats of EU importance were found in the site. The largest cover belongs to Bog woodland (91D0*). They have developed naturally on the edges of the mire, as well as around Lake Deguma. However, the drainage system created in the Nature Reserve and the adjacent territory has contributed to the mineralization of peat and the more intensive growth of pine trees.

1.3.4. Drainage impact in the area

The territory of the Lielais Pelečāre Mire has changed little in the period from the middle of 19th century to the middle of 20th century. At that time the entire territory of the Nature Reserve was only little affected by human economic activity. The first ditches in the mire were built at the beginning of the last century (1920s) and in 1934. Later, around 1952, the ditches are not only at the S and SE parts of Lake Deguma, but also at the N end of the mire. In the late 1980s and early 1990s, ditches were created in the bog woodland along the NW edge of the reserve, as well in the S part of the mire to the E of Lake Deguma. In later years, new changes in the hydrological system of the mire are not observed.
Since the restoration activity aimed at stabilizing the hydrological regime of the area is not yet possible due to delays in document processing, vegetation monitoring has not been repeated so far. It will be carried out during the 2027 vegetation season, as the restoration works are expected to be completed in the autumn or winter of 2026.

1.4. Sudas-Zviedru Mire in the Gauja National Park

1.4.1. Protection status

- Protected area since 1973
- Total area 3516 ha
- Natura 2000 site since 2004, site code LV0200100
- Belongs to the Gauja National Park (total area 91786.74 ha)
- Site-centre location [decimal degrees]: 25.016100, 57.141692.

1.4.2. Nature values

Sudas-Zviedru Mire is the most outstanding raised bog in the Gauja National Park due to the presence of carst phenomena. The three main mire types are represented here – fens, transition mires and raised bogs. Zušu-Staiņu Springs and the beginning of Suda River is in the S part of the mire. Several lakes occur in the mire, forming a joint ecological system. Protected plant species *Trichophorum cespitosum* occurs in the bog. Rare bird species are known in the mire, like Black Stork and Black Grouse. The mire is important for migrating bird species, such as Greater White-fronted Goose, and a nesting place to Common Cranes.

According to the Law on Gauja National Park (in force since 01.01.2000) the territory of Gauja NP is divided into five functional zones: strict nature reserves (4%) (**Figure 1.4.1**), restricted nature areas (31%), neutral zone (18%), landscape protection zone (44%) and zone of cultural and historical value (3%). Sudas-Zviedru Mire is in the S part of the national park, approximately 10 km from Sigulda City. The area is divided in several zones – Sudas Mire Strict Nature Reserve, Ratnieki Lake and Mire Nature Reserve, Mežaki Nature Reserve, and More Nature Reserve.


Figure 1.4.1. *The natural, undrained part of Sudas-Zviedru Mire, where a strict nature reserve zone has been established to preserve protected habitats and locations of rare species. Images: © L. Strazdiņa*

1.4.3. Habitats of EU importance

In total, 15 types of habitats of EU importance have been identified in the Sudas-Zviedru Mire. The total cover of all habitats takes 81% of the Nature Reserve (Appendix 6.1, 6.2).

Fennoscandian mineral-rich springs and springfens (7160), Transition mires and quaking bogs (7140), and Active raised bogs (7110*) are found in Sudas-Zviedru Mire. The largest area is covered by bogs (2089 ha), while fens (0.14 ha) and transition mires (53.5 ha) are located near the edges. In areas where the drainage ditches have been excavated, Degraded raised bogs still capable of natural regeneration (7120) have formed (total area 58.7 ha) (**Figure 1.4.2**).

About 14% from the mire area is taken by different forest habitats, from which the Bog woodland (91D0*) (307 ha) and Western Taiga (9010*) (167 ha) are the most common.

Figure 1.4.2. *Active raised bog (left) and degraded part in 2024 where restoration has been completed in 2017 (right) in Sudas-Zviedru Mire. Images: © M. Pakalne*

1.4.4. Drainage impact in the area

Relatively high human activity has occurred in Sudas-Zviedru Mire. In the 1930's, peat extraction was carried out in the area, therefore a dense system of drainage ditches was installed. Although part of the ditches has already overgrown with vegetation, they still function, and the water is carried away from the mire. As a result of the draining, heather, birch, and pine have become dominant species along the ditches. To reduce the impact of drainage ditches, 67 dams were built (**Figure 1.4.3**) within the LIFE project "Conservation and Management of Priority Wetland Habitats in Latvia" LIFE13 NAT/LV/000578 in 2017.

Figure 1.4.3. *Restored area in Sudas-Zviedru Mire in 2025, eight years after dam building. Images: © L. Strazdiņa*

2. Methods

2.1. Hydrological monitoring

In this report we cover the 2025 hydrological year from October 1, 2024 to September 30, 2025, that is based on a previously established monitoring network. In each of the study sites a network of hydrological, mostly, water level, observation sites were set up. The groundwater monitoring wells are equipped with 25 mm HDPE pipes from the Dutch company Royal Eijkelkamp B.V. The typical construction of the well consists of a 1 m long pipe, followed by 2 m or, less frequently, 1 m slotted filter pipe, with or without a filter fabric sock covering (**Figure 2.1.1**). The head of the well pipe is usually approximately 0.5 m above the soil surface. The monitoring points are equipped with Solints, Canad, Levelogger 5 Junior water level and temperature probes. The water level measurement range is 0 to 5 m and a nominal accuracy ±0.1% of the measurement range, corresponding to ±0.5 cm. The probes are installed in the wells using 1 mm stainless steel wire rope (AISI 316 (A4)), typically at depths corresponding to the lower portion of the filter interval.

In the case of Lielais Pelečāres Mire, two soil water regime monitoring points and two weather stations were installed as well. The soil water regime is monitored with Meter, USA probes Teros 21 (soil water potential) and Teros 11 (soil water content). The soil water potential probes are installed at depths of 0.1 and 0.6 m, while the water content probes are installed at depths of 0.1, 0.3, and 0.6 m below the ground surface (**Figure 2.1.1**).

(a) (b) (c)

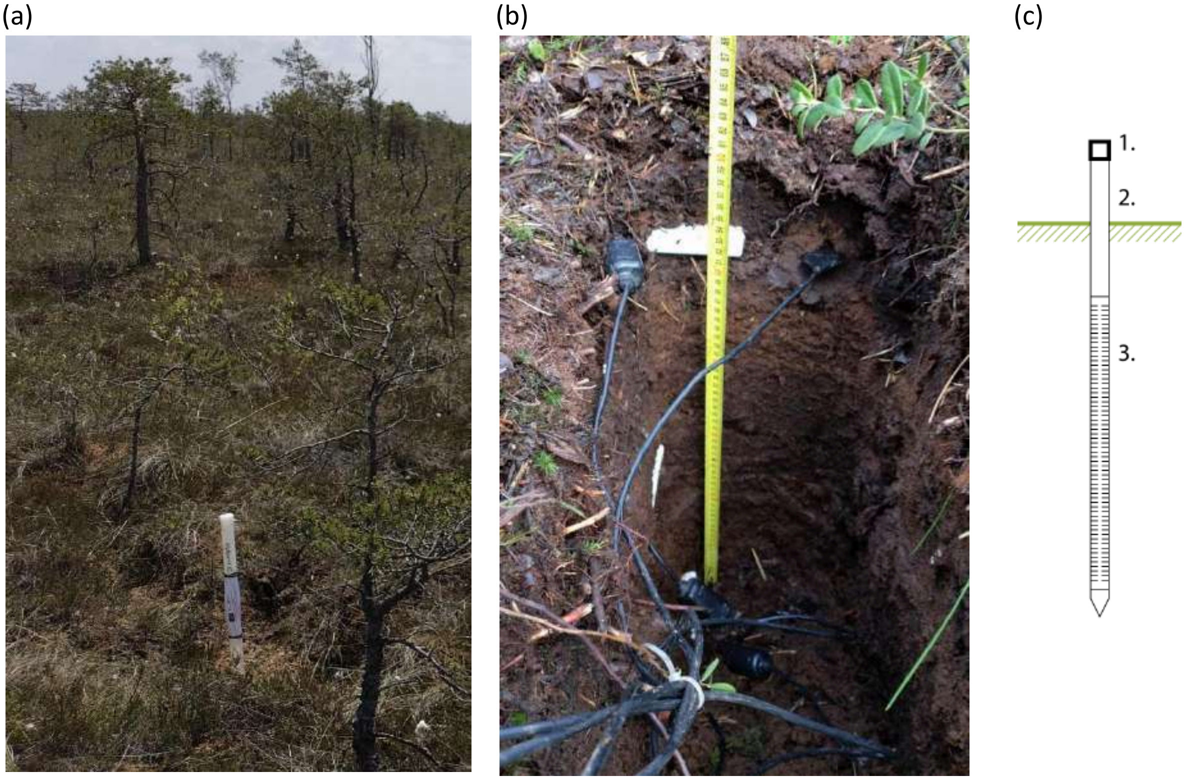

Figure 2.1.1. *Groundwater monitoring well (a) and soil water monitoring probes (b) in Lielais Pelečāres Mire. Schematic monitoring well setup (c): 1 – well cap; 2 – smooth pipe HDPE 25 mm internal diameter, usually 1 m long, about 0.5 m above surface; 3 – filter interval, usually 2 m long in some cases covered with filter fabric sock. Images: © A. Kalvāns*

In total 72 soil and ground water sensors, including 4 barometric probes were planned for procurement (**Table 1-1**). During two procurement rounds in 62 Levelogger5 Junior water level probes, 4 Levelogger5 LTC water level and electrical conductivity probes, 4 Barologger5 barometric pressure probes from Solinst Canada and 2 Atmos 41 integrated weather stations form METER Group GmbH, with capabilities of recording parameters necessary to calculate climatological water balance (precipitation, air humidity, wind speed, solar radiation and air temperature). Four of the procured sensors remain in reserve if a replacement or additional monitoring needs arise.

Hydrological monitoring in Cenas Mire was initiated on June 8, 2023, by establishing six monitoring points equipped with automatic water level sensors (**Figure 2.1.2**, Appendix 6.3), including one point for assessing water flow in a drainage ditch. The second set of groundwater level monitoring probes were installed in spring 2024 on May 7 and 27. In September 2025 a malfunction of a water level probe was detected in monitoring well Cena10. Later that year the Cena11 monitoring well was accidentally damaged while building a new dam on a large drainage ditch. Therefore, on November 11 the probe from well Cena11 was transferred to well Cena10.

The hydrological monitoring in Lielais Pelečāres mire was initiated on June 20, 2023, when the first 13 monitoring wells, including one point in the ditch (Malnupeite) for discharge volume assessment were installed (**Figure 2.1.2**). Most of these monitoring points were equipped with automatic groundwater level (Appendix 6.4) probes. The water level data was retrieved on November 7, 2023. Additionally, in the autumn of 2023, another 12 water level monitoring points were installed. The water level sensors were installed in spring 2024. Furthermore, two soil water regime monitoring points have been set up, where observations of soil water content and potential are conducted using five probes at each site. In Aprils 23, 2024 two weather stations were installed aimed at comparing microclimatological differences in forested site and open raised bog.

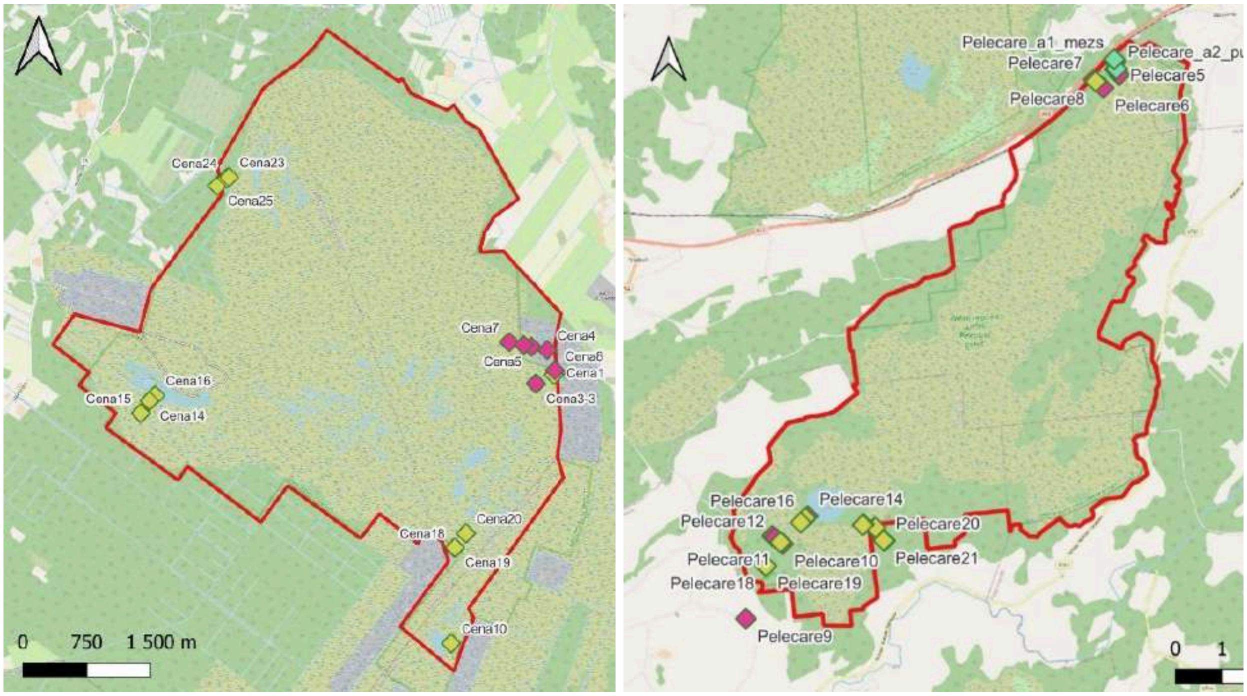

Figure 2.1.2. *Location of the hydrological monitoring points in Cenas Mire (left) and Lielais Pelečāres Mire (right). Legend: ◆ - no probe; ◆ - Levelogger 5 Junior; ◆ - Meter Teros21 and Teros11. Images: © A. Kalvāns*

The water level monitoring network in Sudas-Zveidru mire comprises 7 sites organised along two profiles (Appendix 6.5). One profile (wells Suda1, Suda6 and Suda5) was set up to monitor the water level in a blocked drainage ditch, both at opposite ends of flooded segments of the ditch and at both sides of a dam on the same ditch. The aim of this configuration was to observe the temporal dynamics of water level along the ditch, particularly the development of the resistance to the water flow in the flooded ditch due to development of vegetation. In the case of successful restoration, we expect to see both an increasing water level gradient along the flooded section of the ditch and a decreasing gradient across the dam. The other profile (Suda7, Suda4, Suda3 and Suda2) was placed radial to the slope of the raised bog dome from relatively intact mire, across two blocked ditches to degraded peatland covered by sparce pine forest. In a case of successful mire restoration, over time, the pattern of water level fluctuations is expected to get like observations in the intact mire.

The water level monitoring network in Melnais Lake mire comprises 7 sites organized along three profiles and additional observation points within a strip of dense pine forest in the mire (Appendix 6.6). The aim of establishing three profiles was to examine the development of the water level gradient towards blocked drainage ditch at sits with apparent successful restoration (profiles of wells Melnais4 – Melnais5 and Melnais2- Melnais3) and location with apparently unsuccessful restoration (wells Melnais6- Melnais7). In addition, the well Melnais1 was set up to gain any insights how the forested strip affects the mire water regime and elucidate any reasons for its establishment.

2.1.1. Cena Mire

Hydrological monitoring in Cena Mire was initiated on June 8, 2023, by establishing six monitoring points equipped with automatic water level sensors (Figure 2.3., Appendix 6.3), including one point for assessing water flow in a drainage ditch. However, due to blockage of the installed spillover by eroded peat, the discharge measurement was not possible. In the autumn of 2023, another 15 monitoring points were set up, including two points for mire lake water monitoring (**Figure 2.1.3**). Monitoring at these locations will begin as soon as water level probes become available.

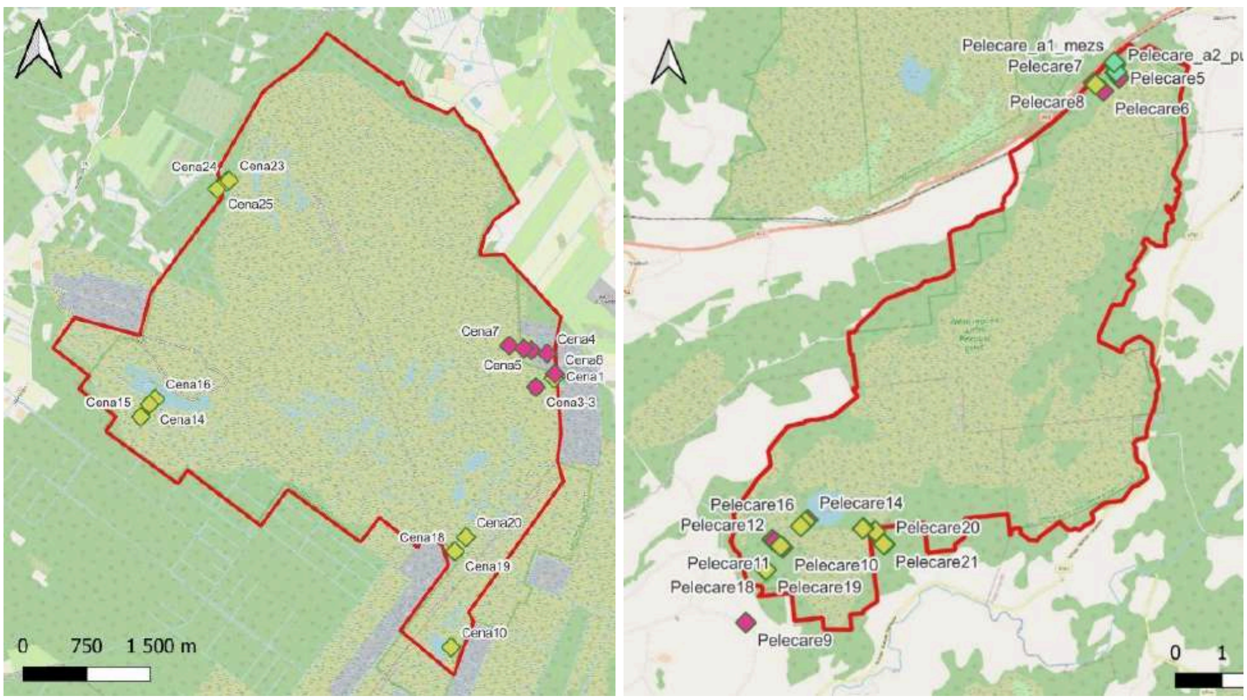

Figure 2.1.3. *Location of the hydrological monitoring points in Cenas Mire (left) and Lielais Pelečāres Mire (right). Legend: ◆ - no probe; ◆ - Levelogger 5 Junior; ◆ - Meter Teros21 and Teros11. Images: © A. Kalvāns*

2.1.2. Lielais Pelečāre Mire

The hydrological monitoring in Lielais Pelečāre Mire was initiated on June 20, 2023, when the first 13 monitoring wells, including one point in the ditch (Malnupeite) for discharge volume assessment were installed (**Figure 2.1.3**). Most of these monitoring points were equipped with automatic groundwater level (Appendix 6.4) probes. The water level data was retrieved on November 7, 2023.

Additionally, in the autumn of 2023, another 12 water level monitoring points were installed, which are not yet equipped with appropriate automatic probes. Monitoring at these points will commence as soon as water level probes become available. Furthermore, two soil water regime monitoring points have been set up, where observations of soil water content and potential are conducted using five probes at each site.

2.1.3. Sudas-Zviedru Mire

The water level monitoring network in Sudas-Zviedru Mire comprises 7 sites organised along two profiles (Appendix 6.5). One profile (wells Suda1, Suda6 and Suda5) was set up to monitor the water level in a blocked drainage ditch, both at opposite ends of flooded segments of the ditch and at both sides of a dam on the same ditch (**Figure 2.1.4**). The aim of this configuration was to observe the temporal dynamics of water level along the ditch, particularly the development of the resistance to the water flow in the flooded ditch due to development of vegetation. In the case of successful restoration, we expect to see both increasing water level gradient along the flooded section of the ditch and decreasing gradient across the dam. The other profile (Suda7, Suda4, Suda3 and Suda2) was placed radial to the slope of the raised bog dome from relatively intact mire, across two blocked ditches to degraded peatland covered by sparse pine forest. In a case of successful mire restoration, over time, the pattern of water level fluctuations is expected to get like observations in the intact mire.

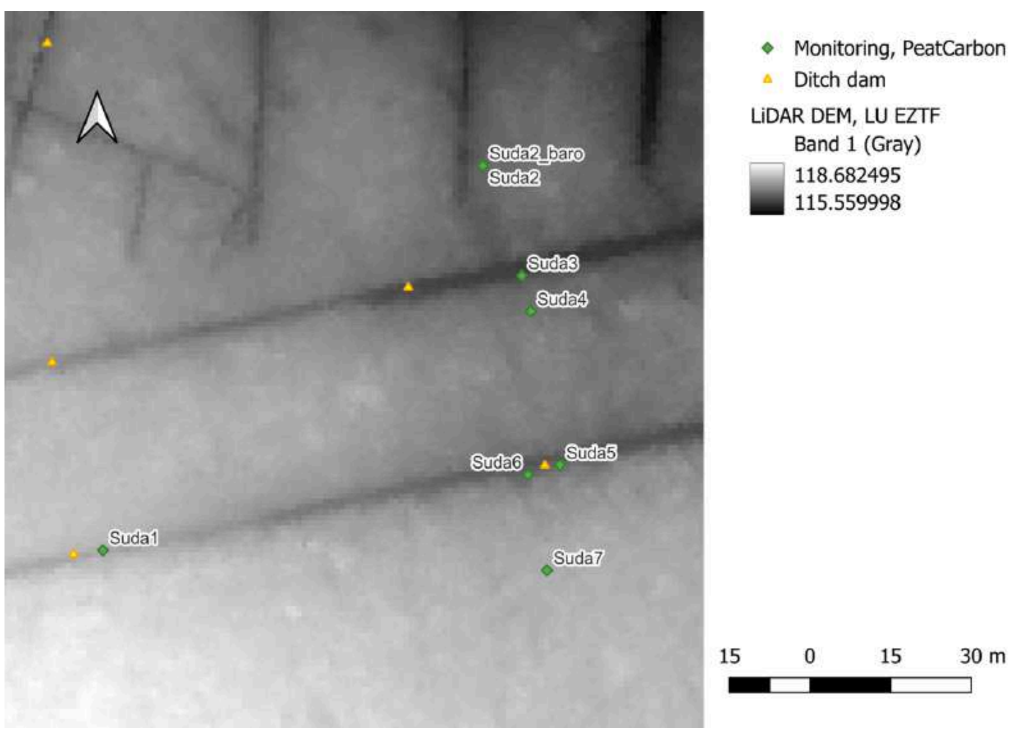

Figure 2.1.4. *Water level monitoring network in Sudas-Zviedru Mire*

2.1.4. Melnais Lake Mire

The water level monitoring network in Melnais Lake mire comprises 7 sites organized along three profiles (**Figure 2.1.5**) and additional observation points within a strip of dense pine forest in the mire (Appendix 6.6). The aim of establishing three profiles was to examine the development of the water level gradient towards blocked drainage ditch at sits with apparent successful restoration (profiles of wells Melnais4 – Melnais5 and Melnais2- Melnais3) and location with apparently unsuccessful restoration (wells Melnais6- Melnais7). In addition, the well Melnais1 was set up to gain any insights how the forested stirp affects the mire water regime and elucidate any reasons for its establishment.

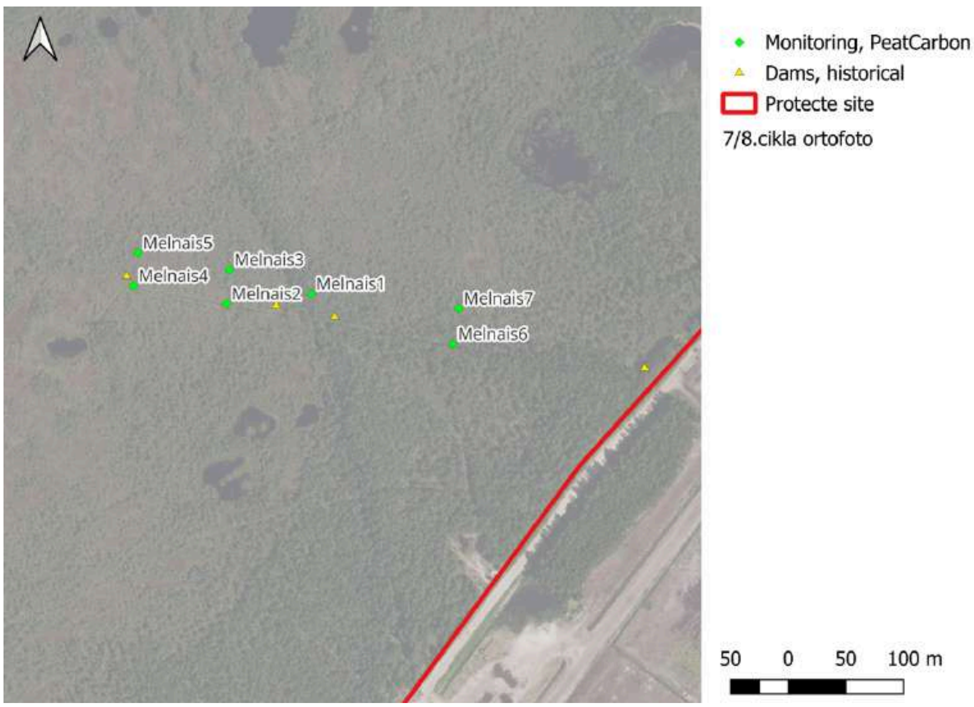

Figure 2.1.5. *Location of water level monitoring wells in Melnais Lake Mire*

2.2. Habitat and vegetation monitoring

The action is mostly implemented in two protected mire habitats of the European Union, i.e. Active raised bog (7110*) and Degraded raised bogs still capable of natural regeneration (7120) (**Table 2.2.1.**, Appendix 6.2). Habitat monitoring is necessary to show the effect of management actions in the project territories. Overall, it is expected that habitat quality and vegetation composition in degraded plots will change after the management actions are completed. According to results of previous similar studies, the number of xerophytes would decrease whereas the occurrence of hygrophytes would significantly increase once the water level in mire is stabilised.

__Table 2.2.1.__ Number of previously and recently established vegetation monitoring plots in project sites in Latvia according to EU habitats (data source: Nature Conservation Agency, 2023).

Year	**Plot size**	**Number of vegetation monitoring plots in EU habitat types**					Outside EU habitats (i.e. peat cutting fields)
		On ditches within the Degraded raised bog (7120)	Degraded raised bog (7120)	Active raised bog (7110*)	Transition mire (7140)	Bog woodland (91D0*)	
Cena Mire							
2005	10*10 m	-	5	2	-	-	-
	1*1 m	-	15	10	-	-	-
	1.5*2 m	25	-	-	-	-	-
2023 [a]	1*1 m	-	6	37	1	2	19
Melnais Lake Mire							
2011	1*1 m	-	30	19	-	-	-
2023	1*1 m	-	18	21	-	-	11
2025	1*1 m	-	3	6	-	-	-
Lielais Pelečāre Mire							
2023	1*1 m	-	3	11	1	16	2
Sudas-Zviedru Mire							
2014	10*10 m	-	-	6	-	-	-
	1*1 m	-	-	60	-	-	-
2023	1*1 m	-	-	20	-	-	-
2025	1*1 m	-	-	9	-	-	-

[a] The number includes vegetation plots at hydrological regime observation points, plots at GHG transects and GEST protocols.

2.2.1. Cena Mire

In 2005, the first habitat monitoring was carried out in Cena Mire where building of dams and habitat management was planned. Permanent plots were established next to hydrological monitoring plots, in places where vegetation changes would be most likely to occur after the planned management actions take place (finished in 2006). In the monitoring design, seven 10*10 m large relevés were planned, each with 3-5 smaller sample plots (1*1 m), and additionally 1.5*2 m plots in drainage ditches. The monitoring scheme also included control plots. In total, there were 25 monitoring plots on ditches and 25 plots in raised bogs (7110*, 7120) in Cena Mire. Plant species composition and the percentage cover, the wetness of the sites, presence of adjacent pools and *Sphagnum* dominated vegetation were evaluated. The monitoring was conducted in 2005, 2007, and 2008 (**Figure 2.2.1**).

Figure 2.2.1. *Vegetation monitoring plots in Cena Mire in 2008 (left) and in 2023 (right). Images: © M. Pakalne, L. Strazdiņa*

In 2023, vegetation monitoring was established in other places than in 2005, in connection with location of water level and GHG measurement plots (**Figure 2.2.1**). However, species composition was compared between the two time periods despite different data collection locations. In total, 29 new vegetation monitoring plots were established (Appendix 6.3). In addition, the species composition in different parts of Cenas Mire can be characterized using GEST protocols. A total of 23 such forms were completed and used for indirect estimation of GHG emissions from the project site.

Vegetation monitoring will be repeated in the summer of 2026, as the restoration activities were completed during the autumn-winter period of 2025.

2.2.2. Melnais Lake Mire

In 2011, permanent vegetation monitoring plots were established in Melnais Lake Mire. In total, 49 plots were in six transects, each with 5–10 vegetation plots. Following parameters were estimated in every plot: species composition and percentage cover, tree cover, heather cover, the total cover of *Sphagnum* species and distance to the nearest drainage ditch.

Monitoring was only partially repeated in 2023 due to unavailability of vegetation monitoring plot coordinates. Both for this reason and because of new groundwater and GHG measurement locations, nine new vegetation plots were established (Appendix 6.3). Like in Cena Mire, the 26 completed GEST protocols can also be used to characterize vegetation of Melnais Lake Mire.

Vegetation monitoring was repeated in 2025 in 9 plots that are associated with GHG measurement points (**Figure 2.2.2**).

Figure 2.2.2. *Part of vegetation monitoring plots in GHG measurement point in Melnais Lake Mire in 2025. Images: © L. Strazdiņa*

Figure 2.2.3. *Vegetation monitoring plots near GHG measurement point with litter collector (left) and near hydrological monitoring point (right) in Lielais Pelečāre Mire in 2023. Images: © L. Strazdina*

2.2.3. Lielais Pelečāre Mire

The area has never been monitored before and the data is only used to characterize the existing situation, but statistical analysis could not be performed. In Lielais Pelečāre Mire, a total of 33 vegetation monitoring plots (1*1 m) were established parallel to 15 water level observation wells and 18 plots around GHG measurement sites (Appendix 6.3, **Figure 2.2.4**).

The restoration will be carried out during the autumn-winter period of 2026; therefore, vegetation monitoring can only be repeated in the summer of 2027.

2.2.4. Sudas-Zviedru Mire

In September 2014, permanent habitat monitoring plots in two transects were established in Sudas-Zviedru Mire. One end of each transect was located near the drainage ditches where management actions were performed, and the other end 150–250 m further leads to natural raised bog where drainage impact is not significant. In total, three plots in size of 10*10m were established on each transect. One plot represents vegetation and habitats of degraded raised bog while the second plot located 50 m further shows less impacted habitats where the drainage effect, however, is still present. The third plot works as a control.

Figure 2.2.4. *Vegetation monitoring plots in Sudas-Zviedru Mire in 2018 (up left) and in 2023 (up right) and in 2025 in GHG measurement points (below). Images: © M. Pakalne, L. Strazdiņa*

Coordinates in the WGS-84 system of each plot were measured using GPS. Following parameters were protocoled for each habitat monitoring plot – cover and vitality of heather, plant community, distance to drainage ditch or bog pool, number and vitality of tree species in different height (<0,5 m, 0,5–1 m, 1–1,5 m, > 1,5 m) of tree level. In each of these plots 10 randomly selected microplots were established. For each microplot following parameters were protocoled – location within the large plot, cover of all species in tree, bush, dwarf-shrub, herb, bryophyte and lichen level. Cover and vitality of heather and trees, most of all pine and downy birch, were used as indicators to recover progress of the whole mire ecosystem after management actions. High-res photos were also taken on site to compare the situation in nature pre and after the management actions. Habitat monitoring in Sudas-Zviedru Mire was repeated in 2015, 2016, 2018, 2020, and 2023 (**Figure 2.2.4**). Only one of the previously established transects with 11 plots will be used in LIFE PeatCarbon project studies (Appendix 6.3). Additionally, nine vegetation plots were established near the GHG measuring points. In 2025, these nine vegetation plots were repeatedly monitored. Vegetation was also surveyed during the GEST analysis, which was conducted in autumn 2025, in 36 plots (**Figure 2.2.5**, Appendix 6.4).

Figure 2.2.5. *Some of the most common GEST types in the Sudas-Zviedru Mire in 2025: Moderately moist forest and shrubberies (OL) (up left); Very moist bog heath (up right); Very moist peat moss lawn (below left); Wet meadows and forbs (below right). Images: © L. Strazdiņa*

2.3. Greenhouse gas emission monitoring

Monitoring of total ecosystem emissions (CO_2 emissions reflecting ecosystem respiration, CH_4 and N_2O emissions) and soil heterotrophic respiration was initiated in June 2023 and has been implemented as part of the monitoring (**Figure 2.3.1, Figure 2.3.2**). In parallel, data are being obtained on environmental parameters that are essential for characterizing changes in GHG emissions: including soil and air temperature, groundwater level, soil water chemical properties, soil chemical properties, aboveground and belowground biomass of ground cover vegetation, including, woody plant litter, herbaceous plants, tree foliar litter, moss and living tree biomass and carbon accumulation in non-living woody plant biomass.

The location and classification of measurement sites is provided in **Table 2.3.1**, the location on the map is shown on the map **Figure 2.3.3, Figure 2.3.4, Figure 2.3.5**. Photos of the study sites and subplots representing different habitat types are provided in the Appendix 6.7.

Figure 2.3.1. *GHG measurement in Melnais Lake Mire. Image: © M. Pakalne*

Figure 2.3.2. *GHG measurement in Melnais Lake Mire. Image: © M. Pakalne*

Table 2.3.1. *Classification of study sites*

Site	Site name	Subplot	Habitat	xcoord WGS84	ycoord WGS84
LPC_1	Sudas-Zviedru Mire	A	Near-natural raised bog	561650	335918
LPC_1	Sudas-Zviedru Mire	B	Rewetted degraded raised bog with direct restoration effect	561641	335948
LPC_1	Sudas-Zviedru Mire	C	Rewetted overgrown raised bog with cumulative restoration effect	561648	335997

Site	Site name	Subplot	Habitat	xcoord WGS84	ycoord WGS84
LPC_2	Lielais Pelečāre Mire	A	Near-natural raised bog	660112	270466
LPC_2	Lielais Pelečāre Mire	B	Drained raised bog with dense tree layer in the strong drainage impact zone	660105	270512
LPC_2	Lielais Pelečāre Mire	C	Drained raised bog with dense tree layer in the weak drainage impact zone	660110	270560
LPC_3	Melnais Lake Mire	A	Near-natural raised bog	499339	299242
LPC_3	Melnais Lake Mire	B	Rewetted degraded raised bog with direct restoration effect	499347	299216
LPC_3	Melnais Lake Mire	C	Degraded bog woodland	499370	299244
LPC_4	Cena Mire	A	Near-natural raised bog	488185	300722
LPC_4	Cena Mire	B	Restored raised bog along ditch with direct restoration effect	488155	300716
LPC_4	Cena Mire	C	Drained raised bog with dense tree layer with cumulative restoration effect	488103	300722
LPC_5	Cena Mire	A	Near-natural raised bog	493086	301066
LPC_5	Cena Mire	B	Peat field along drainage ditch in the strong drainage impact zone	493087	301083
LPC_5	Cena Mire	C	Dry peat field in the strong drainage impact zone	493089	301106
LPC_6	Lielais Pelečāre Mire	A	Natural raised bog	660070	270275
LPC_6	Lielais Pelečāre Mire	B	Natural raised bog	660063	270221
LPC_6	Lielais Pelečāre Mire	C	Natural raised bog	660039	270189
LPC_7	Lielais Pelečāre Mire	A	Near-natural raised bog	660392	263312
LPC_7	Lielais Pelečāre Mire	B	Natural raised bog	660352	263322
LPC_7	Lielais Pelečāre Mire	C	Near-natural raised bog	660299	263326

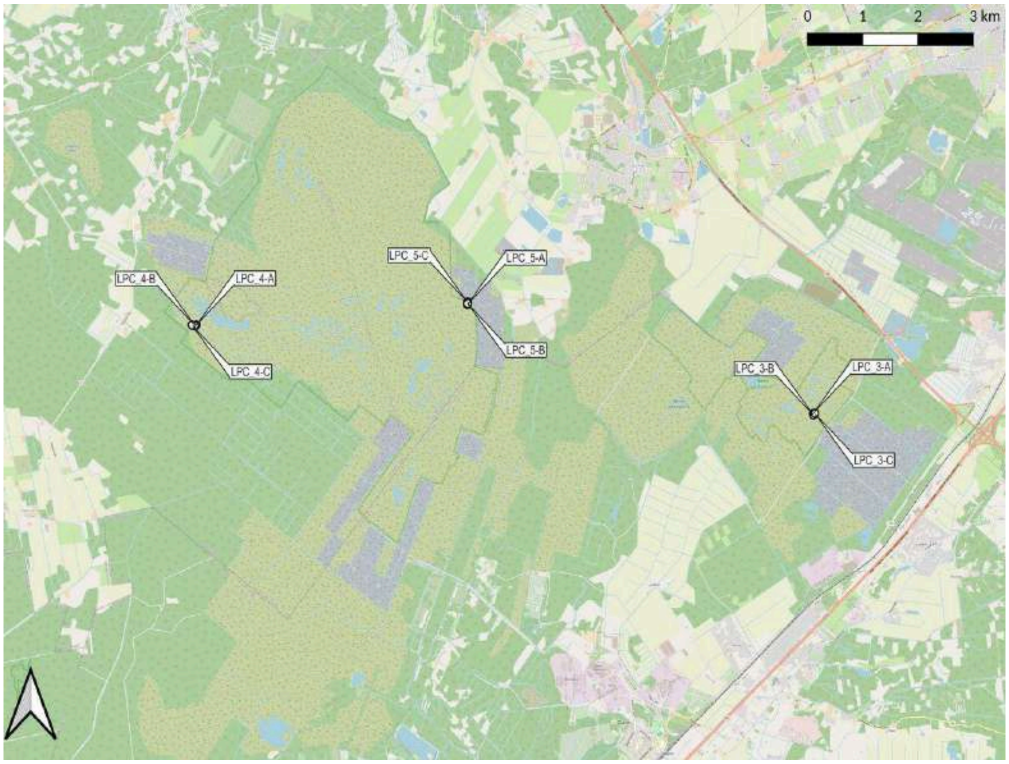

Figure 2.3.3. *Measurement sites in Riga region, Cena & Melnais Lake Mire (LPC_3, LPC_4 rewetted and LPC_5 to be rewetted)*

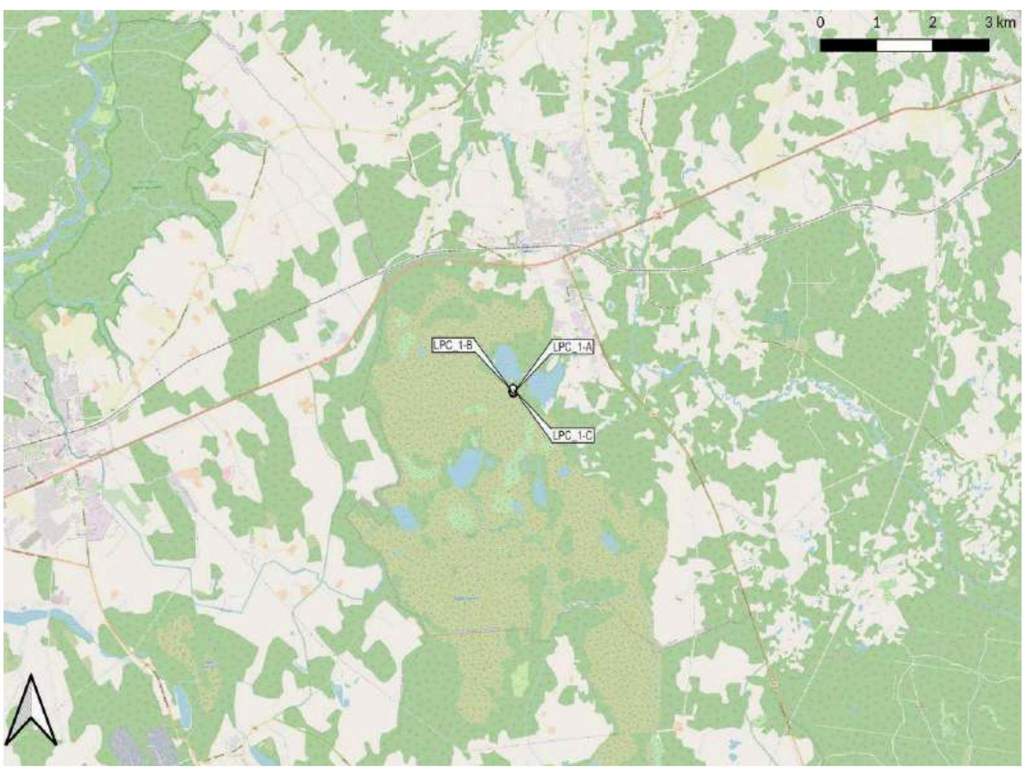

Figure 2.3.4. *Measurement sites in Sudas – Zviedru Mire (rewetted)*

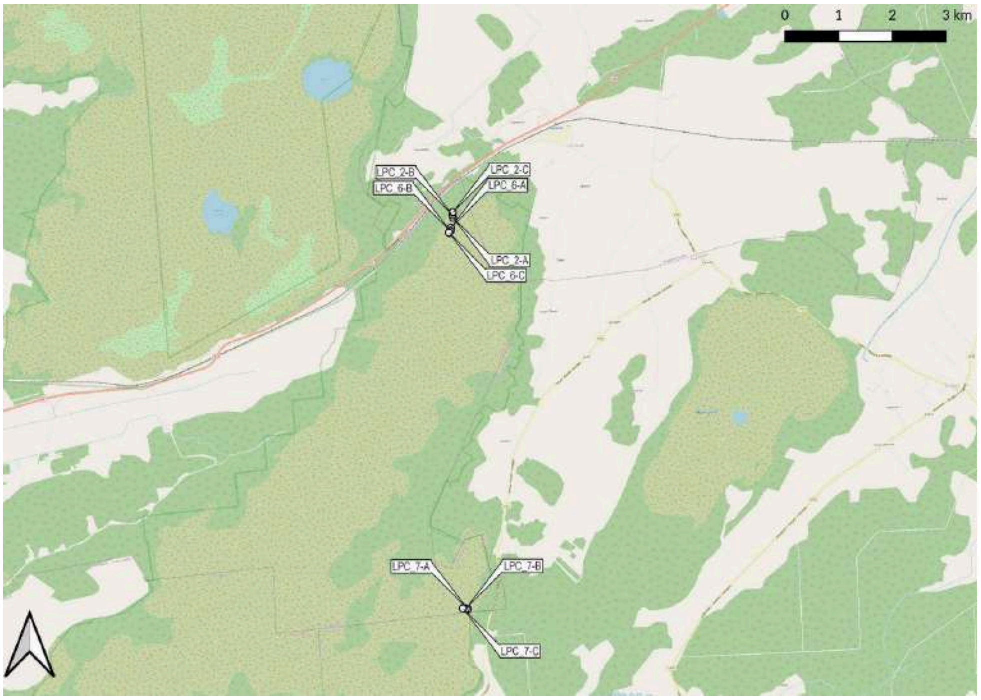

Figure 2.3.5. *Measurement sites in Lielais Pelēčāre Mire (LPC_2 to be rewetted, LPC_6 & LPC_7 pristine)*

Habitats represented in study:			
• Pristine raised bog:	• Degraded • (drained):	• Rewetted:	• Restored
○ Natural, ○ Near-natural	Peat field: • Strong DIZ, • Strong DIZ by ditch Tree cover: • Strong DIZ, • Weak DIZ, • Woodland	With restoration effect: • Not overgrown, • Overgrown, • Dense tree layer	

Table 2.3.2. *Classification of peatland habitats included in the study according to their state of degradation and restoration*

Some images demonstrating different habitats are provided in **Figure 2.3.6**.

Near-natural raised bog

Natural raised bog

Peat field, strong drainage impact zone

Peat field, strong drainage impact zone by ditch

Dense tree layer in strong drainage impact zone

Dense tree layer in weak drainage impact zone

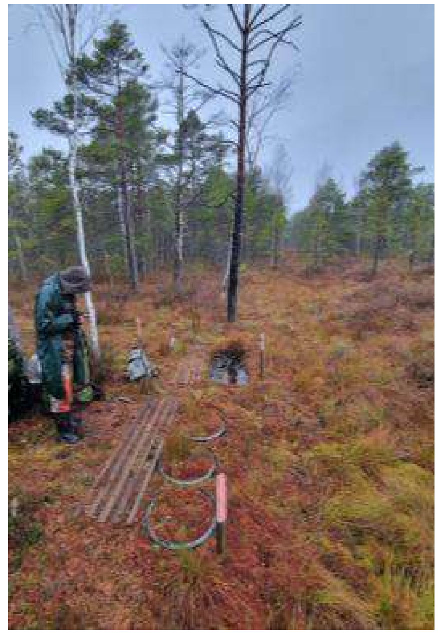

Restoration effect **Restored**

Figure 2.3.6. *Different habitats in study sites. Images: G. Saule*

To conduct observations, 3 sample plots have been established at each monitoring site (at least three months before GHG emission monitoring was initiated), which characterize different ground cover vegetation composition and the impact of expected or already occurred changes in the moisture regime. In addition, 2 study sites (LPC_6 and LPC_7, Table 2.3.1) were established in the Lielais Pelečāre Mire representing natural raised bog and near-natural raised bog habitats (GHG emission monitoring was initiated in May 2024). The sample plots are located at 20-30 m from each other (**Figure 2.3.7.**). Three permanent collars have been installed in each sample plot to characterize total emissions and a sub-sample plot with three sampling points to characterize soil heterotrophic respiration with three gas measurement points. Sub-plots for soil respiration characterization are prepared at least three months before the start of gas exchange measurements (**Figure 2.3.8.**).

Ecosystem respiration – CO_2 (R_{eco} or R_{floor} depending on type of habitat, hereafter R_{tot}), CH_4 and N_2O – is measured using the closed chamber method (Hutchinson & Livingston, 1993). The closed chamber consists of two parts – a chamber made of PVC material and is 40 cm high, with a Ø of 50 cm and a volume of 65 L and a ring that is in the soil throughout the observations. When collecting samples, the chamber is placed on the collar, which is light in colour to prevent excessive temperature increase during monitoring. A groove is made on the upper edge of the collar, which corresponds to the diameter of the chamber. This groove is filled with water, so that when placing the chamber in it, a completely closed environment is ensured (no air can enter the chamber from the atmosphere).

The chambers in the plots are placed 1-2 m from each other to reduce the need to move around the plot during gas sample collection. Gas samples are collected from the chambers using a tube inserted into the chamber and a syringe attached to it, with the help of which the air from the chambers is transferred into 100 mL bottles, from which all air has been sucked out before measurements (residual pressure <0.3 mbar). Four samples are collected from each chamber within half an hour, observing 10-minute intervals – at minute 0 (immediately after placing the chamber on the ring), at minutes 10, 20 and 30 (Bārdule et al., 2023; Butlers et al., 2023). The samples are placed in specially prepared and labelled sample boxes so that each sample has its own cell address depending on which chamber and at what minute the samples will be taken.

The subplots for measuring soil heterotrophic respiration (R_{het}) are 1.5 x 0.6 m in size with vegetation removed(Figure 2.3.8). Soil respiration measurements are performed with an EGM5 spectrometer. The measurement lasts for 3 minutes. Soil respiration chambers are smaller than ecosystem emission measurement chambers. Soil heterotrophic respiration data are analysed using linear regression equations. If the change in CO_2 concentration does not fit the linear regression equation, the measurement is not used in further analysis, assuming that the measurement was disturbed by some external factor. The same approach is used in the analysis of ecosystem emission measurement results.

Gas samples are collected on average once a month – more often during the vegetation season and les often during winter. Every time, when collecting gas samples, the groundwater depth (cm), air temperature, soil temperature and moisture content in the soil surface are measured. Soil groundwater wells are installed for groundwater depth measurements. Groundwater wells – perforated PVC pipes (Ø50 mm), sealed in the lower 0.5 m – are placed at a depth of 1.5 m. Soil temperature is measured at four depths – 5, 10, 20 and 30 cm.

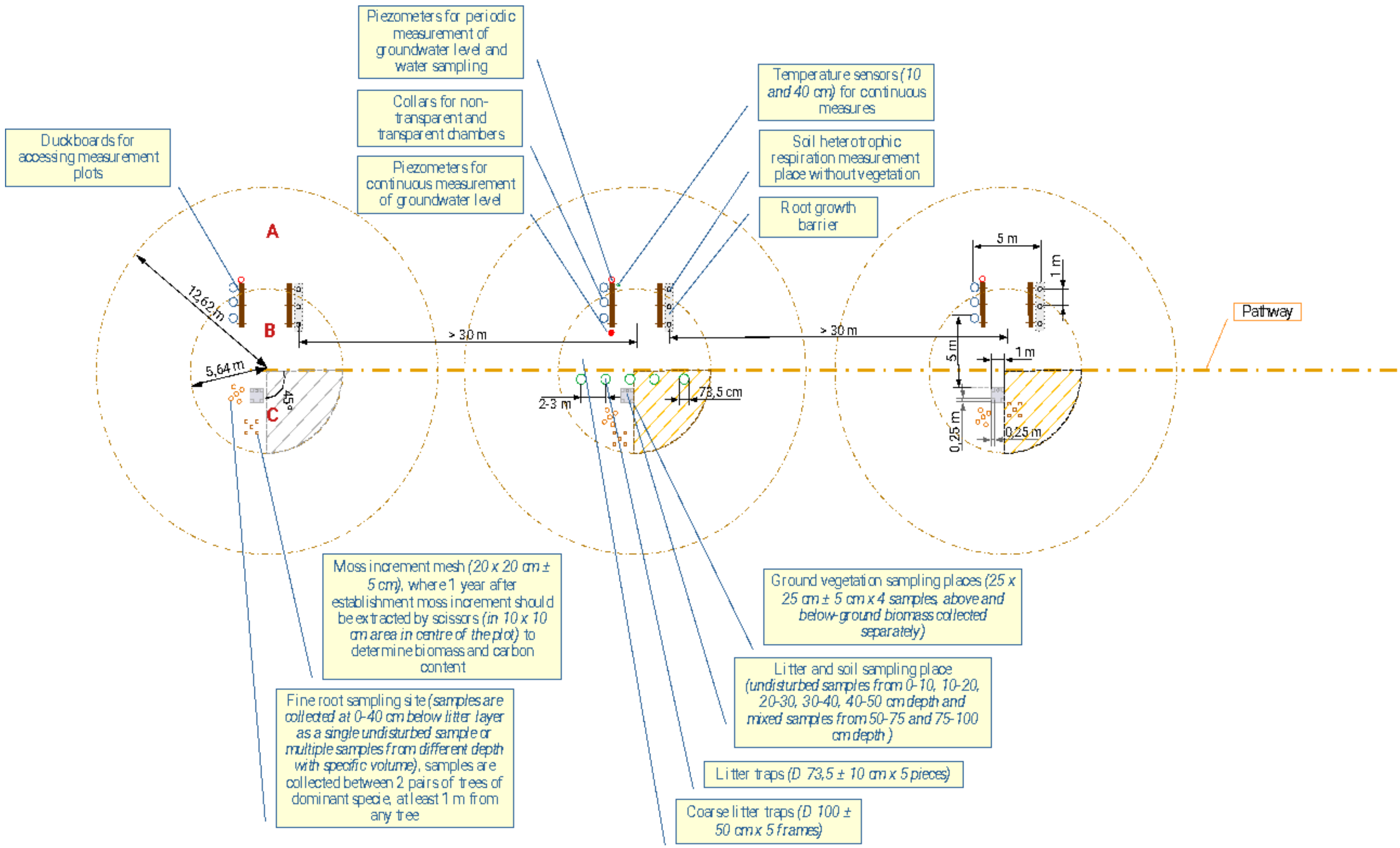

Figure 2.3.7. *Measurement site design*

After measuring the groundwater level, the wells are pumped out to obtain fresh soil water samples for laboratory analyses. The collected water samples (collected during every gas sampling campaign) are delivered to the LSFRI Silava Forest Environmental Laboratory.

Ecosystem emissions or GHG concentrations (CO_2, CH_4 and N_2O) in the collected gas samples are analysed by the LSFRI Silava Forest Environmental Laboratory using a Shimadzu GC-2014 gas chromatograph (equipped with an electron capture detector (ESD), a flame ionization detector and a Loftfield autosampler, designed according to the principles defined by Loftfield et al. (1997). The emission level of each gas is calculated by assuming a linear increase in gas concentration over time, at a given chamber area and volume.

Figure 2.3.8. *Gas measurement plots (heterotrophic respiration on left, total ecosystem exchange (CO_2, CH_4, N_2O fluxes) on the right). Image: © G. Saule*

Simultaneously with the measurement of groundwater level, measurements and observations of factors affecting ecosystem GHG exchange are performed. Typically, groundwater characteristics such as depth, temperature, dissolved oxygen (DO), electrical conductivity, pH and oxidation-reduction potential (ORP) are determined with the ProDSS probe, as well as groundwater samples are collected for determination of the composition of (NO_3^-) and ammonium (NH_4^+) ions, as well as other parameters in the laboratory. In parallel, air and soil temperature measurements are performed at a depth of 5 cm, as well as soil electrical conductivity and soil moisture level are determined with Procheck (**Figure 2.3.9.**).

Figure 2.3.9. *Equipment for measuring soil temperature, moisture content and groundwater properties**.** Image: © G. Saule*

Litter collectors (**Figure 2.3.10**) are installed on the outer perimeter of the plot, 10-15 m from the centre (3 pcs. in each plot) and are emptied once a month, simultaneously with gas exchange measurements. The total dry matter mass, as well as the carbon content, are determined for the litter. Large litter is not evaluated in this study, if carbon input because of natural branching or falling larger tree debris is small. The ICP Forests methodology (Ukonmaanaho et al., 2016) was used for litter collection and analysis.

Figure 2.3.10. *Water and litter sampling plots. Image: © G. Saule*

2.4. GEST monitoring

Land cover mapping at different digitalization is usually performed using spectral remote sensing data (Jakovels et al., 2016; Räsänen & Virtanen, 2019). The choice of target classes depends on available reference data as well as spectral separability. Reference data could be a community type, for instance, following a GEST typology or plant functional types and should be provided as geospatial data polygons or points. In the project, reference data have been collected according to GEST methodology (Jarašius et al., 2022) that required additional vegetation monitoring points for differentiation of all homogeneous vegetation forms present on peatland. The reference information was used directly for GEST classification, but the same information based on vegetation description by projective cover of each species will be recalculated according to their belonging to plant functional type (PFT) thus gaining reference information of PFT composition within each GEST class.
Reference data can be prepared based on existing databases or can be obtained during field visits. If spectral remote sensing data is acquired before field visits, unsupervised classification can be used for effective and targeted planning. An example of such an approach that IES have applied within the project is shown in **Figure 2.4.1**, where unsupervised classification based on Principal Component Analysis (PCA) was used to identify spectrally different areas. Reference GEST type class and polygon borders have been further defined during the site visit. Areas with mixed classes were not included in reference data. Obtained reference data were further used for both training of classification algorithms and the validation of produced data products.

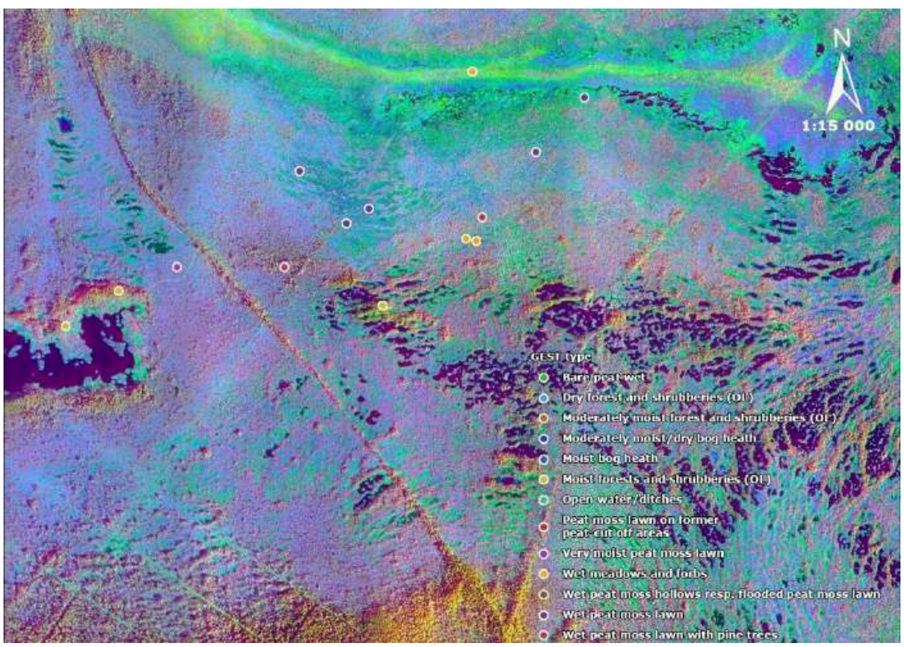

Figure 2.4.1. *Example of gathered reference data for GEST classification as input data for RS algorithm training showed on Principal Component Analysis map of Cena Mire, Latvia. Image: © Institute for Environmental Solutions.*

If reference data is available from existing databases, it is possible to perform a separability analysis on the training data to estimate the expected error in the classification for various feature combinations

(Landgrebe, 2003). The results may identify classes that cannot be separated as well as features that don't provide added value.

The choice of classification algorithms usually depends on the number of available reference data, data specifics as well as researcher's preference. There is not a best option, and the result often depends on the experience of the researcher. In Latvia, IES has previously successfully applied the Support Vector Machine (SVM) based algorithms for the classification of land cover (Jakovels et al., 2016). The SVM-based approach has been chosen as it has demonstrated relatively good performance with small reference data sets and is not sensitive to overfitting. In this case, input data standardization using mean values and standard deviations was applied, as well as RBF or Gaussian kernel was chosen.

RS experts in Luke have mostly used random forest (e.g., Räsänen & Virtanen 2019) but also SVMs and boosted regression trees. Random forest has been among the best-performing classifiers, and it is simple to use compared to some alternative classifiers. Random forest does not usually require tuning of parameters, it rarely overfits, and it is capable of handling multicollinear explanatory data with hundreds of features. Within the project different machine learning techniques will be tested for GEST classification (most probably selecting SVM or random forest) and chosen the one which demonstrates the best performance during the validation of data products.

The performance of classification algorithms was assessed during the validation procedure. It is important to separate training and validation data sets to avoid validation on data that has been already used for training. A common practice is to randomly divide available reference data into two groups where e.g., 80% are used for training and 20% for validation. In the case of small reference data sets, a k-fold cross-validation approach can be applied. For instance, in the k=5 approach training and validation are performed 5 times, each time choosing a different 20% subset for validation, and average classification accuracy is reported at the end. The k might be increased up to the total number of the reference data set where the leave-one-out validation approach is applied in such a case.

The digitalization of classification results primarily depends on the spatial resolution of spectral remote sensing data. Hyperspectral data in the visible-to-near infrared spectral range is optimal to ensure the best spectral separability, however, multispectral data with at least five spectral channels (blue, green, red, red-edge, near-infrared) is also acceptable. Data acquisition should be performed during vegetation season when the most significant spectral and textural differences could be observed among different target classes. Cloud-free sky weather conditions and flight direction in or out of the Sun are recommended to clear data with a maximal signal-to-noise ratio.

The final data products are GEST maps and PFT distribution maps used for spatial GHG emission upscaling. Those shall be based on measured flux data and flux factors, and only for rough estimation, on literature derived values. GEST approach can be tested by producing GHG emission maps using literature-based flux factor values and later validating them by flux factors based on measured GHG fluxes from the monitoring sites. Further, PFT distribution maps will be used by FMI for ecosystem model development of each project site.

2.5. Annualisation of GHG fluxes by temperature dependant interpolation

Soil temperature dependant CO_2 efflux models

Measured CO_2 flux data were first quality-controlled and prepared for modelling. Temperature values stored as character strings were converted to numeric format, and records lacking valid temperature, flux, site or subplot identifiers were excluded. Observations were grouped at the level of individual subplots (Site × Subplot) to preserve microsite-specific hydrological and ecological conditions.

The temperature response of total ecosystem respiration (R_{eco}) was modelled separately for each Site × Subplot combination using the Lloyd–Taylor equation, which describes the exponential dependence of respiration on temperature:

$$R(T) = R_{ref} exp\left(E_0\left(\frac{1}{T-T_0}\right)\right)$$

where T is temperature (K), T_0 is a constant set to −46.02 °C (227.13 K), and T_{ref} is a reference temperature of 10 °C (283.15 K). The parameters R_{ref} (respiration rate at the reference temperature) and E_0 (temperature sensitivity) were estimated using non-linear least squares. Initial parameter values were derived from observed fluxes near 10 °C or. Model fitting was performed independently for each Site × Subplot. Fitted models (**Figure 2.5.1**) were then used to generate continuous predictions of total respiration across the observed temperature range for each subplot.

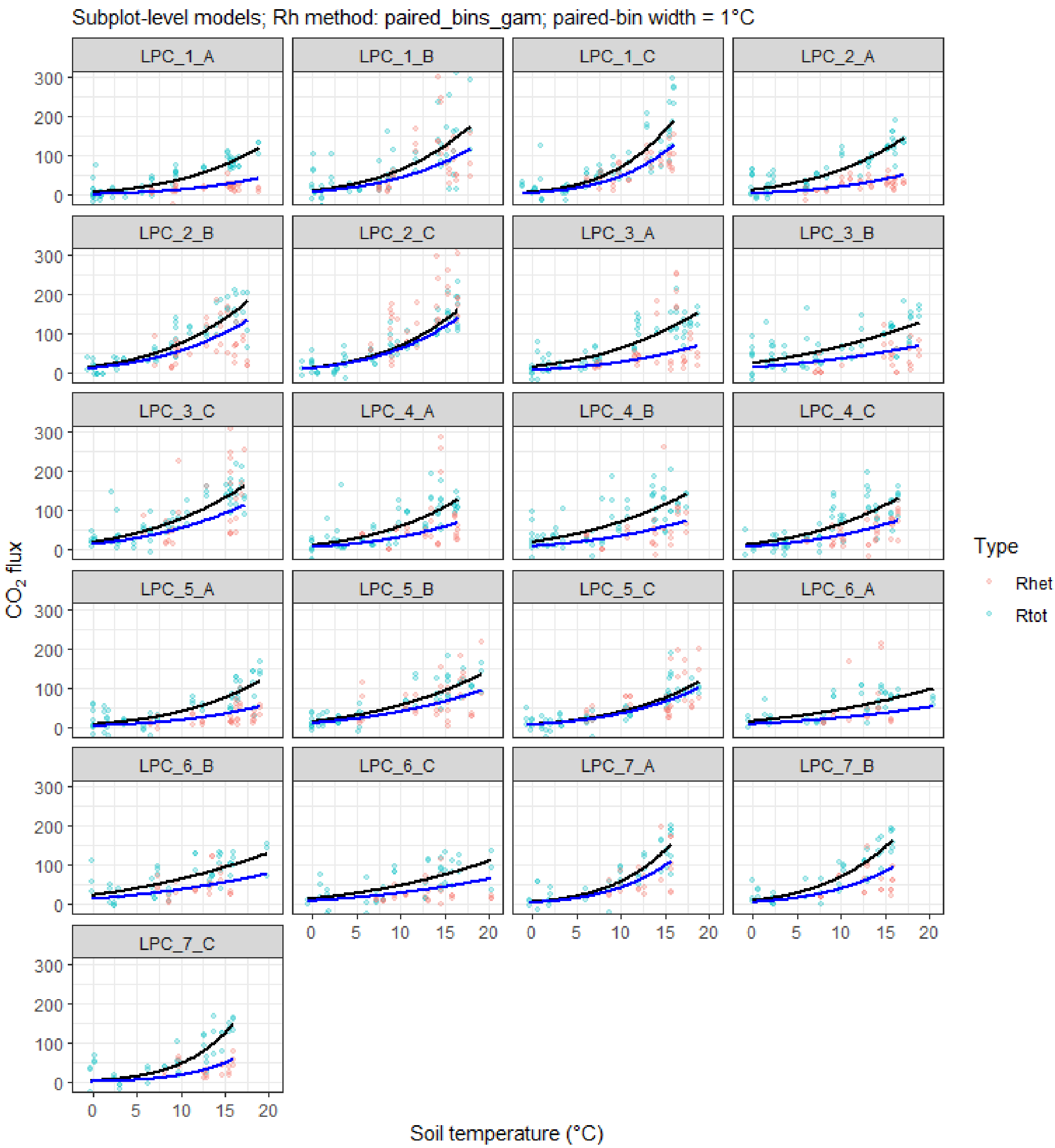

***Figure 2.5.1**. Relationship between soil temperature and CO_2 efflux fitted with the Lloyd–Taylor equation*

To estimate heterotrophic respiration (R_{het}), the ratio between heterotrophic and total respiration ($f = R_{het}/R_{tot}$) was modelled as a function of temperature (**Figure 2.5.2**). Mean values of R_{het} and R_{tot} were calculated for each Site × Subplot within 1 °C temperature bins. Ratios were constrained to the interval 0 to 1.

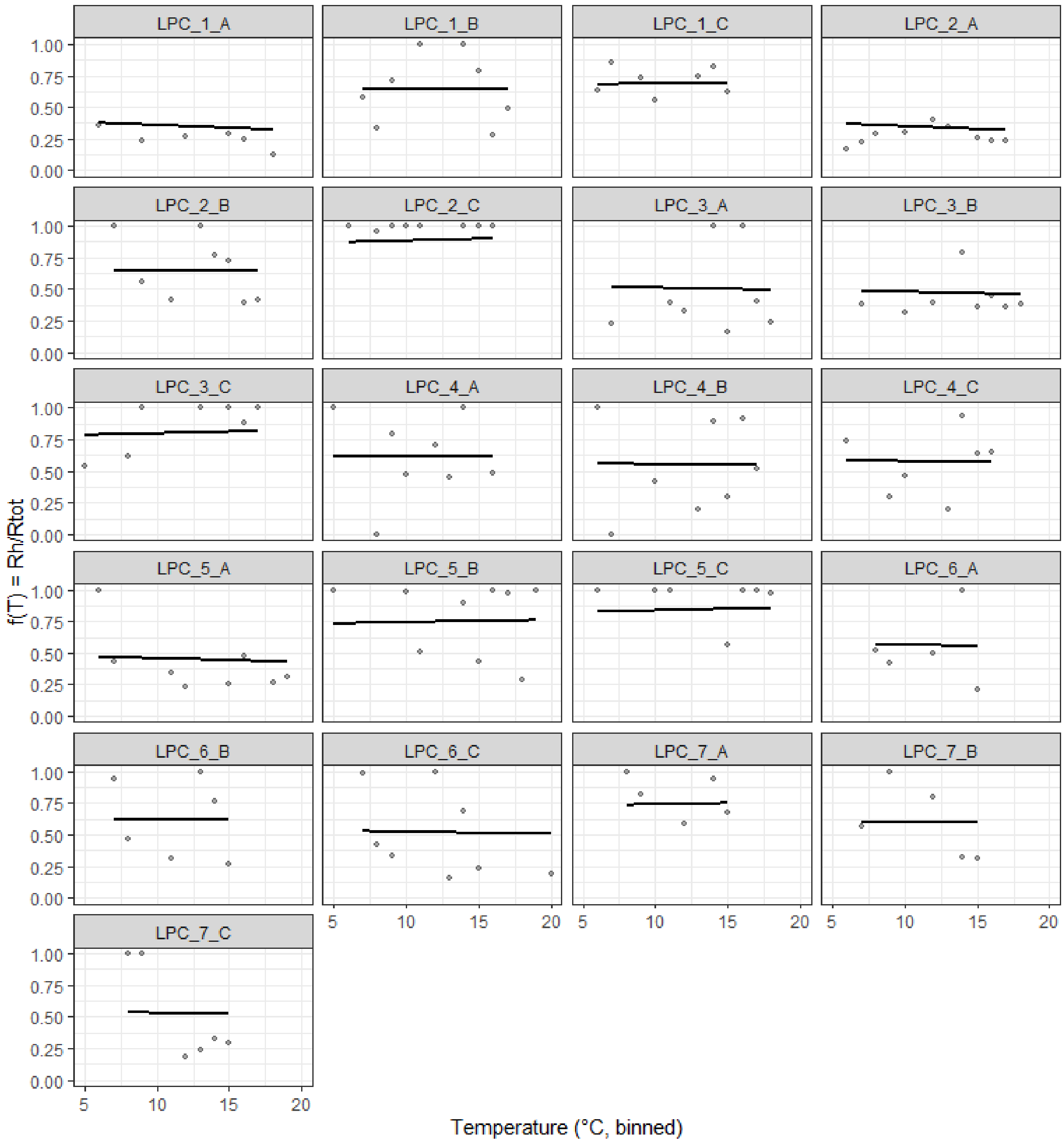

Figure 2.5.2*. Contribution of heterotrophic respiration to total respiration*

A generalized additive model (GAM) with quasibinomial error distribution and logit link was used to describe the temperature dependence of f. Separate smooth functions of temperature were fitted for each Site × Subplot using factor-smooth interactions, allowing the heterotrophic contribution to vary non-linearly with temperature and differ among microsites.

Predicted total respiration from the Lloyd–Taylor model and predicted temperature-dependent ratios $f(T)$ from the GAM were combined to estimate heterotrophic respiration:

$$R_h(T) = f(T) \times R_{tot}(T)$$

Continuous temperature-response curves for both total and heterotrophic respiration were produced for each Site × Subplot and compared with observed fluxes to assess model performance (**Figure 2.5.1**). The two-stage modelling framework allowed robust extrapolation of heterotrophic respiration to low temperatures where direct partitioned measurements were unavailable, while explicitly accounting for the observed heterotrophic fraction within R_{tot}.

If paired temperature bins were too sparse for reliable fraction modelling, a fallback approach was applied. In this case, Lloyd–Taylor models were fitted separately for both Rtot and Rhet, and the fraction $f(T)$ was derived directly from the ratio of the two fitted curves. Under this fallback approach, the derived fraction was constrained to the physically meaningful range between 0 and 1, and predicted Rhet values were restricted not to exceed predicted Rtot.

Summary of models aggregated by habitat categories is illustrated in **Figure 2.5.3.**

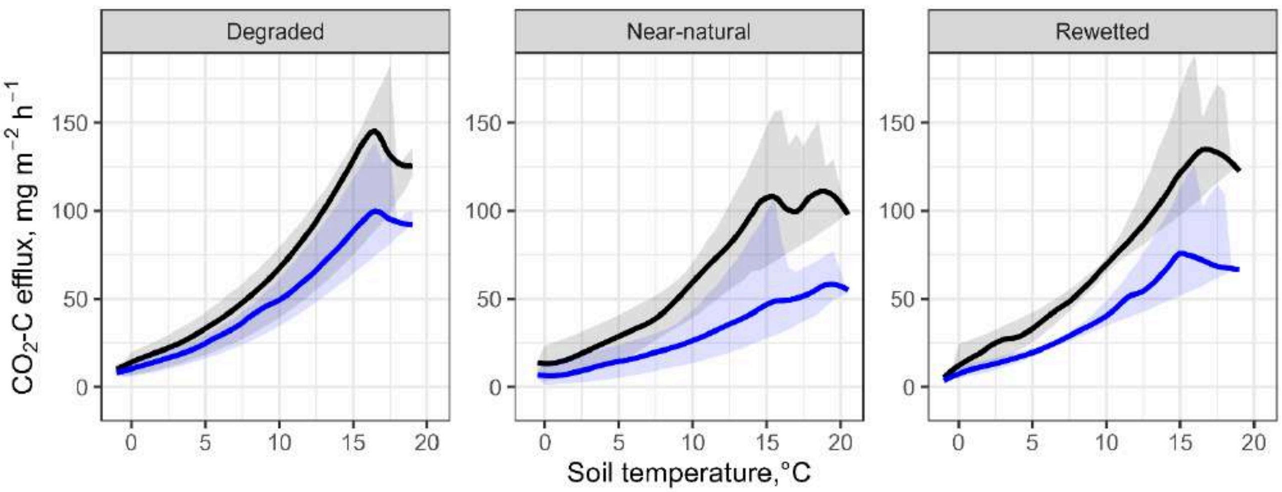

Figure 2.5.3. *Habitat category level CO_2 efflux (blue: R_{het}, black: R_{tot}) temperature response. The figure represents predictions from subplot-level models assigned to habitat categories, grouped into fine temperature bins, and summarised using the median predicted response across subplots. Interquartile ranges (5-95%) were calculated to represent between-subplot variability. Therefore the figure shows median Rtot and Rhet curves, with ribbons representing dispersion among subplot-level predictions.*

Gap-filling and extrapolation of soil temperature time series

Hourly soil temperature time series were constructed for each temperature sensor and completed using a sequential gap-filling approach consisting of short-gap interpolation (≤ 6 h), within-site median borrowing, GAM-based reconstruction of seasonal and diurnal patterns, and minimal last-resort extrapolation. The completed series were then expanded to a common global time window, and remaining gaps were filled using site-level information, GAM predictions, and sensor-specific offsets. All values were labelled by filling stage to ensure traceability, and quality checks confirmed complete temporal coverage and realistic temporal behaviour.

Soil temperature data were harmonized to an hourly temporal resolution for each sensor (defined as Site × Subplot). Raw timestamps were converted to a common time format (UTC), and temperature values were standardized to numeric format. Observations within the same hour were aggregated by calculating the mean, and hours containing only missing values were retained as missing. For each sensor, a continuous hourly time series was constructed spanning the full range between the first and last recorded observation.

Missing values within each sensor-specific time series were filled using a sequential multi-stage procedure. First, observed hourly values were retained. Second, short gaps (≤ 6 hours) were filled using linear interpolation, restricted to avoid extrapolation across longer data gaps. Third, remaining missing values were replaced using the median temperature of other subplots within the same site at the corresponding hour (site-hour median), thereby preserving site-level temporal dynamics. Fourth, any remaining gaps were filled using a generalized additive model (GAM) fitted separately for each sensor, with cyclic smooth terms for day of year and hour of day to represent seasonal and diurnal temperature patterns. GAM-based predictions were only applied when sufficient data were available (≥ 500 observations distributed across ≥ 30 unique days). Finally, any residual missing values were filled using last-observation-carried-forward and backward (LOCF), applied strictly as a last-resort method. Each value in the resulting time series was annotated according to the filling stage (observed, interpolated, site-derived, modelled, or LOCF) to ensure full traceability (**Figure 2.5.4.**).

Following sensor-level gap-filling, all time series were expanded to a common global hourly time window defined by the minimum and maximum timestamps across all sensors. This ensured consistent temporal coverage for subsequent analyses. Missing values introduced during this expansion, including edge gaps and periods of complete sensor outage, were filled using a second sequential procedure. First, available values from the previously gap-filled series were retained. Second, missing values were replaced using the site-hour median derived from other sensors at the same site. Third, where no site-level observations were available for a given hour, a site-level GAM (with cyclic smooth terms for day of year and hour of day) was used to predict temperature. This model was only applied when sufficient data were available (≥ 1000 observations across ≥ 60 unique days). Fourth, to preserve persistent differences among sensors, a group-specific offset was applied to the site-level predictions. This offset was calculated as the median difference between observed sensor values and corresponding site-level estimates during overlapping periods. Finally, any remaining missing values were filled using LOCF as a safety measure.

Quality assurance included verification of complete temporal coverage for all sensors, confirmation of the absence of missing timestamps, and quantification of the contribution of each filling stage. Visual inspection of time series and stage-specific contributions was used to ensure that reconstructed values followed realistic temporal patterns (**Figure 2.5.4**). In cases where individual sensors exhibited implausible behaviour, their time series were replaced using site-level averages.

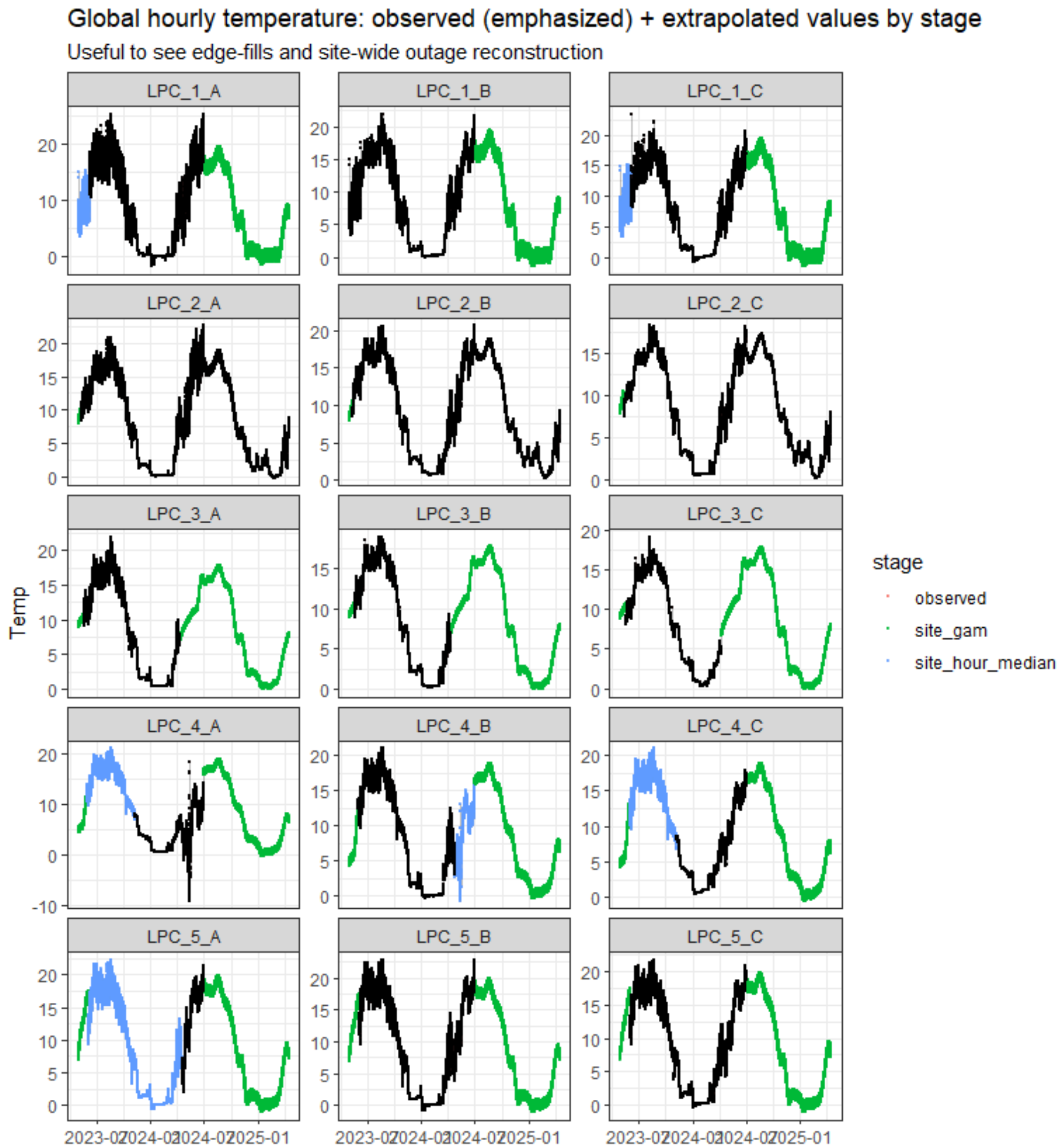

Figure 2.5.4. *Gap-filling and extrapolation of soil temperature time series*

CO_2 efflux annualisation

Hourly CO_2 efflux rates were predicted by combining the fitted temperature-response functions with the previously gap-filled hourly soil temperature series. Hourly total respiration was predicted directly from the Lloyd–Taylor model for each group. Hourly heterotrophic respiration was then estimated either as the product of predicted total respiration and the GAM-derived fraction $f(T)$, or, where the fallback method was used, directly from the Lloyd–Taylor model fitted for Rhet. In all cases, predicted heterotrophic respiration was constrained to be non-negative and not greater than predicted total respiration. The final output consisted of continuous hourly time series of predicted Rtot and Rhet for each subplot across the full study period. These predictions were subsequently exported for further aggregation and analysis.

For annualisation, each hourly prediction was assigned to one of two ecological years, defined as 1 May to 30 April. Thus, the period from 1 May 2023 to 30 April 2024 was treated as Year 1, and the period from 1 May 2024 to 30 April 2025 as Year 2. Only observations falling within these two complete ecological years were retained for annual summary calculations.

Cumulative annual fluxes were then calculated separately for each subplot and ecological year by summing hourly predicted fluxes through time. Annual totals for total and heterotrophic respiration were obtained as the cumulative annual efflux for each subplot and year. These annual sums, initially expressed in g m^{-2} yr^{-1}, were converted to t ha^{-1} yr^{-1} using the factor 0.01. In addition, a 2-year mean annual flux was calculated for each subplot as the arithmetic mean of the two ecological-year totals.

Soil carbon balance estimation

Soil carbon (C) balance was estimated using a mass-balance approach by combining annualised CO_2 efflux with annual soil C inputs to the soil. Soil C inputs were derived from measured litter components, including tree foliar litter, above- and belowground biomass of herbaceous and woody vegetation, and moss.

Annual C input was estimated in two steps: first, by determining the carbon content of annual litter production, and second, by applying factors representing the fraction of carbon entering the soil. For woody ground vegetation, aboveground biomass was converted to annual litter using a turnover rate of 0.25 (Muukkonen, 2006). Total annually collected foliar litter, measured herbaceous aboveground biomass, and annual moss increment were assumed to represent annual litter production (turnover rate = 1.0) (Muukkonen, 2006). Belowground biomass of both herbaceous and woody vegetation was converted to annual litter using a turnover rate of 0.33 (Muukkonen, 2006).

Aboveground litter inputs were further adjusted using a factor of 0.8, assuming that 20% of carbon is oxidised prior to entering the soil (Bragazza et.al., 2009). In contrast, belowground litter was assumed to contribute fully to soil C input (factor = 1.0).

N_2O and CH_4 efflux annualization

N_2O and CH_4 emissions showed weak relationships with temperature; therefore, a simplified approach was applied for annualisation. Instantaneous flux measurements were grouped by calendar month across the entire measurement period, averaged within each month, and subsequently aggregated to derive annual fluxes.

2.6. Hydrological Model of Cenas and Pelecare Raised Bogs, its Calibration, and Impact of Restoration Measures

2.6.1. Model description

The hydrological response of the Cenas and Pelecare raised bogs was simulated using MODFLOW 6. The modelling approach represents groundwater flow and simplified surface runoff within a unified framework. Surface runoff and channel drainage were represented as flow through a highly permeable conceptual upper layer. This formulation allows simulation of ditch networks without explicit surface routing and ensures numerical stability for long-term simulations.

The model domain was discretized using an unstructured triangular mesh with spatial refinement near drainage features. Ditches were represented as narrow linear depressions with a width of approximately four meters. The mesh resolution was selected to ensure adequate representation of drainage features while maintaining computational efficiency.

The model consists of three vertical layers. The upper layer represents a highly permeable material simulating surface storage and rapid lateral flow. The second layer represents upper peat controlling most of the groundwater dynamics. The third layer represents deeper peat with lower hydraulic conductivity. This layered structure allows separation of rapid surface flow and slower groundwater response.

Ground surface elevation was derived from the digital elevation model using percentile filtering. The ground surface corresponds to the median elevation within a moving window, while ditch bottoms are defined using a lower percentile. Lowering the elevation of the upper layer created effective ditch geometries without modifying mesh topology.

Evapotranspiration was simulated using a depth-dependent formulation. Evapotranspiration equals potential evapotranspiration when the water table reaches the surface and decreases with increasing water table depth. Extinction depth varied according to land use classes. Precipitation and potential evapotranspiration were applied as spatially uniform forcing.

Constant head boundary conditions were applied along model boundaries. Initial groundwater levels were set slightly below the ground surface, and a multi-year warm-up period was used to minimize the influence of initial conditions. Identical model structure was used for both study sites, Cenas and Pelecare raised bogs.

2.6.2. Model calibration

Calibration was performed using groundwater level observations from monitoring wells located in degraded peatland areas. Observations were available mainly near drainage ditches and lakes. The calibration period covered 2023–2026, while 2022 was used as a warm-up period.

Calibration was performed manually by adjusting peat hydraulic conductivity, storage parameters, evapotranspiration extinction depth, and geometry of the highly permeable upper layer. The calibration targeted reproduction of mean groundwater levels and temporal variability.

Calibration performance was evaluated using a combination of statistical and visual diagnostics. A composite error metric (*J*) was defined to quantify the agreement between simulated and observed groundwater levels:

$$J = \frac{1}{N}\sum_{i=1}^{N}\left(\left|\Delta\widetilde{h}_i\right| + \left|\Delta\overline{h}_i\right|\right)$$

where:

- N is the number of observation wells,
- $\widetilde{\Delta h}$ is the difference in variability (range or fluctuations) between simulated and observed heads,
- $\Delta\overline{h}_i$ is the difference in mean groundwater level at well i.

This metric ensures that both the temporal variability and the mean state of the groundwater system are simultaneously reproduced. Calibration quality was evaluated using comparison of simulated and observed groundwater levels at monitoring wells. Both mean levels and variability ranges were considered. The calibration results are shown in **Figure 2.6.1.**

The model showed strongest sensitivity to evapotranspiration parameters. Hydraulic conductivity changes had smaller influence within tested ranges. Despite conceptual parameterization, the calibrated model reproduces observed groundwater dynamics sufficiently well, especially, for comparative analysis.

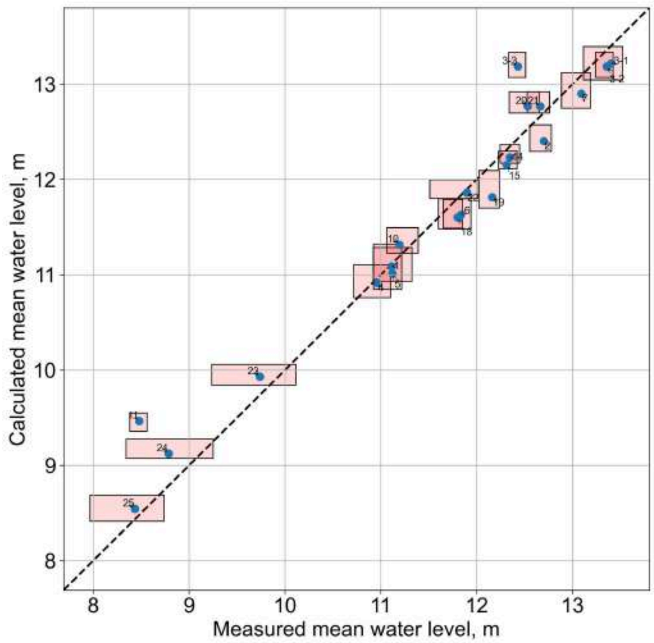

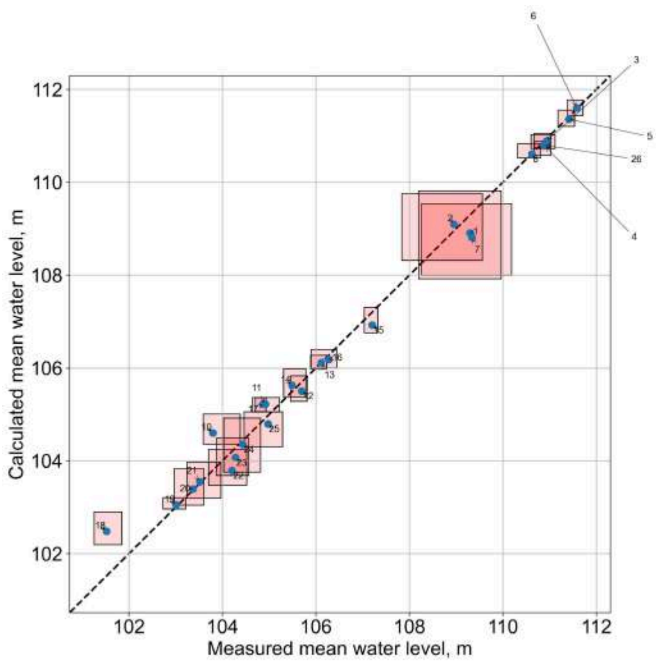

Figure 2.6.1.*: Calculated vs observed water levels for Cenas (left) and Pelecare (right) mires. Boxes illustrate the variability of simulated/observed water levels, while the distance from the diagonal line represents differences in mean water table depth. The surface elevation of the computational mesh was used as the reference level.*

The obtained calibration error was 0.57 cm for Cenas mire and 0.43 cm for Pelecare mire, indicating good agreement between simulated and observed groundwater levels. The agreement between simulated and observed groundwater levels is consistent across wells, with no systematic bias. Minor differences in variability indicate slight smoothing of short-term fluctuations by the model. Overall, calibration results demonstrate that the model reproduces both mean water levels and its temporal dynamics.

3. Results

3.1. Hydrological monitoring

The 2025 hydrological year starting at October 1, 2024, was unusual compared to historically observed conditions (**Figure 3.1.1.** to **Figure 3.1.6.**). The first half of the period was unusually dry and warm. The daily mean temperature reached freezing during the latter half of November, but during December and January flowing remained mostly positive. Permanent freezing conditions established only in February for a period of 2 to 3 weeks. Late April saw an episode of the historically highest air temperature (daily mean close to 20°C, but May to June temperatures remained moderate with a hotter period during the second part of July followed by chilly August, and historically hot September. The precipitation and water balance remained close to historical minimum up to mid-May, when a series of intense precipitation events kicked off one of the wettest summers seen in the study region, particularly in the easternmost study site – Lielais Pelecare mire. In contrast to the usually observed decline of water balance during summer, in 2025 we saw positive water balance – precipitation exceeding evapotranspiration. The conditions switched again during the later part of the hydrological year – September was unusually dry, with neutral water balance, rather than historically observed slight excess of precipitation over evapotranspiration.

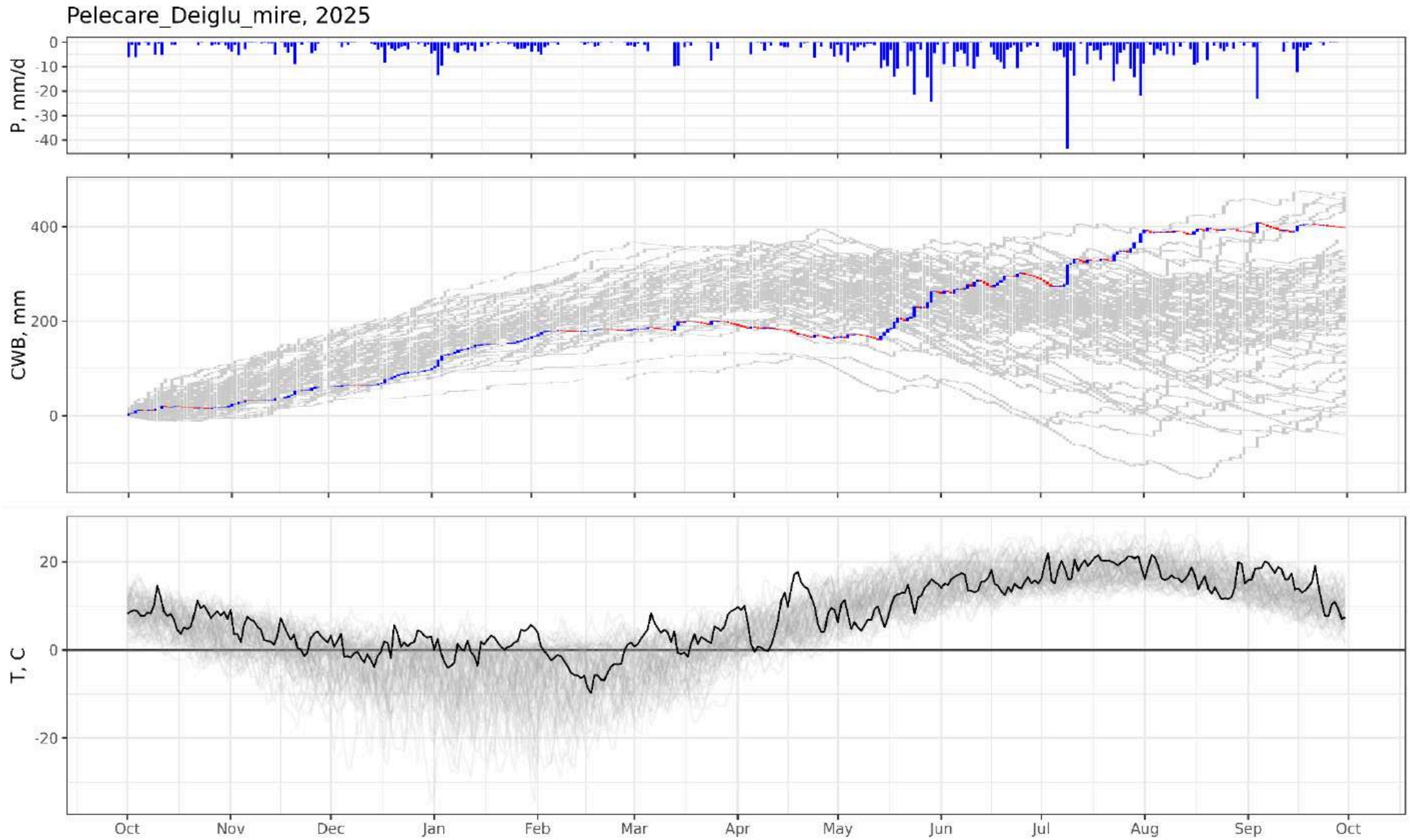

Figure 3.1.1. *Hydrometeorological conditions during 2025 hydrological year starting at October 1, 2024 in the northern part of the Pelecare mire (Diegļu bog), ERA5-land data (Copernicus Climate Change Service 2019), the grey background lines are historical conditions since 1950: P – precipitation, CWB – climatic water balance, T – air temperature*

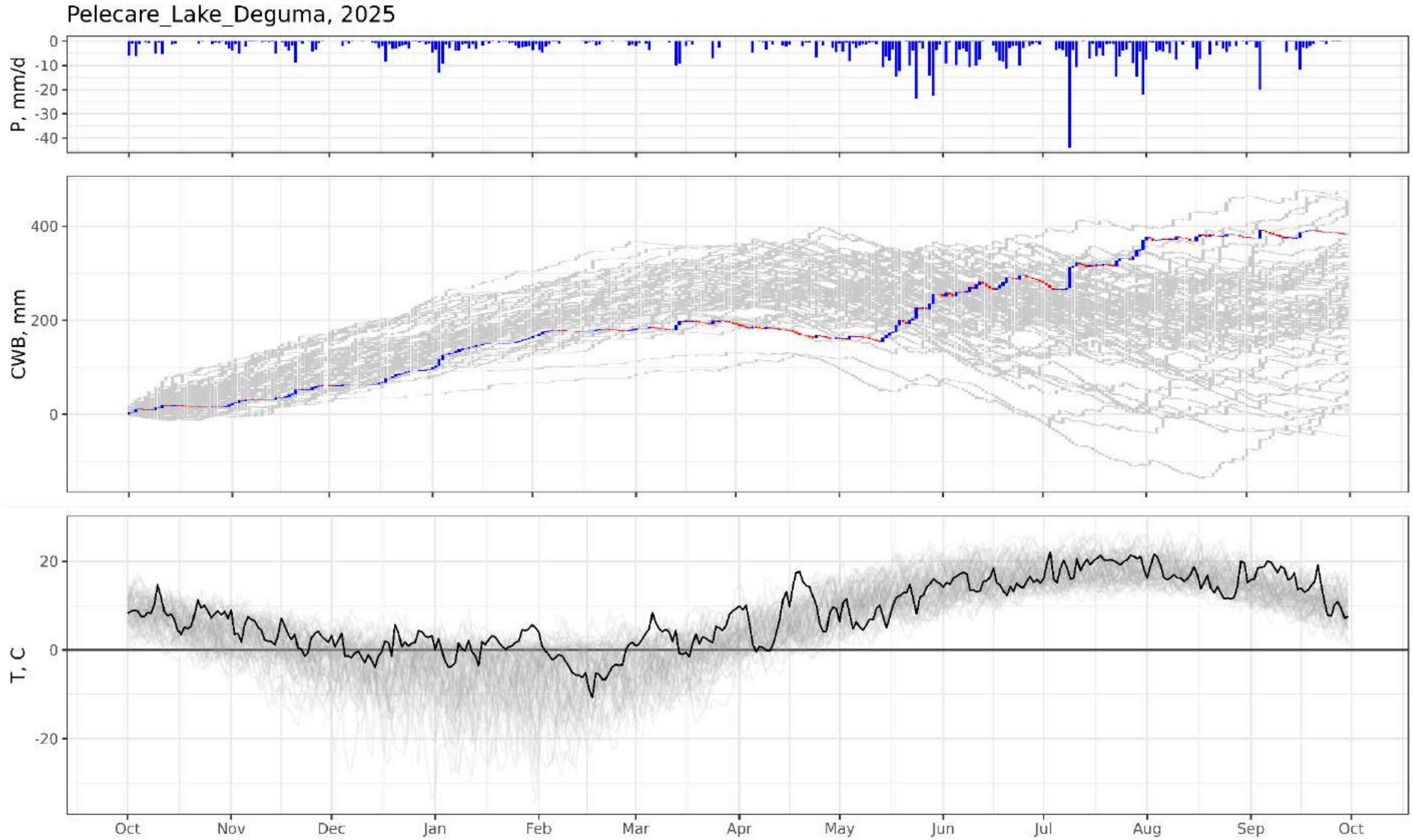

Figure 3.1.2. *Hydrometeorological conditions during 2025 hydrological year starting at October 1, 2024 in the southern part of the Pelecare mire (Lake Deguma), ERA5-land data (Copernicus Climate Change Service 2019), the grey background lines are historical conditions since 1950: P – precipitation, CWB – climatic water balance, T – air temperature*

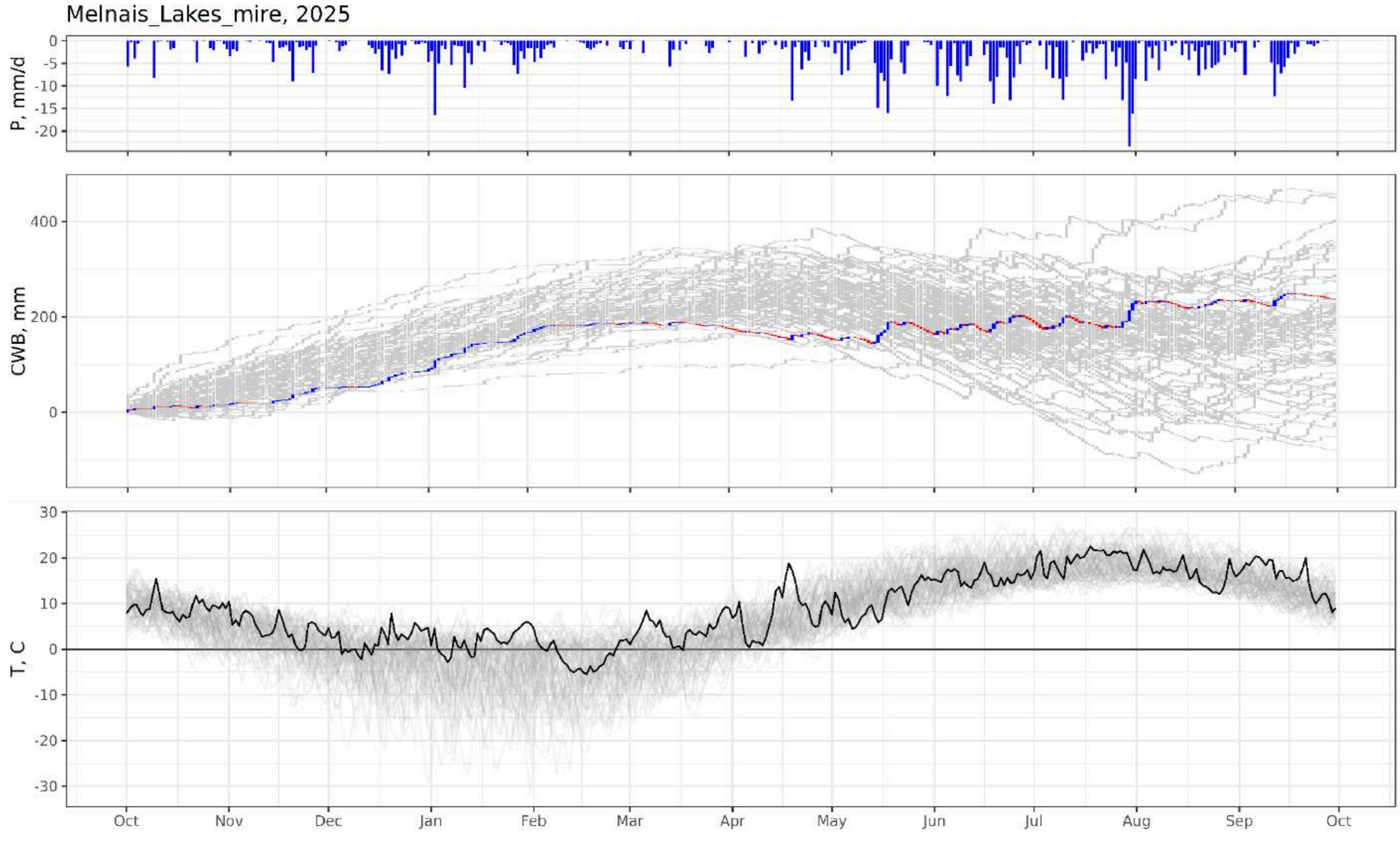

Figure 3.1.3. *Hydrometeorological conditions during 2025 hydrological year starting at October 1, 2024 in the southern part of the Melnais Lajke mire, ERA5-land data (Copernicus Climate Change Service 2019), the grey background lines are historical conditions since 1950: P – precipitation, CWB – climatic water balance, T – air temperature*

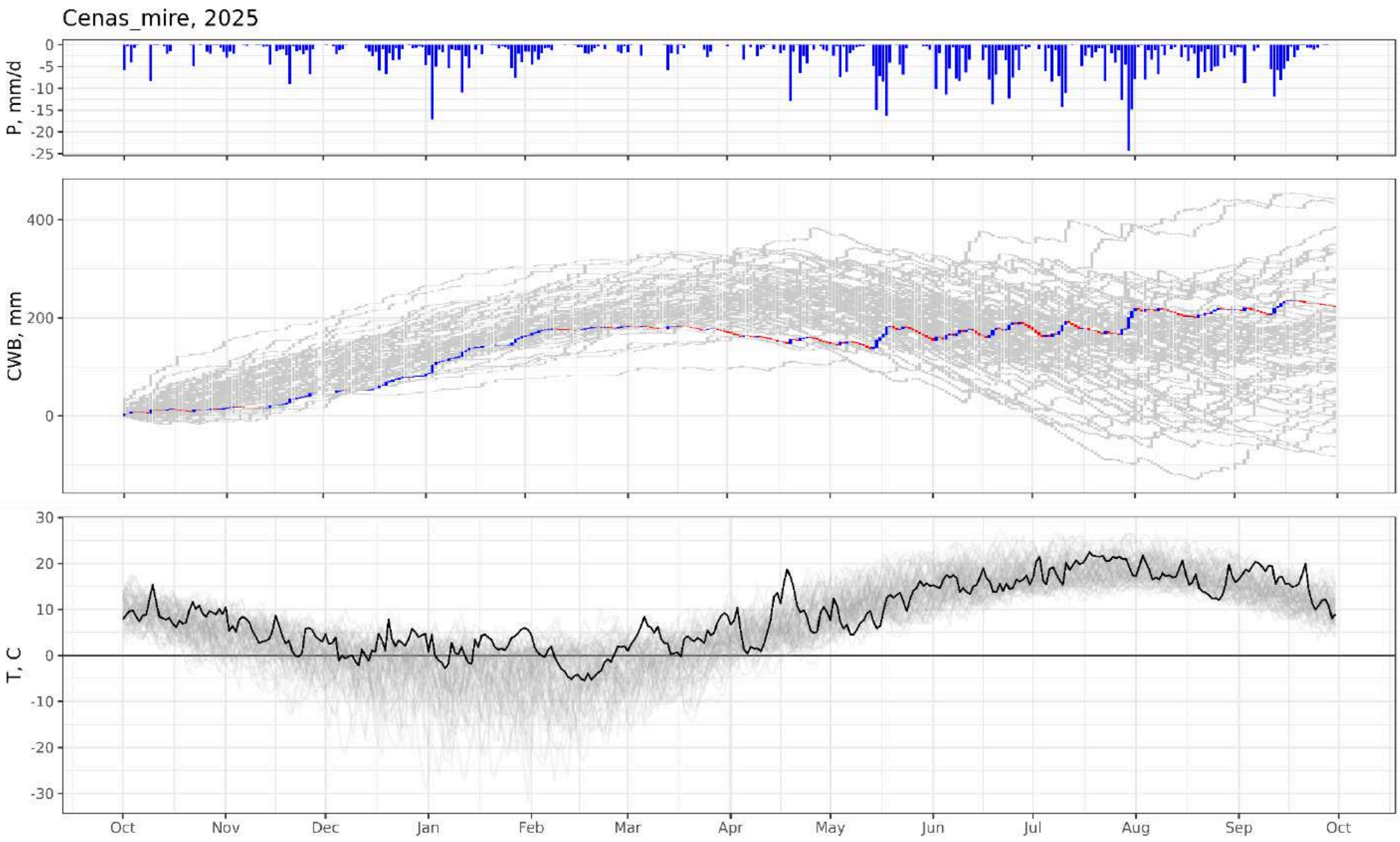

Figure 3.1.4. *Hydrometeorological conditions during 2025 hydrological year starting at October 1, 2024 in the southern part of the Cena mire, ERA5-land data (Copernicus Climate Change Service 2019), the grey background lines are historical conditions since 1950: P – precipitation, CWB – climatic water balance, T – air temperature*

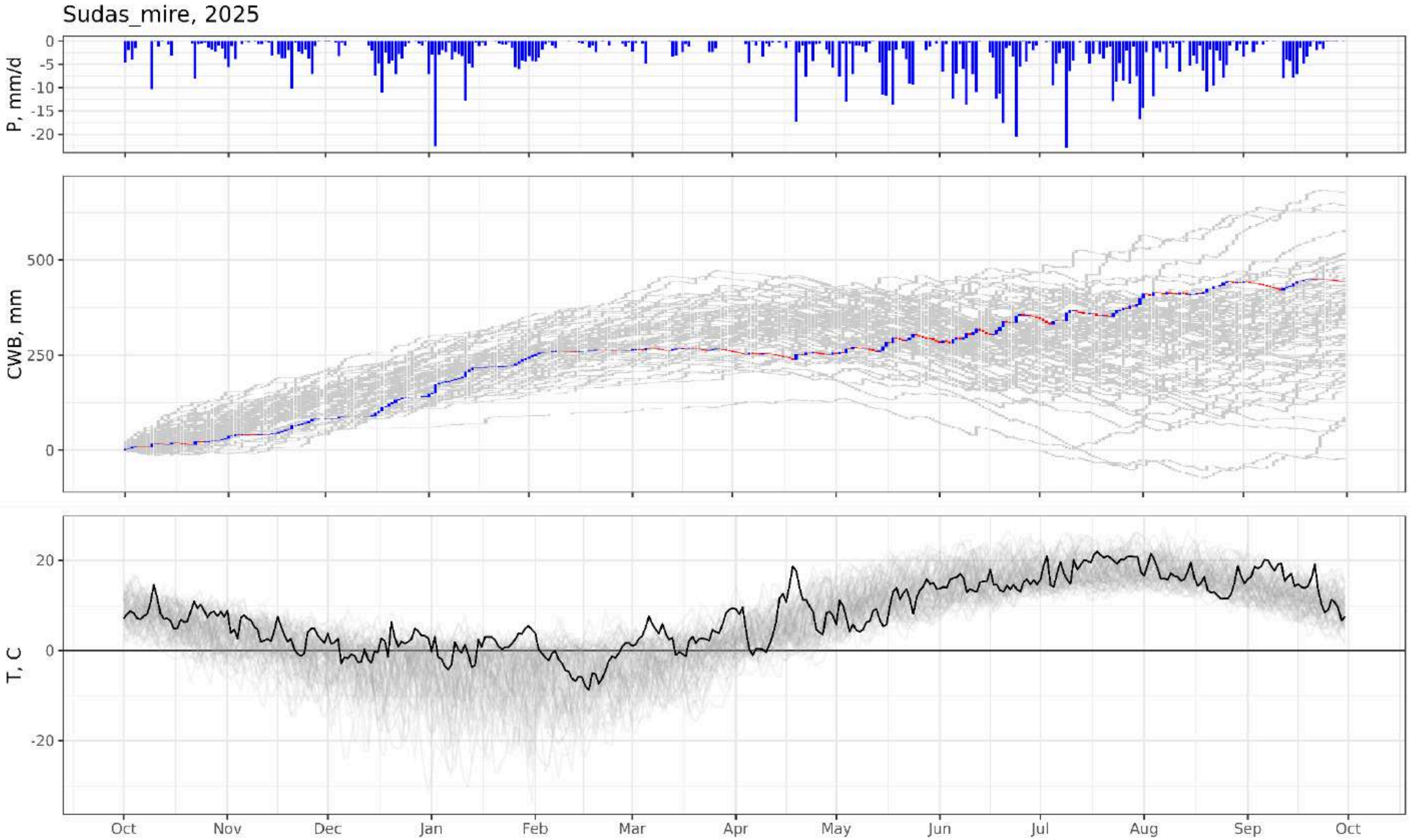

Figure 3.1.5. *Hydrometeorological conditions during 2025 hydrological year starting at October 1, 2024 in the southern part of the Sudas-Zviedru mire, ERA5-land data (Copernicus Climate Change Service 2019), the grey background lines are historical conditions since 1950: P – precipitation, CWB – climatic water balance, T – air temperature*

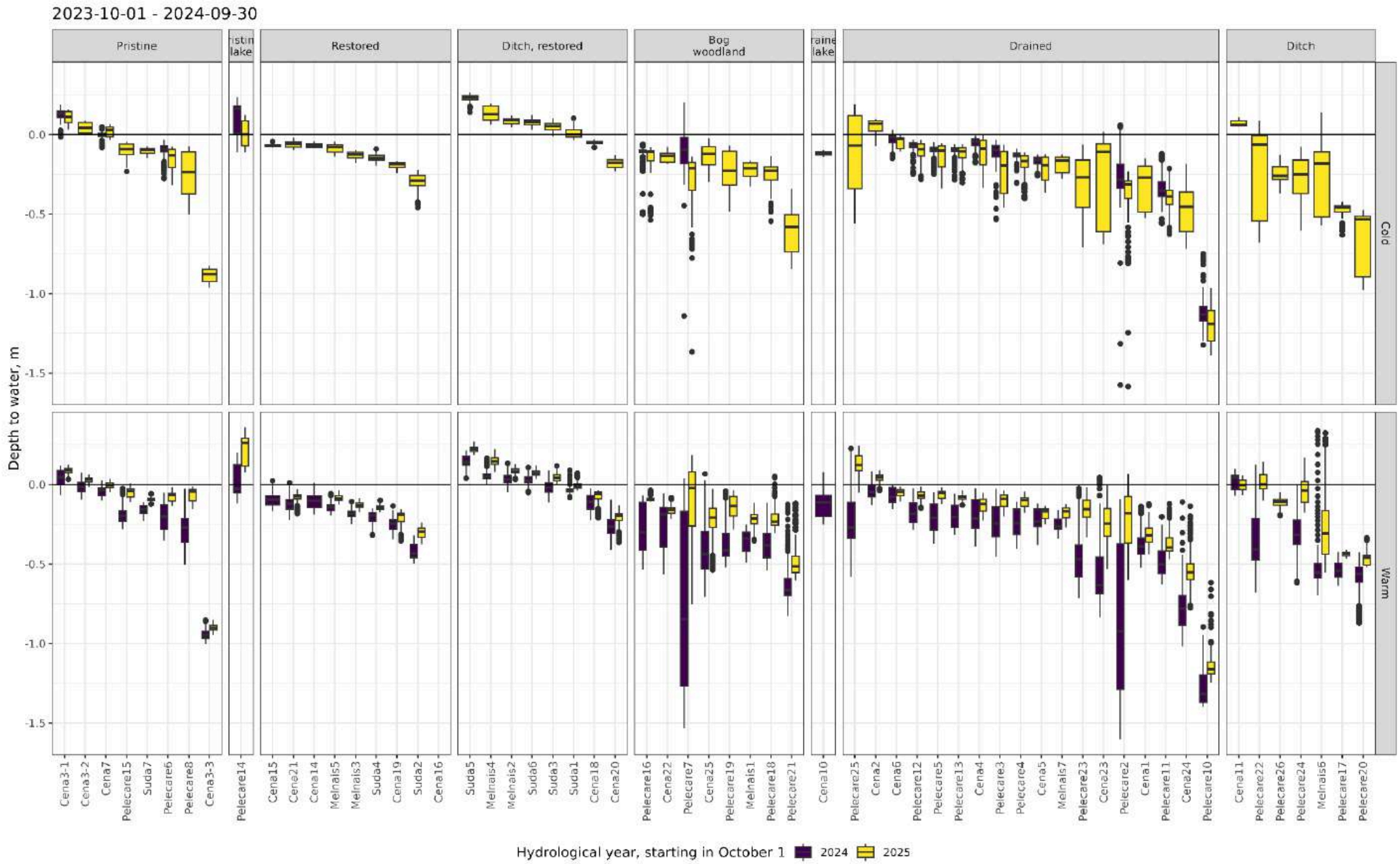

Figure 3.1.6. *Summary of the observed water level distribution during 2024 and 2025 hydrological years from October 1 to September 30*

The unusual hydrometeorological conditions of the 2025 hydrological year are reflected in the observed water level regime as well (**Figure 3.1.6., Table 3.1.1**): at many observations points the warm season (April to September) water table was higher than during the preceding cold season (October 2024 to March 2025) – opposition of usual conditions. Generally the cold season water table was deeper during the 2025 hydrological year than during 2024, and the reverse during the warm season – 2025 saw much wetter conditions than 2024.

Grouping of observation sites by the restoration / degradation status a clear trend is revealed (**Figure 3.1.6**): the highest relative water table is in restored (dammed) ditches followed by pristine and restored wetland sites. These sites have the least water level fluctuations as well. In contrast, degraded wetland sites and bog woodlands generally have deeper groundwater levels and an increasing range of seasonal fluctuations. Drainage ditches or wells near ditches have both on average deepest water level and highest range.

Table 3.1.1. *Summary statistics of the observed water level in 2025 hydrological year from October 1, 2024, to September 31, 2025 in meters: Q10 and Q90 is the 10% and 90% percentile respectively of the hourly water table observations*

ID	*Absolute mean*	*Relative mean*	*Relative min*	*Relative max*	*Relative Q10*	*Relative Q90*	*Full Range*	*Relative range Q90-Q10*
Cena1	10.31	-0.31	-0.53	-0.1	-0.49	-0.18	0.43	0.31
Cena2	11.88	0.05	-0.07	0.1	-0.01	0.09	0.17	0.1
Cena3-1	12.56	0.1	0.03	0.16	0.05	0.15	0.13	0.1
Cena3-2	12.5	0.04	-0.02	0.09	0	0.08	0.11	0.08
Cena3-3	11.71	-0.89	-0.96	-0.82	-0.93	-0.84	0.14	0.09
Cena4	10.42	-0.12	-0.34	0	-0.23	-0.03	0.34	0.2
Cena5	10.69	-0.2	-0.37	-0.12	-0.32	-0.14	0.25	0.18
Cena6	11.32	-0.05	-0.11	0	-0.1	-0.01	0.11	0.09
Cena7	12.63	0.01	-0.05	0.07	-0.03	0.05	0.12	0.08
Cena10	11.07	-0.12	-0.14	-0.1	-0.13	-0.1	0.04	0.03
Cena11	8.82	0.03	-0.07	0.11	-0.03	0.09	0.18	0.12
Cena14	12.33	-0.07	-0.08	-0.04	-0.08	-0.05	0.04	0.03
Cena15	12.23	-0.07	-0.08	-0.04	-0.08	-0.06	0.04	0.02
Cena18	12.06	-0.06	-0.21	-0.03	-0.1	-0.04	0.18	0.06
Cena19	12.04	-0.2	-0.35	-0.15	-0.24	-0.17	0.2	0.07
Cena20	12.74	-0.2	-0.37	-0.13	-0.24	-0.15	0.24	0.09
Cena21	13	-0.07	-0.18	-0.02	-0.1	-0.04	0.16	0.06
Cena22	12.88	-0.15	-0.22	-0.08	-0.18	-0.1	0.14	0.08
Cena23	9.41	-0.26	-0.69	0.02	-0.63	-0.03	0.71	0.60
Cena24	8.6	-0.5	-0.77	-0.14	-0.67	-0.32	0.63	0.35
Cena25	8.5	-0.18	-0.54	-0.02	-0.32	-0.05	0.52	0.27
Melnais1	13.07	-0.22	-0.35	-0.12	-0.29	-0.17	0.23	0.12
Melnais2	13.56	0.08	0.03	0.13	0.06	0.11	0.1	0.05
Melnais3	13.41	-0.13	-0.18	-0.08	-0.16	-0.11	0.1	0.05
Melnais4	13.62	0.14	0.06	0.22	0.08	0.18	0.16	0.1
Melnais5	13.62	-0.09	-0.14	-0.04	-0.12	-0.06	0.1	0.06
Melnais6	12.28	-0.26	-0.57	0.31	-0.54	-0.01	0.88	0.53
Melnais7	13.47	-0.18	-0.28	-0.12	-0.26	-0.13	0.16	0.13
Pelecare1	108.43	-2.14	-3.42	-1.58	-3.09	-1.67	1.84	1.42
Pelecare2	109.16	-0.27	-0.81	0.07	-0.46	-0.05	0.88	0.41

ID	Absolute mean	Relative mean	Relative min	Relative max	Relative Q10	Relative Q90	Full Range	Relative range Q90-Q10
Pelecare3	110.78	-0.17	-0.46	-0.04	-0.4	-0.06	0.42	0.34
Pelecare4	110.81	-0.15	-0.4	-0.04	-0.25	-0.08	0.36	0.17
Pelecare5	111.19	-0.1	-0.34	-0.02	-0.23	-0.04	0.32	0.19
Pelecare6	111.55	-0.12	-0.32	-0.01	-0.23	-0.05	0.31	0.18
Pelecare7	109.43	-0.16	-0.76	0.19	-0.44	0.1	0.95	0.54
Pelecare8	110.57	-0.16	-0.5	-0.01	-0.4	-0.03	0.49	0.37
Pelecare9	98.65	-1.72	-1.9	-1.12	-1.84	-1.58	0.78	0.26
Pelecare10	103.54	-1.17	-1.39	-0.67	-1.34	-1.06	0.72	0.28
Pelecare11	104.74	-0.39	-0.63	-0.13	-0.47	-0.28	0.5	0.19
Pelecare12	105.48	-0.09	-0.28	-0.01	-0.17	-0.04	0.27	0.13
Pelecare13	106	-0.11	-0.3	-0.04	-0.17	-0.07	0.26	0.1
Pelecare14	105.38	0.11	-0.11	0.36	-0.09	0.3	0.47	0.39
Pelecare15	107.16	-0.08	-0.23	0.01	-0.14	-0.02	0.24	0.12
Pelecare16	106.15	-0.14	-0.54	-0.04	-0.2	-0.08	0.5	0.12
Pelecare17	104.76	-0.46	-0.63	-0.41	-0.52	-0.42	0.22	0.1
Pelecare18	102.49	-0.24	-0.54	0.04	-0.31	-0.16	0.58	0.15
Pelecare19	103.41	-0.19	-0.49	-0.04	-0.38	-0.07	0.45	0.31
Pelecare21	106.31	-0.55	-0.85	-0.13	-0.77	-0.41	0.72	0.36
Pelecare22	103.82	-0.1	-0.68	0.14	-0.59	0.07	0.82	0.66
Pelecare23	104.06	-0.24	-0.71	-0.02	-0.51	-0.08	0.69	0.43
Pelecare24	104.17	-0.17	-0.6	0.16	-0.4	0.03	0.76	0.43
Pelecare25	104.34	0	-0.56	0.24	-0.45	0.19	0.8	0.64
Pelecare26	110.49	-0.17	-0.37	-0.04	-0.28	-0.09	0.33	0.19
Suda1	117.53	0	-0.04	0.1	-0.03	0.04	0.14	0.07
Suda2	116.35	-0.3	-0.46	-0.23	-0.36	-0.25	0.23	0.11
Suda3	116.49	0.05	-0.01	0.11	0.01	0.08	0.12	0.07
Suda4	116.72	-0.15	-0.2	-0.09	-0.17	-0.12	0.11	0.05
Suda5	117.09	0.22	0.14	0.27	0.19	0.25	0.13	0.06
Suda6	117.22	0.08	0.03	0.13	0.05	0.1	0.1	0.05
Suda7	117.41	-0.1	-0.15	-0.06	-0.12	-0.08	0.09	0.04

Quality Assessment of Water Level Observations

The quality of the hydrological monitoring was assessed by validating the automatic groundwater level measurements by comparing to manual readings (**Figure 3.1.7**). Overall, the quality of the monitoring can be considered as satisfactory – 95% of the readings were within 5.6 cm while 75% within 3.2 cm, that is close to combined uncertainty of automatic and manual measurements. The exception is one reading at well Cena23, where the difference is more than 15 cm. The manual measurement was taken during a episode of rapid groundwater level rise, explaining the discrepancy between manual and automatic measurements. Similar sudden groundwater level increase has been observed in other wells (e.g. Pelecare2, Pelecare7) in the marginal zones of the mires.

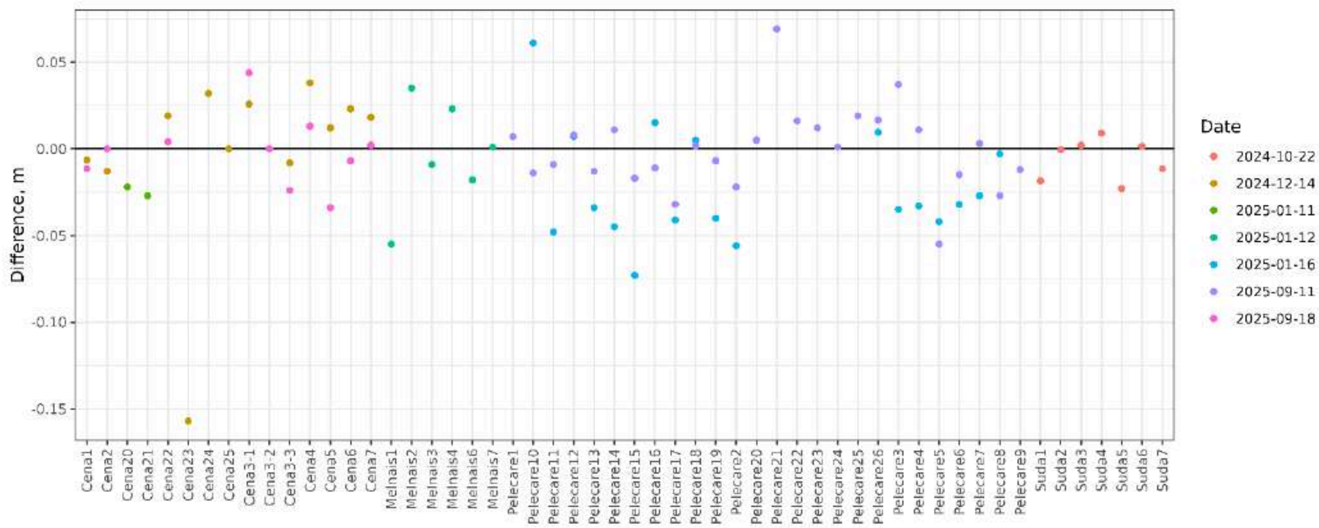

Figure 3.1.7. *The difference between automatic and manual water level measured in most observation points is 0.05 m or less, indicating overall good measurement quality.*

3.1.1. Cenas Mire

The latest data download for groundwater level probes took place on September 17 and October 30, 2025. The summary statistics is provided in **Table 3.1.1,** and the time series are described in **Figure 3.1.2**. The observations at 22 wells are grouped in 6 stations:

1. 2006 restoration - Lake Skaista
2. 2006 restoration - drainage area
3. Bog woodland, restoration area No. 4
4. Mire lake dam, restoration area No. 2
5. Peat extraction area, restoration area No. 1
6. Profile from degraded to pristine raised bog

Figure 3.1.2 *Description of hydrological monitoring results in Cena mire for 2025 hydrological year*

Observations	Location and description
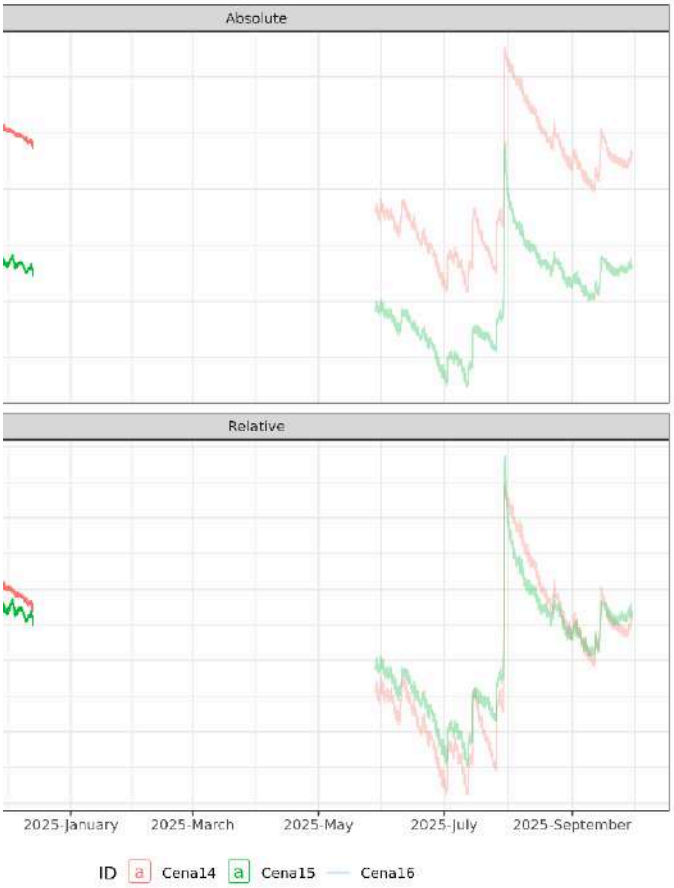	**2006 restoration - Lake Skaista** 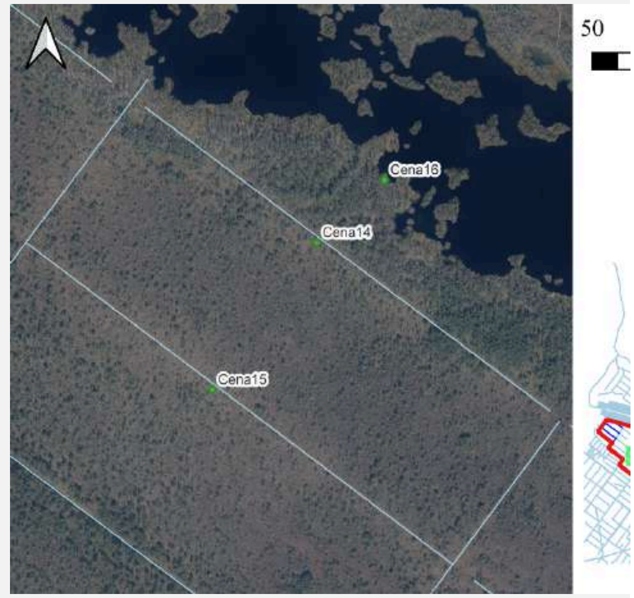 No new data in 2025

Observations

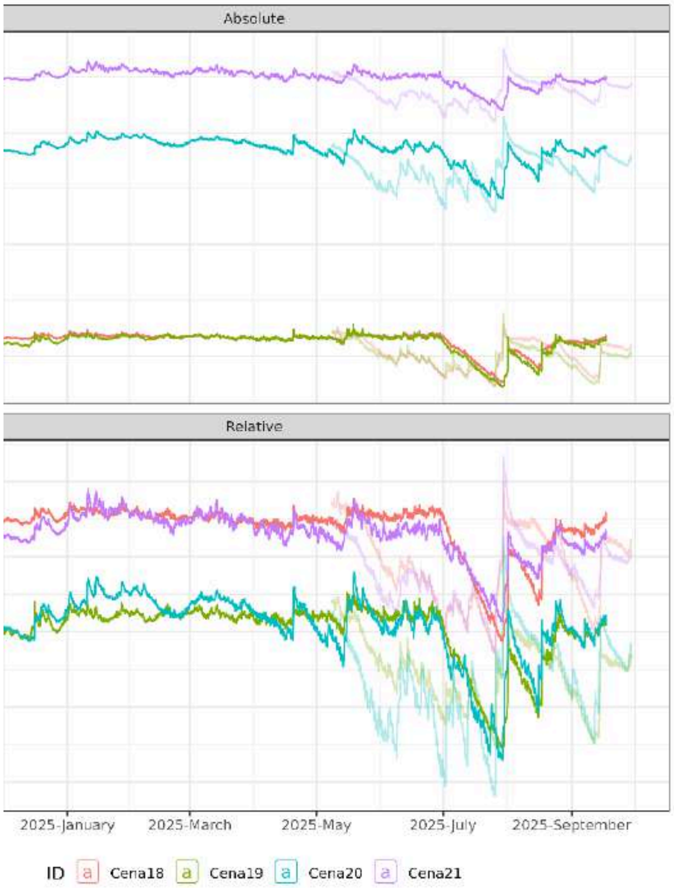

Location and description

2006 restoration - drainage area

In the historical restoration area, a slight warm-season water table decrease is observed only in July, resulting in a water table fluctuation range 0.16 to 0.24 m. This is slightly higher than in the relatively pristine locations like Cena3-1 or Cena7 but less than drainage or marginal forested locations like Cena4, Cena23 or Cena25.

Observations	*Location and description*
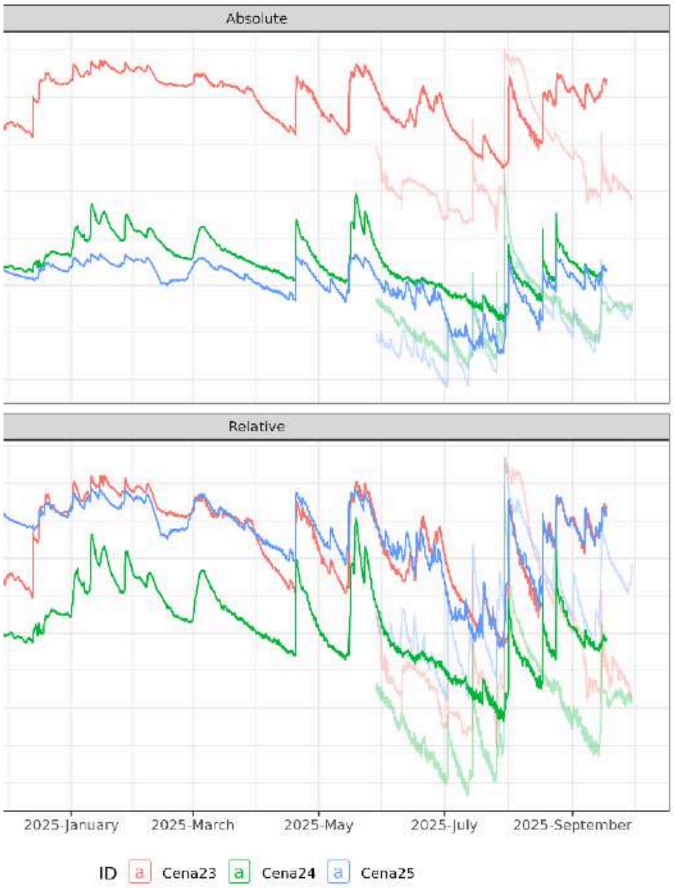	**Bog woodland (restoration area No. 4)** 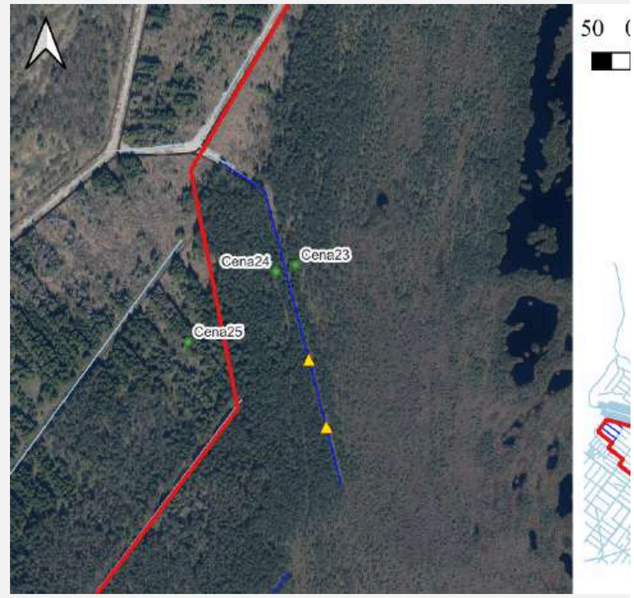 Relatively strong fluctuations (range 0.52 to 0.71 m) of the water level are observed at these wells near drainage ditch and wet forests at the marginal zone of Cena mire. The drainage ditch effectively intercepts the filtration flow from the mire, resulting in 0.79 m over mean water table at distal setting. Rapid water level fluctuations reflect the precipitation events and strong influence of the established drainage system.

Observations	*Location and description*
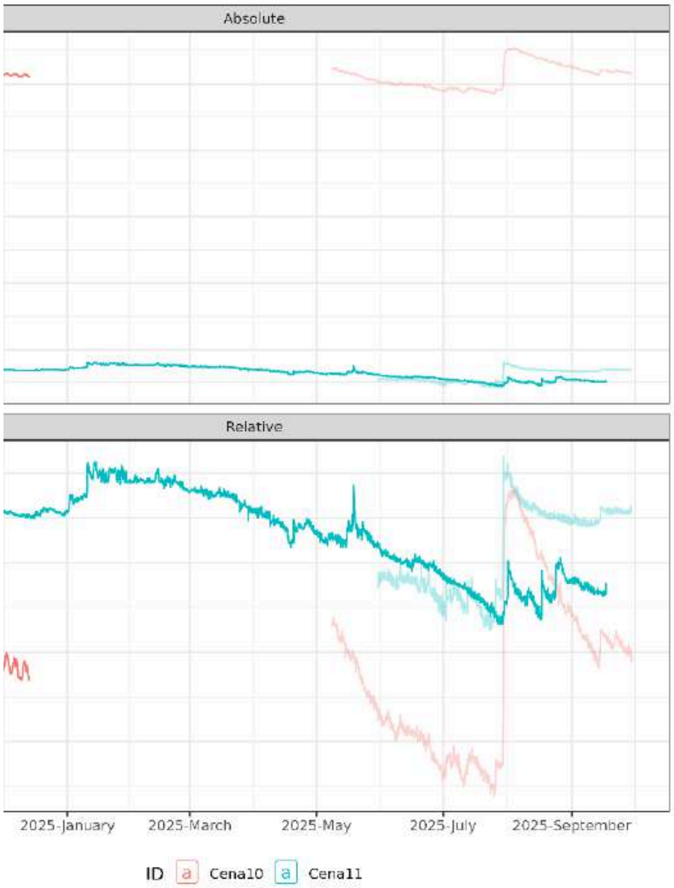	**Mire lake dam, restoration area No. 2** 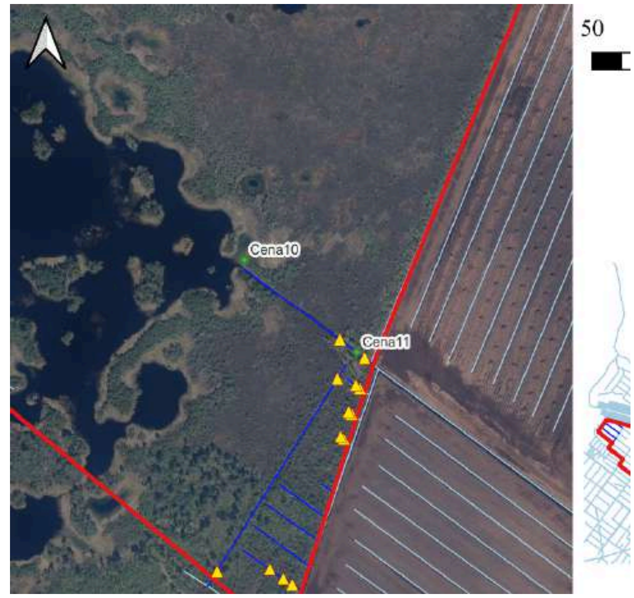 Unfortunately, the water level probe installed at partly drained mire lake (Cena10) malfunctioned, resulting in data loss for the most part of reporting period. Water level in drainage ditch sharply rose in early January 2025 associated with strong precipitation events and periodically freezing temperatures, flowed by gradual decline in contrast to other, pristine, locations, demonstrating strong drainage effect of the ditch network.

Observations	Location and description

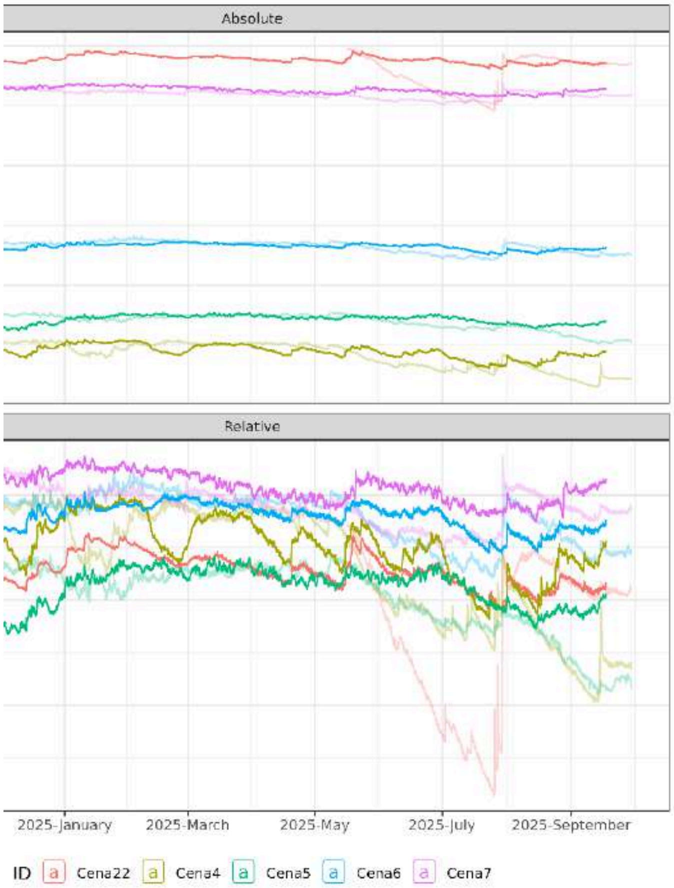

Peat extraction area, restoration area No. 1

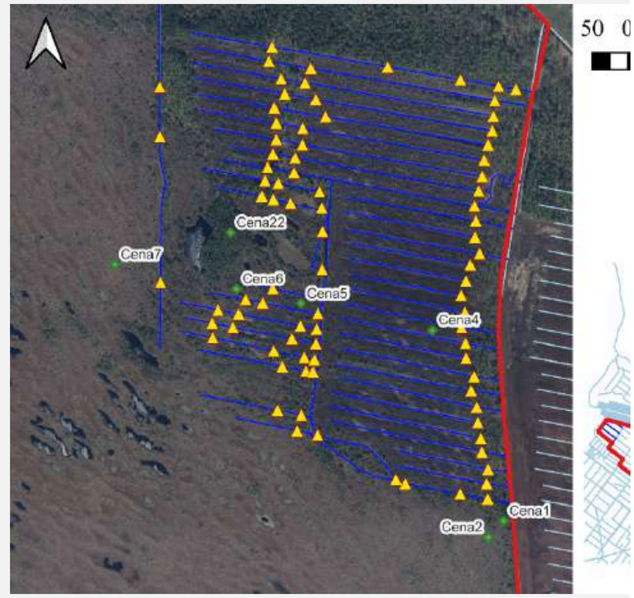

The deepest water tables are observed in the early part of the observation period, reflecting the legacy of summer 2024, but during the rest of the hydrological year were relatively high and stable due to excessive precipitation. Highest fluctuations (range 0.34m) are observed in Cena4, that is proximal to the main contouring drainage ditch. The next is Cena22 (range 0.14 m) located in a densely forested section of the mire – in contrast to 2024 no significant summer water table decline was noticed at this location.

Observations	***Location and description***
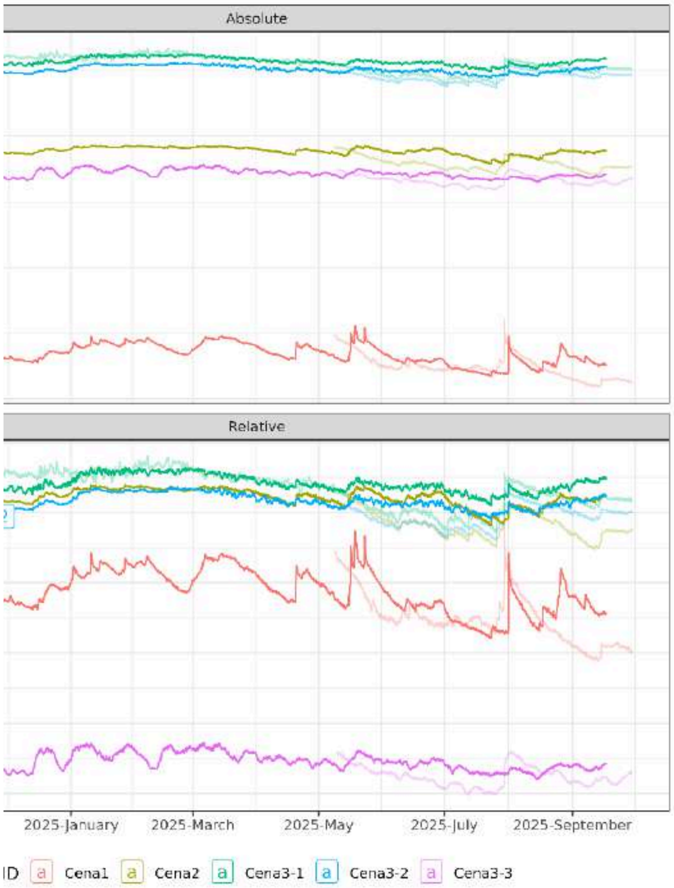	**Profile from degraded to pristine raised bog** 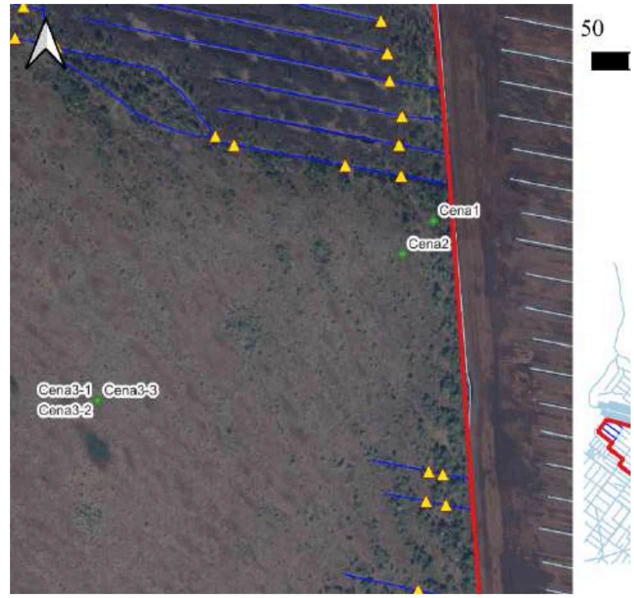 Well near the deep contouring ditch (Cena1) shows characteristic water level decline during the summer as well as strong fluctuations with range exceeding 0.3 m, reflecting intense precipitation events, demonstrating impact of the ditch. In wells more distant from the ditch (Cena2, Cena3-1) water level is remarkably stable, the fluctuations range 0.17 and 0.13 m respectively. At the pristine site the water pressure in at the base of peat layer (4.34-5.34 m depth, Cena3-3) remains 0.89 m below surface, but still 1.4 m higher than near the contour ditch at well Cena1.

Automatic water level observation probes in Cena Mire were installed on June 8 and the latest data download took place on November 11, 2023. Along with data download, manual groundwater level measurements took place using acoustic water level probes. The manual measurements are used to control the validity of automatic measurements. Water quality parameters were not measured during the reporting period.

Assessment of Water Level Observation Quality

In Cena Mire, good agreement was found between manual and automatic water level measurements (**Figure 3.1.8**). Differences in most cases are less than 5 cm, which overall corresponds to the uncertainty sum of manual and automatic measurements. The exception is the monitoring well No. Cena23, where in one case the difference is more than 15 cm. Reasons for the deviance and any corrective measures need to be established during future monitoring.

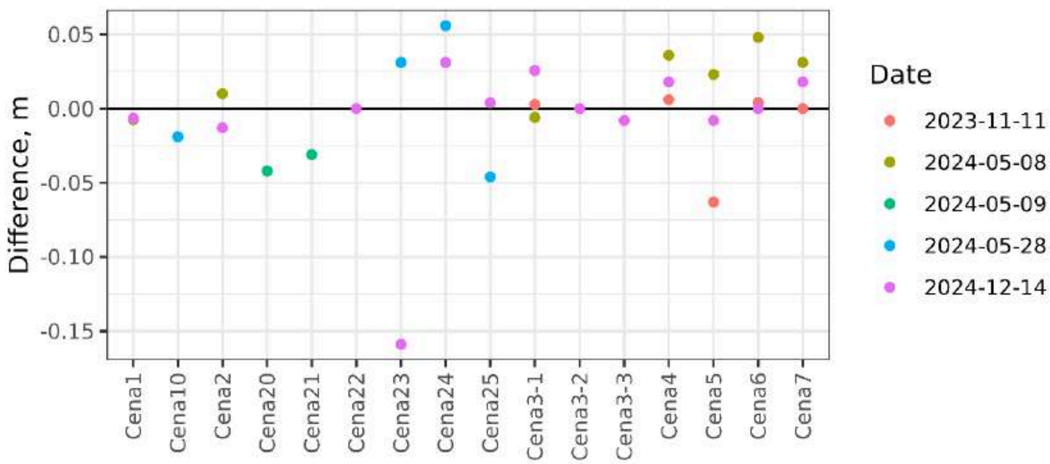

Figure 3.1.8. *The difference between automatic and manual water level measured in most observation points is 0.05 m or less, indicating overall good measurement quality.*

Results of the groundwater level monitoring

In Cena Mire 6 groups of water table measurements are distinguished:

7. 2006 restoration - Lake Skaista (Wells No. Cena14, Cena15)
8. 2006 restoration - drainage area – 2 (Wells No. Cena20, Cena21)
9. Bog woodland (Wells No. Cena23, Cena24, Cena25)
10. Mire lake dam (Wells No. Cena10, Cena11)
11. Peat extraction area (Wells No. Cena22, Cena4, Cena5, Cena6, Cena7)
12. Profile from degraded to pristine raised bog (Wells No. Cena1, Cena2, Cena3-1, Cena3-2, Cena3-3)

The water level probes at the 2006 restoration site near Lake Skaista (Wells No. Cena14, Cena15) were installed May 27, 2024, the data were downloaded in early 2025, however the analysis is limited to hydrological year up to September 30, 2024. We see that the water level range at both sites was about 20 cm with peak corresponding to July 29, when extreme precipitation occurred (**Figure 3.1.9**). Noticeably, during the summer water table decline was faster in well Cena14, that is higher on the bog dome than in Cena15, that is located further downstream in part of the bog with higher remaining tree cover. The reason for this difference remains to be investigated once a longer data time series is accumulated.

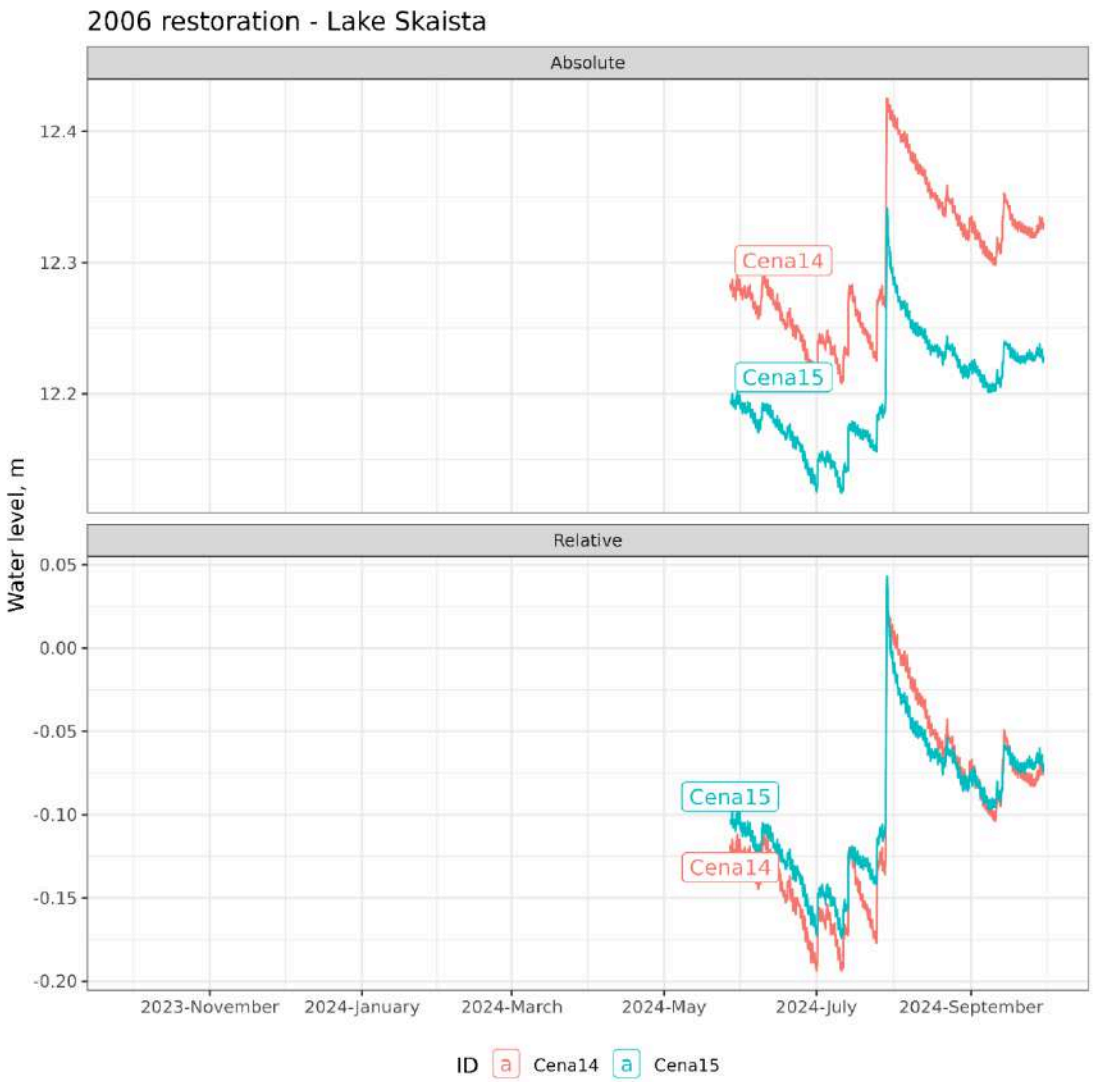

Figure 3.1.9. *Water level dynamics in a small, blocked ditch (well Cena15) and in between two small ditches (well Cena14) in a drained mire section restored in 2006.*

Table 3.1.3. *Water level monitoring data summary for Cena Mire*

Well ID	***Mean relative water table, m***	***Min relative water table, m***	***Max relative water table, m***	***Mean absolute water table, m***	***Range of the daily mean, m***
Cena1	-0.38	-0.52	-0.16	10.24	0.36
Cena10	-0.12	-0.25	0.08	11.06	0.33
*Cena11**	0.01	-0.07	0.1	8.8	0.17
*Cena14**	-0.1	-0.19	0.02	12.3	0.21
*Cena15**	-0.1	-0.17	0.02	12.2	0.19
Cena2	-0.04	-0.13	0.08	11.79	0.21
*Cena20**	-0.27	-0.41	-0.1	12.67	0.31
*Cena21**	-0.12	-0.22	0.01	12.95	0.23

*Cena22**	-0.26	-0.56	-0.06	12.77	0.5
*Cena23**	-0.55	-0.83	0.05	11.94	0.88
*Cena24**	-0.77	-1.02	-0.16	8.33	0.86
*Cena25**	-0.4	-0.72	0.06	8.28	0.78
Cena3-1	0.08	-0.06	0.19	12.55	0.25
*Cena3-2**	-0.01	-0.09	0.07	12.45	0.16
*Cena3-3**	-0.94	-1	-0.86	11.66	0.14
Cena4	-0.13	-0.39	-0.01	10.42	0.38
Cena5	-0.2	-0.38	-0.12	10.69	0.26
Cena6	-0.05	-0.15	0.03	11.32	0.18
Cena7	-0.02	-0.1	0.05	12.6	0.15

* incomplete time series, starting from May 2024

Figure 3.1.10 *Installation of the groundwater level probe in Cena21 well in a 2006 restoration site with a dense network of drainage ditches, May 7, 2024. Image: © A. Kalvāns*

Figure 3.1.11*. Installation of the water level monitoring well Cena4 in the degraded part of the Cena Mire, PeatCarbon restoration site, June 8, 2023. Image: © A. Kalvāns*

In the 2006 restoration site with a dense network of drainage ditches, data from two observation wells are available – one placed directly in the blocked ditch (Cena20) and the other in between ditches (**Figure 3.1.10**). Here the pattern of water level fluctuations is very similar (**Figure 3.1.11**), but the ditch has a slightly smaller range of the water level (23 cm in comparison to 31 cm, **Table 3.1.3**) This indicates that the restoration measures are effectively keeping the water in the bog.

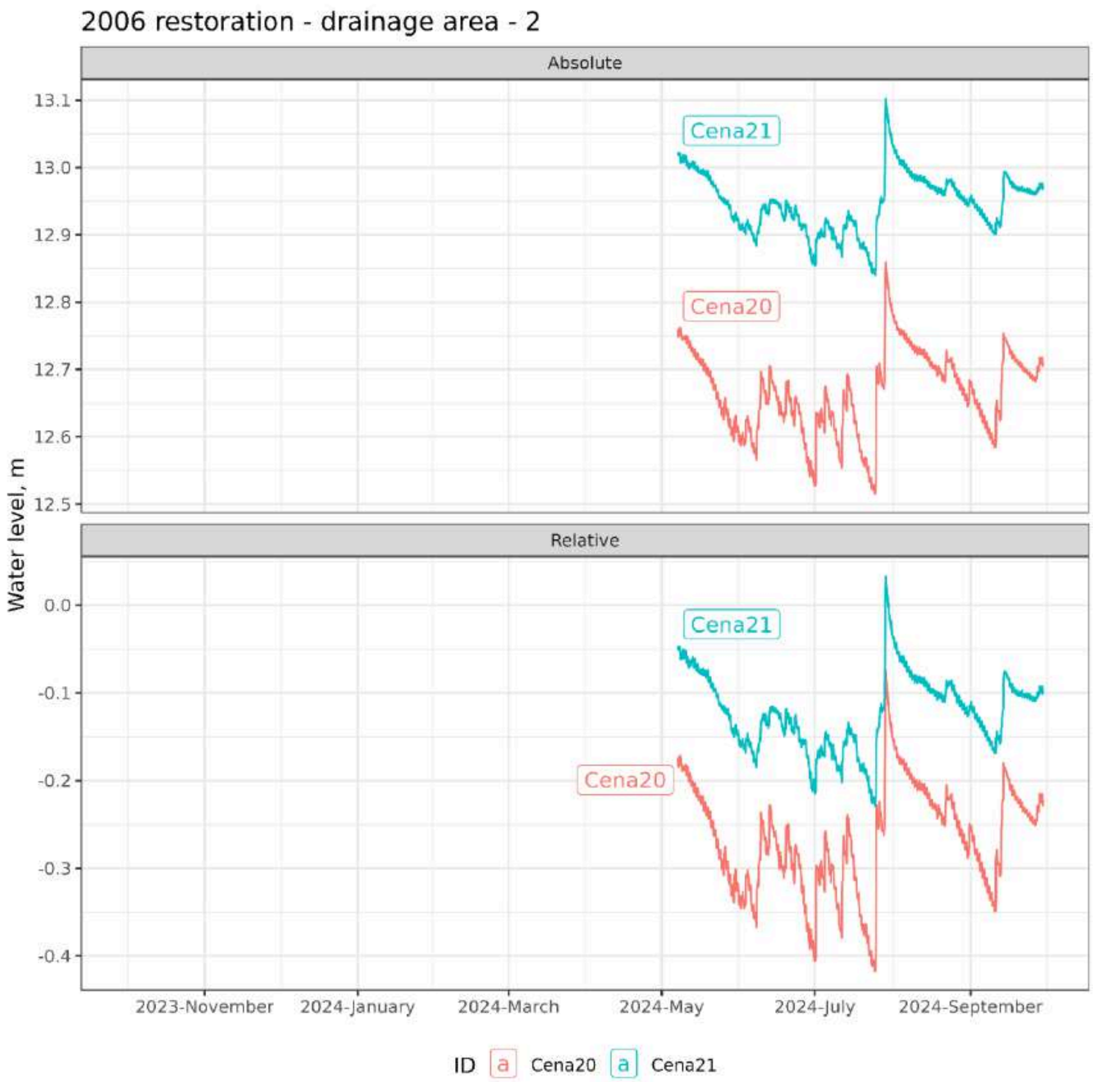

Figure 3.1.12. *Water level dynamics in observation sites near Lake Skaista where mire hydrological regime was restored in 2006.*

At the site that was prepared for peat extraction (wells No Cena4 to Cena7 and Cean22, **Figure 3.1.12**, **Figure 3.1.13**) we see a clear trend in increasing depth and range of the water table towards the main drainage ditches. However, we notice that the yearly water table range in some of these wells (Table 3.1.1) was less than in the pristine raised bog site Cena3-1. This seems to be due to deep water pooling in the pristine part of the bog during the winter, which seems to result from interaction between snow, ice and bog microtopography. It appears that in the site affected by drainage, during the autumn-winter-spring seasons the surface water is effectively drained by remaining drainage capacity of existing dens ditch network. However, during the warm season the drainage of the soil water is limited by the natural clogging of the ditches.

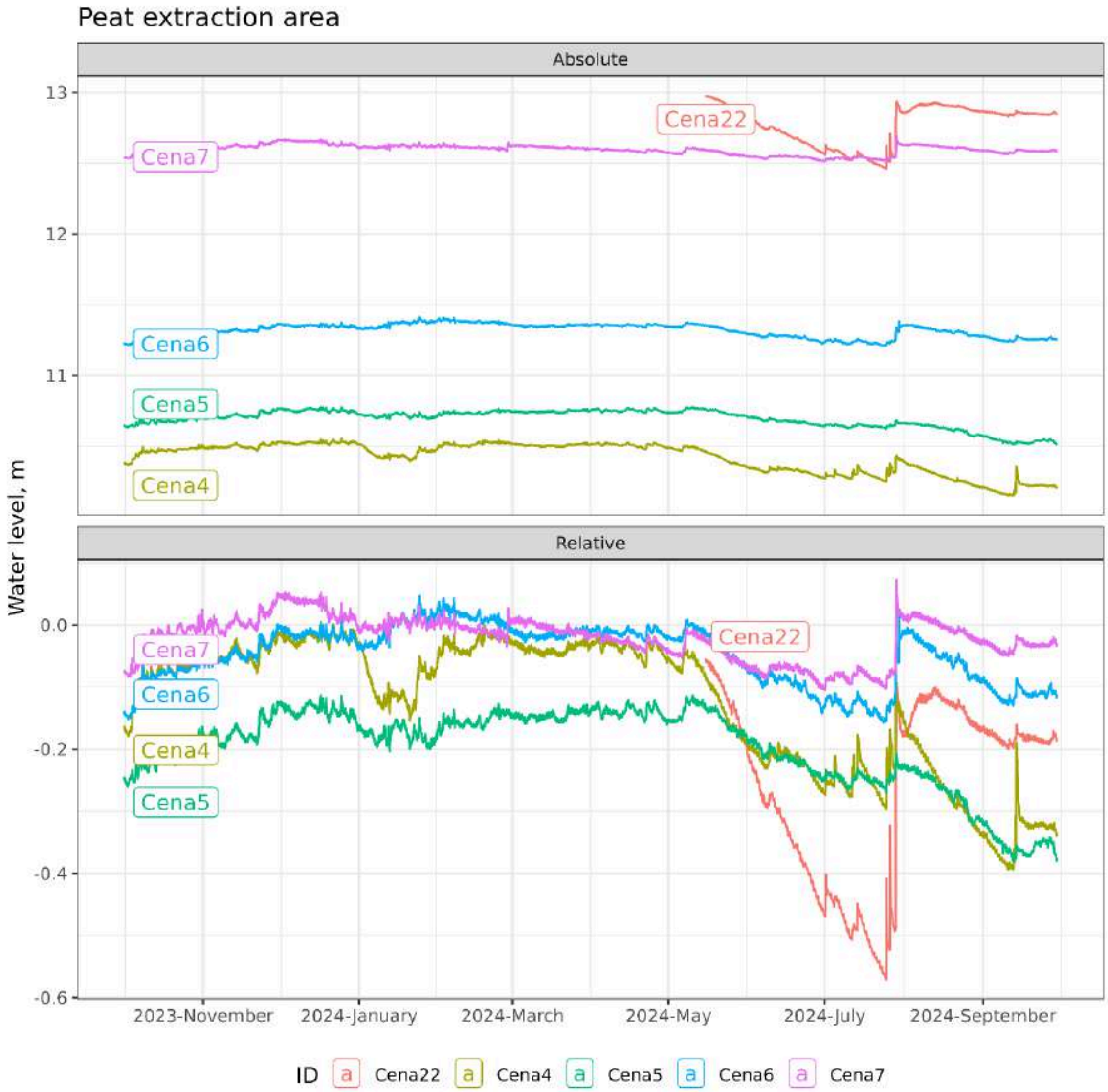

Figure 3.1.13. *Water level dynamics in observation sites in a drained bog with dens network of drainage ditches (planed restoration area No 1 "Kūdras lauks (Atpūtas)"), forming a gradient from heavily degraded bog with bare peat surface (Cena4) to largely intact mire (Cena7); well, Cena22 is at location within a patch of dense young pine tree stand.*

Figure 3.1.14. *Water level monitoring wells Cena3-1, Cena3-2 and Cena3-3 in relatively undisturbed part of the Cenas Mire, Jun 8, 2023*

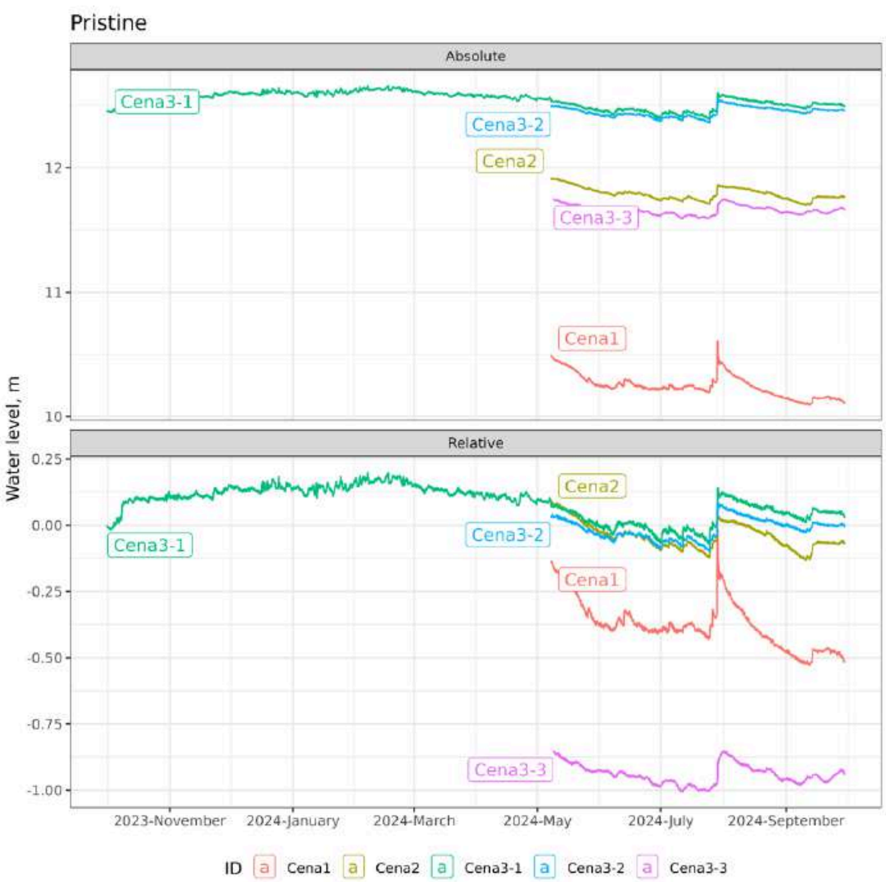

Figure 3.1.15. *Absolute (top) and relative (bottom) water level time series in radial profile at the Cena mire for hydrological year from October 1, 2023, to September 30, 2024.*

At the observation profile (**Figure 3.1.14**) from a drained bog margin to largely pristine raised bog we notice that the water level fluctuation range is least further away from the drainage system (Well3-1, **Figure 3.1.15**) however the measurements cannot be directly compared as the only Cena3-1 cover the full hydrological year from October 1, 2023, to September 31, 2024. However, we do notice that the range and average depths at wells affected by drainage (Cena1 and Cena2) is greater than for those deeper in the pristine raised bog. In addition, we notice that in the well Cena3-3, that penetrates the 5 m peat layer, the water table is about 1 m below the surface, demonstrating that there is downwards filtration of the water from peat into sandy mineral subsoil. Thus, the sand layer at the base of the bog keeps draining water from it and thus drainage systems penetrating this layer in the surrounding nature conservation area do affect the water balance deep within the bog.

Discharge measurements

The water discharge (runoff) monitoring in Cena Mire was planned in the hydrological regime restoration area No. 1 (Kūdras lauks (Atpūtas)), at observation point Cena8. Upon inspecting the installed observation point in the autumn of 2023, it was discovered that the constructed spillway had become clogged with eroded peat (Figure 3.1.9.), rendering the measurement results unusable. It is planned to relocate the discharge monitoring point to a ditch where the accumulation of such peat erosion material is not anticipated in a restoration area No.2 “Akača dambis”.

Figure 3.1.16. *A discharge measurement spillway (monitoring point Cena8) clogged with eroded peat, November 10, 2023. Image: © A. Kalvāns*

3.1.2. Lielais Pelečāre Mire

Latest data download for groundwater level probes took place during September 2025. The summary statistics is provided in **Table 3.1.1,** and the time series are described in **Table 3.1.4**. The data from the meteorological station installed in the Lielais Pelecare mire is presented in **Figure 3.1.17**, providing a reliable source for air temperature. However, the precipitation data, during freezing temperatures need to be considered with caution, as the probe is not well equipped for measuring snowfall. The observations at 26 wells are grouped in 9 stations, where some of the wells are included in several of the stations:

1. Azara grovs – a ditch draining Lake Deguma
2. Drained wetland forest with sparse tree cover
3. Drained wetland forest with moderate tree cover
4. Deigļu bog: gradient from mineral soil to drained bog
5. Deigļu bog: gradient from marginal setting to relatively pristine bog
6. Lake Deguma
7. Malnupeite marginal bog woodland
8. Malnupeite drained bog
9. River Malnupeite, longitudinal section

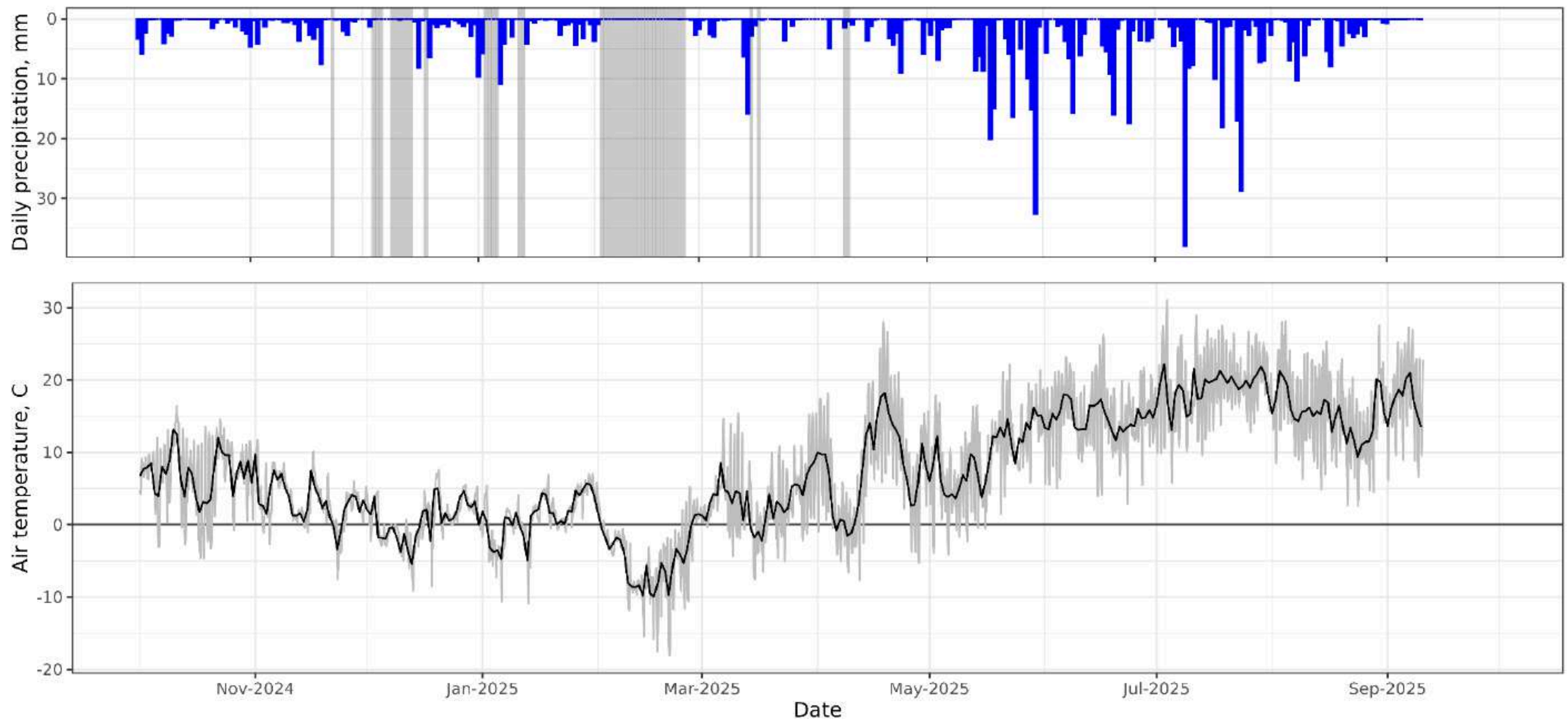

Figure 3.1.17. *Daily precipitation and air temperature in Lielais Pelečāre Mire, open raised bog site (Pelecare_a3_atklats_purvs), the grey bands in the topmost image represent days with expected snow as dominant form of precipitation (T < -1°C)*

Figure 3.1.4. *Description of hydrological monitoring results in Lielais Pelecare mire for 2025 hydrological year*

Observations	***Description***

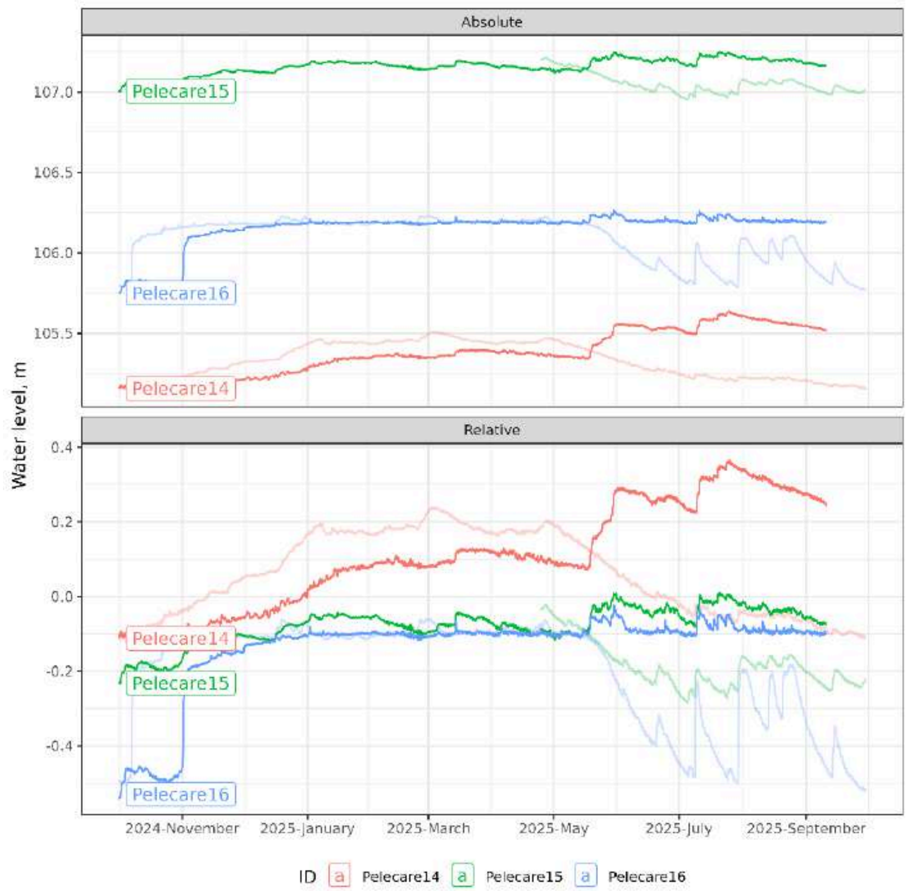

Lake Deguma

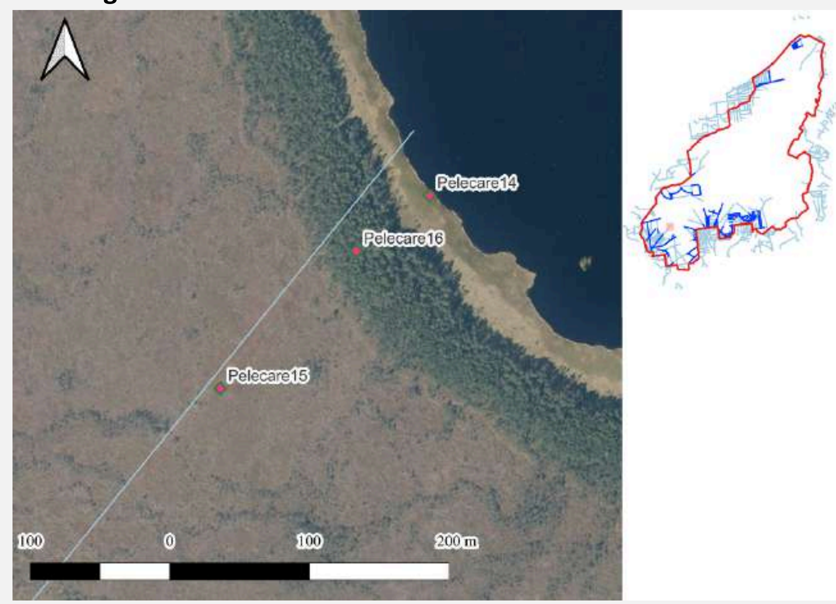

The water tables climb up to January 2025 and remain static up to mid-May downpours, when the lake level (Pelecare14) continues to rise to reach its maximum at late July almost 0.5 higher than in the beginning of the hydrological year. In contrast the wetland forest (Pelecare16) and open bog (Pelecare15) maintain stable levels indicating the local threshold for unrestricted surface runoff. Another interesting feature is the sudden groundwater rise by 0.28 m during 4-day period in forest rim around the Lake Deguma (Pelecare16) in early November 2024 – similar feature were observed in 2023 and in other, wetland marginal, settings (wells Pelecare7, Pelecare2).

Observations	*Description*
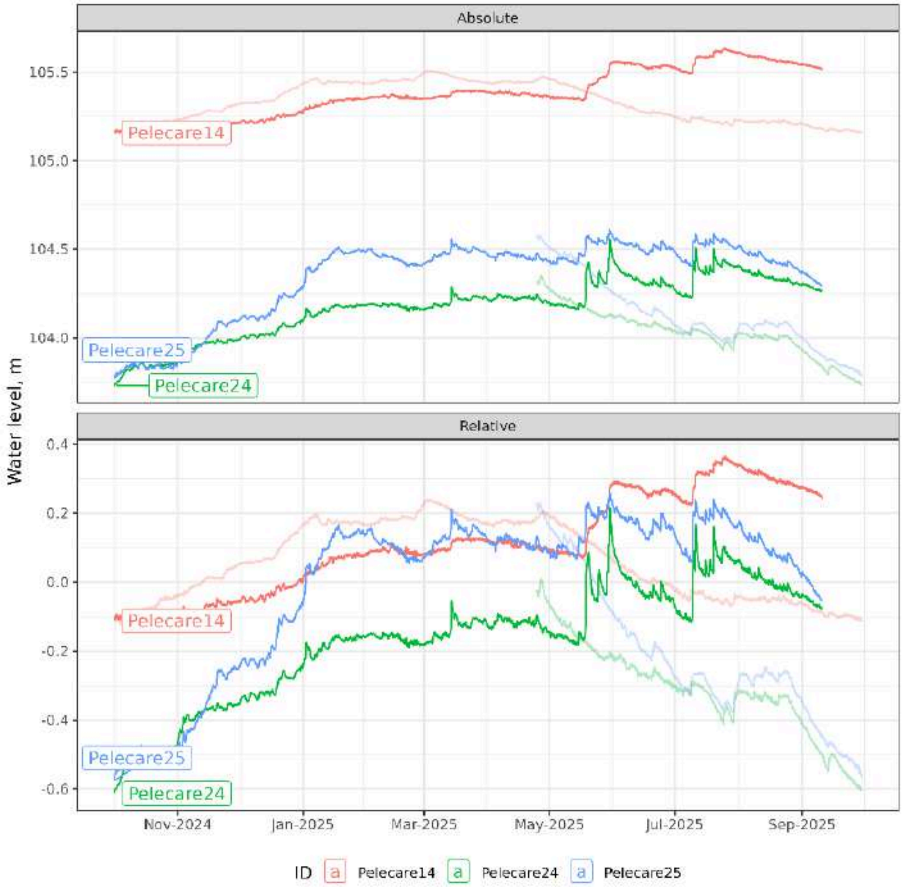	**Azara grovs – a ditch draining Lake Deguma** 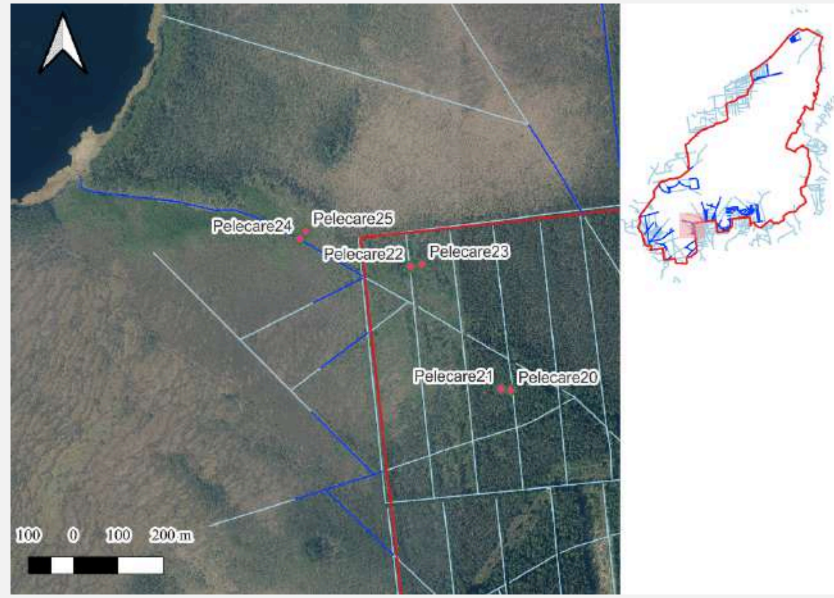 The water table rises during the fall 2024, reaching stability in January 2025. In later part of 2024 hydrological year (shaded curves) and early 2025 hydrological year (solid curves) the water table in both wells – ditch (Pelecare24) and in forest regrows after a fire (Pelecare25) are similar suggesting that it is controlled by soil water processes at both sites – root water uptake and precipitation in filtration, and there is no runoff in the ditch. Starting from December 2025 the water levels diverge – regrowth location water level is higher. However, during distinct precipitation events in May and July 2025 the water level in the ditch is almost as in the bank location suggesting local flooding.

Observations	*Description*
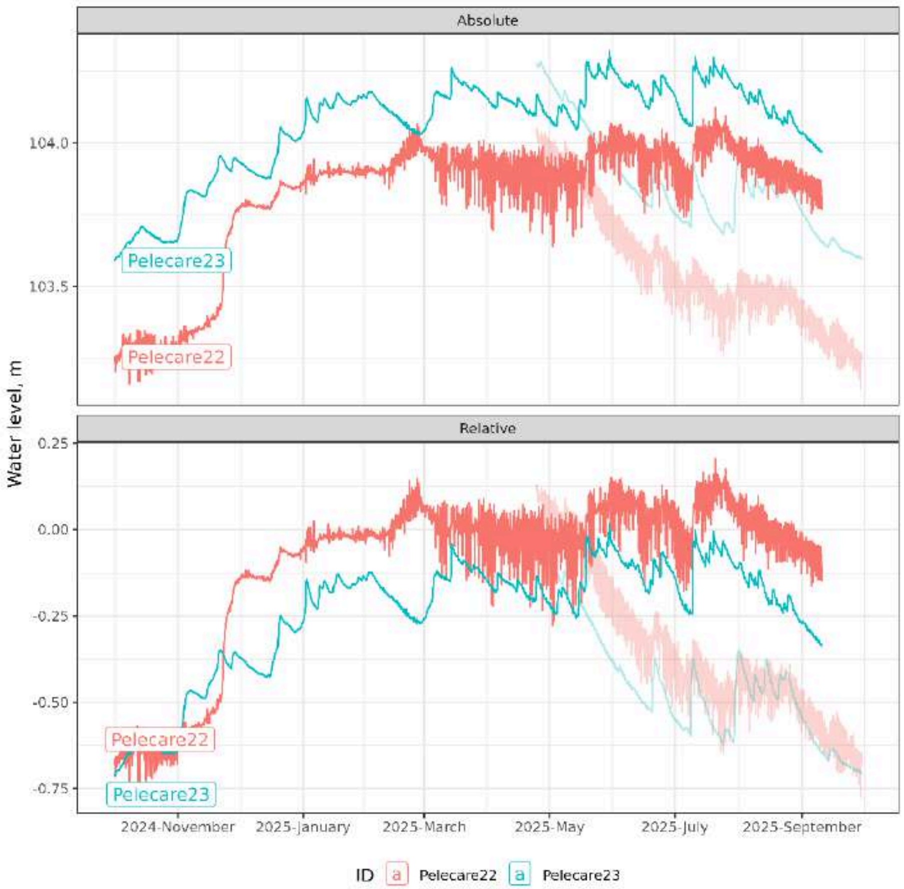	**Drained wetland forest with sparse tree cover** The water level in the forest section (Pelecare23) is about 0.24 m higher than in the ditch (Pelecare22). The phase of fluctuations matches at both locations except one case in late-February 2025 – a prolonged cold spell, thus the discrepancy is likely due to freezing-induced variations of water pressure – either water suction to freezing front in soil resulting in decrease of pressure at Pelecare23 or ice-blocking of well in Peleacre22. There are extreme daily fluctuations in the Pelecare22, that appears to be an artefact rather than genuine hydrological signal.

Observations	*Description*
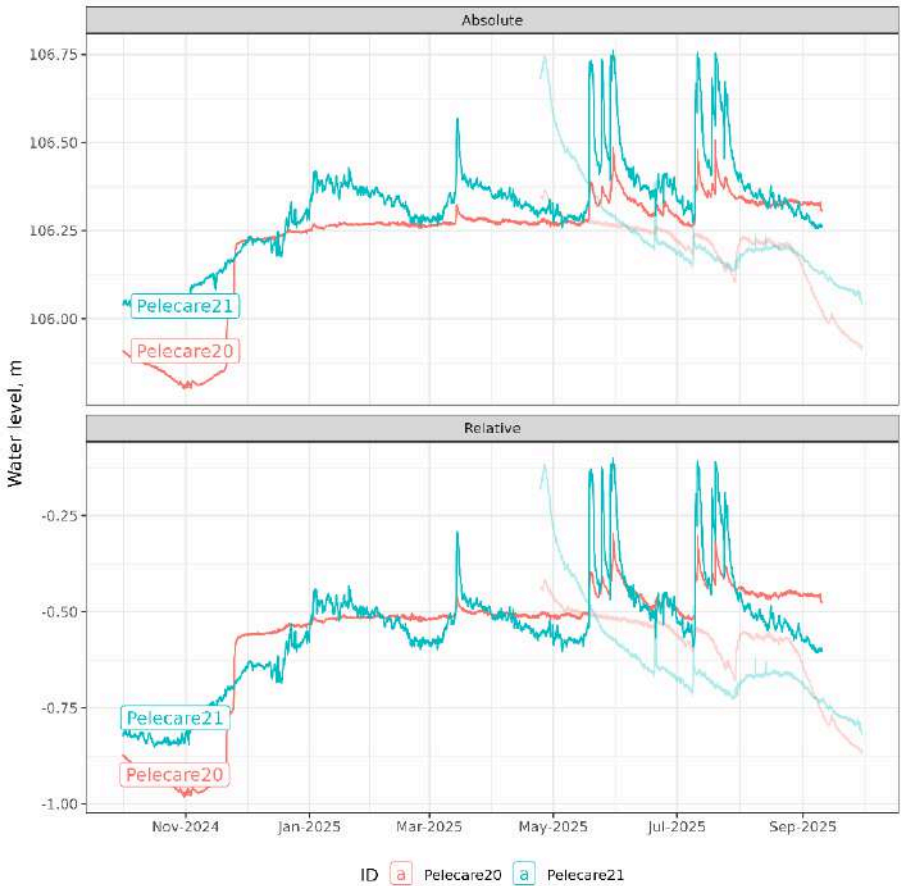	**Drained wetland forest with moderate tree cover** Water level in 2025 was higher than during the period with available data in 2024. In forest wells (Pelecare21) the water level fluctuates strongly in response to precipitation events, suggesting flooding from upstream areas and rapid floodwater recession. The ditch well (Pelecare20) has a more moderate range of water level and the minimum water levels in 2025 appears to be controlled by impeded flow by drift in the ditch that evolves during the season. On a few occasions in 2024 and late 2025 the absolute water level at forest well (Pelecare21) drops below the ditch well (Pelecare20), suggesting significant draw-down by forest evapotranspiration.

Observations	*Description*

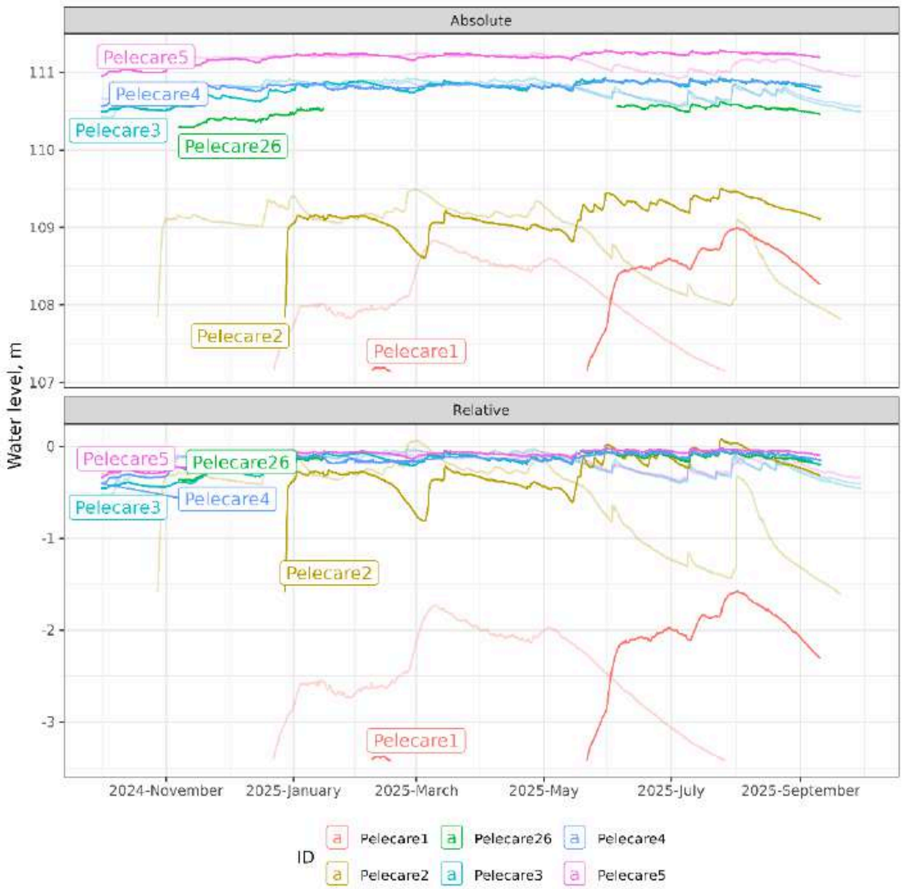

Deigļu bog: gradient from mineral soil to drained bog

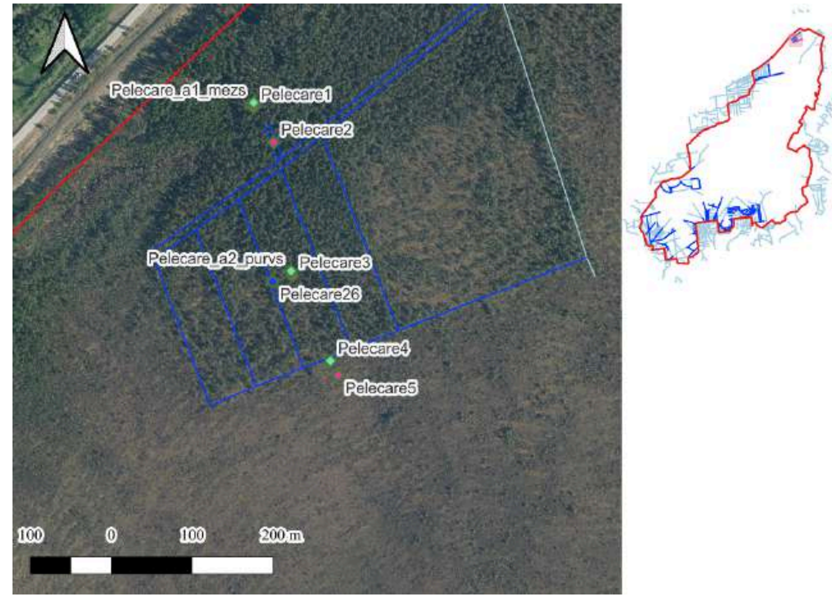

The well located deeper in the relatively pristine bog (Pelecare5) has the least water level range, excluding the initial low water level period (0.13 m), while the well near the ditch (Pelecare4) and the on located within central part of the bog woodland (Pelecare3) delimited by ditches has fluctuation range 0.19 and 0.30 m respectively. The well in the marginal setting (Pelecare2) has characteristic water level rise in late December, a minimum in late-February – early-March, associated with a cold spell and a second minimum in mid-May, before the start of the rainy period.

Both the marginal well (Pelecare2) and well in mineral soil next to the bog have a decreasing water level trend starting from late-July, indicating the onset of relatively dry conditions.

Observations ***Description***

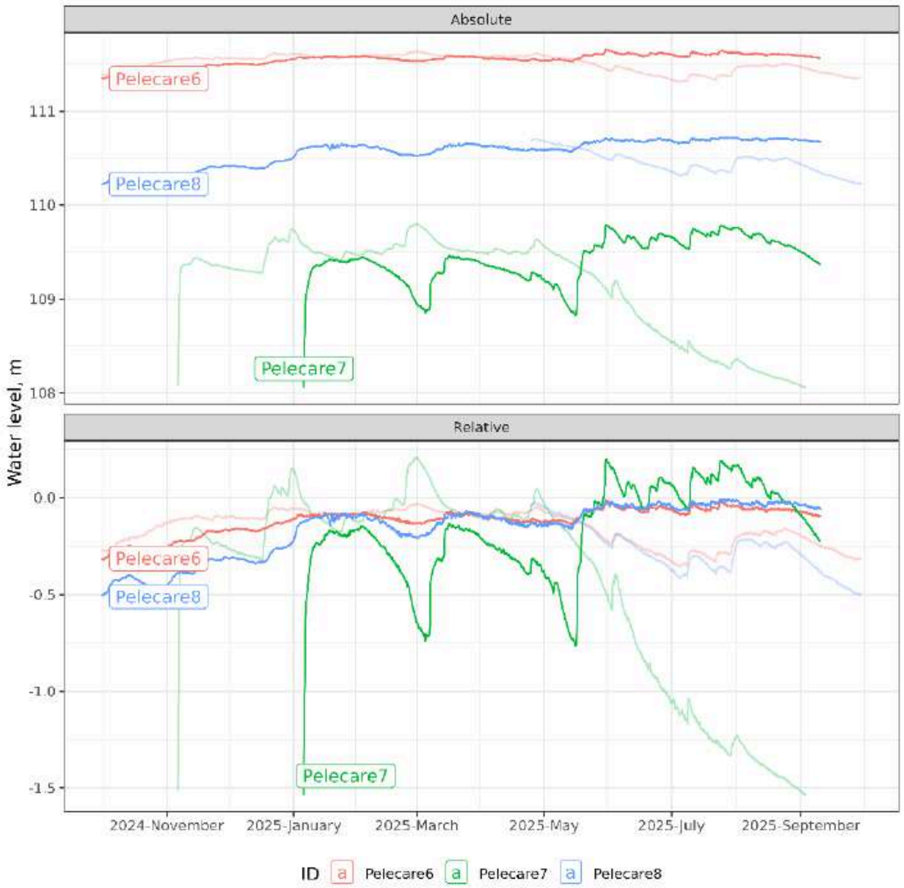

Deigļu bog: gradient from marginal setting to relatively pristine bog

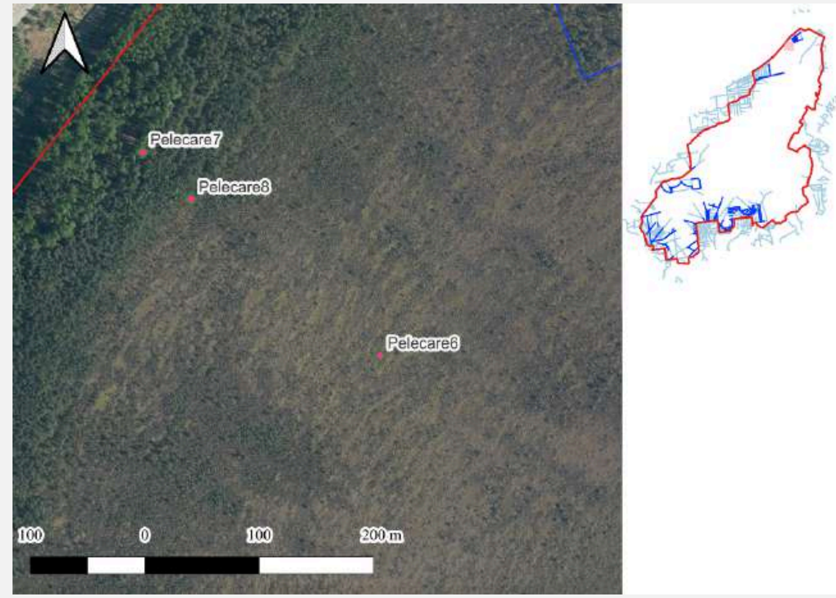

The lowest water level is observed in autumn 2025, it gradually climbs up to January 2025, and, in bog locations (Pelecare6 and Pelecare8) remains close to the surface during the rest of the year. Within the marginal well Pelecare7 a sudden groundwater rise by more than 1.0 m is observed in early January, like one observed a year earlier.

Noticeably, in late-February to early-March there is a prominent water table decline in the marginal well Pelecare7 and to lesser extent at marginal bog well Pelecare8. This follows a period of almost two weeks of freezing temperatures. The pater can be explained by the water loss to the groundwater filtration or water suction by freezing front. Another water table minimum was during the first half of May, before the onset of the rainy period, after the late-April hot wave. This second minima probably was denoted by both increased evapotranspiration and groundwater filtration.

Observations	***Description***
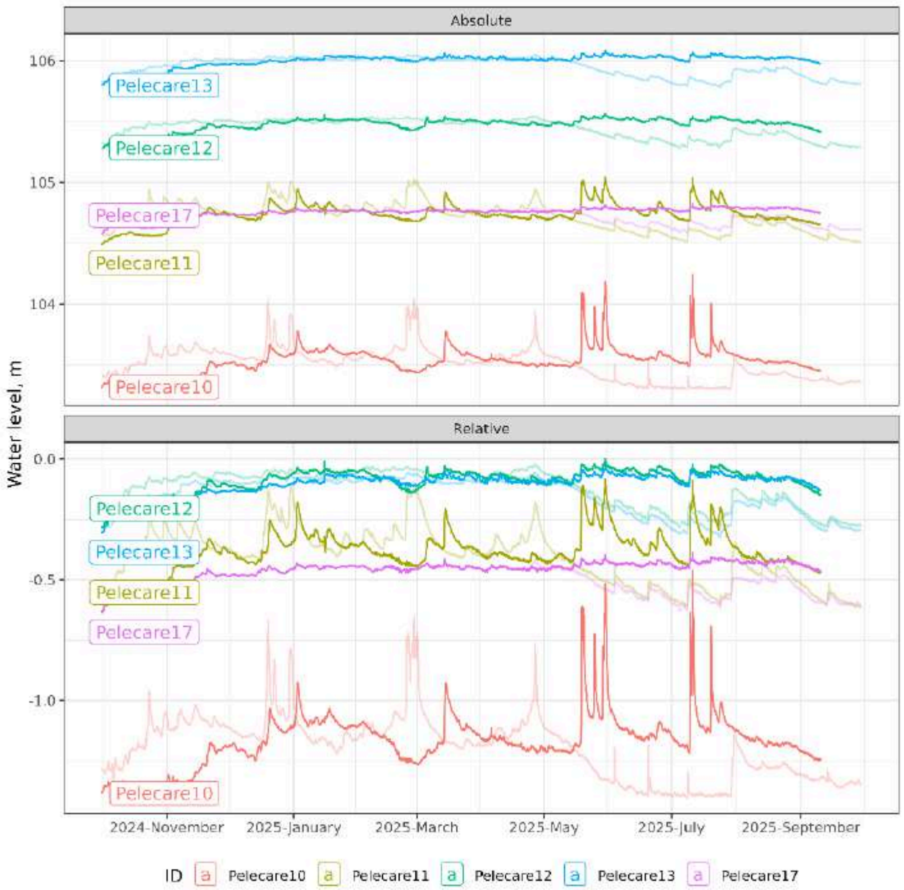	**Malnupeite drained bog** 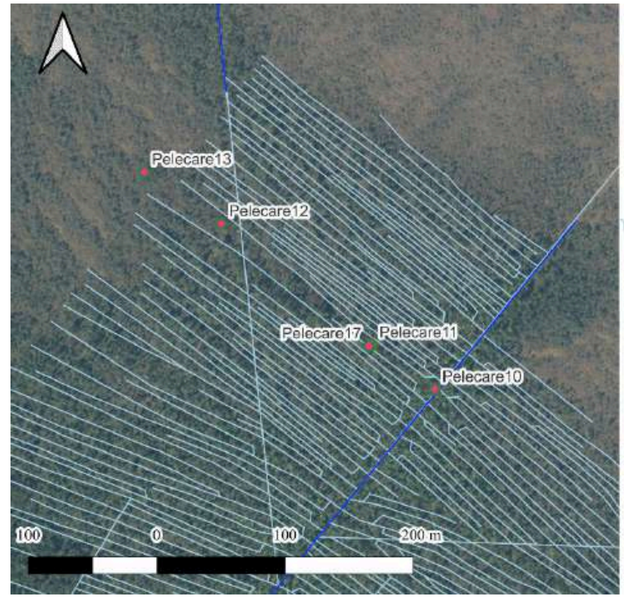  More distal wells from the large drainage ditch (Pelecare12, Pelecare13) have very little water level fluctuations – if the initial relatively low water level is not considered, the fluctuation range is less than 0.1 m. A similar pattern is for the well Pelecare17, installed in a small ditch, near the main ditch (Malnupiet itself) – probably reflecting slow water influx from upstream areas. The paired well in-between small ditches – Pelecare11, has more flushy nature, with rainfall peaks and lows going deeper than the Pelecare17, likely reflecting direct filtration to the main ditch via the deeper peat layers.

Observations	Description
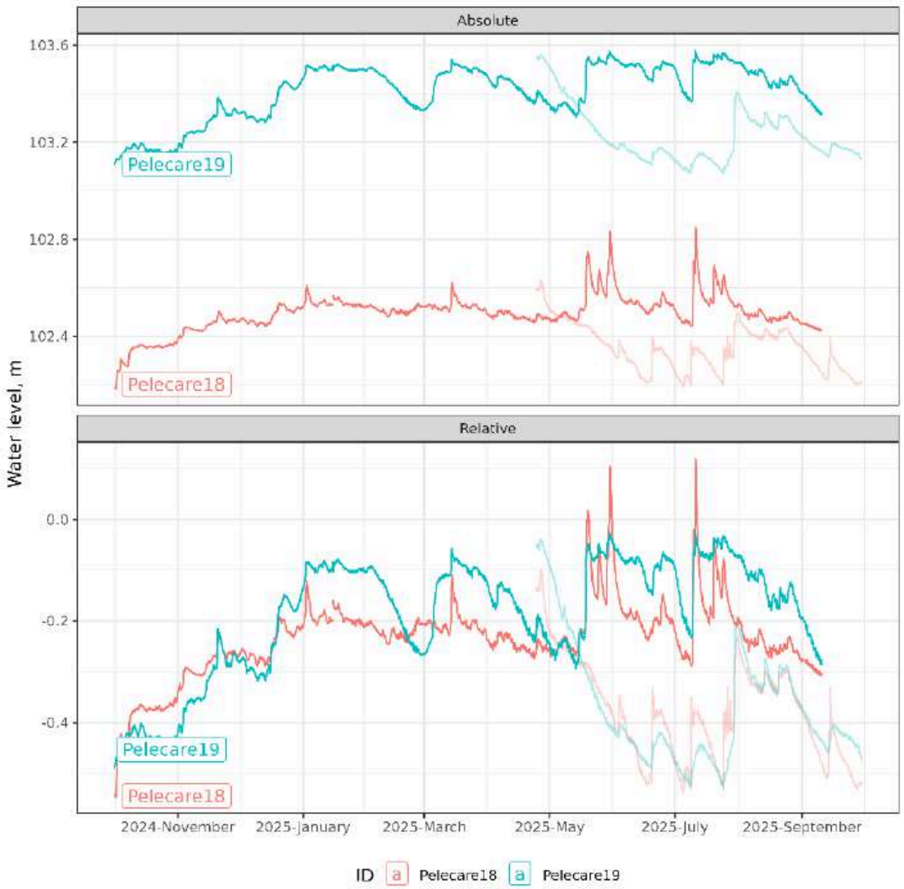	**Malnupeite marginal bog woodland** The water level range in bog woodland is 0.45m. but if the initial low-stand period is excluded, 0.29 m – more than in pristine bog settings (e.g. Pelecare15 or Pelecare6).

Observations	Description
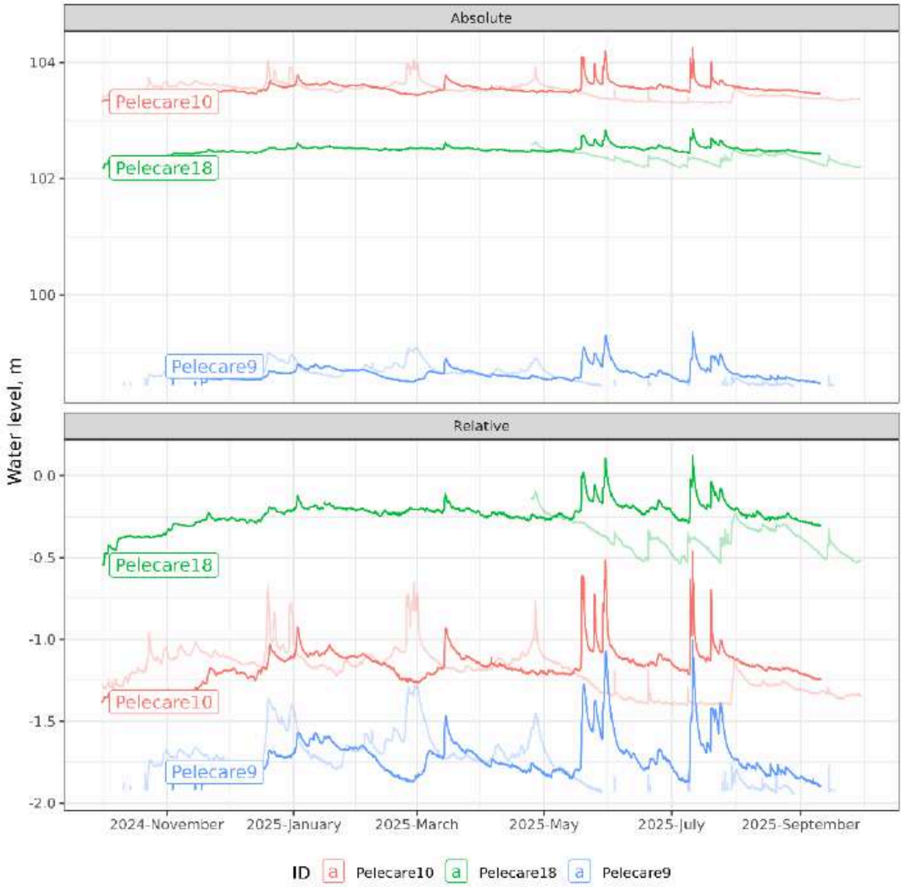	**River Malnupeite, longitudinal section** 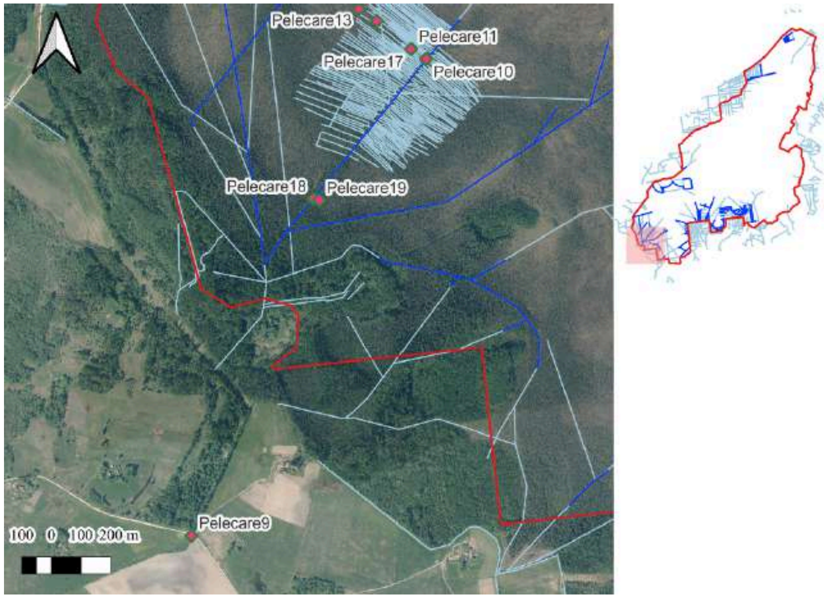 In contrast to 2024, Malnupeitei does not dry up during the summer of 2025. A stable water level is reached in late December 2024, remaining high during the year. The highest level is observed during the precipitation peaks in late May and July.

Water quality measurements were taken in Lielais Pelecare Mire at 4 locations: at the source of stream Malnupeitei within the bog and near level observation sites Pelecare10, Pelecare18 and Pelecare9. In 2025 hydrological year samples were collected on January 16, June 5 and September 11. In the water quality data we see a clear trend toward increased nutrient (N, P) concentrations, alkalinity, electrical conductivity Pelecare10, Pelecare18 and Pelecare9 and pH downstream, but particularly after transition from wetland area (Malnupeite-source, Pelecare10, Pelecare18) to nearby forested and grazed lands (Pelecare9, **Figure 3.1.18**).

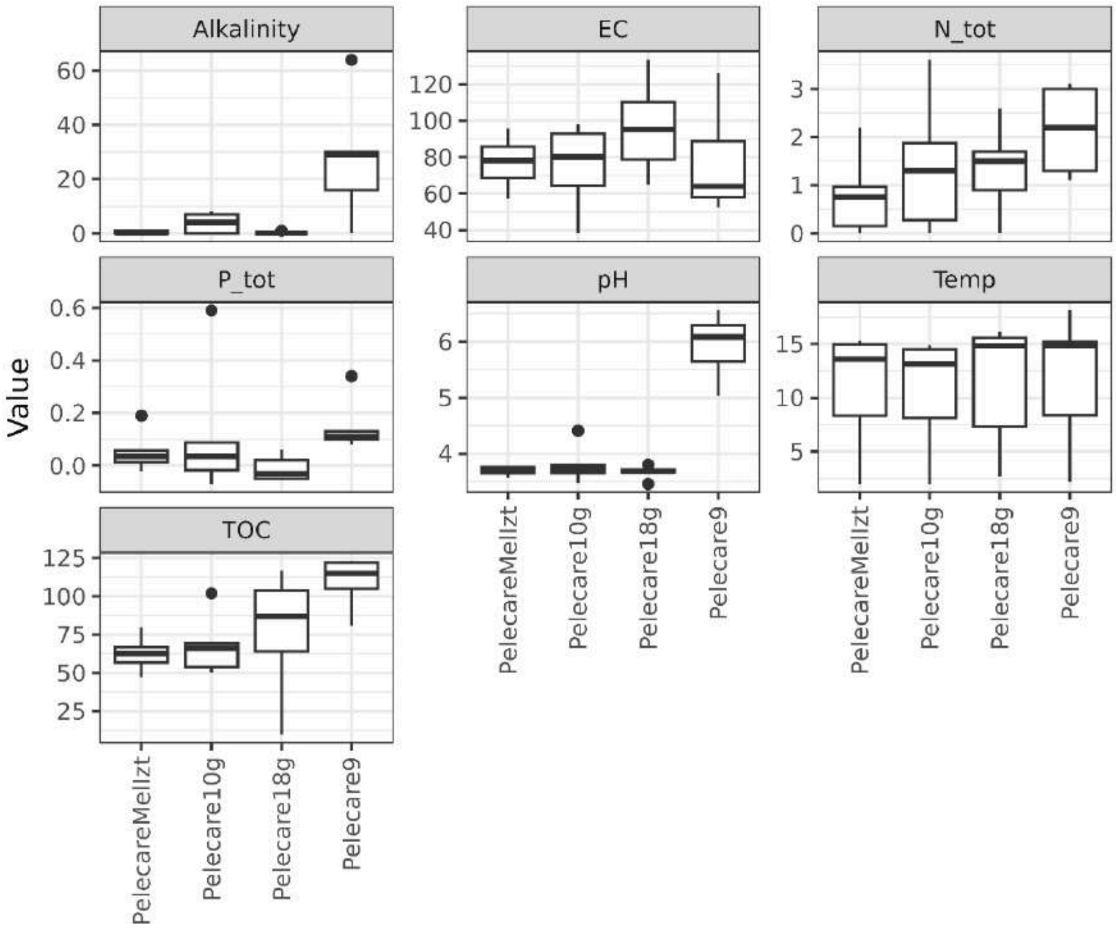

Figure 3.1.18. *Summary of the water quality measurements in stream Malnupeite since the inception of monitoring program in 2023: PelecareMelIzt is the source of stream Malnupete within the raised bog, Pelecare10g, Pelecare18g and Pelecare9 are sampling sites near respective monitoring wells; Alkalinity is alkalinity expressed in mg-$CaCO_3$/L, EC – electrical conductivity µS/cm, N_tot – total nitrogen mg/L, P_tot – total phosphorus mg/L, pH – acidity, Temp – water temperature °C and TOC – total organic carbon mg/L.*

The discharge of the stream Malnupeite is measured with salt tracing (bucked) method based on EC measurements along with water quality sampling. A calibration curve was constructed and respective discharge calculated (**Figure 3.1.19**) from the observed water level at the culvert gauged by Pelecare9 well. The estimated catchment area is 375 ha. In the 2025 hydrological year most of the runoff was during the warm season, in contrast to 2024 (**Table 3.1.5**).

A

B

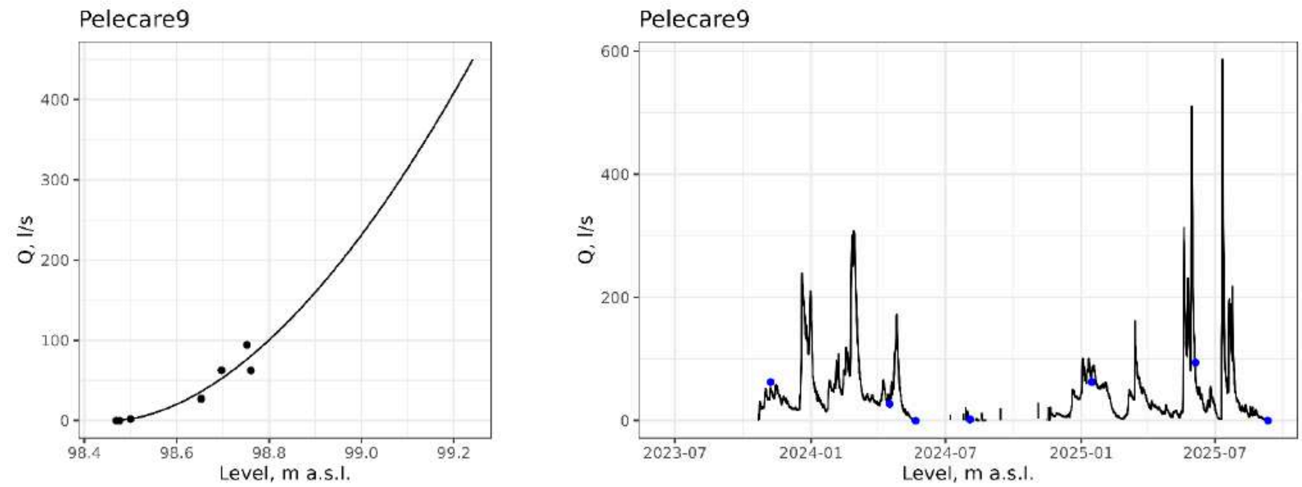

Figure 3.1.19. *A – calibration curve for the discharge at the Pelecare9 location; B – Reconstructed hydrographs (discharge) at Pelecare9 location – a stream Malnupeite culvert: blue dots are measured discharge*

Table 3.1.5. *Runoff summary mm/season Malnupeite at Peleacre9 location*

Hydrological year	*Warm*	*Cold*	*Year*
2024	48	246	294
2025	190	120	310

Meteorological conditions

During most of the available observation period from April 23, the temperature in Lielais Pelečāre Mire was relatively high, reaching peak in late July and August, daily maximum exceeding 30°C and average above 20°C (**Figure 3.1.20**). From mid-May to late mid-September the daily maximum was consistently above 20°C. Notable precipitation events were recorded in early June, second and third decade of July and middle of August. April and May as well as late August and September have seen little precipitation.

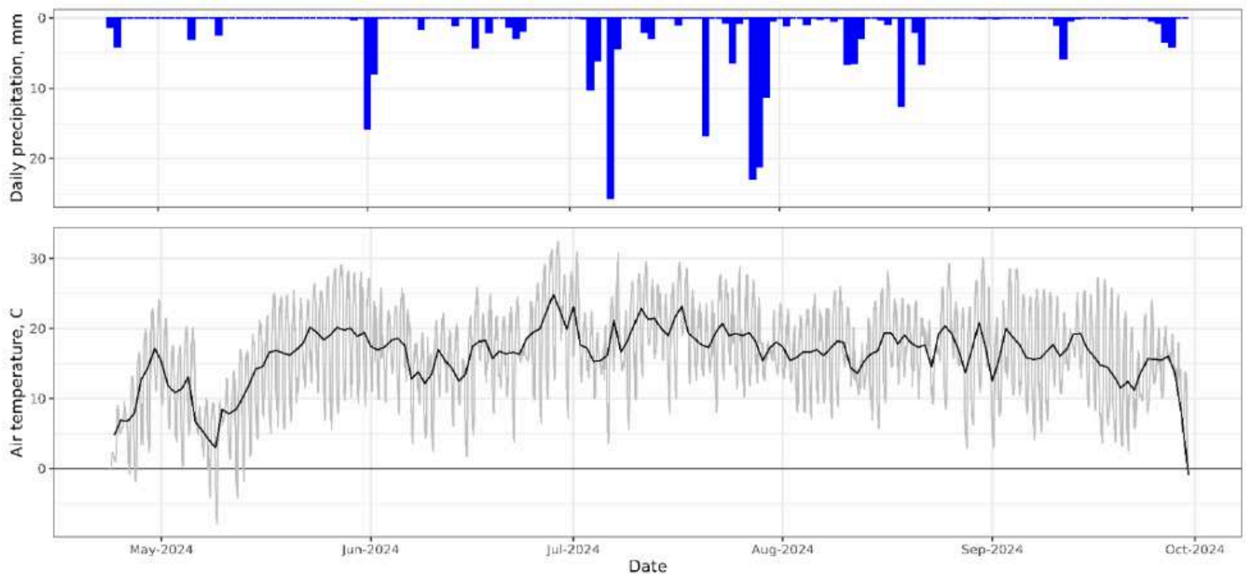

***Figure 3.1.20**. Daily precipitation and air temperature in Lielais Pelečāre mire, open raised bog site (Pelecare_a3_atklats_purvs)*

Automatic water level observation probes in Lielais Pelečāres Mire were installed on June 22, 2023, additional data loggers were installed on April 23, 2024. The latest data download took place on January 15, 2025. Along with data download manual groundwater level measurements took place using acoustic water level probes. The manual measurements are used to control the validity of automatic measurements. Water quality parameters were not systematically measured during the reporting period. The analysis in this report is limited to the hydrological year from October 1, 2023 to September 30, 2024.

Water level observations in Pelečāre mire is subdivided into 6 groups: Deiglu bog, drained; Deiglu bog, pristine; Lake Deguma; Malnupeite, bog woodland; Malnupeite, drained and Malnupeite, stream.

Two weather stations and soil water monitoring sites have been set up in the Lielais Pelečāre mire to study microclimatological differences between open raised bog landscape and woodland. The water quality monitoring of selected parameters is organized along the Malnupeite River cores in the Southern part of Lielais Pelečāre Mire.

Mostly, the depth of the water level determined by automatic probes aligns well with manual control measurements, falling within the summative uncertainty limits (<5 cm). Initial measurements during setup in wells No. Pelecare3 to Pelecare6 and Pelecare18, show large deviations, but subsequent control measurements show reasonably good consistency **Figure 3.1.21**).

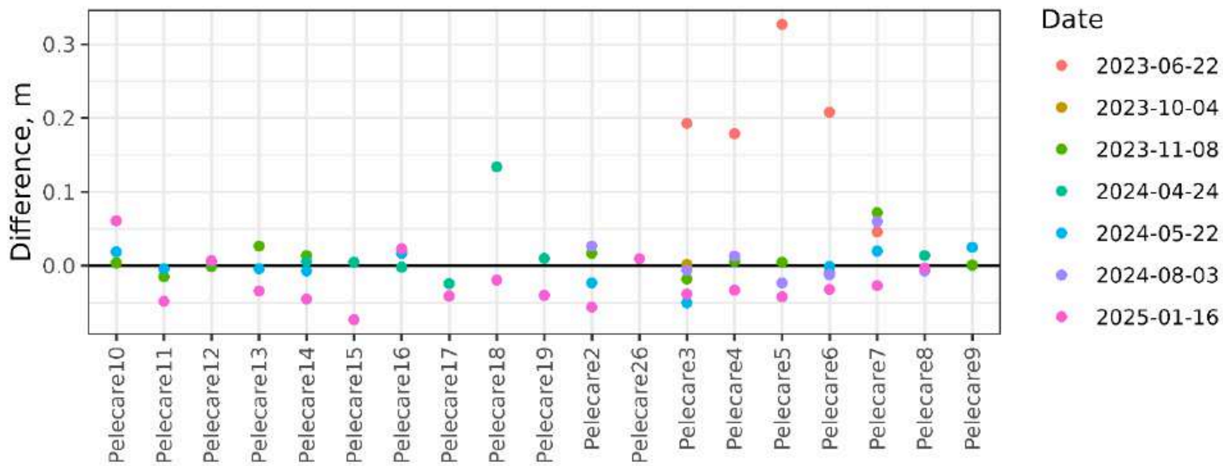

Figure 3.1.21*. The difference between automatic and manual water level measured in Lielais Pelečāres Mire*

Table. 3.1.6. *Summary statistics for the water table below soil surface in Lielais Pelečāre Mire.*

Group of observations	***Well ID***	***Mean relative water table, m***	***Min relative water table, m***	***Max relative water table, m***	***Mean absolute water table, m***	***Range of the daily mean, m***
Deiglu bog, drained	Pelecare1	-2.48	-3.41	-1.74	108.09	1.67
	Pelecare2	-0.57	-1.59	0.06	108.86	1.65
	Pelecare3	-0.19	-0.54	-0.03	110.77	0.51
	Pelecare4	-0.19	-0.41	-0.09	110.77	0.32
	Pelecare5	-0.16	-0.37	-0.05	111.14	0.32
Deiglu bog, pristine	Pelecare6	-0.15	-0.35	-0.03	111.51	0.32
	Pelecare7	-0.44	-1.53	0.2	109.16	1.73
	Pelecare8*	-0.27	-0.51	-0.03	110.45	0.48
Lake Deguma	Pelecare14	0.06	-0.12	0.24	105.33	0.36
	Pelecare15*	-0.19	-0.28	-0.02	107.05	0.26
	Pelecare16	-0.2	-0.54	-0.06	106.09	0.48
Malnupeite, bog woodland	Pelecare18*	-0.38	-0.54	-0.11	104.42	0.43
	Pelecare19*	-0.37	-0.52	-0.04	107.98	0.48
Malnupeite, drained	Pelecare10	-1.2	-1.4	-0.74	103.51	0.66
	Pelecare11	-0.41	-0.63	-0.12	104.72	0.51
	Pelecare12	-0.12	-0.29	-0.02	105.44	0.27
	Pelecare13	-0.16	-0.32	-0.06	105.95	0.26

	Pelecare17*	-0.54	-0.64	-0.43	104.68	0.21
Malnupeite, stream	Pelecare9	-1.71	-1.93	-1.29	98.66	0.64

* Incomplete time series starting from April 23, 2024

Results of the water level observations in a section of the Deigļu Mire least affected by drainage

At this location, there are 3 wells equipped with automatic water level probes: Pelecare6 on the slope of the raised bog dome; Pelecare8 at a hinge of the raised bog dome and Pelecare7 in the bog woodland, forming the transition zone between the raised bog and the upland forest (**Figure 3.1.22, 3.1.23**). We see gradual increase of the mean groundwater depth and the range of groundwater level fluctuations in a direction from bog dome to the marginal bog woodland. At the slope of the dome the yearly range of the water level was 32 cm, while at the marginal hinge of the dome (Pelecar8), for an incomplete series it was already 48 cm and more than 173 cm at bog woodland (Pelecare7), where the minimum levels were not detected as the water table plunged below the well depth (**Table 3.1.6**). Interestingly, at this site temporal flooding we detect only at the bog woodland, but not in the raised bog itself.

Figure 3.1.22. *Monitoring wells Pelecare6 (left) and Pelecare7 (right) forming a profile from relatively undisturbed raised bog to bog forest at its margin, June 21, 2024. Image: © A. Kalvāns*

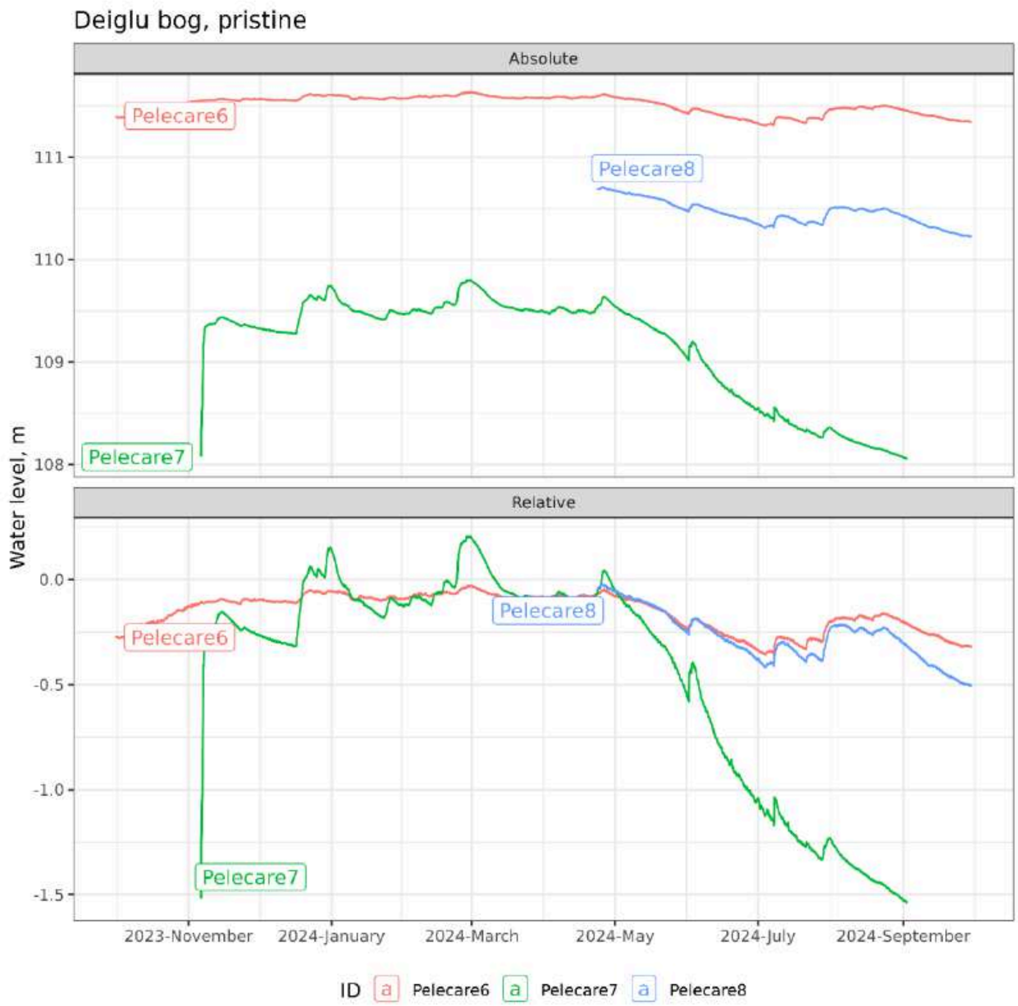

Figure 3.1.23. *Observed water level in the less affected by drainage part of the Lielais Pelečāre Mire, Deigļu Mire section: Pelecare6 – observation point located on the slope of the raised bog dome; Pelecare7 – observation point in the bog woodland in the transition zone between the raised bog and dry forest.*

Results of the water level observation in the section of the Deigļu Mire affected by drainage

In the drained part of the Deigļu Mire, 5 water level observation points have been set up, forming a profile line from the dry forest (Pelecare1), continuing through the bog woodland formed drained peatland (Pelecare2, Pelecare3, Pelecare4), and into the raised bog less affected by the drainage (Pelecare5; **Figure 3.1.24**).

Here we see that the water level in mineral soil near the bog margin (No. Pelecare1 and Pelecare2) (**Figure 3.1.25**) is consistently lower than in the bog, indicating groundwater recharge – infiltration of the water emanating from the raised bot. This has implications for the planned restoration measures – simple dams on the ditches will not completely stop water loss from the bog woodland, still some of the water will infiltrate into the sandy subsoil. Full closure of the ditches would provide better restoration results.

Figure 3.1.24. *One of two weather stations for microclimatological analysis and data logger at the Pelecare_a1_mezs observation site near well Pelecare1. Image: © A. Kalvāns*

Water level observations in the Lake Deguma

A water level monitoring profile towards the lake Deguma consists of monitoring points No. Pelecare15, Pelecare16 and Pelecare14, the latter recording the water level in the lake **Figure 3.1.25**).

The range of the Lake Deguma water level in 2024 hydrological year was 36 cm (Error! Reference source not found.), that is like that seen in other monitoring sites with pristine raised bog conditions. The water level peak was recorded in March 2024, probably reflecting the meltwater input. Meanwhile the extreme precipitation event at the end of July, that is prominent in many of the groundwater monitoring sites, is barely seen in lake Deguma hydrograph. The Pelecare16 site is located at the elevation hinge between raised bog dome and bog lake, covered by a strip of pine forest. Here the water level dynamics were much like one observed in the margins of the raised bog (wells No. Pelecare2 and Pelecer7) – sharp rise of the water level in late autumn or early winter, stable levels in winter, and decline in summer and autumn with peaks corresponding to major precipitation events.

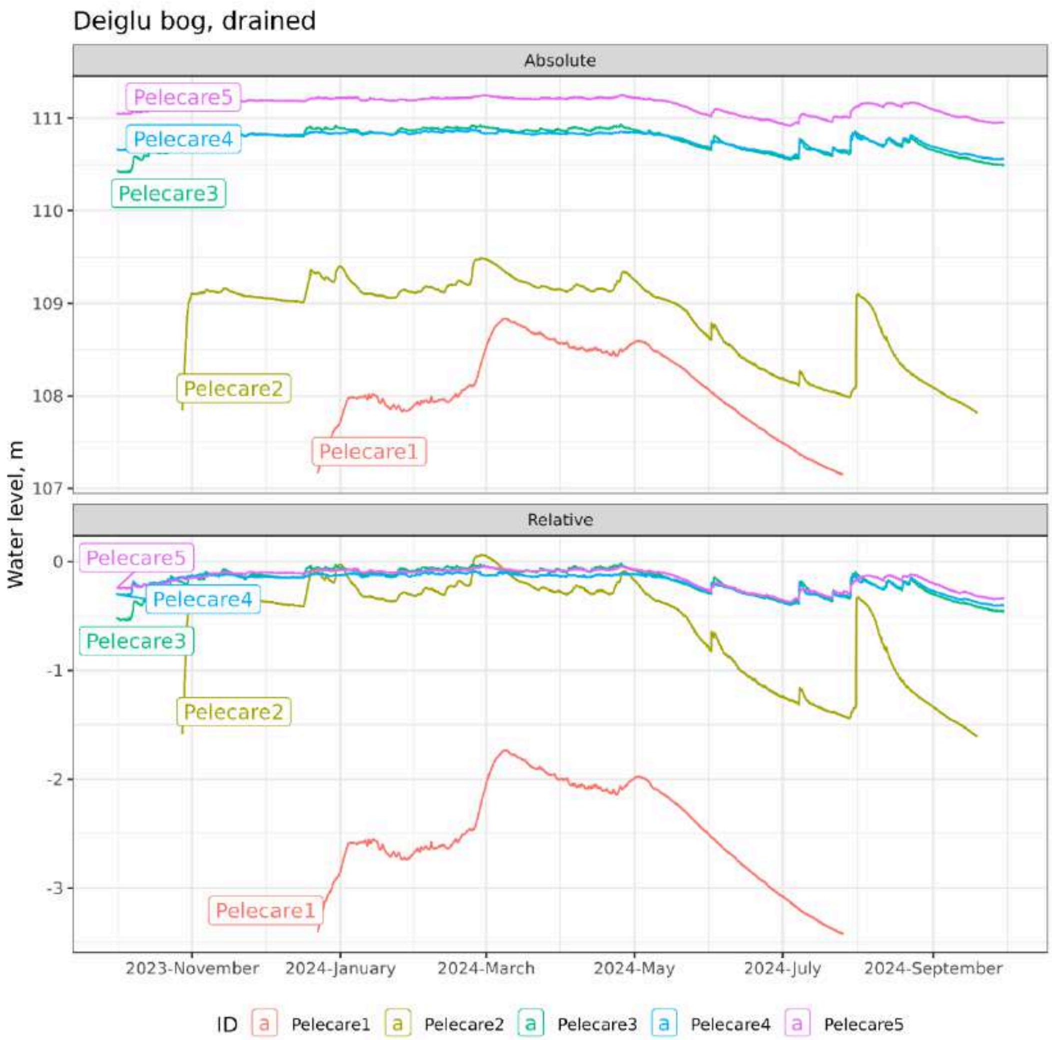

Figure 3.1.25. *Observed water level in the drained part of the Deigļu Mire (southern part of the Lielais Pelečāre Mire): Pelecare1 – dry forest at the edge of the bog; Pelecare2, Pelecare3, Pelecare4 – bog woodland, partially formed because of drainage on the slope of the raised bog dome; Pelecare5 – observation point least affected by the drainage at the bog side of the last drainage ditch.*

Figure 3.1.26. Installation of the water level monitoring equipment at the floating shore of the Lake Deguma, June 20, 2023. Image: © A. Kalvāns

Figure 3.1.27. A deep drainage ditch cut into the peat that is known as river Malnupeite, near water level monitoring well Pelecare10, August 27, 2022. Image: © A. Kalvāns

Water level observations in the drained section of the Malnupeite River catchment

The group of water level observation points in the drained section **(Figure 3.1.28**) of Malnupeite River catchment consists of 5 water level monitoring wells. Here we see a clear pattern of increasing depth to water table and range of water table fluctuations towards the main drainage ditch, that is about 2 m deep near the water level monitoring profile (**Table 3.1.6**).

We can note an interesting pattern: in the drained section of the bog further away from the main, deep drainage channel (Malnupeite) the yearly range of the groundwater level (26 to 27 cm) is slightly less than in more pristine locations (Pelecare6, 32 cm). Similar patterns we can notice in Cena mire as well. One explanation for this might be that the derelict drainage system does not affect the water level once it is below soil surface, but still effectively evacuates any above-surface water consists of water level observations in the watercourse of national significance named “Nr.25”, that collects water from Malnupeite River outside the raised bog (Pelecare9), a profile of four observation points in a raised bog section drained by a dense network of small ditches (Pelecare10, Pelecare11, Pelecare12, Pelecare13) drained by deep collector ditch named Malnupeite River, and an observation point of the Deguma Lake water level (Pelecare14, **Figure 3.1.29**).

During the reporting period, water flow in ditch Nr.25 (Pelecare9) outside the Lielais Pelečāre Mire appeared only in the second half of October 2023 (**Figure 3.1.19**), presumably due to an increase in groundwater levels because of autumn rains. During the observation period, one instrumental flow measurement was carried out there using the salt tracer method: on November 7, 2023, at 12:26, the calculated discharge was 32.6 l/s and the corresponding relative water level was -1.66 m relative to the zero mark of the observation point.

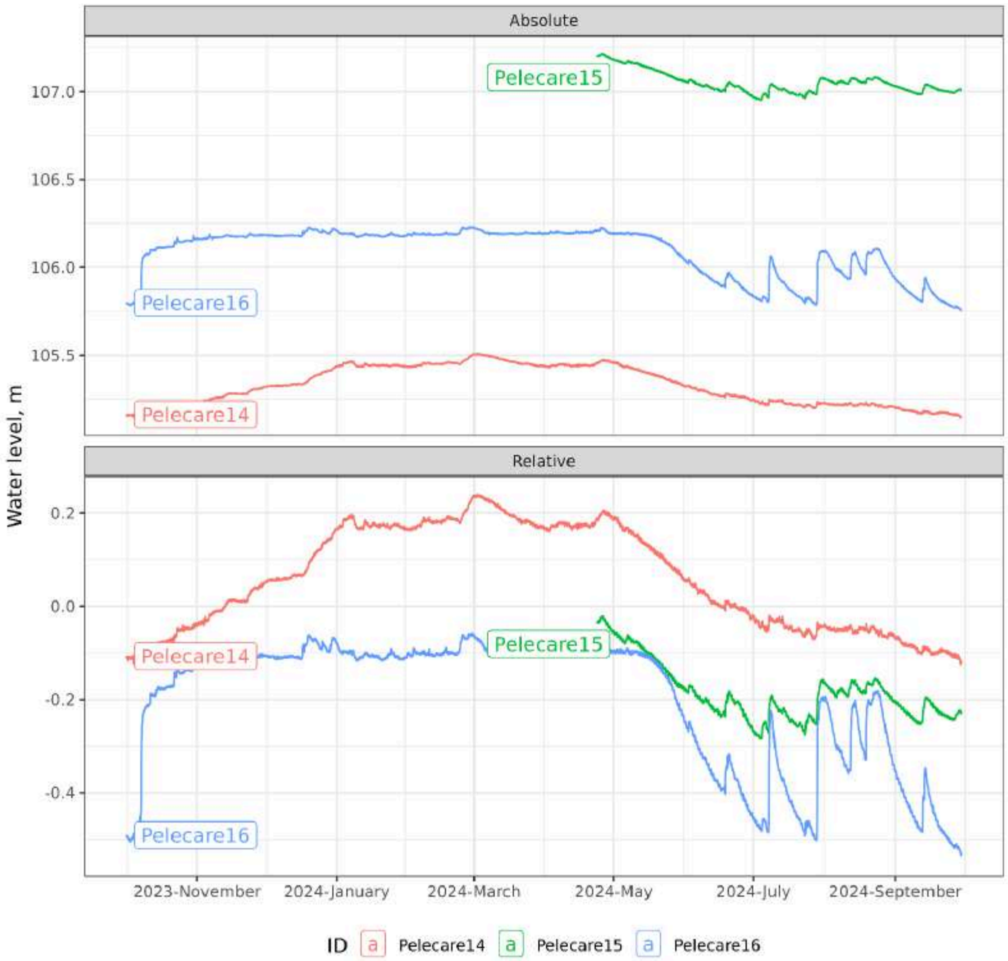

Figure 3.1.28*. Observed water level near Lake Deguma: Pelecare 14, Pelecare 16 – bog woodland along lake shore; Pelecare 15 – open raised bog.*

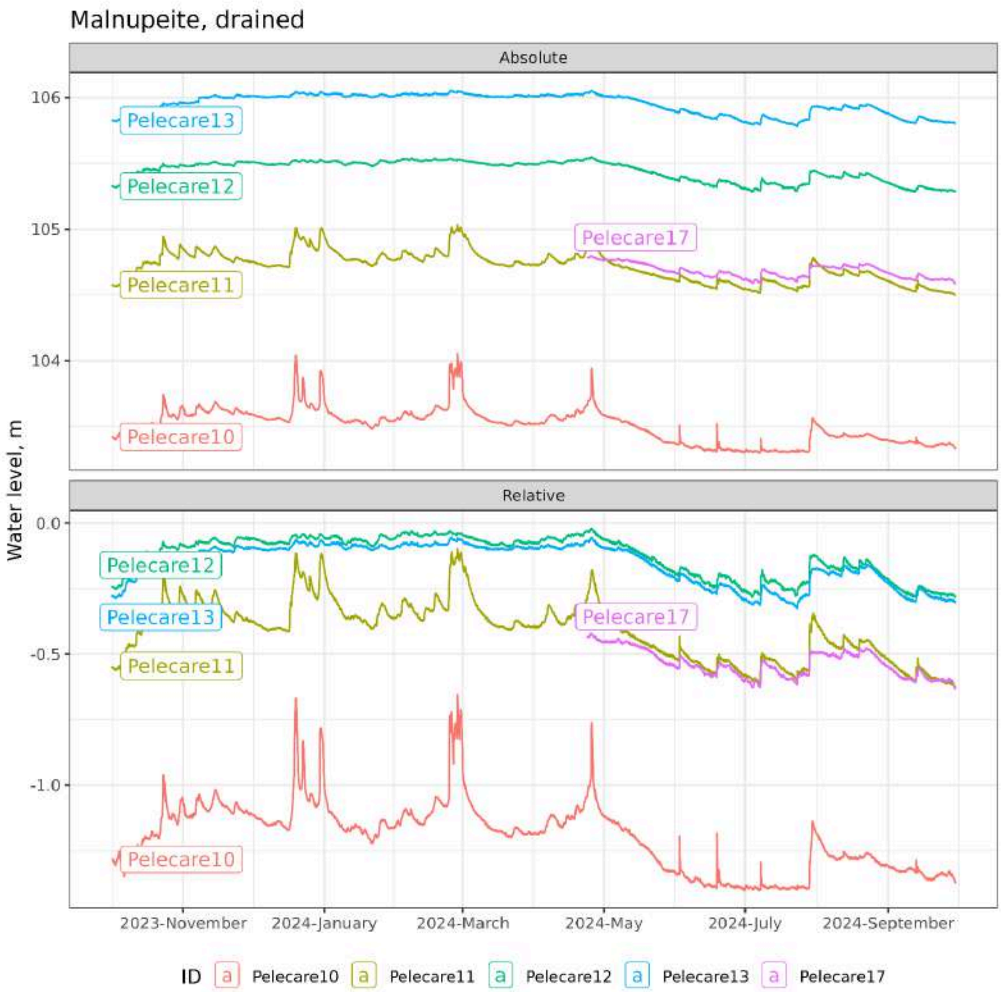

Figure 3.1.29. *Observed water level in the southern part of Lielais Pelečāres Mire, within the drainage basin of watercourse of national significance named "Nr.25" (Malnupeite) and Deguma Lake: Pelecare9 – Malnupeite River (watercourse of national significance named "Nr.25"); Pelecare10, Pelecare11, Pelecare17, Pelecare12, Pelecare13 – profile of observation points perpendicular to the deep collector ditch (Malnupeite) within the Lielais Pelečāre Mire.*

Water level observations in bog woodland in Malnupeite River catchment

A profile of two wells (No. Pelecare18 and Pelecare19) were installed near Malnupeite River channel in the bog woodland in the forested marginal zone of the Lielais Pelečāre Mire. The two wells since April 2024 had a similar range of groundwater level fluctuations for the observation (43 to 48 cm, Table 3.1.2. (**Figure 3.1.30**), however the well near the channel had more flashy behaviour with higher increase of water level in response to moderate precipitation events, showing the impact of the drainage from upstream catchment.

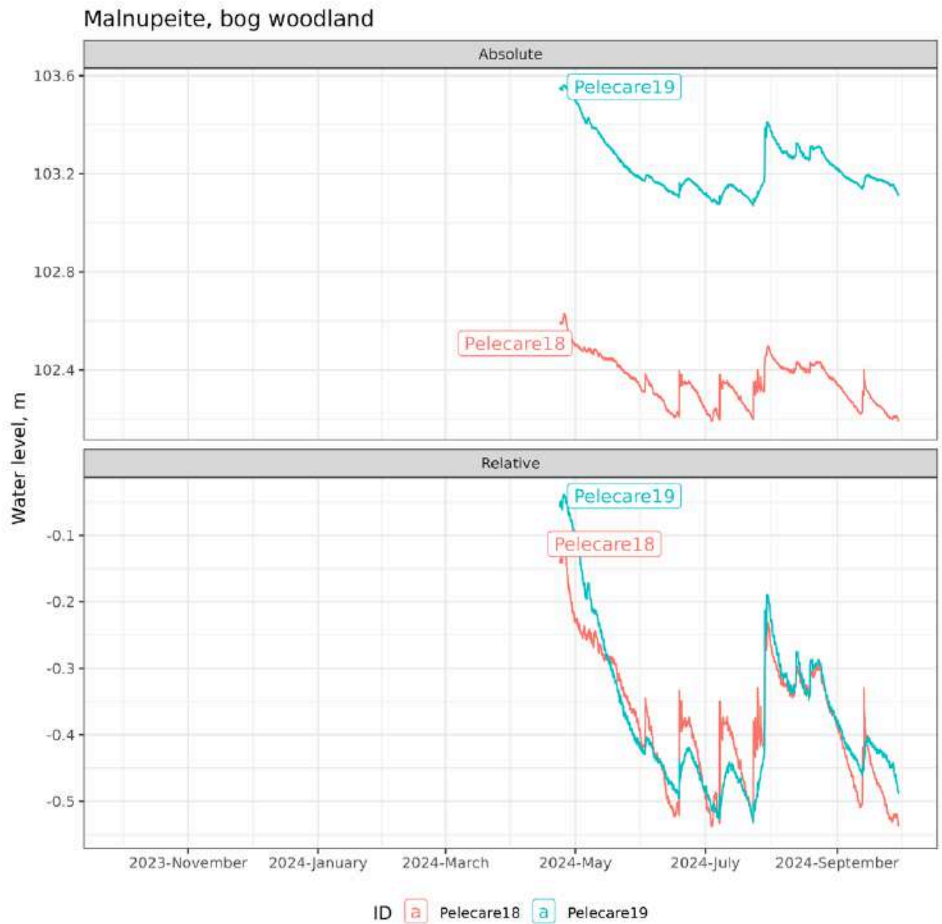

Figure 3.1.30. *Observed water level at a profile towards the Malnupeite ditch at the bog woodland located at the margin of the raised bog: Pelecare19 – 20 m distance from the ditch; Pelecare18 – within 0,5 from the ditch.*

The along-stream water level of Malnupeite River

Three monitoring wells record the water level along the stream of the Malnupeite River: No. Pelecare10, Pelecare18 and Pelecare9, **Figure 3.1.31**). Strictly speaking, only Pelecare9 records the river water level, while the rest are placed in the sediments near the stream channel. Along the stream some sensitive chemical parameters were measured. At the Pelecare9 site the discharge was periodically measured using salt tracing method (**Table 3.1.7**).

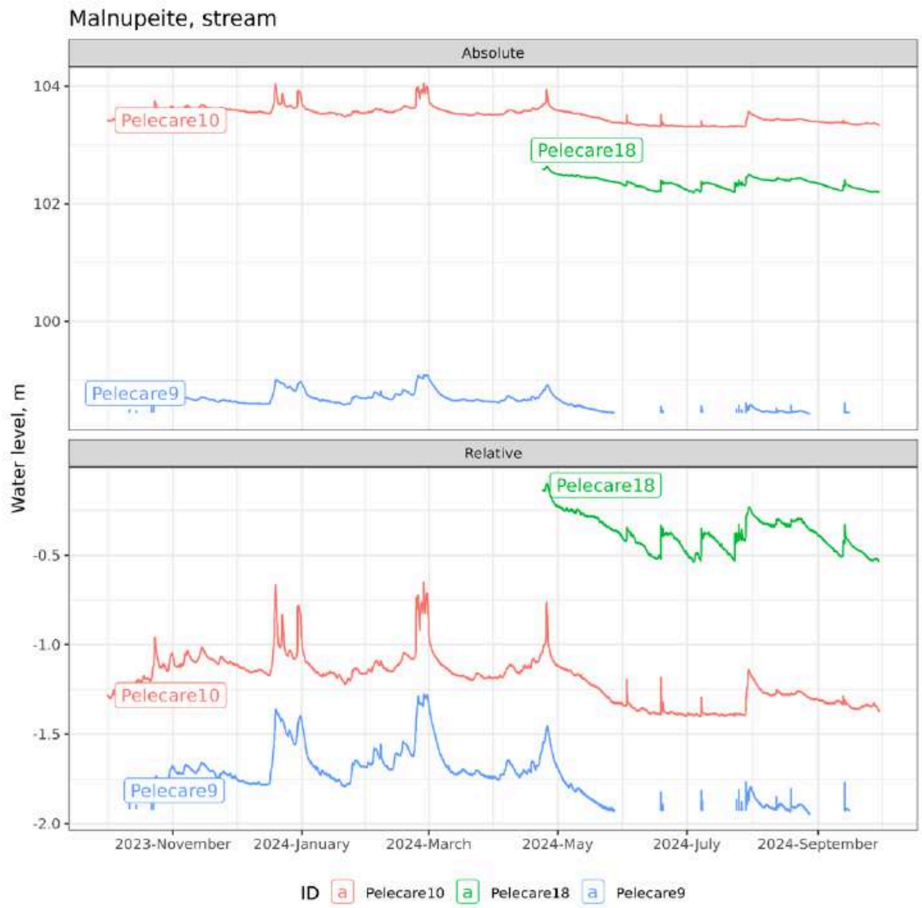

Figure 3.1.31. *Observed water level observed in wells near the Malnupeite ditch from the heavily drained raised bog (Pelecre10), to bog woodland between raised bog and dryland (Pelecare18) to a ditch outside the bog (Pelecare8).*

Table 3.1.7. *Water quality monitoring results along the Malnupeite stream*

ID	*Date*	*pH*	*EC, µS/cm*	*N-total, Mg/l*	*P-total PO_4 mg/l*	*Alkalinity, $CaCO_3$ mg/l*	*TOC, C-mg/l*	*Q, l/s*
Pelecare10g	2023-03-08	4.409	38.2	3.6	0.84	7	50	
PelecareMellzt	2023-03-08	3.774	67.7	0.9	0.44	1	59	
Pelecare9	2023-07-11							62.6
Pelecare9	2024-16-04	6.085	52.7	1.3	0.33	16	81	27.1
Pelecare18g	2024-16-04	3.715	78.6	2.6	0.22	1	64	
Pelecare10g	2024-16-04	3.701	69.7	1.1	0.18	4	51	
PelecareMellzt	2024-16-04	3.729	57.3	0.6	0.26	1	66	
Pelecare9	2024-21-05							0
Pelecare9	2024-03-08	6.29	88.6	3	0.36	29	105	1.88
Pelecare18g	2024-03-08	3.674	95.2	1.5	0.2	<1	87	
Pelecare10g	2024-03-08	3.645	90.5	1.5	0.34	<1	102	

PelecareMelIzt	2024-03-08	3.648	95.9	2.2	0.31	<1	80	
PelecareMelIzt	2025-15-01	3.57	84.9	<0.1	0.23	<1	56	
Pelecare9	2025-15-01	5.645	64.1	1.1	0.35	<1	122	62.5
Pelecare10g	2025-15-01	3.47	98.1	<0.1	0.24	<1	69	
Pelecare18g	2025-15-01	3.458	110.1	<0.1	0.2	<1	104	

3.1.3. Sudas-Zviedru Mire

Assessment of Water Level Observation Quality

Latest data download for groundwater level probes took place on October 30 2025. The summary statistics is provided in **Table 3.1.1,** and the time series are described in **Figure 3.1.8.** The observations at 7 wells are grouped in 2 stations, where some of the wells are included in both stations:

1. Along dammed drainage ditch
2. Across two dammed drainage ditches

Figure 3.1.8. *Description of hydrological monitoring results in Sudas-Zviedru mire for 2025 hydrological year*

Observations | **Description**

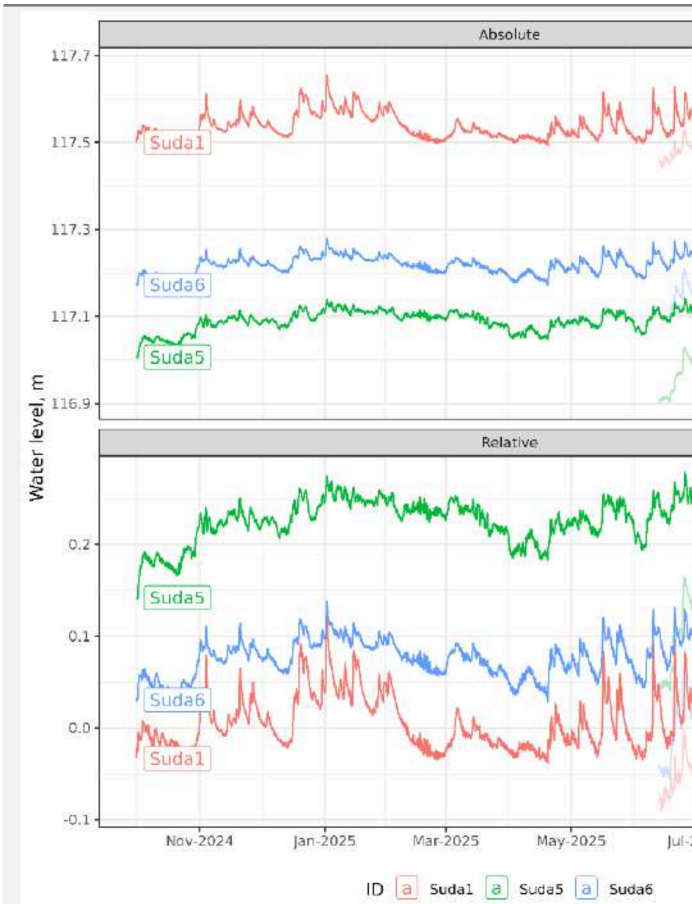

Along dammed drainage ditch

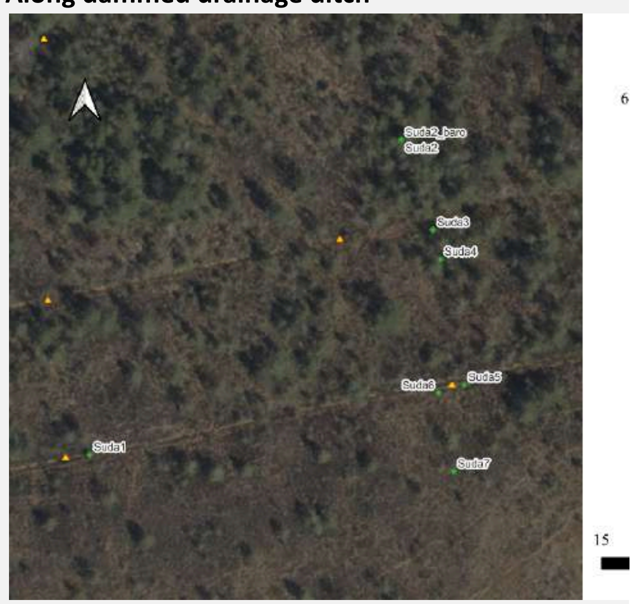

The range of water level fluctuations in the ditch in all three monitoring wells in 2025 are moderate (0.10 to 0.14 m), with highest value at the upstream location. The small range to some extent is determined by the extremely wet summer. The largest range and swiftest fluctuations are at the upstream location (Suda1), while downstream locations above (Suda5) and below (Suda6) dam are progressively smaller. This pattern reflects buffering capacity of the impoundments created by ditch damming at the two downstream locations, while the upstream site remains partly above the impoundment level.

Across two dammed drainage ditches

The well profile is established in the up-slope direction, across two dammed ditches that are oriented tangentially to the slope.

It can be observed that both there is a gradient of decreasing water level fluctuation from lower to higher elevation (0.23 m at Suda2 and 0.09m at Suda7) and decreasing depth to water, indicating drained conditions at down-slope side of the ditches and increasingly water saturated conditions at up-slope sites.

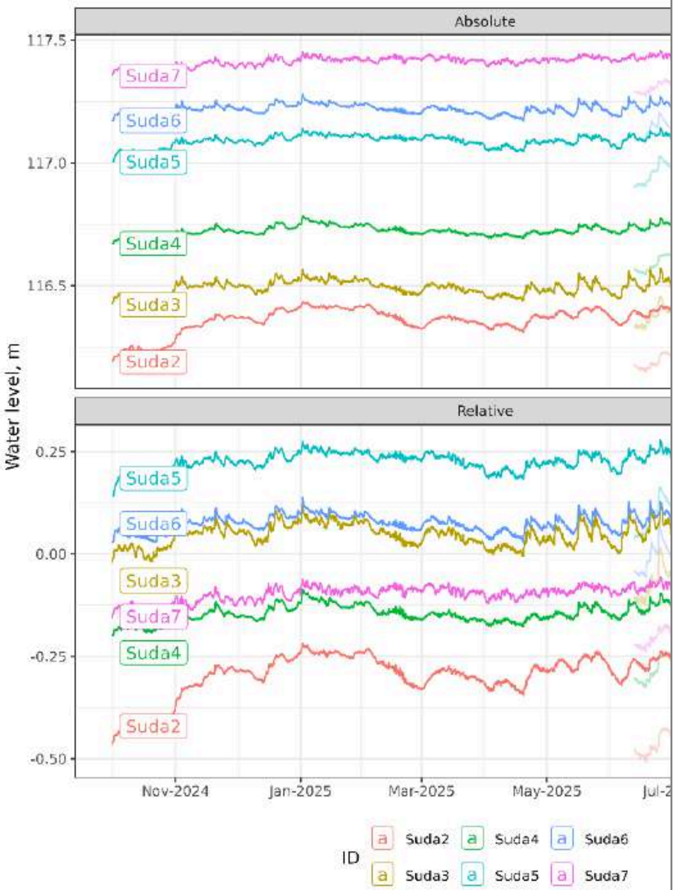

Water level probes in Sudas-Zviedru mire were installed on June 11, 2024 while the data were downloaded on October 21, 2024, however for consistency we limit the data set to the end of the water year (September 30, 2024). The water level measurements at Sudas-Zviedru Mire shows an excellent agreement between automatic and manual measurements – in most cases the difference is less than 2 cm (**Figure 3.1.32.**).

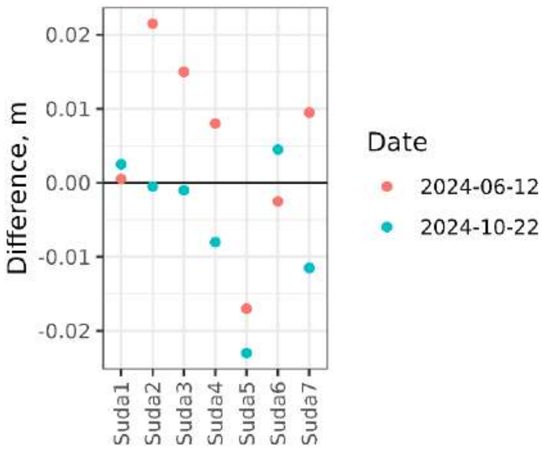

Figure 3.1.32. *The difference between automatic and manual water level measured at all observation points is 0.05 m or less, indicating overall good measurement quality.*

Figure 3.1.33. *Water level monitoring well in Suda6 in Sudas-Zviedru Mire was restored in 2017, June 22, 2024. Image: © A. Kalvāns*

Results of the groundwater level monitoring

We analyse the water level observations in two overlapping profiles. One is oriented radially in respect to the raised bog dome, across the two parallel ditches that have been blocked in previous project, from bog woodland closest to the margin to the open raised bog (wells No. Suda2 to Suda7). The other is along the ditch axis, tangential in respect to the bog dome (wells No. Suda5, Suda6 and Suda1) (**Figure 3.1.34**).

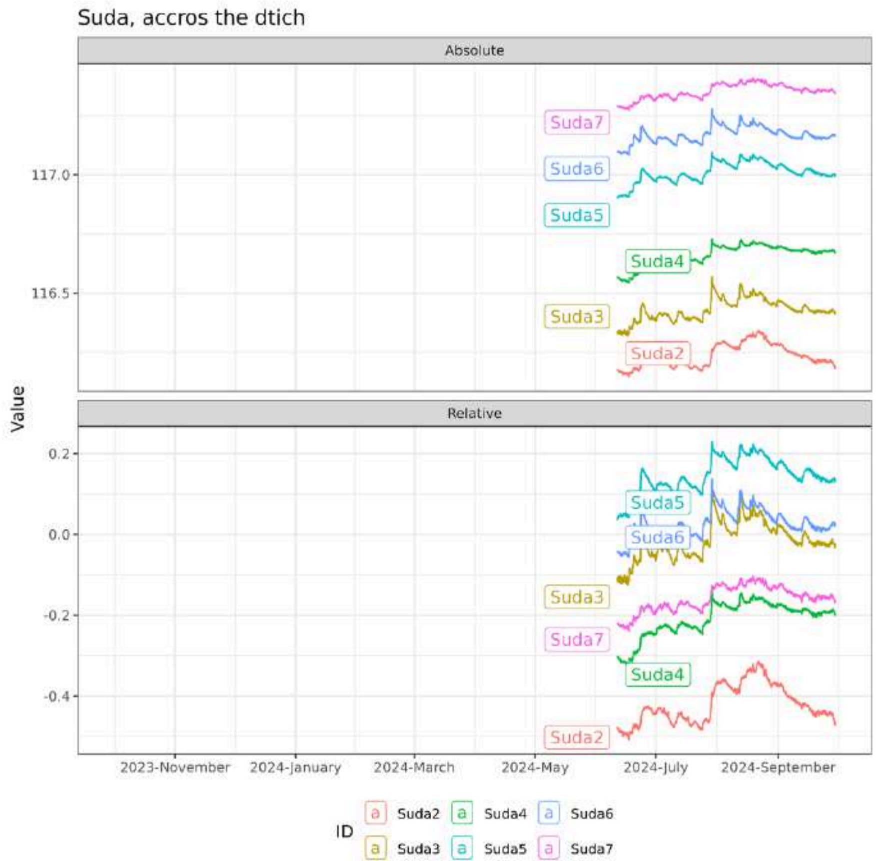

Figure 3.1.34. *Absolute (top) and relative (bottom) water level time series in radial profile at the Sudas-Zviedru Mire.*

In the radial profile we see a gradually lower water table from the open raised bog to the bog woodland (**Figure 3.1.35**). The similar albeit less clear trend is in the relative water table as well, it is on average deepest in the bog woodland (well No. Suda2) and shallower between blocked drainage ditches (Suda4) and open raised bog (Suda7) except for the wells located directly in the water of drainage ditches (Suda3, Suda5 and Suda6). A clear trend is seen for the water depths range (**Table 3.1.9.**) as well – it is highest in the forested bog (Suda2, 18 cm) and least in open raised bog (Suda7, 12 cm).

Table 3.1.9. *Summary statistics of the water table measurements in Sudas-Zviedru Mire for the period from June 11 to September 30, 2024.*

Well ID	***Mean relative water table, m***	***Min relative water table, m***	***Max relative water table, m***	***Range of the daily mean, m***	***Mean absolute water table, m***

*Suda1**	-0.03	-0.09	0.15	0.18	117.50
*Suda2**	-0.42	-0.51	-0.31	0.18	116.24
*Suda3**	-0.02	-0.12	0.12	0.22	116.43
*Suda4**	-0.21	-0.33	-0.14	0.17	116.66
*Suda5**	0.15	0.04	0.23	0.18	117.01
*Suda6**	0.03	-0.06	0.14	0.16	117.17
*Suda7**	-0.16	-0.24	-0.1	0.12	117.35

* limited observation period from June 11 to September 30, 2024

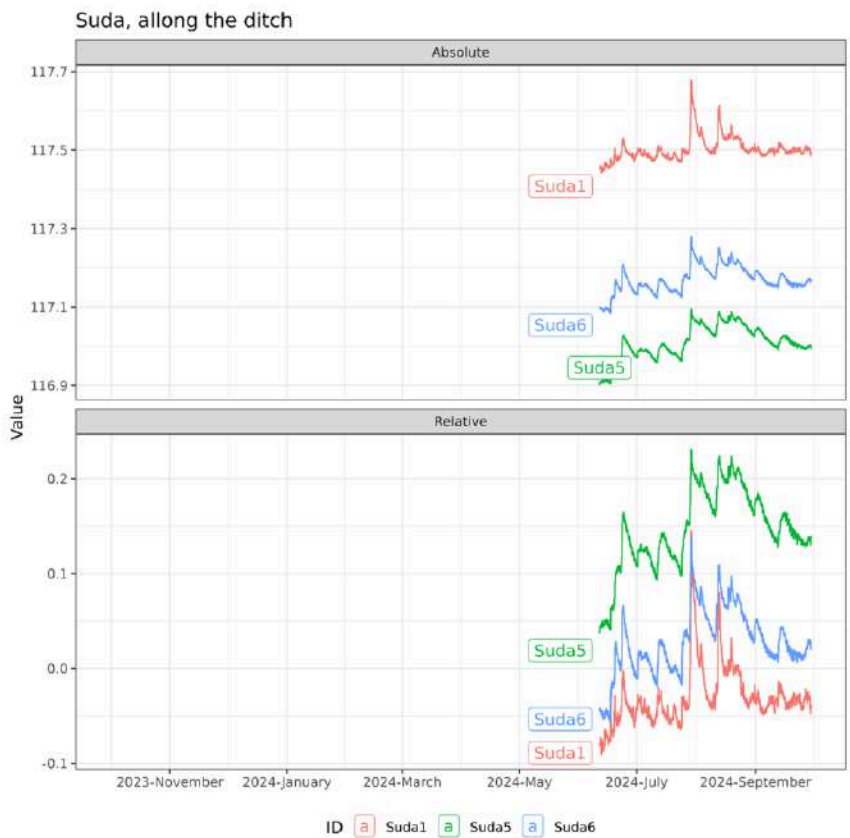

Figure 3.1.35. *Absolute (top) and relative (bottom) water level time series in a profile along a blocked drainage ditch at the Sudas-Zviedru Mire.*

The profile along a drainage ditch (**Figure 3.1.35**) shows the water table difference along a flooded (continuous open water surface) drainage ditch section without dams in between (Suda1 to Suda6, 80 m) and on two sides of a dam (Sufa 6 to Suda1). Here we see a water table gradient in the flooded ditch of 0.004 m/m, indicating that the vegetation in the ditch offers some resistance to the water flow so that a permanent water table gradient can develop

3.1.4. Melnais Lake Mire

Latest data download for groundwater level probes took place on November 11, 2025. The summary statistics is provided in **Table 3.1.1,** and the time series are described in **Figure 3.1.10**. The observations at 7 wells are grouped in 4 stations, where some of the wells are included in more than one station:

1. Water level in a dammed drainage ditch
2. A gradient towards dammed ditch
3. A gradient towards dammed ditch
4. Degraded peripheral part of the bog

Figure 3.1.10. *Description of hydrological monitoring results in Lake Melnais mire for 2025 hydrological year*

Observations	***Description***
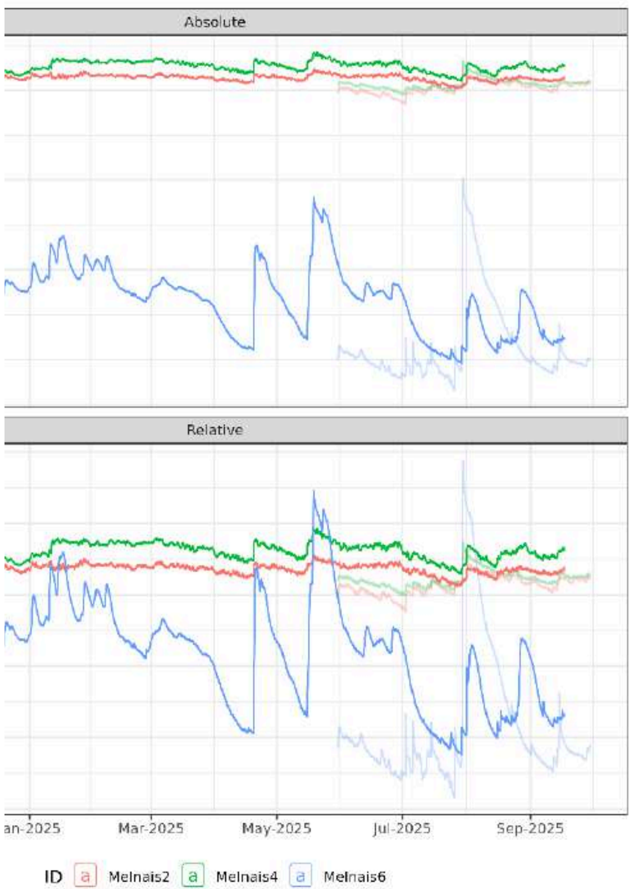	**Water level in a dammed drainage ditch**

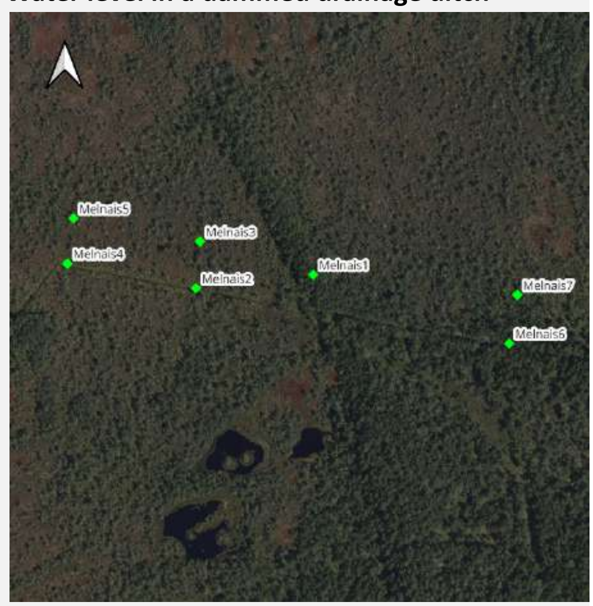

During 2025 hydrological year, except its initial months the water level at the upstream location (Melnais4) remained about 0.06 m higher than at a 80 m downstream location (Melnais2) at the same impoundment created by a dam on the ditch – a gradient similar to changes in bog surface elevation between two wells, suggesting that resistance to the flow in the ditch is gradually built up by development of submerged and surface vegetation such as *Sphagnum cuspidatum*. However, 200 m downstream (Melnais6) the water regime remains flushy demonstrating runoff accumulation from the catchment and gradual water loss, by infiltration to the groundwater in sandy mineral subsoil.

Observations	*Description*
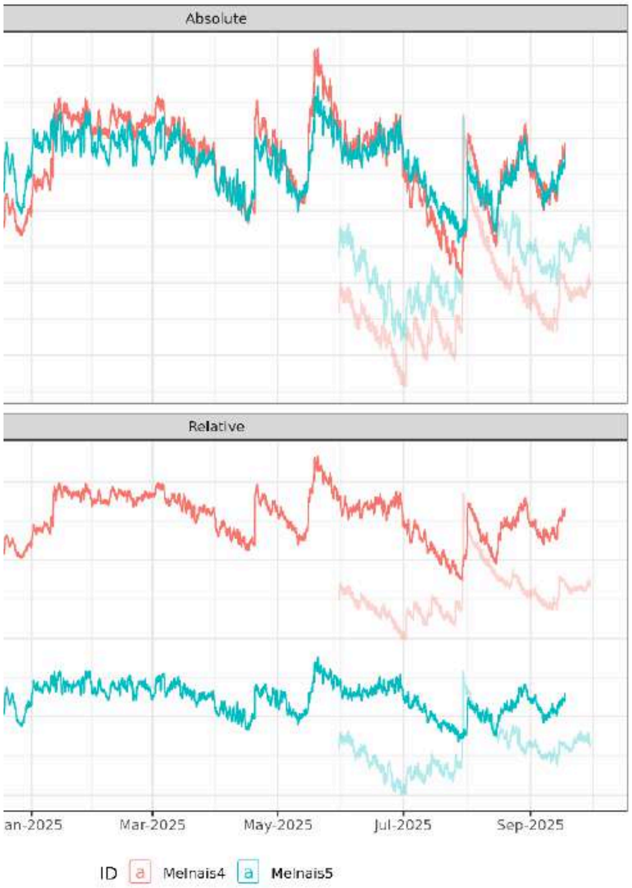	**A gradient towards dammed ditch** The water level at the two wells is very similar. The ditch well (Melnais4) has slightly higher range of fluctuations, indicating contribution by upstream catchment and slightly enhanced drainage conditions than at bog location (Melnais5).

Observations	***Description***
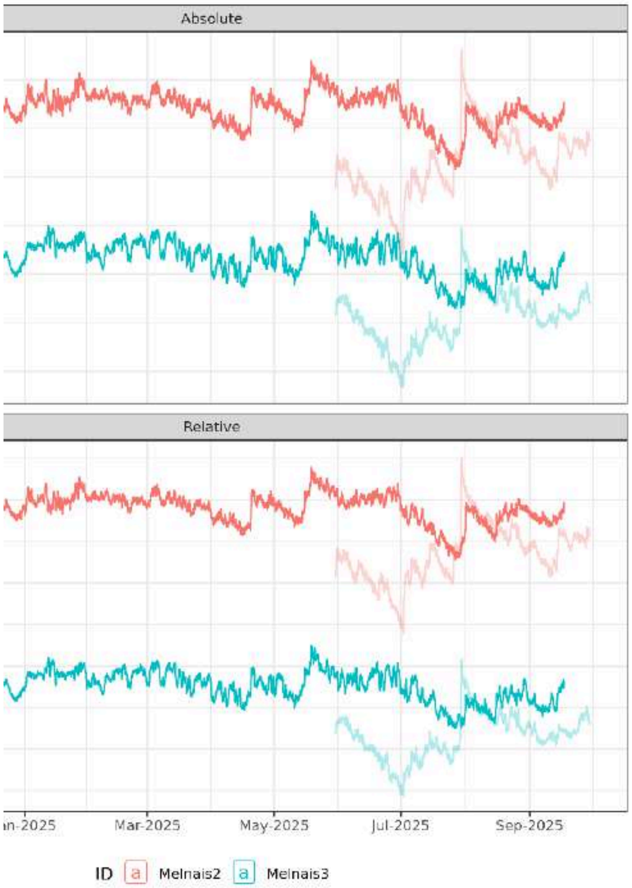	**A gradient towards dammed ditch** The water level gradient is from impoundment in the dammed ditch (Melanis2) towards the bog location (Melanis3). This demonstrates that the damming of the ditch is effectively retarding the water runoff from the bog. It can be suggested that the water filtration direction within the upper layer of the bog is towards the downstream part of the ditch where damming was not successful.

Observations | ***Description***

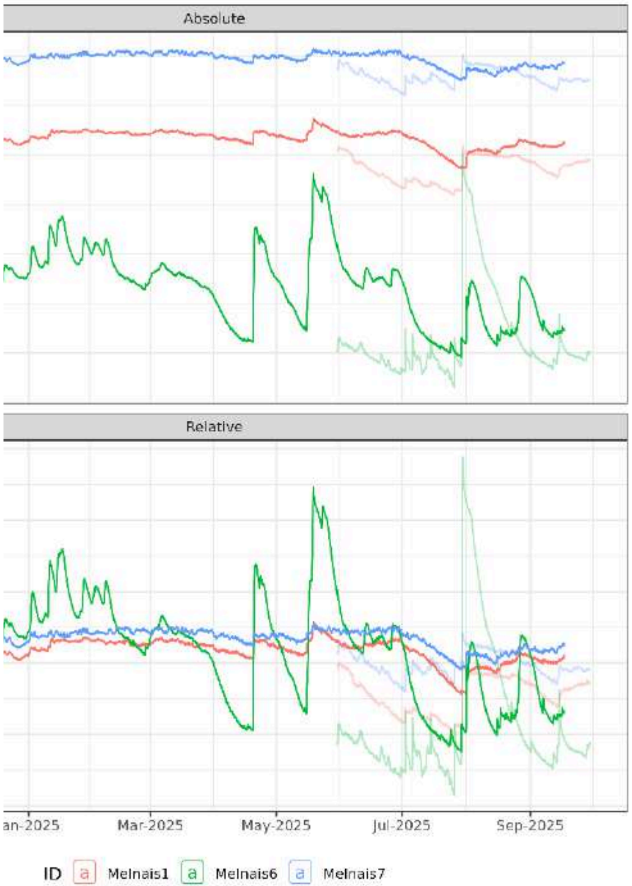

Degraded peripheral part of the bog

Both wells in the bog (Melanis1 and Melanis7) always have higher water levels than in the ditch (Melanis6), demonstrating water loss towards the ditch. Noticeably the well located in forested belt (Melanis1) has lower water level and higher range of fluctuations than the well in degraded bog (Melanis7), 0.23 and 0.16 m respectively, that is most pronounced during the dry episode in July, 2025, suggesting either higher evapotranspiration by the forest or lover water capacity of the compacted peat under the forested belt.

Water level monitoring equipment in Melnais Lake Mire was installed on May 30, 2024. The data download took place in early 2025, however the data for barometric water pressure level compensation was available up to December 13, 2024. The water level monitoring network in Sudas-Zviedru Mire comprises 7 sites organised along two profiles (Appendix 6.5).

Assessment of Water Level Observation Quality

Comparing the manual and automatic water level measurements (**Figure 3.1.36**) we see that at 5 out of 7 observation points the difference is less than 5 cm, that is rather close to combined measurement uncertainty. For the remaining two observation wells, reasons for rather large discrepancies need to be clarified and eliminated during future monitoring, when more of the control data will be available. The manual reading was taken during the installation of the groundwater pressure probes, several hours before the actual start of probe operation. Thus, one of the explanations of the discrepancy can be the water level changes during this lag period.

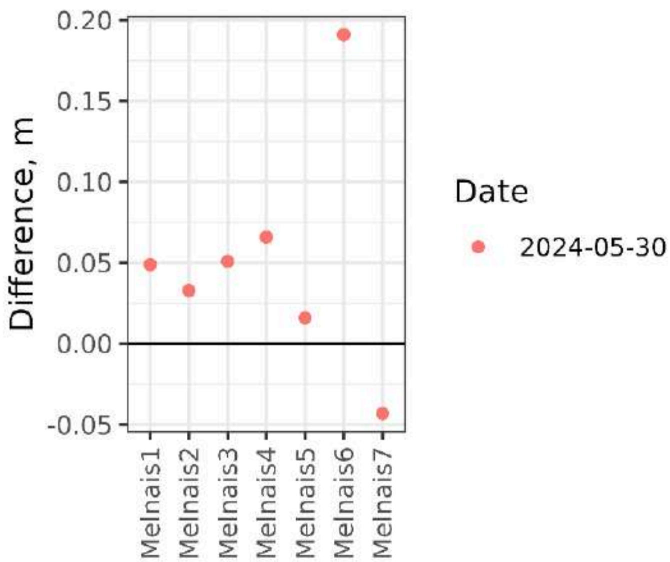

Figure 3.1.36. *The difference between automatic and manual water level measured at all but two observation points is 0.05 m or less, indicating overall good measurement quality*

Results of the groundwater level monitoring

The groundwater level monitoring results in Melnais Lake Mire can be analysed in respect to profiles (pairs of observation wells) perpendicular to the blocked drainage ditch and along the axis of the same ditch.

Two pairs (profiles) of wells (**Figure 3.1.37, Figure 3.1.38.**) located in apparently successfully restored part of the raised bog show groundwater level range of only about 15 cm. It must be noted that the highest water level was observed on July 29 associated with extreme precipitation events. The water level fluctuation range is only slightly higher in wells located in the former ditch (Melnais2 and Melnais4) compared to those located some 20 m from the ditch. At a location closer to the bog canter, the water level in the ditch just below a ditch dam (Melnais4) is lower than in the surrounding bog (Melnais5) indicating a remaining drainage towards the ditch at the study site. While in the profile closer to the margin of the mire water level in the ditch just above a dam (Melnais2) is somewhat higher than in a 20 m distance (Melnais3), that, probably, is due to water filtration around the dam towards the remaining open ditch.

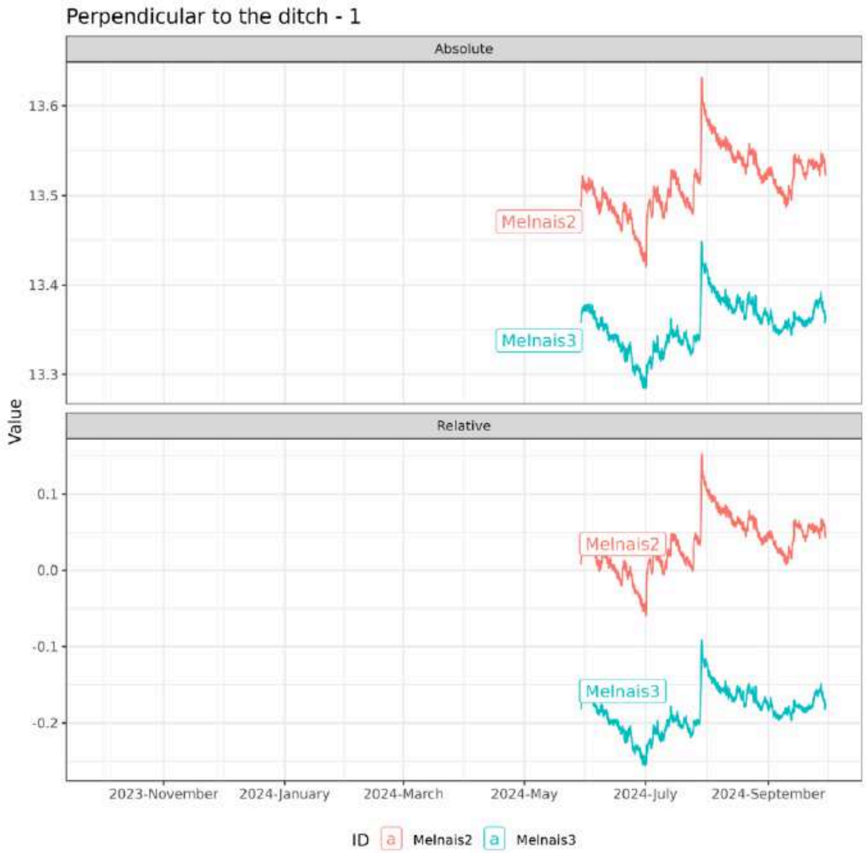

Figure 3.1.37. *The absolute (top) and relative (bottom) water level in profile towards successfully blocked drainage ditch.*

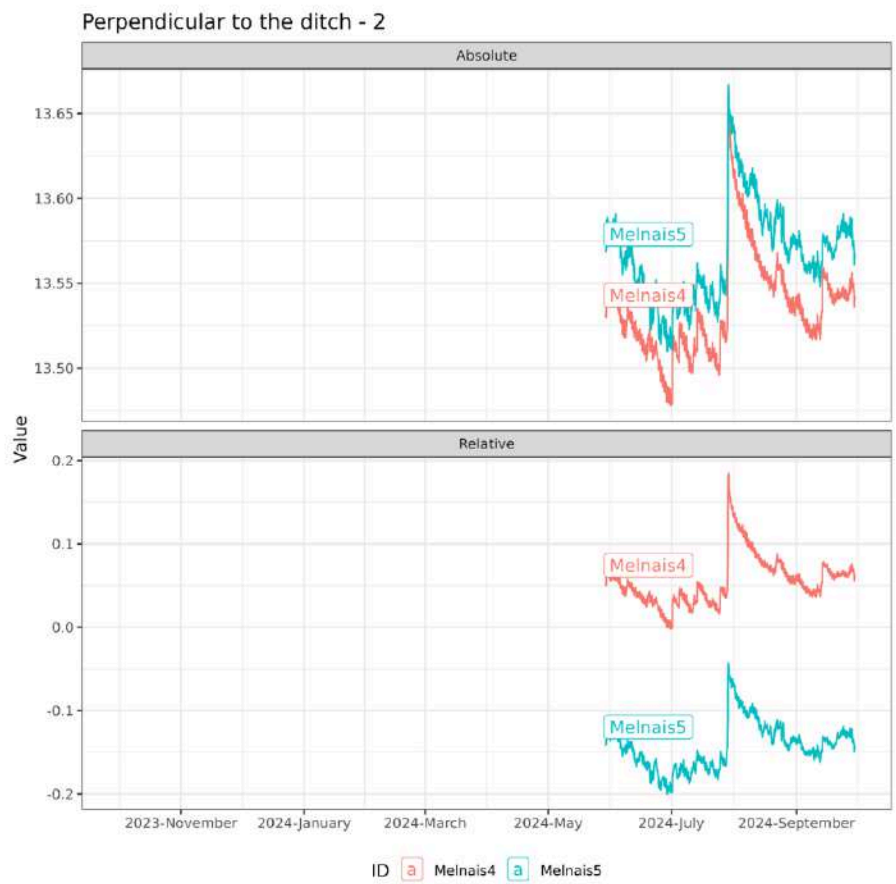

Figure 3.1.38. *The absolute (top) and relative (bottom) water level in profile towards successfully blocked drainage ditch.*

Table. 3.1.11. *Summary statistics of the water table measurements in Lake Melnais for the period from May 30 to September 30, 2024.*

Well ID	***Mean relative water table, m***	***Min relative water table, m***	***Max relative water table, m***	***Range of the daily mean, m***	***Mean absolute water table, m***
*Melnais1**	-0.36	-0.49	-0.24	0.24	12.93
*Melnais2**	0.03	-0.06	0.15	0.18	13.51
*Melnais3**	-0.18	-0.26	-0.09	0.14	13.36
*Melnais4**	0.06	0	0.18	0.16	13.54
*Melnais5**	-0.14	-0.2	-0.04	0.13	13.57
*Melnais6**	-0.47	-0.71	0.47	1.05	12.07
*Melnais7**	-0.33	-0.43	-0.22	0.18	13.32

* incomplete time series from May 30 to September 30.

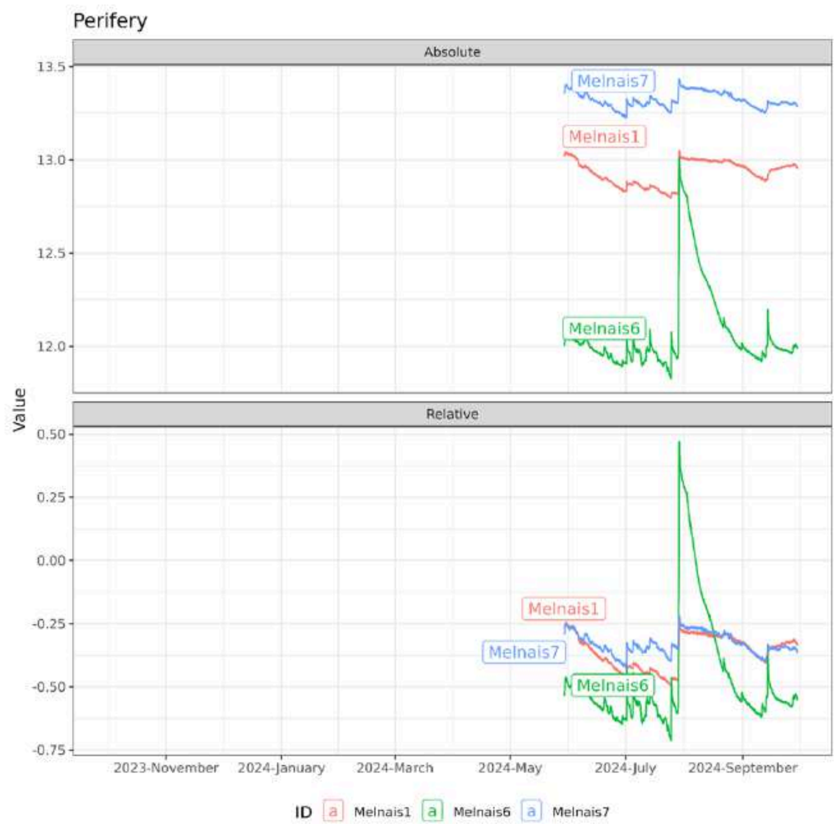

***Figure 3.1.39**. The absolute (top) and relative (bottom water level in profile towards unsuccessful blocked drainage ditch (Melanis6 and Melnais7) and dens pine forest strip in a zone between successful and unsuccessful restoration (Melnais1).*

***Figure 3.1.40**. Monitoring well Melnais6 installed in the successfully blocked ditch in Melnais Lake Mire, May 29, 2024.*

In the observation wells located at the peripheral zone of the Lake Melnais Mire near the section of the ditch that was not successfully blocked higher water level fluctuations were observed (**Figure 3.1.41**). Within the ditch (Melnais6) the water table range was more than 1.0 m (**Table 3.1.11**). Already at 20 m distance from the ditch (Melnais7) the range was less than 20 cm, however on average the water table was relatively deep - 33 cm below the surface. Within a dense pine forest strip in the peatland (Melnais1) the average water table debs were similar, but a more rapid decline rate in spring can be noticed, suggesting that higher water volume was lost to the evapotranspiration than at other locations. Alternatively, the faster water table drawdown can be due to small water capacity of the degraded peat at forest strip or localized infiltration mineral subsoil.

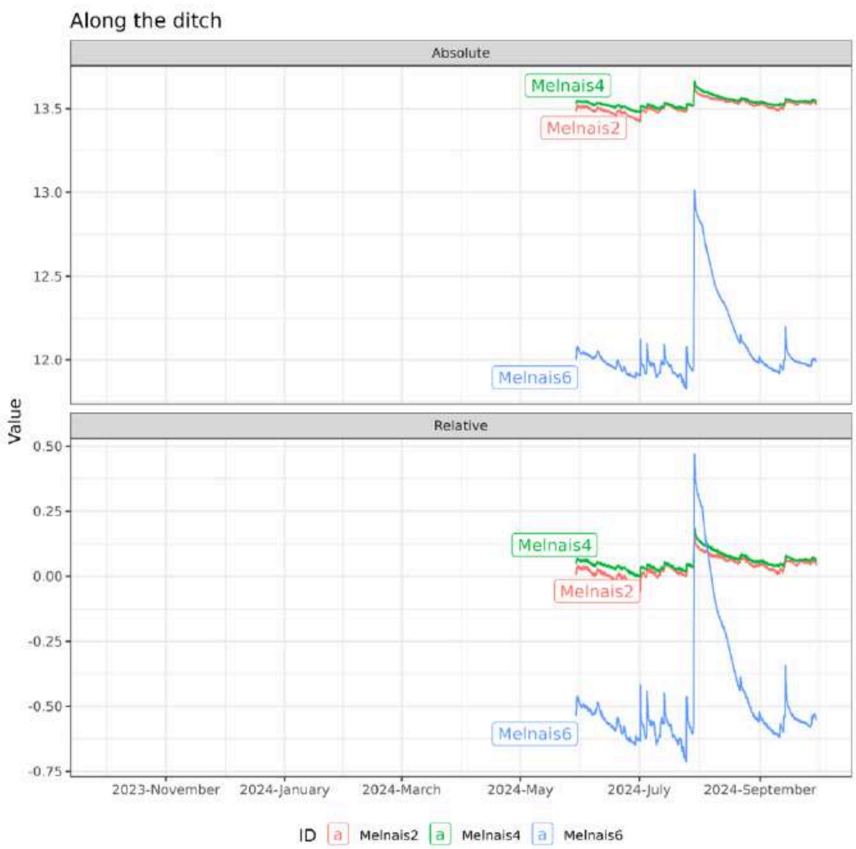

***Figure 3.1.41.** The absolute (top) and relative (bottom) water level is along the axis of the blocked drainage ditch.*

Considering the water level along the blocked ditch (**Figure 3.1.41**) we notice an encouraging sign: there water table at well Melnais4 remains higher than at downstream well Melnais2 both during periods of relatively high and low water table, although the difference (3 cm for 82 m distance) is close to measurement uncertainty. Particularly, differences in the water table after the extreme rainfall on July 29, 2024 indicates that the vegetation development in the flooded ditch creates sufficient resistance to the water flow so that a water table gradient is maintained, despite the fact the former ditch excavation is full to the brink with water.

3.2. Habitat and vegetation monitoring results

The species composition from all vegetation monitoring plots (including plots from GHG transects and GEST points) shows that the highest species richness was in Melnais Lake Mire (53), followed by Cena Mire with 44 species and the Lielais Pelečāre Mire with a total of 39 species of vascular plants, bryophytes, and lichens.

The lowest number of species was found in Sudas-Zviedru Mire with 32 species (Appendix 6.4). Altogether, 68 species were found at least in one monitoring plot. Some of the most common species that were recorded in all project sites are *Betula pendula, Pinus sylvestris, Andromeda polifolia, Calluna vulgaris, Drosera rotundifolia, Empetrum nigrum, Eriophorum vaginatum, Ledum palustre, Oxycoccus palustris, Rhynchospora alba, Rubus chamaemorus, Vaccinium uliginosum, Dicranum polysetum, Pleurozium schreberi, Sphagnum cuspidatum, S. fuscum,* and *S. medium*.

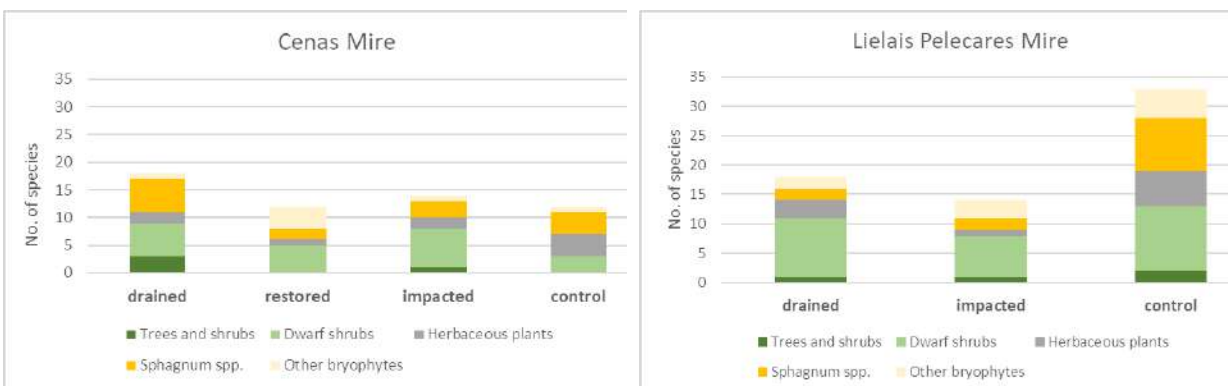

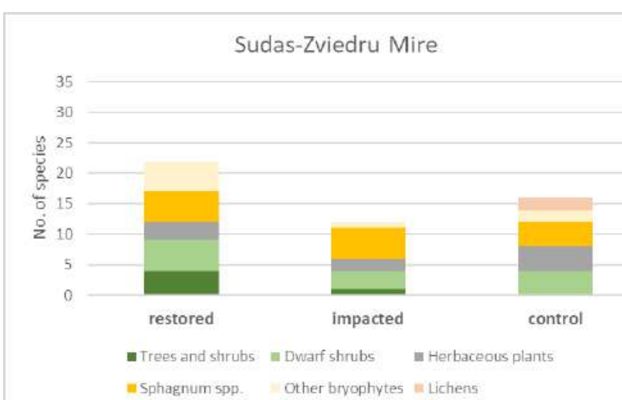

Figure 3.2.1. *Number of species in vegetation layers in vegetation monitoring plots at the water level measurement points with different drainage impact in project sites in Latvia.*

Next, the species composition is analysed among vegetation monitoring plots that were (i) close to water level measurement points or (ii) in GHG measurement transects.

The vegetation at the water level measurement points varies greatly between the sample plots with different drainage impacts – depending on whether they have been previously restored, significantly or only indirectly drained, or not affected by changes in the water regime at all. Accordingly, the number of trees, shrubs and dwarf shrubs is higher in the drained plots, while the number of herbaceous plants is higher in the natural habitats (**Figure 3.2.1**).

The most common tree species are *Betula pendula* and *B. pubescens, Pinus sylvestris*, occasionally also *Frangula alnus* and *Picea abies*. Dwarf shrub layer is species rich and especially in Lielais Pelečāre Mire with 11 species. The most common species are *Andromeda polifolia, Calluna vulgaris, Chamaedaphne calyculata, Ledum palustre, Oxycoccus palustris, Rubus chamaemorus, Vaccinium uliginosum*. *Sphagnum spp.* does not show a certain relationship with the drainage impact, as in Lielais Pelečāre Mire they are more common in the natural part of the bog, in Cenas Mire – in the degraded part, while in Sudas-Zviedru Mire the number of *Sphagnum* is relatively similar in all plot types. The other bryophyte species like *Pleurozium schreberi, Dicranum polysetum* and other forest mosses are more common in restored bog monitoring plots.

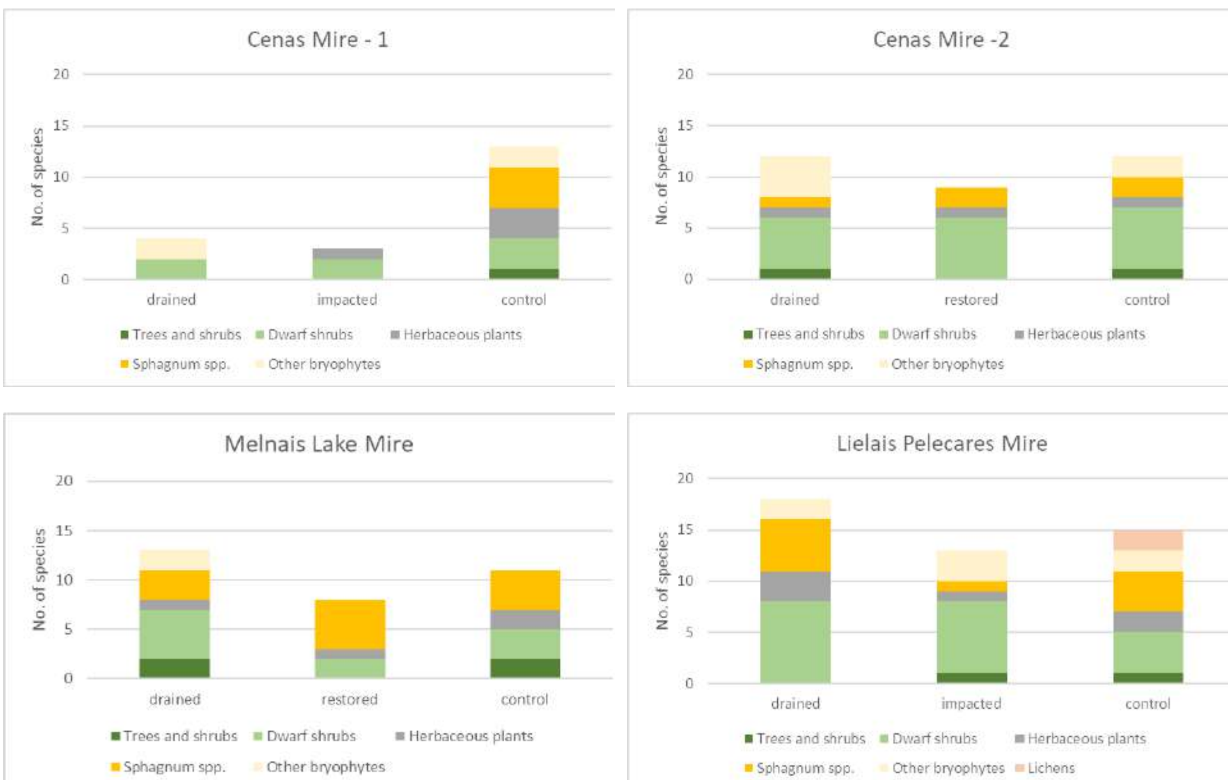

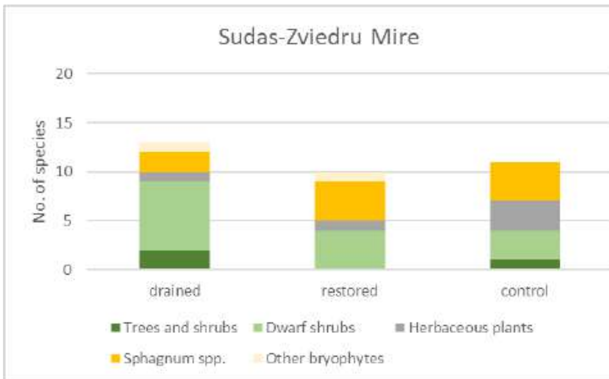

Figure 3.2.2. *Number of species in vegetation layers in vegetation monitoring plots at GHG measurement points with different drainage impact in project sites in Latvia. For the Melnais Lake Mire and Sudas-Zviedru Mire, the graphs have been updated with the 2025 monitoring data. For all other project sites, the situation from the initial monitoring conducted during the 2023 vegetation season is shown.*

Some of the species richness trends described above are also found in the GHG measurement transects (**Figure 3.2.2**). The number of drought resistant dwarf shrub species is higher in drainage impacted plots in all project sites except Cena Mire. Whereas the number of herbaceous plants and *Sphagnum* species shows relation with natural plots in all plots except Lielais Pelečāre Mire.

In the 2025 GHG monitoring of vegetation plots, no major changes were observed compared to previous periods (Appendix 6.5). However, it is noteworthy that in all three plot types of the Melnais Lake Mire an increase in *Sphagnum* species was recorded. The newly observed species are as follows: in the drained type – *Sphagnum capillifolium* and *S. divinum*; in the restored type – *S. flexuosum, S. rubellum* and *S. russowii*; in the control type – *S. tenellum*. It is possible that these species have newly colonised the plots from the surrounding area, or that they had already been present but previously undetected. Nevertheless, the rainy summer of 2025 may have prompted their improved growth and more favourable habitat conditions. It should also be noted that all *Sphagnum* species (as well as all other bryophyte and vascular plant species) recorded in earlier years in these plots were also observed during this year's monitoring.

A similar trend has also been observed in the Sudas-Zviedru Mire, namely an increase in the number of *Sphagnum* species. Accordingly, in the drained plot type *Sphagnum capillifolium* was recorded for the first time; in the restored type – *S. angustifolium, S. capillifolium* and *S. cuspidatum*; and in the control type – *S. flexuosum*. Unlike in the Melnais Lake Mirem where species composition remains relatively stable, the Sudas-Zviedru Mire shows a more dynamic pattern of species change, with either new species arriving or others disappearing across all vegetation layers. Continued monitoring is necessary to understand the causes of these changes. It is possible that the dynamics are linked to the effects of restoration measures, which may still be influencing species composition and preventing it from reaching a stable state.

In general, it cannot be argued that a natural, active raised bog has a higher species diversity than a degraded mire. However, it can be observed that the species composition is more balanced between different vegetation layers in natural habitats. Whereas in the drained parts of the mire, one of the species groups clearly dominates and disrupts the balance. Since the data series of the vegetation monitoring are still relatively short, it is not possible to analyse the restoration progress after the stabilization of the hydrological regime.

A more detailed data analysis could be performed only for the Sudas-Zviedru Mire, where the previously recorded data were directly compared with the existing species composition. In other project sites (i.e. Cena Mire and Melnais Lake Mire), some important information is missing from the historical vegetation monitoring data – either the coordinates of the sample plots or the species lists, so they can only be used to observe changes in the general species composition, but not to specifically characterize the monitoring transects. Results of this study was published in the previous Monitoring reports.

3.2.1. Vegetation monitoring data analysis for Sudas-Zviedru Mire

Data were collected six times in the same monitoring plots in the mire. The total number of plots has been reduced, so only half of the previously recorded data was used in the analysis. As indicated by the DCA ordination succession vectors, the species composition is almost similar between the natural (or control) plots and the impacted plots (**Figure 3.2.3**).

In addition, the species composition does not change significantly between monitoring years, so the points of these plots form a relatively compact cluster in the left side of DCA ordination. With monitoring sample plots in the restoration area, exactly the opposite situation is observed - from 2014 to 2023, the composition of species has changed, so they "move" away from each other in the DCA ordination. In addition, the species composition becomes more like the natural part of the mire.

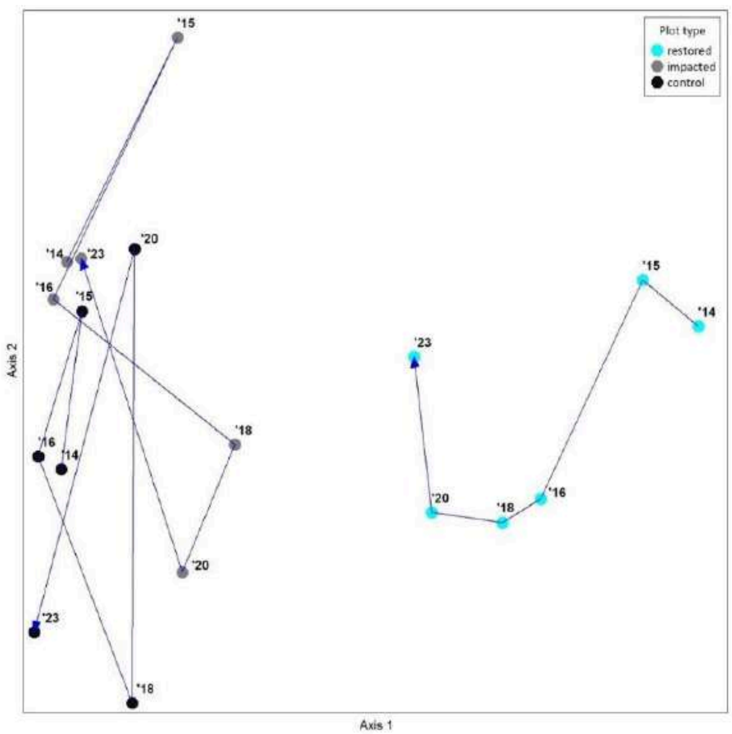

Figure 3.2.3. *DCA ordination of vegetation monitoring plots of Sudas-Zviedru Mire during nine years from 2014 to 2023.*

The total cover of species in different vegetation layers in Sudas-Zviedru Mire was compared between six monitoring years **(Figure 3.2.4)**. The curve shows almost no fluctuations in the control and the little impacted monitoring plots. On the other hand, in the restored part of the mire, there is a significant drop immediately after the restoration works, because machinery moved mechanically or operated in the sample plots. During the following four years, the vegetation has stabilized and shows tendencies to approach the natural part of the mire.

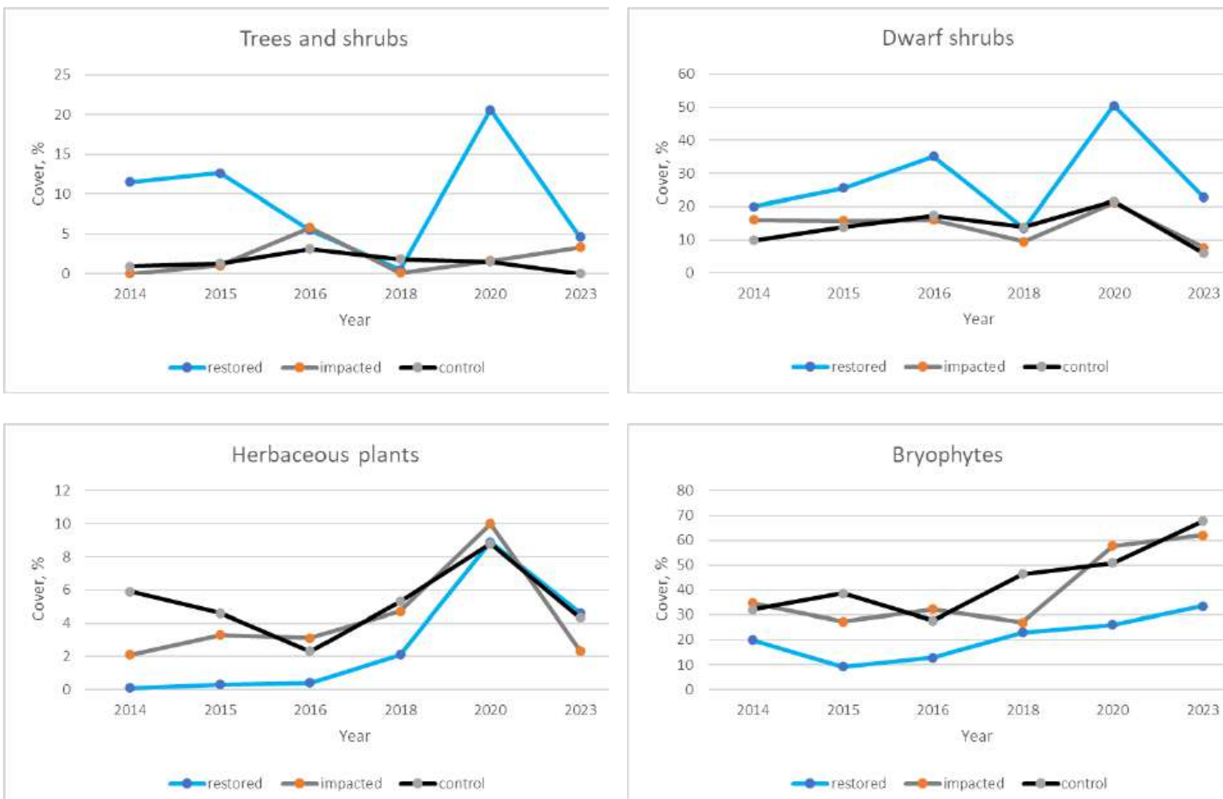

Figure 3.2.4. *Changes of the total cover (%) of species in different vegetation layers ((i) trees and shrubs; (ii) dwarf shrubs; (iii) herbaceous plants; (iv) bryophytes) during nine years in Sudas-Zviedru Mire. Hydrology stabilization in the mire was completed in 2017.*

The withering of trees near the restored ditches was also visually assessed. Positive changes over time are also expected in the dwarf shrub layer. The total cover of *Calluna vulgaris* could slowly decrease and be replaced by herbaceous plants or *Sphagnum* species.

3.3. Greenhouse gas emission monitoring

The monitoring results indicate that the Latvian case study sites form a coherent ecological gradient from near-natural raised bog conditions through rewetted systems to degraded drained peatland habitats. The habitat sequence shown in the presentation encompasses natural and near-natural raised bogs, strongly drainage-affected peat fields, sites influenced by drainage ditches, tree-covered degraded peatlands, dense tree-layer stands under both strong and weak drainage impact, and rewetted or restored sites with varying vegetation cover. This gradient is important because it provides the ecological background against which the observed greenhouse gas fluxes, soil properties, and vegetation-derived carbon inputs can be interpreted. Rather than representing isolated site classes, these categories describe different positions along a peatland transformation continuum in which hydrology, vegetation structure, substrate quality, and biogeochemical functioning co-vary.

A central outcome of the monitoring is that the different greenhouse gas components do not respond in the same direction across the site categories. The results suggest lower soil carbon mineralisation and a tendency towards stronger carbon sink behaviour in near-natural and rewetted sites than in degraded sites, but this is accompanied by elevated non-CO_2 emissions, especially CH_4 and at some sites N_2O, in the wetter categories. This combination is characteristic of rewetted peatlands globally: hydrological restoration tends to suppress aerobic peat oxidation and reduce CO_2 losses, yet the return of anaerobic conditions creates environmental space for methanogenesis and, depending on nutrient status and redox oscillation, can also generate episodic or persistent N_2O emissions. Comparable behaviour has been reported in Danish bog and fen mesocosms, where rewetting reduced cumulative CO_2-equivalent emissions from heterotrophic respiration while CH_4 responses remained highly site-specific and strongly linked to peat geochemistry.

GHG efflux variation

Variation in ecosystem CO_2 emissions (R_{eco}) in areas without tree cover and forest floor CO_2 emissions (R_{floor}) in forested areas during the study period by different seasons and habitat types is shown in Figure 3.3.1 and Appendix 6.7. Statistically significant differences in variation of ecosystem CO2 emissions between different habitat types were observed ($p < 0.05$).

The highest CO_2 emissions (R_{eco} or R_{floor} depending on habitat type, including both soil heterotrophic respiration and autotrophic respiration) were observed during summer months (June – August).

In summer months, the highest ecosystem CO_2 were observed in drained raised bog with dense tree layer (mean 153.9 mg CO_2-C m^{-2} h^{-1}) followed by degraded bog woodland (mean 145.1 mg CO_2-C m^{-2} h^{-1}) and restored and rewetted raised bog (mean 135.9 mg CO_2-C m^{-2} h^{-1}), while the lowest ecosystem CO_2 emissions were observed in peat fields (108.8 mg CO_2-C m^{-2} h^{-1}) and natural and near-natural raised bog (mean 115.1 mg CO_2-C m^{-2} h^{-1}).

Specifically in drained raised bog with dense tree layer, the highest mean CO_2 flux value (in summer months) was observed in drained raised bog with dense tree layer in the strong drainage impact zone (200.1 mg CO_2-C m^{-2} h^{-1}). In general, the lowest CO_2 fluxes were observed in winter months (December – February). Further steps include estimation of net annual CO_2 emissions considering share of soil heterotrophic respiration (R_{het}) and carbon input into soil with above- and belowground litter of vegetation (**Figure 3.3.2.**)

Subplot A (near-natural raised bog) in LPC_1 Sudas-Zviedru Mire. Image: © G. Saule

Subplot B (rewetted degraded raised bog with direct restoration effect) in LPC_1 Sudas-Zviedru Mire. Image: © G. Saule

Subplot C (rewetted overgrown raised bog with cumulative restoration effect) in LPC_1 Sudas-Zviedru Mire. Image: © G. Saule

Subplot A (near-natural raised bog in LPC_2 Lielais Pelečāre Mire. Image: © G. Saule

Subplot B (drained raised bog with dense tree layer in the strong drainage impact zone) in LPC_2 (Lielais Pelečāre Mire). Image: © G. Saule.

Subplot C (drained raised bog with dense tree layer in the weak drainage impact zone) in LPC_2 (Lielais Pelečāre Mire). Image: © G. Saule.

Figure 3.3.1. *Greenhouse gas emission monitoring study sites and subplots representing different habitat types*

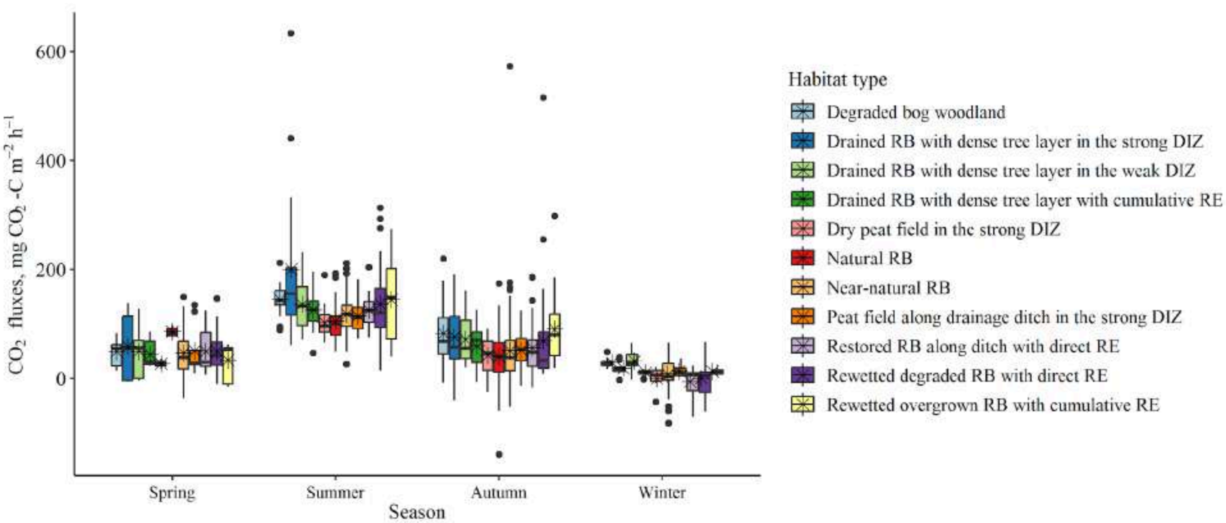

Figure 3.3.2. *Variation in ecosystem CO_2 emissions (R_{eco}) in areas without tree cover and forest floor CO_2 emissions (R_{floor}) in forested areas during the study period by different seasons and habitat types*[1]

[1] DIZ – drainage impact zone; RE – restoration effect; RB – raised bog. The boxes show 25th and 75th percentiles, horizontal line – median value, asterisk – mean value, whiskers – minimal and maximal values or 1.5 time the interquartile range if outlier values are presented (points).

Variation in soil heterotrophic respiration (R_{het}) during the study period by different seasons (spring, summer, autumn) and habitat types is shown in **Figure 3.3.3**. Among all studied habitat type, the highest mean soil heterotrophic respiration was observed during summer months (June – August). In summer months, the highest mean soil heterotrophic respiration was observed in degraded bog woodland, while the lowest in natural and near-natural raised bog. Furthermore, statistically significant differences in variation of soil heterotrophic respiration between different habitat types were observed ($p < 0.05$). Further steps include estimation of net annual CO_2 emissions considering carbon input into soil with above- and belowground litter of vegetation.

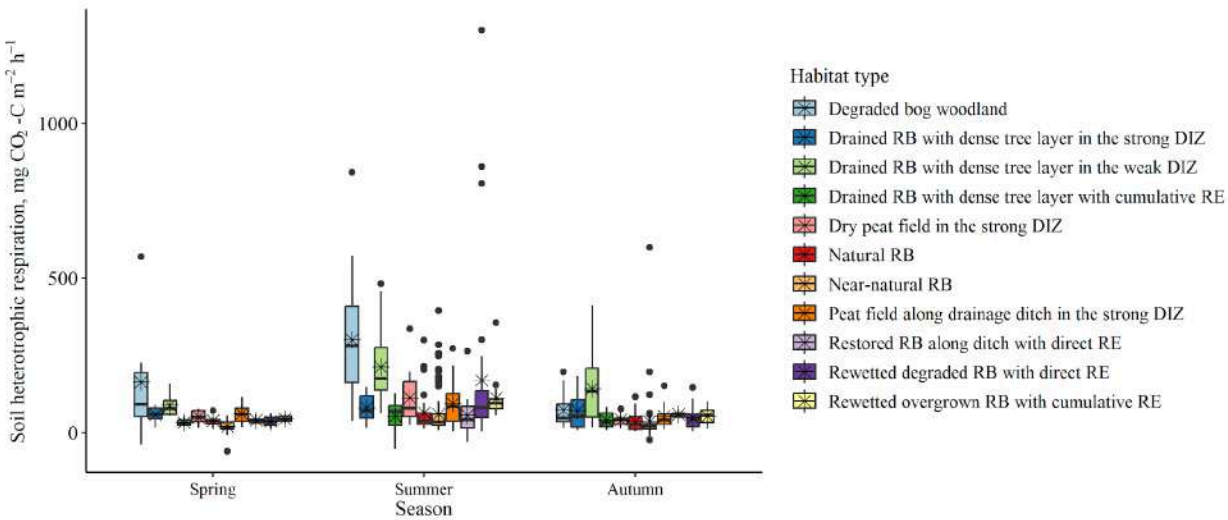

Figure 3.3.3. *Variation in soil heterotrophic respiration (R_{het}) during the study period (vegetation period) by different habitat types*[2]

Variation in CH_4 emissions during the study period by different seasons and habitat types is shown in **Figure 3.3.4.** According to the preliminary estimates (June 2023 – December 2024), the highest mean CH_4 fluxes were observed in rewetted degraded raised bog with direct restoration effect (5036.9 µg CH_4-C m^{-2} h^{-1} in summer months June – August and 3389.8 µg CH_4-C m^{-2} h^{-1} in autumn months September – November), followed by restored raised bog along ditch with direct restoration effect (2609.9 µg CH_4-C m^{-2} h^{-1} in summer months June – August and 2714.4 µg CH_4-C m^{-2} h^{-1} in autumn months September – November), while soils in drained raised bog with dense tree layer with cumulative restoration effect during autumn months (September-November) were sink of CH_4 (CH_4 removals were observed, mean -65.7 µg CH_4-C m^{-2} h^{-1}). Statistically significant differences in variation of CH_4 emissions between different habitat types were observed ($p < 0.05$).

2 DIZ – drainage impact zone; RE – restoration effect; RB – raised bog. The boxes show 25th and 75th percentiles, horizontal line – median value, asterisk – mean value, whiskers – minimal and maximal values or 1.5 time the interquartile range if outlier values are presented (points).

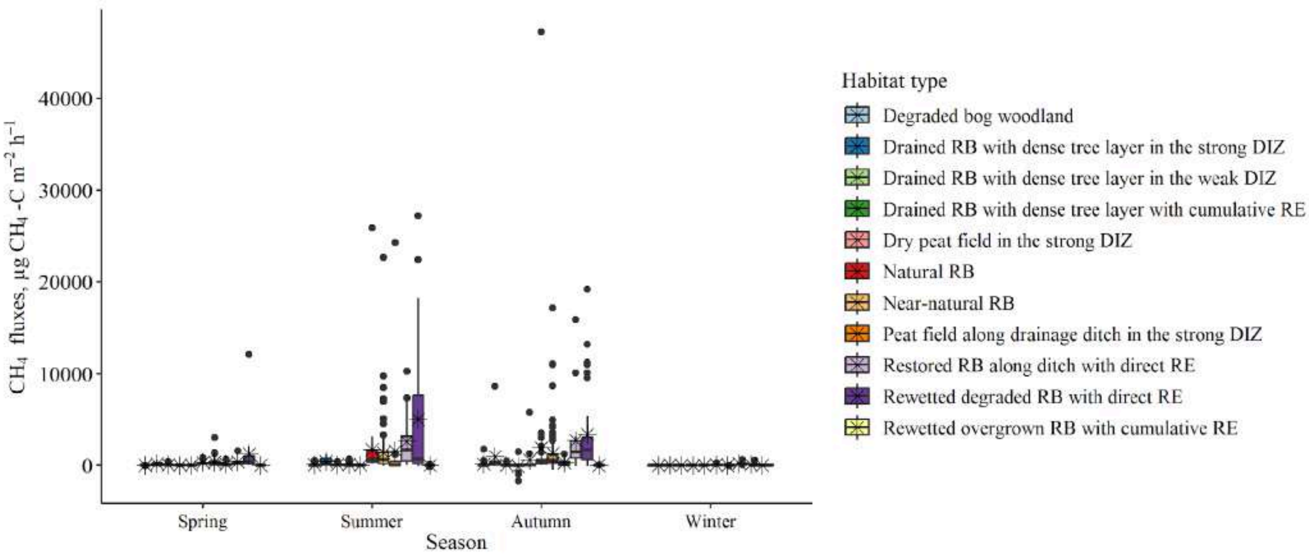

Figure 3.3.4. *Variation in CH_4 emissions during the study period by different seasons and habitat types*[3]

Variation in N_2O emissions during the study period by different seasons and habitat types is shown in **Figure. 3.3.5.** According to the preliminary estimates (June 2023 – December 2024), the highest mean N_2O fluxes (64.4 µg N_2O-N m^{-2} h^{-1}) were observed in peat field along drainage ditch in the strong drainage impact zone in spring months (March – May) followed by restored raised bog along ditch with direct restoration effect in summer months (June – August, mean 50.3 µg N_2O-N m^{-2} h^{-1}). Statistically significant differences in variation of N_2O emissions between different habitat types were observed ($p < 0.05$).

[3] DIZ – drainage impact zone; RE – restoration effect; RB – raised bog. The boxes show 25th and 75th percentiles, horizontal line – median value, asterisk – mean value, whiskers – minimal and maximal values or 1.5 time the interquartile range if outlier values are presented (points).

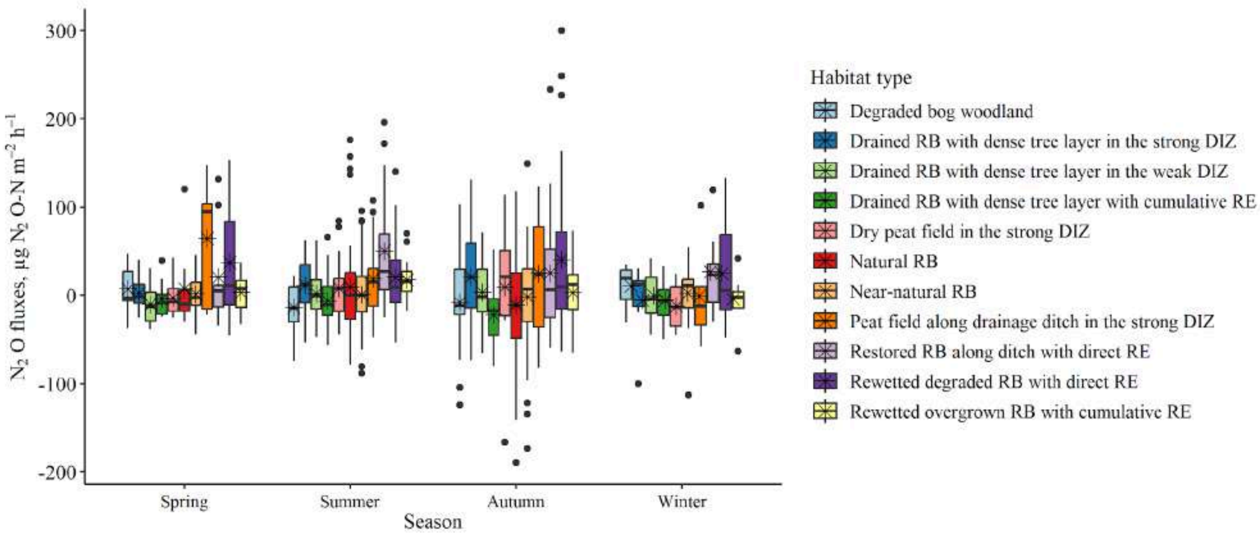

Figure 3.3.5. *Variation in N_2O emissions during the study period by different seasons and habitat types*[4]

In general, preliminary estimates of GHG emissions including CO_2 (both ecosystem respiration and soil heterotrophic respiration), CH_4 and N_2O emissions showed significant variation in GHG emissions between different habitat types including restored/rewetted raised bog and areas that will be rewetted (for instance, peat fields). Seasonal (temperature) effect were particularly noticeable in relation to CO_2 emissions, while groundwater level, which directly depends on management activities, showed impact on magnitude of CH_4 emissions. Further steps include estimation of total net GHG emission balance (annual) across different habitats including estimation of net annual CO_2 emissions (soil CO_2 balance) considering carbon input into soil with above- and belowground litter of vegetation.

Soil chemical properties

The main soil chemical properties in different topsoil layers (O horizon if presented in the study sites, 0-10 cm and 10-20 cm soil layer) in different habitat types are shown in **Figure 3.3.6** (soil bulk density), **Figure 3.3.7** (soil pH $CaCl_2$), **Figure 3.3.8** (organic carbon (OC) concentration), **Figure 3.3.9** (total nitrogen (TN) concentration) and **Figure 3.3.10** (concentrated nitric acid (HNO_3) extractable potassium (K) concentration). Among studied habitat types mean soil bulk density in 0-10 cm soil layer ranged from 40.4 kg m^{-3} (in rewetted degraded raised bog with direct restoration effect) to 160.1 kg m^{-3} (dry peat field in the strong drainage impact zone), while in 10-20 cm soil layer mean soil bulk density ranged from 67.0 kg m^{-3} (in natural raised bog) to 481.6 kg m^{-3} (in degraded bog woodland). In deeper analysed soil layers (20-50 cm), soil bulk density among studied habitat types ranged from 33.6 to 256.5 kg m^{-3}.

4 DIZ – drainage impact zone; RE – restoration effect; RB – raised bog. The boxes show 25th and 75th percentiles, horizontal line – median value, asterisk – mean value, whiskers – minimal and maximal values or 1.5 time the interquartile range if outlier values are presented (points).

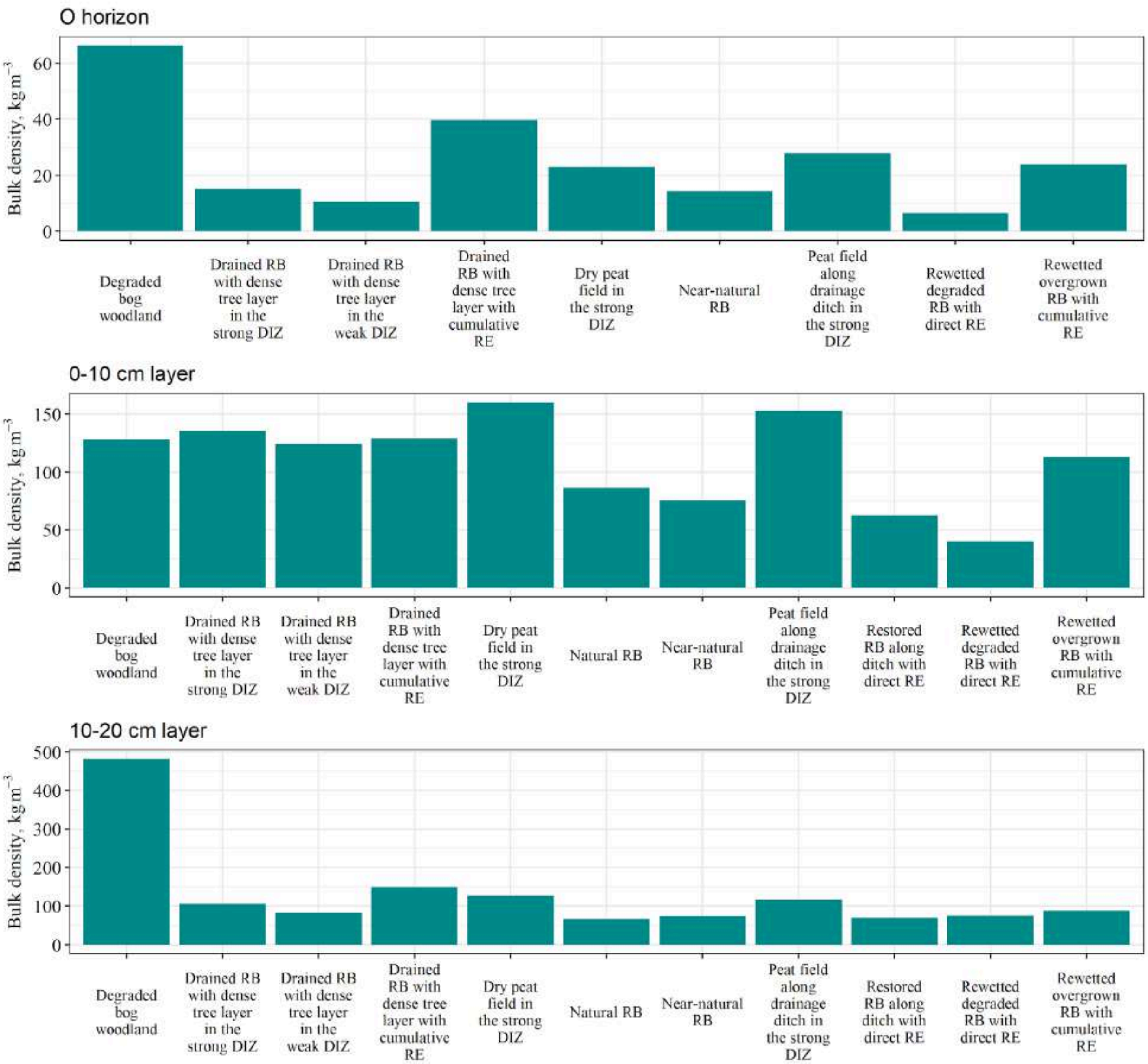

Figure 3.3.6. *Soil bulk density (O horizon, 0-10 cm and 10-20 cm soil layer) by habitat types*[5]

Among studied habitat types mean soil pH ($CaCl_2$) in topsoil layers (0-10 cm and 10-20 cm soil layer) ranged from 2.4 (in drained raised bog with dense tree layer with cumulative restoration effect and in restored raised bog along ditch with direct restoration effect) to 3.1 in natural raised bog (**Figure 3.3.7.**). In deeper analysed soil layers (20-50 cm), soil pH ($CaCl_2$) ranged from 2.4 to 3.7.

[5] DIZ – drainage impact zone; RE – restoration effect; RB – raised bog.

Figure 3.3.7. *Soil pH ($CaCl_2$) in different soil layers (O horizon, 0-10 cm and 10-20 cm soil layer) by habitat types*[6]

Among studied habitat types, organic carbon (OC) concentration in 0-10 cm soil layers ranged in a relatively narrow range – from 492.5 g kg^{-1} in natural raised bog to 528.9 g kg^{-1} in drained raised bog with dense tree layer in the strong drainage impact zone. In the 10-20 cm soil layer, OC concentration ranged from 379.3 g kg^{-1} in degraded bog woodland to 540.8 g kg^{-1} in restored raised bog along the ditch with direct restoration effect (**Figure 3.3.8**). In deeper analysed soil layers (20-50 cm), OC concentration ranged from 433.8 to 539.7 g kg^{-1} reflecting organic matter rich (peat) soil also in deeper soil layers.

6 DIZ – drainage impact zone; RE – restoration effect; RB – raised bog.

Figure 3.3.8. *Organic carbon (OC) concentration in different soil layers (O horizon, 0-10 cm and 10-20 cm soil layer) by habitat types*[7]

Among studied habitat types, total nitrogen (TN) concentration in 0-10 cm soil layers ranged from 12.2 g kg^{-1} in natural raised bog to 17.0 g kg^{-1} in peat fields along drainage ditch in the strong drainage impact zone. In the 10-20 cm soil layer, TN concentration ranged from 9.5 g kg^{-1} in drained raised bog with dense tree layer in the weak drainage impact zone to 19.4 g kg^{-1} in drained raised bog with dense tree layer in the strong drainage impact zone (**Figure 3.3.9**). In deeper analysed soil layers (20-50 cm), TN concentration ranged from 7.8 to 20.3 g kg^{-1}.

[7] DIZ – drainage impact zone; RE – restoration effect; RB – raised bog.

Figure 3.3.9. *Total nitrogen (TN) concentration in different soil layers (O horizon, 0-10 cm and 10-20 cm soil layer) by habitat types*[8]

Among studied habitat types mean concentrated nitric acid (HNO_3) extractable potassium (K) concentration in 0-10 cm soil layer ranged from 0.25 g kg^{-1} in drained raised bog with dense tree layer in the strong drainage impact zone to 1.11 g kg^{-1} in rewetted degraded raised bog with direct restoration effect. In the 10-20 cm soil layer, K concentration ranged from 0.14 g kg^{-1} in drained raised bog with dense tree layer in the weak drainage impact zone to 0.62 g kg^{-1} in drained raised bog with dense tree layer in the strong drainage impact zone (**Figure. 3.3.10**). In deeper analysed soil layers (20-50 cm), K concentration ranged from 0.02 to 0.48 g kg^{-1}.

[8] DIZ – drainage impact zone; RE – restoration effect; RB – raised bog.

Figure 3.3.10. *Concentrated nitric acid (HNO_3) extractable potassium (K) concentration in different soil layers (O horizon, 0-10 cm and 10-20 cm soil layer) by habitat types*[9]

The soil property charts provide an explanatory context for the respiration and carbon balance gradients. Mean topsoil nitrogen was approximately 12.68 g kg^{-1} in near-natural sites, 14.38 g kg^{-1} in rewetted sites, and 14.39 g kg^{-1} in degraded sites. Mean topsoil phosphorus was about 0.473, 0.533, and 0.417 g kg^{-1}, respectively, while topsoil potassium averaged 0.535, 0.617, and 0.381 g kg^{-1}. Soil pH declined from about 2.92 in near-natural sites to 2.70 in rewetted and 2.57 in degraded sites. Thus, compared with near-natural sites, degraded sites combined higher topsoil nitrogen with lower pH and lower phosphorus and potassium, whereas rewetted sites appeared relatively enriched in P and K and intermediate in pH.

[9] DIZ – drainage impact zone; RE – restoration effect; RB – raised bog.

The most straightforward interpretation is that nutrient availability alone does not explain the carbon-balance gradient, but interacts with hydrology and peat decomposition history. Degraded sites have experienced prolonged drainage, which likely exposed peat to aerobic decomposition, mineralised organic matter, and altered nutrient pools. Their high heterotrophic respiration despite comparatively low mean P and K suggests that aeration and the legacy of decomposed surface peat are stronger controls than current macronutrient concentrations alone. Near-natural sites, despite having lower N, showed the lowest heterotrophic respiration and the strongest estimated soil sink. This is consistent with classic bog biogeochemistry: low pH, low nutrient availability, and sustained saturation, slow decomposition and favour organic matter accumulation. Rewetted sites fall between these states and appear to combine restored hydrological control with still-elevated nutrient availability from earlier drainage or post-restoration mobilisation (Albert-Saiz et al., 2025).

The elevated P and K in rewetted sites may also be relevant to methane and nitrous oxide dynamics. Rewetting can mobilise nutrients from previously oxidised surface peat and from redox-sensitive soil phases. Urbanová and co-authors showed that peat rewetting can alter nutrient fluxes and CH_4 production potential, and later work has reinforced that rewetted peatlands may experience a phase of nutrient leaching or solute mobilisation, especially where the surface peat is strongly decomposed or hydrology remains unstable. The higher electrical conductivity observed in rewetted sites in the Latvian presentation is consistent with that possibility (Urbanová et al., 2011).

Environmental variables

The variation in main environmental variables during the study period in different habitat types is shown in **Figure 3.3.11** and **Figure 3.3.12** (groundwater level below soil surface and soil moisture), **Figure 3.3.13** (air and soil temperature).

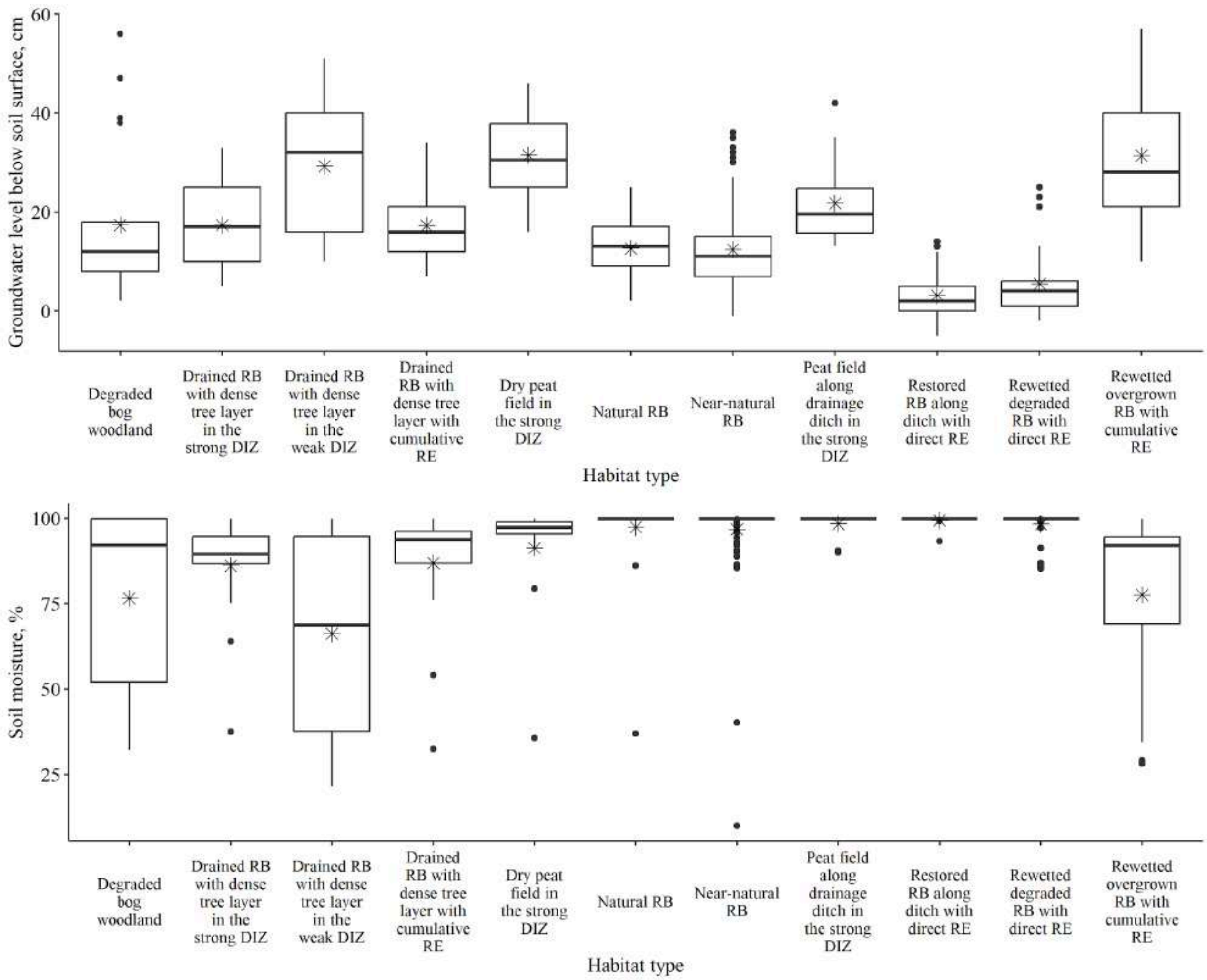

***Figure 3.3.11**. Variation in groundwater level below soil surface and soil moisture during the study period by habitat types*[10]

[10] DIZ – drainage impact zone; RE – restoration effect; RB – raised bog. The boxes show 25th and 75th percentiles, horizontal line – median value, asterisk – mean value, whiskers – minimal and maximal values or 1.5 time the interquartile range if outlier values are presented (points).

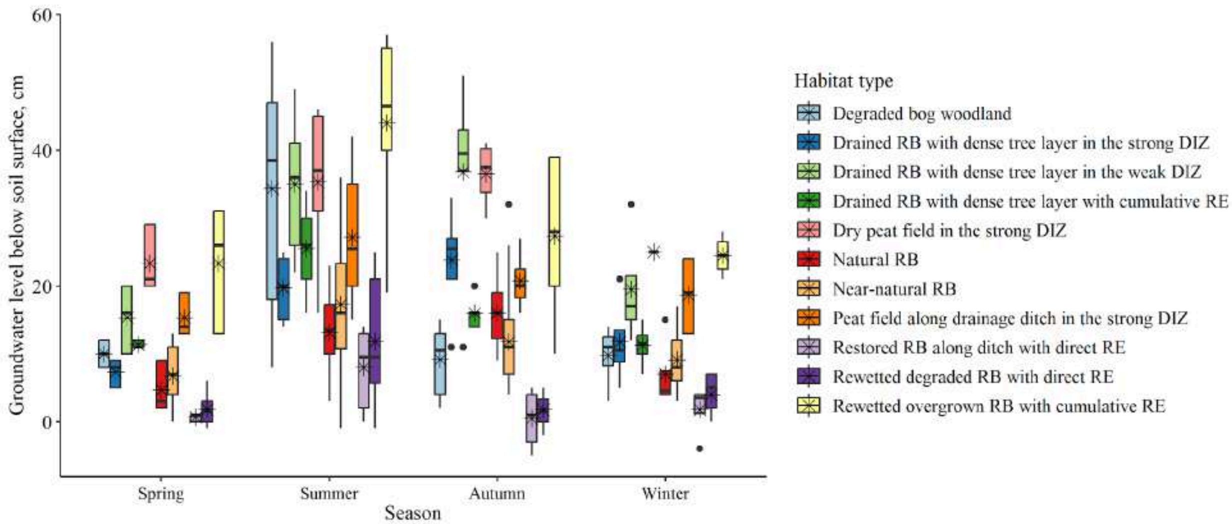

Figure 3.3.12. *Variation in groundwater level below soil surface during the study period (different seasons) by habitat types*[11]

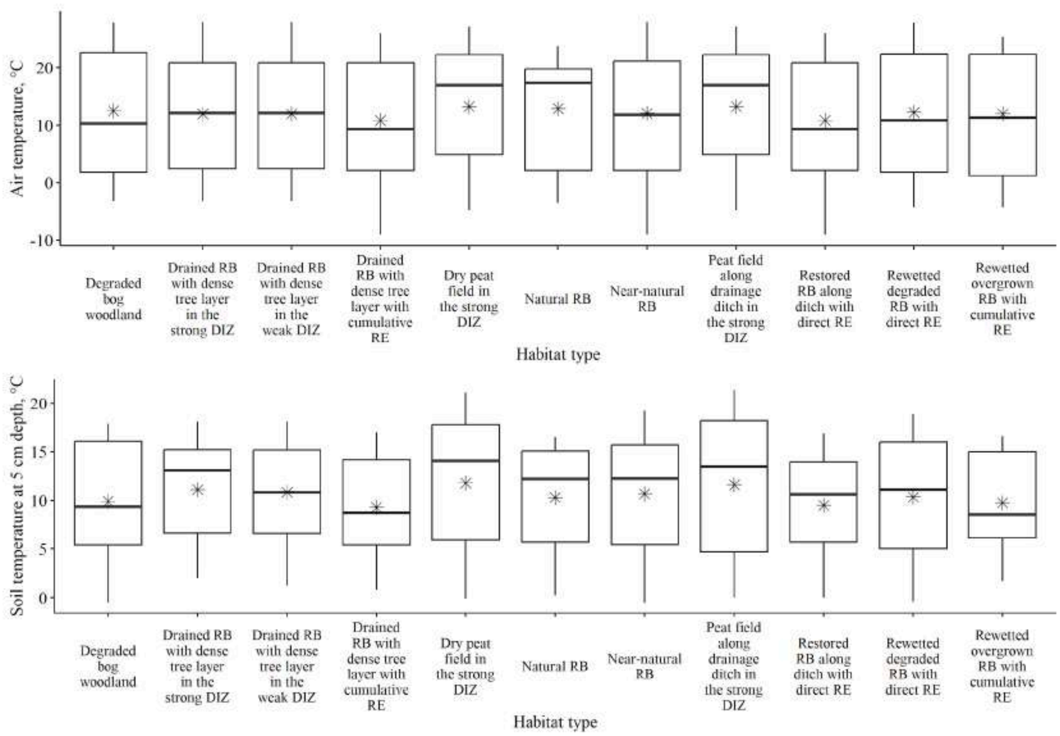

Figure 3.3.13. *Variation in air and soil temperature during the study period by habitat types*[12]

11

12 DIZ – drainage impact zone; RE – restoration effect; RB – raised bog. The boxes show 25th and 75th percentiles, horizontal line – median value, asterisk – mean value, whiskers – minimal and maximal values or 1.5 time the interquartile range if outlier values are presented (points).

3.3.1. Biomass

The biomass results show that vegetation structure differed among near-natural, rewetted, and degraded site categories, but not in a uniform way across all biomass pools. Aboveground vascular plant biomass remained within a relatively narrow interval across the categories, with mean values close to 2.5-2.9 t C ha^{-1} yr^{-1}. Near-natural sites appear to centre around roughly 2.5-2.6 t C ha^{-1} yr^{-1}, rewetted sites around 2.8-2.9 t C ha^{-1} yr^{-1}, and degraded sites around 2.5-2.6 t C ha^{-1} yr^{-1} (**Figure 3.3.14**). The medians are similarly close, implying that the herbaceous or low-stature vascular component was not the principal source of divergence among site categories. Instead, the larger differences emerge in the woody component and in moss production.

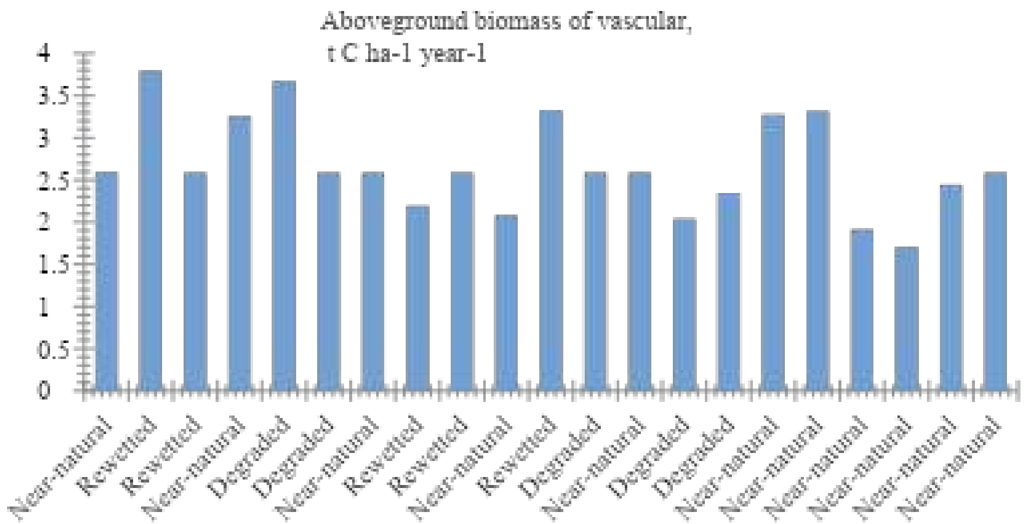

Figure 3.3.14. *Aboveground biomass of vascular plants*

Aboveground woody biomass was markedly higher and more variable in rewetted and degraded sites than in near-natural sites. The mean in near-natural sites is visually close to 4.7–4.8 t C ha^{-1} yr^{-1}, with a relatively tight box and only a few higher points. In rewetted sites the mean is approximately 5.0 t C ha^{-1} yr^{-1}, but the distribution is much broader, extending from about 3 to almost 11 t C ha^{-1} yr^{-1}. In degraded sites the mean appears still higher, around 6.0–6.2 t C ha^{-1} yr^{-1}, again with very wide variability and upper values near 11 t C ha^{-1} yr^{-1} (**Figure 3.3.15**). This pattern indicates that woody encroachment or retention of woody biomass remains important in the altered peatland states, especially where drainage has promoted tree establishment and where rewetting has not yet fully reversed vegetation legacy effects. In practical terms, the degraded category appears to preserve the clearest signal of long-term drainage-driven secondary woodland development.

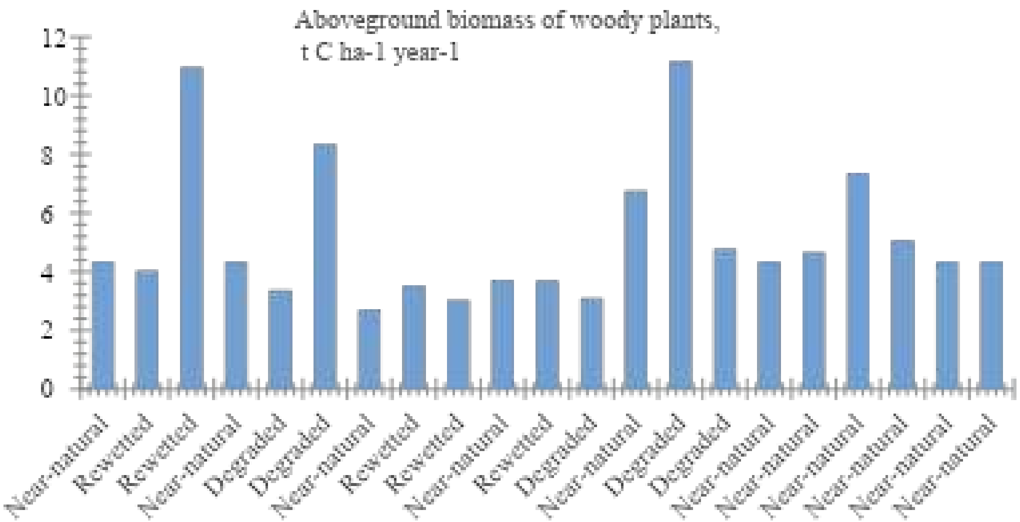

Figure 3.3.15. *Aboveground biomass of woody plants*

Belowground vascular biomass was less variable than aboveground woody biomass. Approximate means are around 1.5–1.6 t C ha^{-1} yr^{-1} in near-natural and rewetted sites and around 1.2–1.3 t C ha^{-1} yr^{-1} in degraded sites. The smaller belowground vascular biomass in degraded sites may reflect lower contribution from mire-type herbaceous species and higher dominance of woody vegetation (**Figure 3.3.16**). Belowground woody biomass was comparatively low in all categories, with approximate means around 0.8–1.0 t C ha^{-1} yr^{-1} in near-natural and rewetted sites and somewhat lower values, roughly 0.6–0.7 t C ha^{-1} yr^{-1}, in degraded sites **Figure 3.3.17**). Although this pool is small in absolute terms relative to the carbon already stored in peat, it remains relevant because root turnover can supply fresh carbon to the upper soil layers and can influence rhizosphere processes, including methanogenesis and methane oxidation.

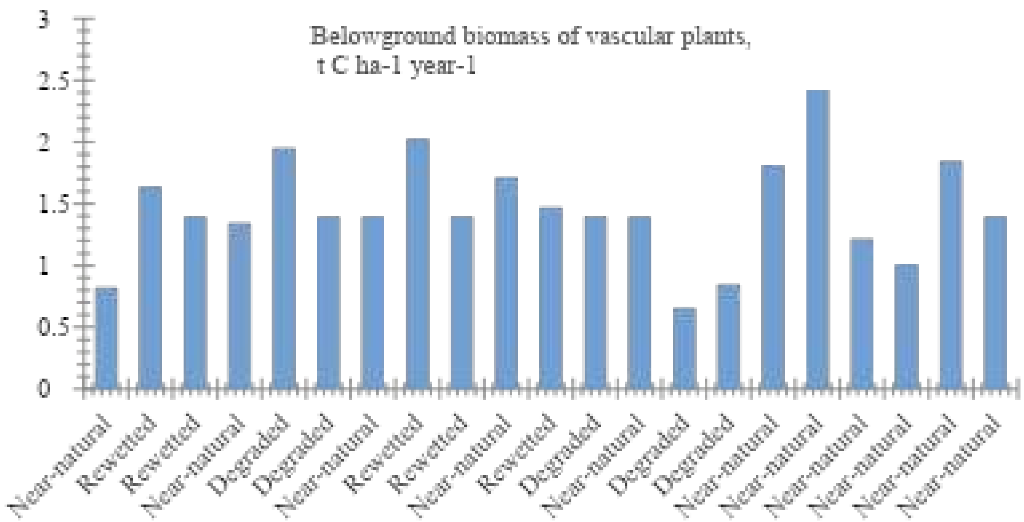

Figure 3.3.16. *Belowground biomass of vascular plants*

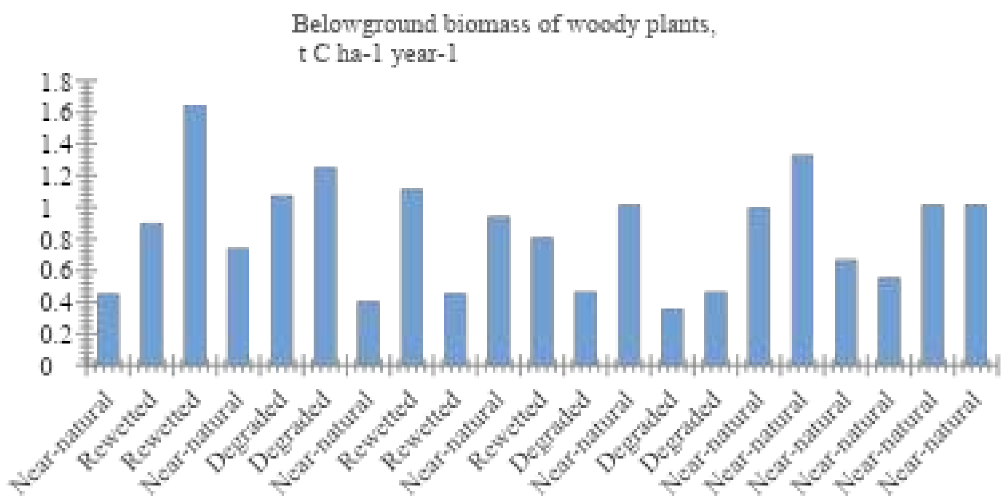

Figure 3.3.17. *Belowground biomass of woody plants*

Fine litterfall showed the lowest values among the plotted production terms. Near-natural sites were close to zero, rewetted sites approximately 0.5–0.6 t C ha^{-1} yr^{-1} on average, and degraded sites around 0.2–0.3 t C ha^{-1} yr^{-1} (**Figure 3.3.18**). Moss production, in contrast, showed a clearer ecological differentiation. Approximate means are about 1.2–1.3 t C ha^{-1} yr^{-1} in near-natural sites, about 1.8–1.9 t C ha^{-1} yr^{-1} in rewetted sites, and around 1.1–1.2 t C ha^{-1} yr^{-1} in degraded sites. The rewetted sites also showed the broadest range, with upper values exceeding 4 t C ha^{-1} yr^{-1} (**Figure 3.3.19**). This is one of the most important biological signals in the presentation because mosses, especially Sphagnum-dominated communities, are central to long-term peat formation. High moss production in rewetted sites implies that hydrological restoration is promoting one of the key pathways through which peatlands rebuild their carbon-accumulating function, even if greenhouse gas balances remain mixed during early or intermediate stages of restoration.

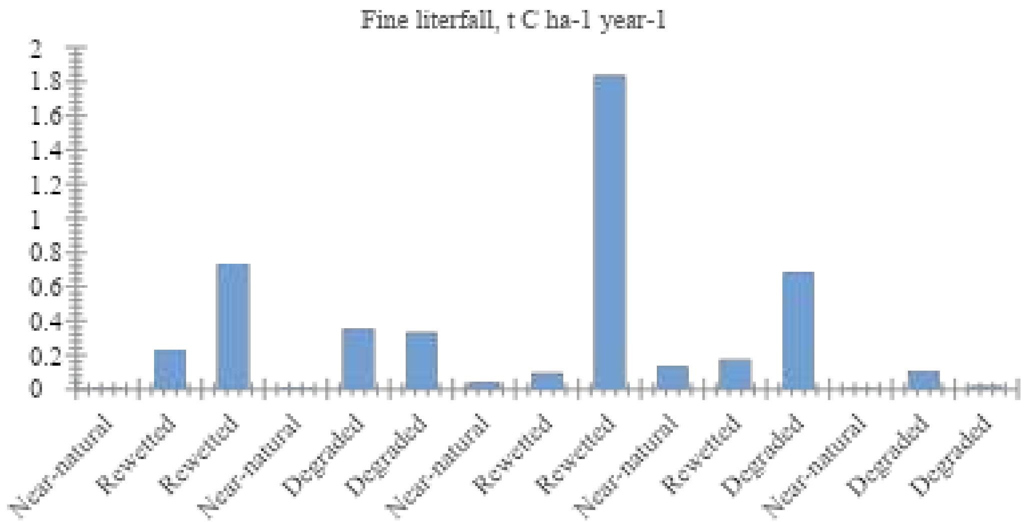

Figure 3.3.18. *Fine litterfall*

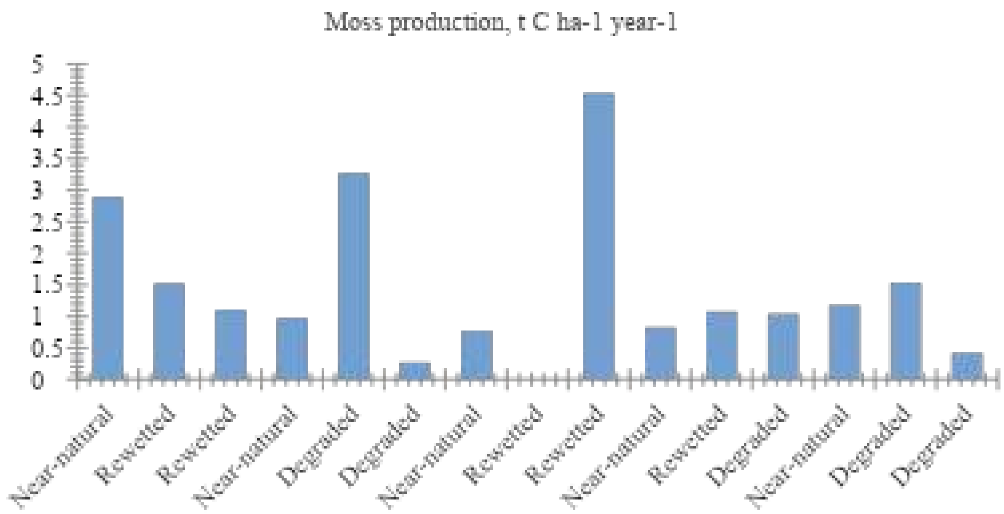

Figure 3.3.19. *Moss production*

These biomass patterns are consistent with the general expectation for peatland restoration. Rewetting does not necessarily produce an immediate return to pristine vegetation structure; instead, intermediate states often combine legacy woody biomass with a recovering moss layer and a partially reorganised vascular plant community. The relatively high moss production in rewetted sites is encouraging from a restoration perspective because successful peat accumulation in raised bog systems ultimately depends on sustained bryophyte productivity. A broader restoration synthesis has similarly concluded that many restored peatlands regain carbon sink characteristics even while methane emissions remain elevated, implying that vegetation recovery and gaseous losses need to be interpreted jointly rather than separately. In a global synthesis of freshwater wetland restoration, most restored peatlands were carbon sinks despite higher CH_4 emissions, whereas most degraded peatlands were carbon sources.

GHG fluxes

The study results show a clear distinction between measured heterotrophic respiration and total ecosystem respiration. The heterotrophic respiration results displays an approximately monotonic increase in category means from near-natural to rewetted to degraded sites (**Figure 3.3.20**). Visual extraction suggests a mean of about 3.1 t C ha^{-1} yr^{-1} in near-natural sites, 4.8 t C ha^{-1} yr^{-1} in rewetted sites, and 5.8 t C ha^{-1} yr^{-1} in degraded sites. Median values appear somewhat lower than means in rewetted and degraded categories, indicating that several sites with elevated fluxes increased the arithmetic average. Approximate ranges are about 1.0–5.4 t C ha^{-1} yr^{-1} in near-natural sites, about 2.9–7.4 t C ha^{-1} yr^{-1} in rewetted sites, and about 2.7–11.1 t C ha^{-1} yr^{-1} in degraded sites. This large spread is ecologically plausible and points to strong site-level dependence of soil organic matter mineralisation.

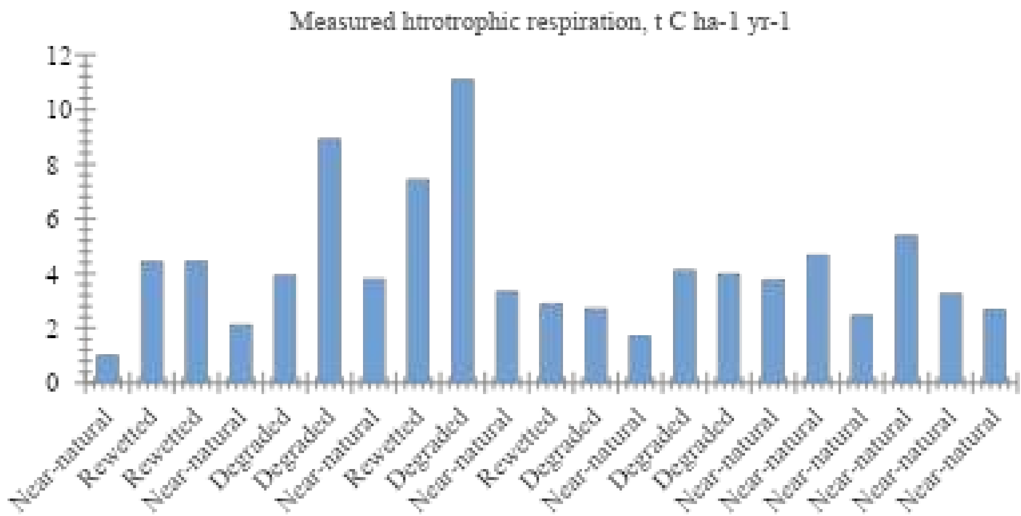

Figure 3.3.20. *Heterotrophic respiration measurement results*

By contrast, total respiration varied much less across categories. Approximate mean values are close to 4.9–5.0 t C ha^{-1} yr^{-1} in near-natural sites, about 6.0 t C ha^{-1} yr^{-1} in rewetted sites, and about 5.6–5.7 t C ha^{-1} yr^{-1} in degraded sites (**Figure 3.3.21**). The distributions overlap strongly, and the apparent between-category separation is smaller than for heterotrophic respiration. The chart embedded in the presentation contains the exact point data for the scatter relationship between total respiration and heterotrophic respiration, and these values further support the impression that total respiration occupies a relatively narrow band while heterotrophic respiration spans a broader gradient. In other words, the major category difference is not simply that degraded sites respire more in total, but that a larger share of their respiration is attributable to decomposition-driven carbon loss from soil organic matter.

This distinction is mechanistically important. Total respiration integrates both autotrophic respiration, linked to living plants and roots, and heterotrophic respiration, linked to microbial decomposition of organic substrates. An ecosystem can therefore show similar total respiration across different site conditions even while soil carbon stability differs substantially. In the present results, degraded sites combine relatively high heterotrophic respiration with only moderately elevated total respiration, which implies that plant-associated respiration is not the dominant driver of the category difference. Rather, deeper water tables and more aerated peat in degraded sites appear to support enhanced microbial oxidation of accumulated peat carbon. Rewetting suppresses this process to some extent, though not uniformly to near-natural levels.

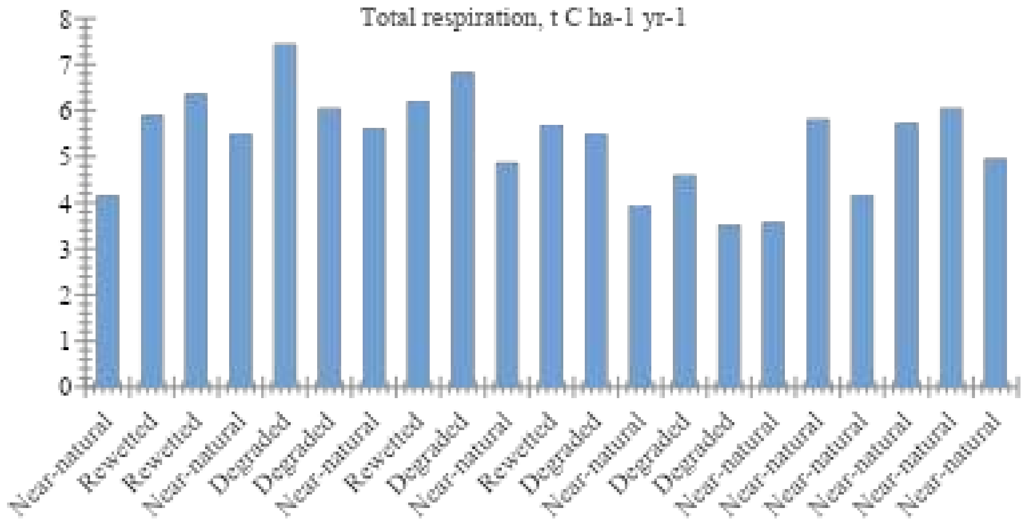

Figure 3.3.21. *Total respiration measurement results*

Figure 3.3.22. Measurements of total (on the left) and heterotrophic respiration

Two soil carbon balance approaches are used in the project: one based on directly measured heterotrophic respiration and one based on recalculation from total respiration using an assumed conversion coefficient (Ojanen et al., 2012). The extracted means from the chart labelled “net CO_2-C, t ha^{-1} yr^{-1} (by Rhet)” were approximately −1.61 t C ha^{-1} yr^{-1} for near-natural sites, −0.57 t C ha^{-1} yr^{-1} for rewetted sites, and +0.02 t C ha^{-1} yr^{-1} for degraded sites (**Figure 3.3.23**). In that sign convention, negative values indicate stronger net soil carbon accumulation or lower net soil carbon loss, whereas positive values indicate a net source. The direct-Rhet method therefore places near-natural sites as the strongest sinks, rewetted sites as weaker but still net sinks on average, and degraded sites as approximately in equilibrium or a slight source. The within-group spread remained high: near-natural sites ranged from roughly −4.66 to +1.66 t C ha^{-1} yr^{-1}, rewetted sites from −2.28 to +3.87, and degraded sites from −3.57 to +3.85.

The recalculated approach based on total respiration produced a similar ranking but somewhat more negative mean balances: approximately −2.60 t C ha^{-1} yr^{-1} for near-natural sites, −1.69 t C ha^{-1} yr^{-1} for rewetted sites, and −1.27 t C ha^{-1} yr^{-1} for degraded sites (**Figure 3.3.24**). The difference between the two methods illustrates how sensitive annual peat carbon balance estimates are to assumptions regarding the partitioning of total respiration, the proportion of plant-derived inputs entering persistent soil carbon pools, and the time frame over which vegetation production is assumed to translate into stable peat accumulation. Nonetheless, both methods support the same main ecological conclusion: the site categories follow a gradient from weaker sink or source conditions in degraded sites towards stronger sink conditions in rewetted and especially near-natural sites.

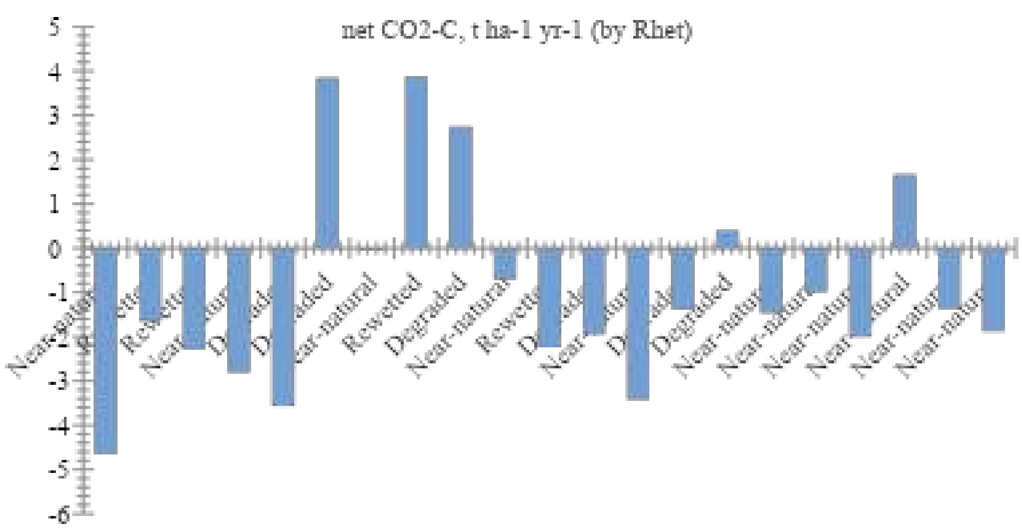

Figure 3.3.23. *C balance calculation using Rhet method*

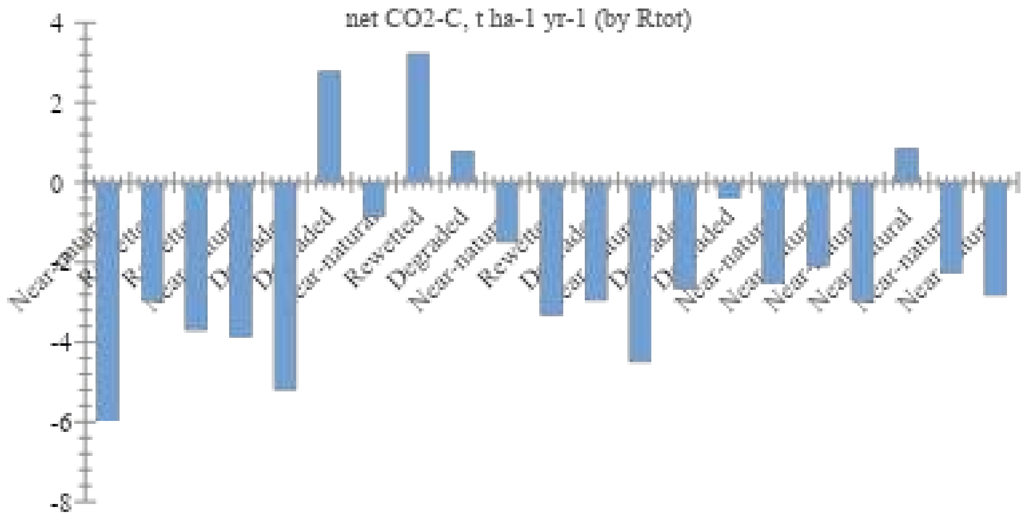

Figure 3.3.24. *C balance calculation using Rtot method*

This is an important result because it indicates that the restoration sites are not merely shifting gases among pools; they appear to be moving towards reduced net peat oxidation. That interpretation is well aligned with the broader literature. A recent meta-analysis concluded that rewetting previously drained peatlands reduces CO_2 emissions on average, although the magnitude depends strongly on ecosystem type and restoration context (Jauhiainen et al., 2023). At the same time, global assessments emphasise that peatland rewetting produces climate benefits precisely because it halts the long-term cumulative burden of CO_2 from drained peat oxidation, even if CH_4 emissions return after rewetting. The Latvian results fit this logic well: the strongest evidence for restoration success lies in the suppressed heterotrophic respiration and more negative net soil CO_2-C balance relative to degraded conditions.

At the same time, caution is warranted in interpreting absolute annual sink values. Peat accumulation is typically a slow process, and annual soil carbon balances derived from component-based calculations can be highly sensitive to spatial heterogeneity, vegetation turnover assumptions, and the representativeness of chamber-based measurements. In the present case, the value of the results lies less in claiming a precise annual peat accumulation rate for each habitat and more in demonstrating the direction of change across the drainage–rewetting–near-natural continuum. That directional signal is robust and ecologically interpretable.

Methane was the clearest non-CO_2 greenhouse gas signal in the monitoring. Mean CH_4 emissions were approximately 202 kg ha^{-1} yr^{-1} in near-natural sites, 240 kg ha^{-1} yr^{-1} in rewetted sites, and 69 kg ha^{-1} yr^{-1} in degraded sites (**Figure 3.3.25**). The rewetted category had the highest upper value, around 580 kg ha^{-1} yr^{-1}, with near-natural sites reaching roughly 538 kg ha^{-1} yr^{-1} and degraded sites only about 203 kg ha^{-1} yr^{-1}. In parallel, mean water-table level below the surface was about 8.5 cm in near-natural sites, 11.4 cm in rewetted sites, and 21.3 cm in degraded sites (Figure 3.3.26). The summary scatter plot shows a strong non-linear decline of CH_4 with increasing water-table depth below the surface, with highest CH_4 emissions clustered where the water table is within roughly the upper 5–10 cm and very low emissions where it lies deeper than about 20–25 cm.

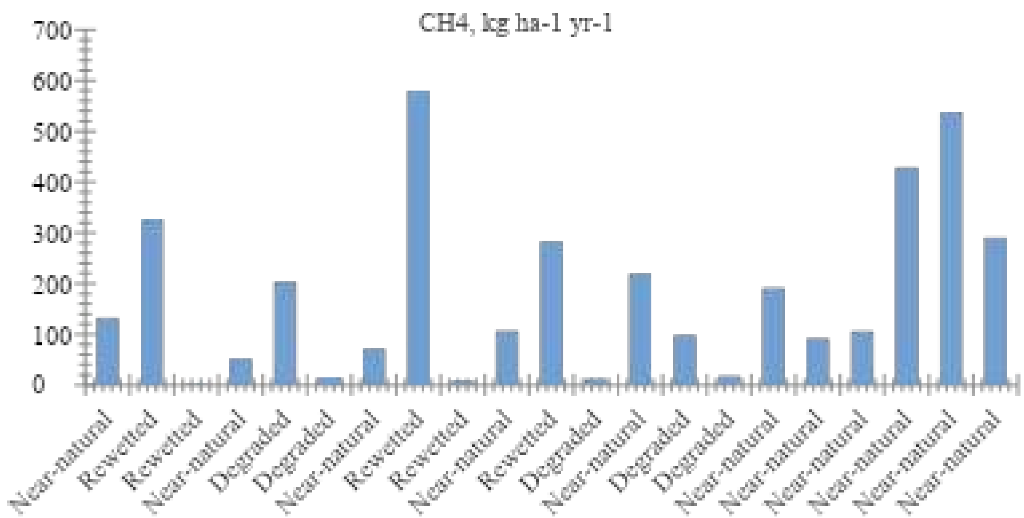

Figure 3.3.25. *Methane fluxes in study sites*

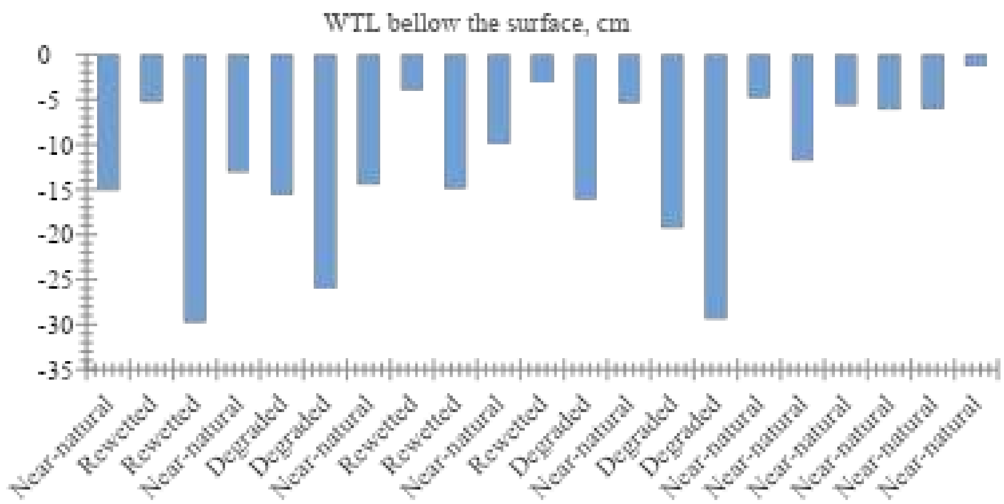

Figure 3.3.26. *Average groundwater level during measurement period*

The mechanism is straightforward and well supported in peatland biogeochemistry. A shallow water table limits oxygen diffusion, promotes anoxic microsites and methanogenesis, and reduces the thickness of the oxic layer through which methane must pass and be oxidised before reaching the atmosphere. A deeper water table does the opposite: it suppresses methanogenesis, expands the oxidising zone, and thereby reduces net CH_4 release. The Latvian data align very well with this conceptual model and with published field studies showing strong control of peatland CH_4 fluxes by water-table depth. Studies from ombrotrophic bogs and other northern wetlands have repeatedly shown that shallower water tables are associated with larger CH_4 fluxes, although vegetation type, temperature, substrate supply, and microtopography modify the exact relationship (Goodrich et al., 2015).

The relative ranking of categories is also fully plausible from a restoration perspective. Drainage strongly suppresses CH_4 emissions; a review of northern peatlands reported that drainage reduces CH_4

emissions by about 84% on average relative to unmanaged conditions. Rewetting, conversely, commonly increases CH_4 relative to drained states, and a meta-analysis found that restoration by rewetting or vegetation/rewetting increased CH_4 emissions on average compared with pre-management conditions. Another more recent meta-analysis reported that rewetting reduced CO_2 emissions but increased CH_4 emissions by about 0.033 Mg CH_4-C ha^{-1} yr^{-1} on average. The Latvian results therefore fall squarely within the broad global pattern: degraded sites had the lowest CH_4, rewetted sites the highest, and near-natural sites remained substantial CH_4 emitters because natural bog functioning itself includes methane production under high water tables (Abdalla et al., 2016).

What is notable in the dataset is that rewetted sites were only modestly higher in mean CH_4 than near-natural sites, while degraded sites were much lower. This suggests that rewetting has not produced an anomalous methane pulse far beyond the natural range of wet bog systems; rather, it has shifted the system back towards the methane-emitting domain typical of waterlogged peatlands. That distinction matters scientifically and for policy communication. Methane increases after rewetting are often perceived negatively when compared only with drained conditions, but the appropriate ecological comparator is frequently the near-natural peatland state, not the degraded state alone. The monitoring indicates that the rewetted category is broadly converging towards the natural wet end of the methane spectrum, even though large variability persists.

Mean N_2O fluxes were approximately 0.065 kg ha^{-1} yr^{-1} in near-natural sites, 2.40 kg ha^{-1} yr^{-1} in rewetted sites, and 0.68 kg ha^{-1} yr^{-1} in degraded sites (**Figure 3.3.27**). The rewetted category showed the highest central tendency and a wide range, from about −1.51 to 4.62 kg ha^{-1} yr^{-1}, while degraded sites ranged roughly from −0.89 to 4.33 and near-natural sites from −1.91 to 2.75 kg ha^{-1} yr^{-1}. Mean redox potential was about 204 mV in near-natural sites, 254 mV in rewetted sites, and 201 mV in degraded sites. Electrical conductivity averaged around 19.9 µS in near-natural sites, 33.3 µS in rewetted sites, and 30.8 µS in degraded sites (**Figure 3.3.28**).

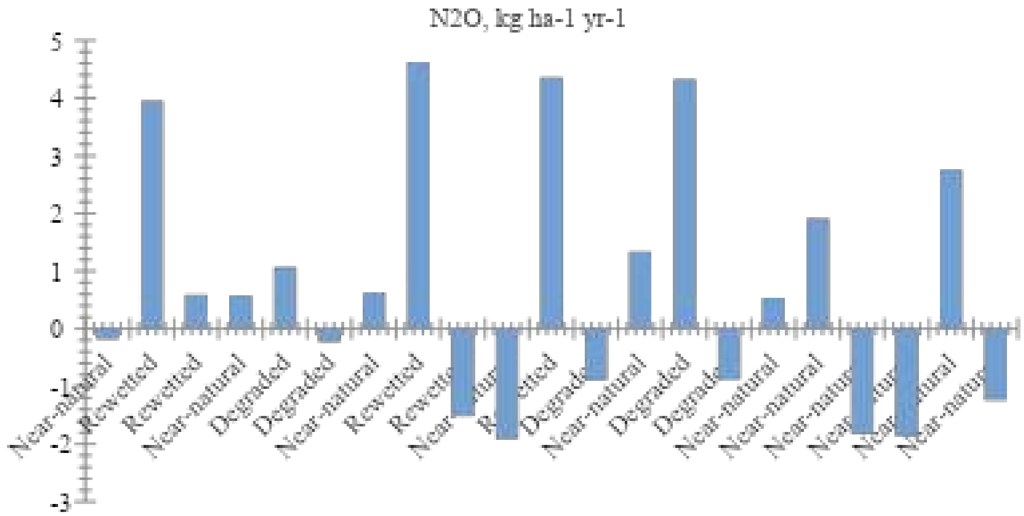

Figure 3.3.27. *Nitrous oxide fluxes in study sites*

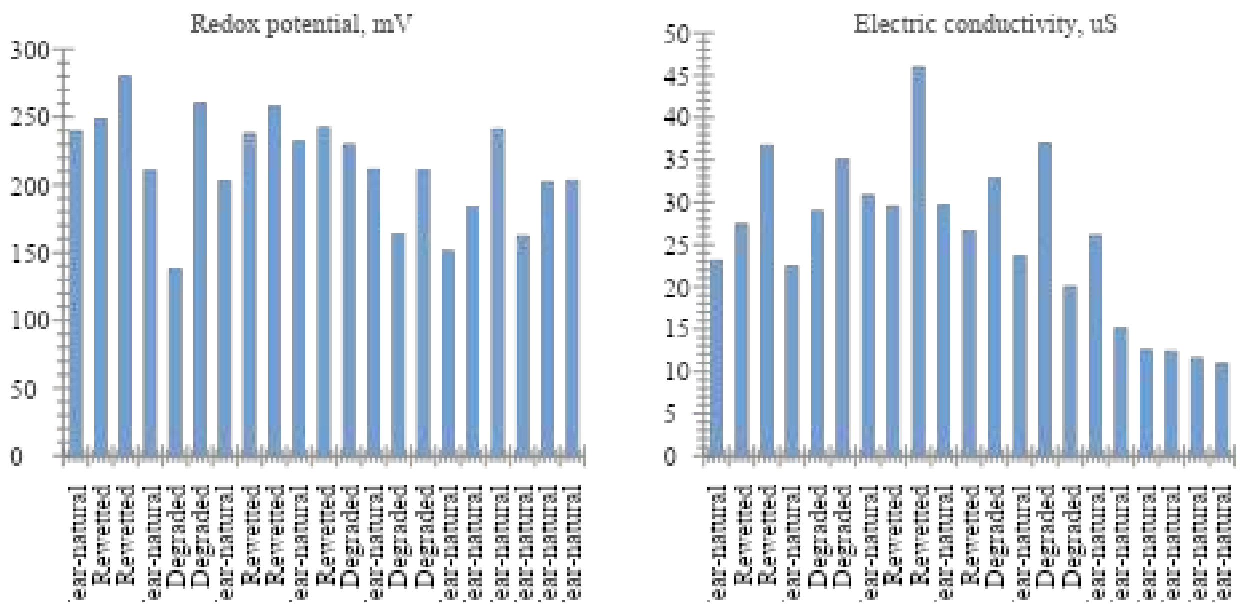

Figure 3.3.28. *Redox potential and electric conductivity in study sites*

The low mean N_2O in near-natural sites is entirely consistent with classical understanding of nutrient-poor, persistently wet bog systems. Such systems tend to have limited nitrification, low available inorganic nitrogen, and redox conditions that suppress sustained N_2O production. Degraded sites can emit N_2O when drainage enhances aeration and nitrogen cycling, but in bogs and nutrient-poor forested peatlands the absolute fluxes may still remain modest relative to nutrient-rich agricultural peat soils. In contrast, rewetted sites can show variable N_2O responses depending on nutrient status, restoration stage, and whether fluctuating water tables create alternating oxic and anoxic microsites. The elevated mean N_2O in the rewetted category therefore suggests that some restored sites remain in a transitional biochemical state with sufficient mineral nitrogen and redox oscillation to support N_2O formation (Liu et al., 2020).

This interpretation is reinforced by the redox and conductivity patterns. Rewetted sites showed both the highest redox potential and the highest conductivity. This may at first appear counterintuitive if one expects low redox values under stronger saturation, but restoration sites are rarely uniform anaerobic systems. Instead, they often display high spatial and temporal variability, with alternating wetting and drying, nutrient mobilisation from previously oxidised peat, and small-scale contrasts among hummocks, hollows, old drainage lines, and rewetted depressions. Under such conditions, both denitrification and nitrification-derived N_2O can occur in sequence, particularly during water-table fluctuations. Recent continental-scale work has shown that rewetting can reduce cumulative N_2O emissions overall, especially when highly degraded peatlands are prioritised, yet individual rewetted sites may still produce non-trivial N_2O during transitional stages. The Latvian results are therefore better interpreted as evidence of restoration-stage heterogeneity than as a contradiction of the broader mitigation benefit of rewetting (Liu et al., 2020).

Another plausible explanation is nutrient leaching or solute release from decomposed surface peat after rewetting. The presentation itself points to higher electrical conductivity and possible nutrient leaching in rewetted sites. That interpretation agrees with published studies showing that rewetting may generate a period of elevated DOC and nutrient export, especially in previously drained peatlands with oxidised upper peat. If such mobilisation occurred in the Latvian sites, it would help explain why the rewetted category combined relatively strong CH_4 emissions with elevated N_2O and conductivity. This would imply that the rewetted sites are already moving towards reduced peat oxidation, but have not yet reached the hydrochemical stability of near-natural bogs (Urbanová et al., 2011).

The integrated net soil greenhouse gas balance on a GWP100 basis highlights the trade-off among gases very clearly. The extracted mean values were approximately −0.21 t CO_2 eq. ha^{-1} yr^{-1} for near-natural sites, 7.14 t CO_2 eq. ha^{-1} yr^{-1} for rewetted sites, and 1.78 t CO_2 eq. ha^{-1} yr^{-1} for degraded sites. Variation within categories was large. Rewetted sites ranged from about −8.14 to 31.66 t CO_2 eq. ha^{-1} yr^{-1}, degraded sites from −7.12 to 14.47, and near-natural sites from −13.42 to 17.59 (**Figure 3.3.29**). The stacked category shows that CH_4 was the dominant positive contributor in all three categories, approximately 5.66, 8.34, and 1.64 t CO_2 eq. ha^{-1} yr^{-1} in near-natural, rewetted, and degraded sites, respectively (**Figure 3.3.30.**). N_2O contributed only about 0.02, 0.90, and 0.08 t CO_2 eq. ha^{-1} yr^{-1}, while the CO_2 component was negative in near-natural (−1.61) and rewetted (−0.57) categories and close to zero but slightly positive in degraded sites (+0.02 t CO_2 eq. ha^{-1} yr^{-1}).

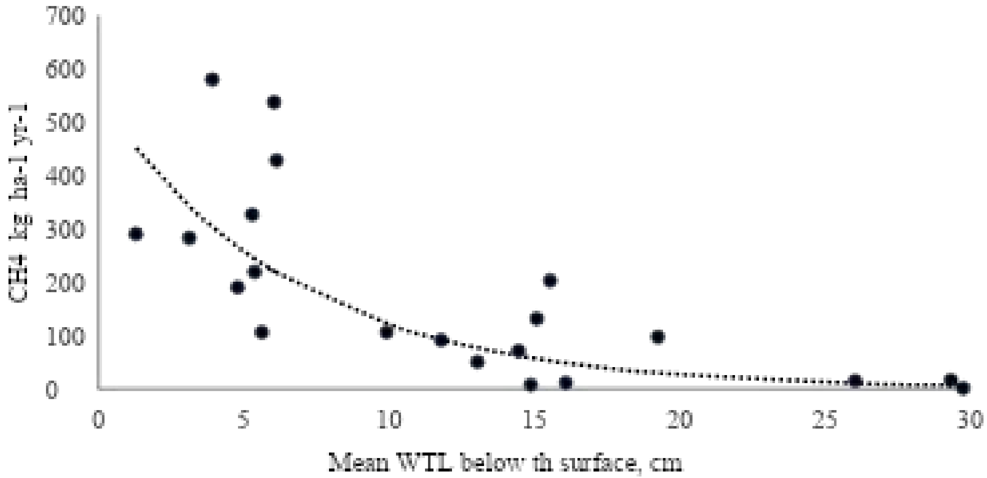

Figure 3.3.29. *Correlation between WTL and methane emissions*

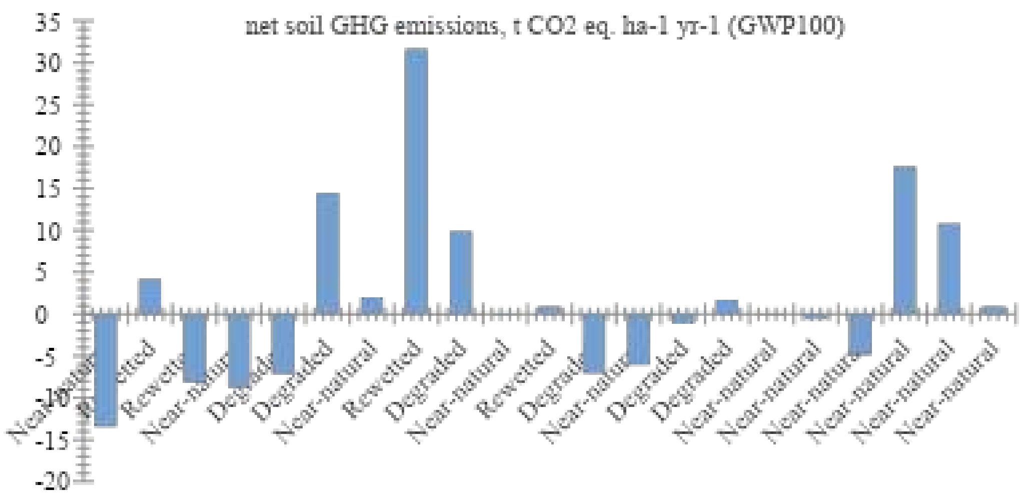

Figure 3.3.30. *Variation of summed site-specific fluxes*

These numbers show that, under a 100-year GWP framework, methane largely determines the annual integrated greenhouse gas balance of the wettest site categories. In other words, near-natural and rewetted systems can function as net soil carbon sinks or near-sinks while still appearing as annual GHG sources in CO_2-equivalent terms because CH_4 carries a high radiative forcing weight. This apparent paradox is widely recognised in peatland climate science. Drained peatlands produce sustained long-term CO_2 emissions from oxidising centuries to millennia of accumulated peat, whereas rewetted peatlands reduce those CO_2 losses but re-establish CH_4 emissions characteristic of wet anaerobic conditions. Whether a rewetted site appears favourable in any given year therefore depends strongly on the selected metric and time horizon.

The results fit this conceptual framework closely. Rewetted sites had the highest mean annual CO_2-equivalent balance because their CH_4 contribution exceeded the gain from reduced soil CO_2 loss. However, the same rewetted sites also had a more favourable soil carbon balance than degraded sites.

The scientific implication is not that rewetting failed, but that the sites are located in the expected transition zone where CO_2 mitigation has become visible before the CH_4 component has stabilised at a lower level. Such trajectories are common in restoration chrono sequences. Some restored peatlands remain net GHG sources for years after rewetting, particularly where nutrient-rich conditions, unstable hydrology, open water, or decomposed surface peat favour CH_4 production. Over longer time horizons, however, the avoided CO_2 from halted peat oxidation generally dominates the mitigation outcome (Darusman et al., 2023).

The acquired CH_4 values are also plausible relative to published ranges for northern peatlands. Near-natural sites averaging around 202 kg CH_4 ha^{-1} yr^{-1} and rewetted sites around 240 kg CH_4 ha^{-1} yr^{-1} indicate substantial methane activity, but not values outside the known range for wet bog and restored peatland systems. Reviews and field studies report considerable variability in CH_4 fluxes among northern peatlands due to differences in water-table depth, vegetation, microtopography, and climate. The fact that some Latvian rewetted and near-natural sites exceeded 500 kg CH_4 ha^{-1} yr^{-1} while others remained much lower is therefore consistent with the strong spatial heterogeneity typical of peatland CH_4 dynamics (Liu et al., 2020).

The respiration partitioning result is perhaps the most distinctive feature of the dataset. Compared with an ombrotrophic bog, where heterotrophic respiration can contribute a much smaller fraction of ecosystem respiration under intact conditions, the rewetted and degraded sites appear more strongly decomposition-driven. This likely reflects site history. Post-drainage and post-extraction surfaces commonly contain more decomposed peat, altered vegetation, and stronger hydrochemical perturbation than long-intact peat-forming bogs. Under such conditions, even after rewetting, the microbial decomposition signal may remain relatively strong for years. Thus, the difference from pristine ombrotrophic bog studies should not be read as inconsistency, but as an indicator of restoration stage and legacy effects.

The elevated N_2O in rewetted sites deserves particular attention because some syntheses report declines in N_2O after rewetting. However, those syntheses generally describe average long-term tendencies across many peatland types. The Latvian rewetted sites still appear hydrochemically transitional, with higher conductivity and variable water tables, which can support patchy and episodic N_2O production. Studies from Europe indicate that N_2O responses are strongly conditioned by peat nutrient status, prior land use, and rewetting strategy. In nutrient-poor bogs N_2O can be very small, whereas in richer or more disturbed peatlands temporary N_2O release may occur during restoration (Liu et al., 2020).

When the entire dataset is considered jointly, the results support a strong ecological interpretation. The degraded sites are characterised by deeper water tables, the highest heterotrophic respiration, the weakest soil carbon balance, the lowest methane emissions, and moderate conductivity. This combination is typical of peatlands where drainage has suppressed methanogenesis but allowed sustained aerobic peat mineralisation. Rewetted sites show shallower water tables, reduced heterotrophic respiration relative to degraded sites, stronger carbon balance, but also the highest CH_4, highest N_2O, highest conductivity, and highest redox potential. This indicates that rewetting has succeeded in limiting peat oxidation, yet the sites remain biogeochemically dynamic and partially unstable. Near-natural sites combine shallow water tables with the lowest heterotrophic respiration, the strongest estimated soil sink, low N_2O, moderate CH_4, low conductivity, and relatively higher pH than the degraded category. That is the signature of a peat-forming state in which hydrology and biogeochemistry are comparatively well coupled (**Figure 3.3.31**).

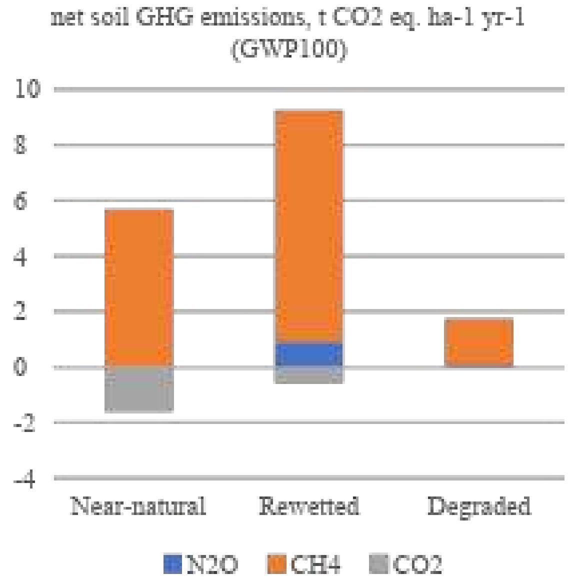

Figure 3.3.31. *Summed within the category averaged fluxes*

In that trajectory, rewetting first shifts the system out of the drainage-dominated decomposition regime, thereby reducing heterotrophic respiration and improving the soil CO_2-C balance. The CH_4 response is immediate because methanogenesis reacts rapidly to anoxia. Nutrient mobilisation and unstable redox conditions can temporarily maintain or elevate N_2O and solute concentrations. With time, if the water table remains high and vegetation shifts towards peat-forming communities, hydrochemical variability should decline, CH_4 emissions may become more spatially organised around wet microforms, and the system may converge towards the near-natural state. Published studies of long-term restored peatlands support such a trajectory, showing that hydrological and biogeochemical functions can recover gradually over many years or decades rather than immediately after restoration actions.

The results demonstrate why a single-gas or single-year evaluation would be inadequate for restoration assessment. If only methane were considered, rewetted sites would appear unfavourable relative to degraded sites. If only heterotrophic respiration or soil carbon balance were considered, rewetted sites would appear clearly improved. If only GWP100 annual totals were considered, near-natural sites would seem only marginally better than neutrality despite functioning as peat-forming ecosystems. The scientific value of the Latvian monitoring lies precisely in showing that all of these statements can be true simultaneously, depending on the metric selected. This is not a methodological weakness; it is an accurate reflection of peatland climate feedback (Kim et al., 2012).

The results also suggest that water-table level alone is not sufficient to explain all restoration outcomes. Mean WTL clearly explained much of the CH_4 pattern, but N_2O and conductivity indicate that hydrochemical state and perhaps the degree of previous peat decomposition are also important. For management, this implies that successful rewetting should aim not only to raise the water table, but also to reduce its amplitude of fluctuation, minimise nutrient release from severely oxidised surface peat, and support the re-establishment of peat-forming vegetation. The results already hint at this by linking rewetted-site non-CO_2 emissions to water-table variation and nutrient leaching. That interpretation is strongly supported by the broader literature.

In summary, the monitoring results show that the study sites follow a consistent biogeochemical gradient. Near-natural sites had the lowest measured heterotrophic respiration, averaging about 3.13 t C ha^{-1} yr^{-1}, and the strongest estimated soil carbon sink, with mean net soil CO_2-C balance around −1.61 t C ha^{-1} yr^{-1} by the direct Rhet approach. Rewetted sites were intermediate in soil carbon response, with heterotrophic respiration of about 4.82 t C ha^{-1} yr^{-1} and mean net soil CO_2-C balance of −0.57 t C ha^{-1} yr^{-1}, but they had the highest CH_4 and N_2O emissions and the highest conductivity. Degraded sites showed the deepest mean water table, about 21 cm below the surface, the highest heterotrophic respiration, 5.81 t C ha^{-1} yr^{-1}, and an approximately neutral to slightly positive mean net soil CO_2-C balance, indicating continued peat mineralisation.

The integrated GWP100 balance demonstrates that methane currently dominates annual net soil greenhouse gas emissions in the wettest categories. Mean net soil GHG emissions were approximately −0.21 t CO_2 eq. ha^{-1} yr^{-1} in near-natural sites, 7.14 t CO_2 eq. ha^{-1} yr^{-1} in rewetted sites, and 1.78 t CO_2 eq. ha^{-1} yr^{-1} in degraded sites. However, this does not negate the restoration benefit of rewetting. Rather, it shows that the studied rewetted sites are in the expected transition phase where CO_2 mitigation through reduced peat oxidation is already detectable, but CH_4 remains high and hydrochemical conditions have not yet stabilised. This interpretation is fully consistent with contemporary peatland science, which recognises that prompt rewetting can provide long-term climate benefit despite short-term methane trade-offs.

Overall, the results support four main scientific conclusions. First, rewetting clearly reduces the intensity of peat decomposition relative to degraded drained conditions. Second, methane responds strongly and predictably to shallow water tables and becomes the dominant contributor to annual GWP100 balances in rewetted and near-natural systems. Third, rewetted sites may show elevated N_2O and conductivity where nutrient mobilisation and variable redox conditions persist. Fourth, the transition from degraded to rewetted to near-natural states is best understood as a long-term restoration trajectory, not as an immediate categorical switch. Continued monitoring is therefore essential to determine whether the present rewetted sites will converge towards the lower-decomposition, lower-conductivity, low-N_2O state represented by the near-natural category.

3.4. GEST monitoring

In 2025, project activities focused primarily on the mapping of GEST types in Lielais Pelečāre Mire using acquired airborne data and on the development of Global Warming Potential (GWP) maps based on the derived classifications. Furthermore, an analysis of Plant Functional Type (PFT) distribution within the identified GEST types was conducted for Cena Mire, Melnais Lake Mire, and Lielais Pelečāre Mire.

In Sudas–Zviedru Mire, airborne data acquisition was carried out on 15 June 2025. Subsequent change detection analysis was conducted using airborne datasets from 2018 and 2025, complemented by available satellite imagery to ensure temporal consistency. Two field campaigns were organised on 7 and 15 October 2025 to collect *in situ* reference data for the validation of mapped GEST types and to verify detected changes within the restoration areas. The complete overview of GEST field campaigns is provided in **Table 3.4.1**.

Table 3.4.1. *PeatCarbon GEST type field campaigns.*

Project sites	Dates of data gathering
Cena Mire	17., 19.10.2023
Melnais Lake Mire	02.11.2023
Lielais Pelečāre Mire	21.-22., 30.-31.05.2024
Sudas-Zviedru Mire	**7., 15.10.2025**

The potential for upscaling high spatial resolution (1 m/pixel) airborne GEST type mapping using lower spatial resolution (10 m/pixel) Sentinel satellite data was assessed for Melnais Lake Mire and Lielais Pelečāre Mire. The analysis demonstrated that the 10 m spatial resolution data are not sufficient to reliably distinguish all identified GEST types. Consequently, the number of classification classes was reduced by merging spectrally similar categories. The results indicate that the existing GEST classification scheme should be reviewed and potentially simplified if future mapping is to rely on freely available Sentinel satellite data.

In addition, a wetland habitat type classification for Latvia was developed to serve as input data for greenhouse gas (GHG) modelling. This approach demonstrates an alternative methodology for developing country-specific GEST-type maps based on freely available Sentinel satellite imagery.

A detailed description of the results achieved under each specific task is provided below.

GEST type mapping – Lielais Pelečāre Mire

GEST type mapping was carried out using airborne hyperspectral data acquired on 16 August 2023 and GEST reference data collected during field campaigns conducted on 21–22 May and 30–31 May 2024. A supervised Random Forest (RF) classifier was trained using airborne hyperspectral reflectance data, local terrain variables, and supplementary land cover information as input features. The objective was to upscale locally collected GEST field observations into a high spatial resolution GEST type map covering the entire area of interest. The resulting GEST type map for Lielais Pelečāre Mire (**Figure**

3.4.1.) comprises 16 GEST classes, including 7 low-vegetation types, 8 high-vegetation types, and 1 open water class.

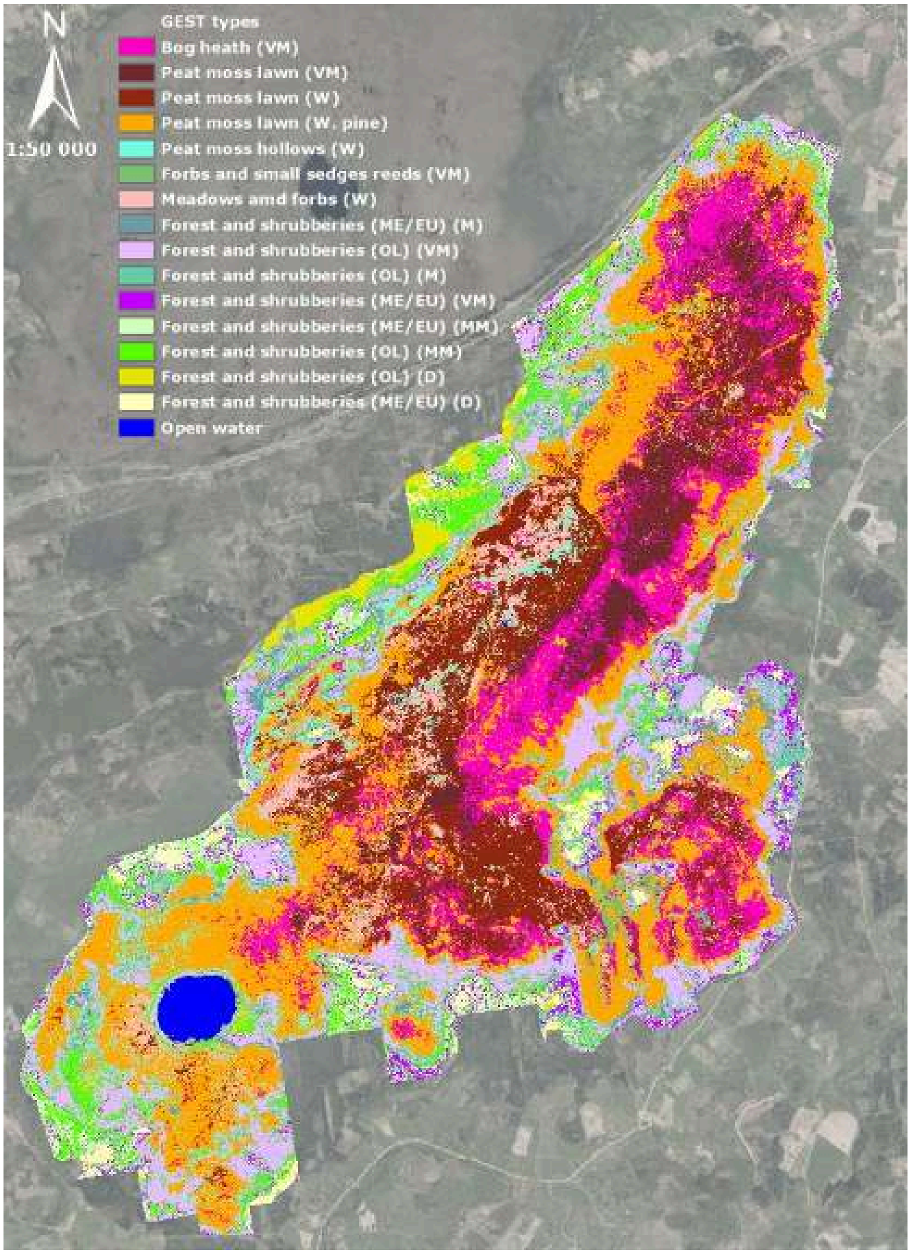

Figure 3.4.1. *Lielais Pelečāre Mire: GEST type map.*

Field campaign data were used to generate both training and validation datasets. Due to the limited number of reference samples, a k-fold cross-validation approach was applied to assess classification performance. The resulting confusion matrix is presented in **Figure 3.4.2**. Class-specific accuracies ranged from 67% to 86%, resulting in an overall classification accuracy of 74%. Additional performance metrics, including precision, recall, and F1-score, are presented in the classification report heatmap (**Figure 3.4.3**).

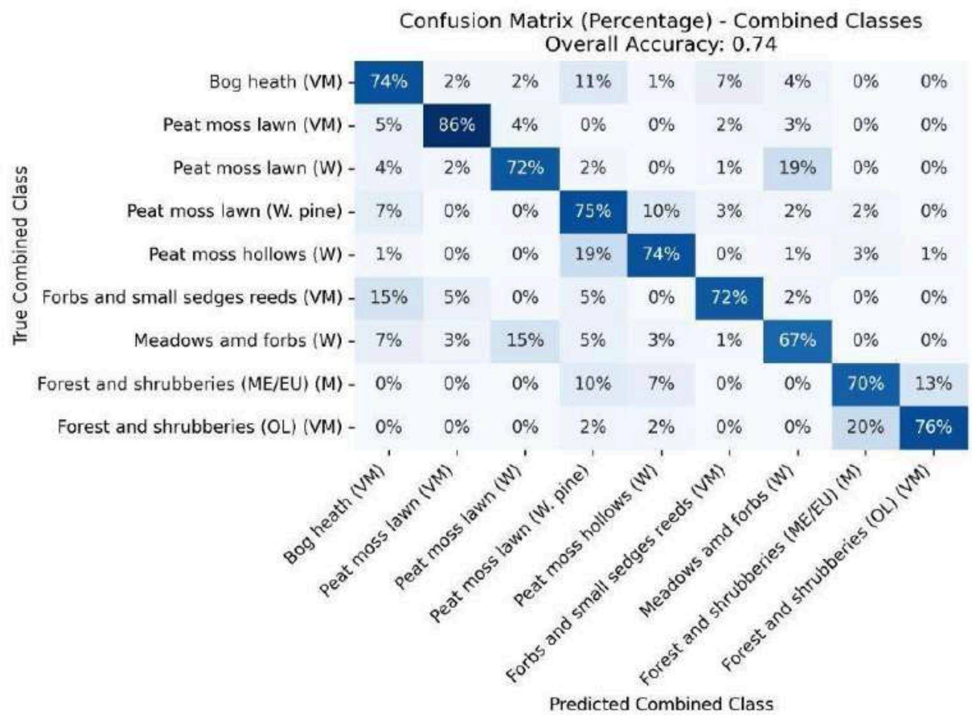

Figure 3.4.2. *Lielais Pelečāre Mire: GEST type mapping confusion matrix.*

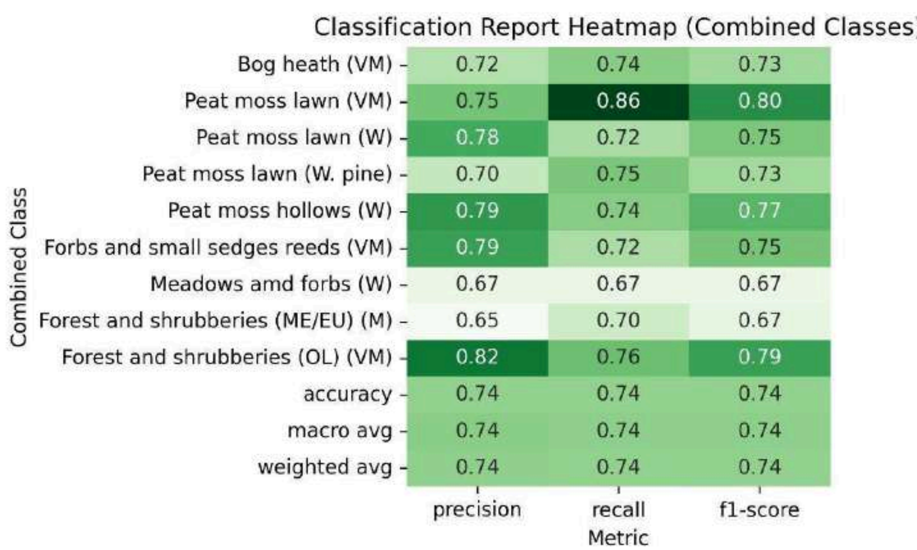

Figure 3.4.3. *Lielais Pelečāre Mire: GEST type classification report heatmap.*

The updated list of GEST types identified within the pilot areas, together with the corresponding greenhouse gas (GHG) emission factors derived from the GEST handbook, is provided in **Table 3.4.2**. For certain GEST types, specific emission factors were not available (indicated in red in **Table 3.4.2**). In such cases, emission factors from the most comparable GEST class were applied as proxies. These emission factors were subsequently used to generate spatially explicit Global Warming Potential (GWP) distribution maps for the area of interest (**Figure 3.4.4**).

The total Global Warming Potential (GWP) for the area of interest was calculated by summing GWP values across all mapped GEST types (**Figure 3.4.5**). The results indicate a substantial difference in total GWP depending on whether tree biomass was included in the calculation. When tree biomass was considered, the total GWP amounted to 12,182 t CO_2 eq. per year, whereas excluding tree biomass resulted in a total GWP of 34,560 t CO_2 eq. per year. This nearly threefold difference highlights the significant influence of biomass components on greenhouse gas (GHG) emission accounting and underlines the importance of consistent methodological assumptions in peatland GHG assessments.

Table 3.4.2. *GEST types and GHG emission factors [t CO2 eq./ha/year].*

	Presence in pilot area				HG emission factors (without tree biomass)				GHG emission factors (with tree biomass)			
GEST type	Cenas tirelis	Melnā ezera	Lielās Pelēčāres	Sudas-Zviedru purvs	Water level	CO_2	CH_4	GWP	Water level	CO_2	CH_4	GWP
Bare peat wet	X	X			4+	1,5	0,1	1,6	4+	1,5	0,1	1,6
Bare peat moist (OL)		X			3+	6,2	0	6,2	3+	6,2	0	6,2
Bare peat dry (OL)		X			2-/3-	7	0,4	7,5	2-/3-	7	0,4	7,5
Open water/ditches	X		X	X	6+	1,42	2,8	4,22	6+	1,42	2,8	4,22
Very moist bog heath		X	X		4+	1,7	3	4,6	4+	1,7	3	4,6
Moist bog heath	X				3+	9,4	0	9,4	3+	9,4	0	9,4
Moderately moist/dry bog heath	X				2+/2-	13,5	0,1	13,6	2+/2-	13,5	0,1	13,6
Wet peat moss hollows resp. flooded peat moss lawn	X	X	X	X	5+	-3.1	12	8.9	5+	-3.1	12	8.9
Peat moss lawn on former peat-cut off areas	X	X			5+	1,5	0,4	1,9	5+	1,5	0,4	1,9
Wet peat moss lawn	X	X	X	X	5+	-0.5	0,3	-0.3	5+	-0.5	0,3	-0.3
Wet peat moss lawn with pine trees	X	X	X		4+	3,9	0,2	4,1	4+	**1,17**	**0,2**	**1,37**
Very moist peat moss lawn	X	X	X		4+	-1.1	3,4	2,3	4+	-1.1	3,4	2,3
Wet meadows and forbs	X	X	X		5+	0	5,8	5,8	5+	0	5,8	5,8
Very moist meadows, forbs and small sedges reeds			X	X	4+	-0,5	2,3	1,9	4+	-0,5	2,3	1,9
Moderately moist (forb) meadows		X			2+	20	0	20	2+	20	0	20
Wet tall reeds		X			5+	-2.3	6,3	4	5+	-2.3	6,3	4
Very moist forest and shrubberies (OL)			X		4+	1,7	3	4,7	4+	-2,3	1,75	-0,55
Moist forests and shrubberies (OL)	X	X	X	X	3+	9,4	0	9,4	3+	**-2,2**	**-1,8**	**-4**
Moderately moist forest and shrubberies (OL)	X	X	X	X	2+	20	0	20	2+	**-3,1**	**-0,11**	**-3,22**
Dry forest and shrubberies (OL)	X	X	X		2-/3-	26	0	26	2-/3-	**-3,1**	**-0,11**	**-3,22**
Very moist forest and shrubberies (ME/EU)			X		4+	-0,5	2,1	1,6	4+	-10,72-(-5,97)	0,81-4,27	-9,91-(-1,7)
Moist forests and shrubberies (ME/EU)			X		3+	4,6	7,5	12,2	3+	21,59-24,98	0,004-5,35	21,59-30,33
Moderately moist forest and shrubberies (ME/EU)			X		2+	20	0	20	2+	1	**0,004-5,35**	**1,004-6,35**
Dry forests and shrubberies (ME/EU)		X	X		2-/3-	43,4	0	43,4	2-/3-	**1**	**0,004-5,35**	**1,004-6,35**

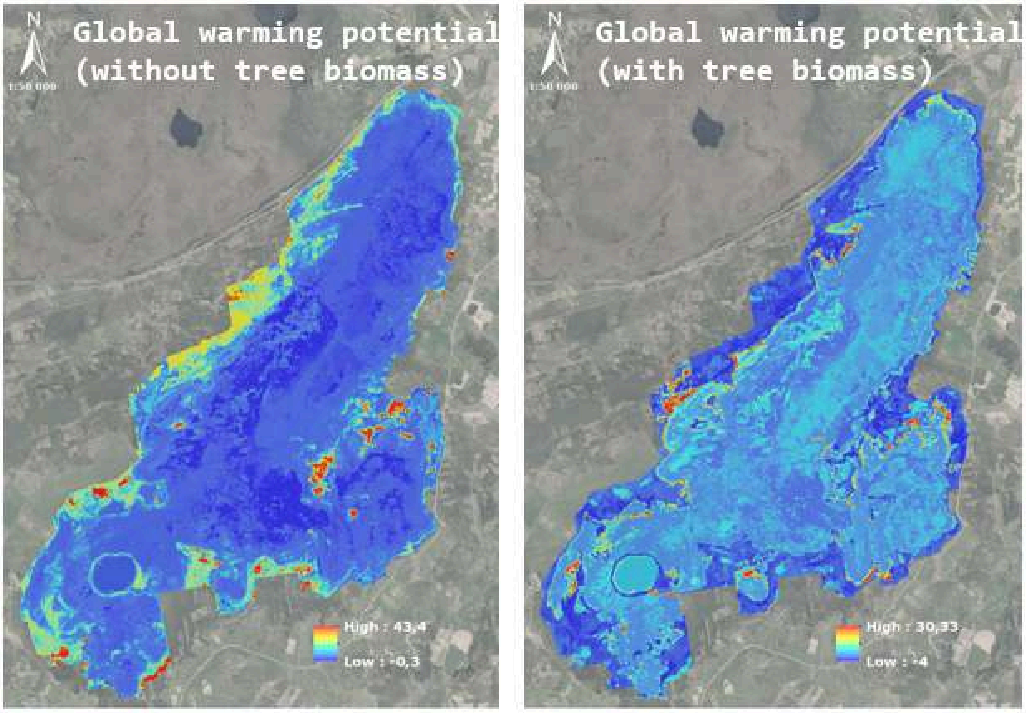

Figure 3.4.4. *Lielais Pelečāre Mire: Global Warming Potential [t CO2 eq./ha/year] maps (without and with tree biomass).*

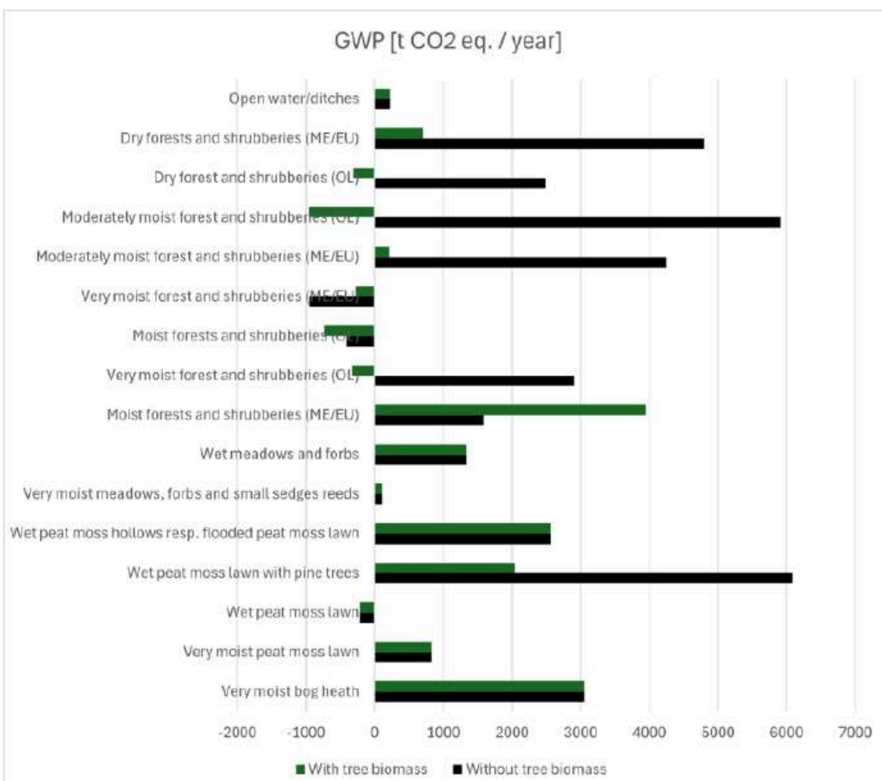

Figure 3.4.5. *Lielais Pelečāre Mire: Global Warming Potential [t CO2 eq./ha/year] sum for each GEST class (without and with tree biomass).*

GEST type mapping – Sudas-Zviedru Mire

In Sudas–Zviedru Mire, airborne data acquisition was conducted on 15 June 2025. False-colour composite images were generated from the acquired airborne dataset to enhance the visual differentiation of spectrally distinct vegetation patches. These composites were used to support the targeted planning of field survey routes and the selection of representative sampling locations. Subsequently, change detection analysis was performed using airborne datasets from 2018 and 2025, complemented by available satellite imagery to ensure temporal consistency and improve the robustness of the assessment. Two field campaigns were carried out on 7 and 15 October 2025 to collect *in situ* reference data for the validation of mapped GEST types and to verify detected changes within the restoration areas (**Figure 3.4.6**).

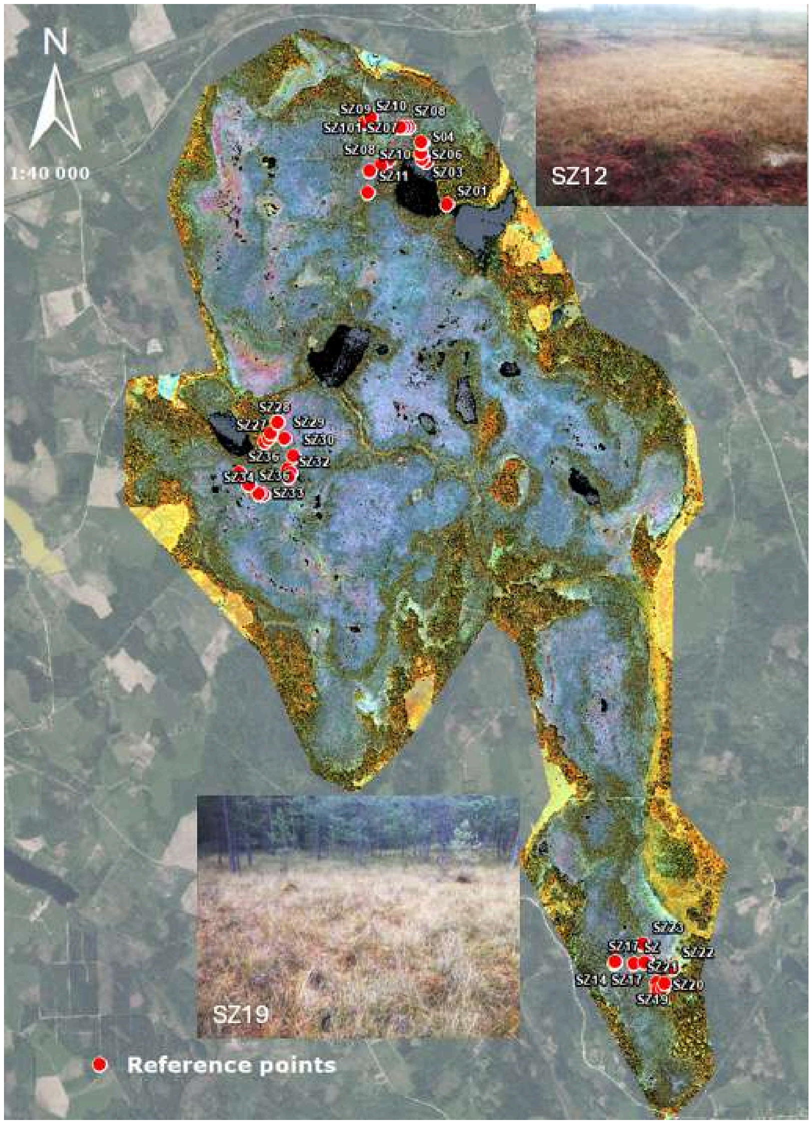

Figure 3.4.6. *Sudas-Zviedru Mire: False color image composite with reference points from two field campaigns in October 2025.*

Detected land cover changes in Sudas–Zviedru Mire between 2018 and 2025 are presented in Figure 7. In several areas, the observed differences may be attributable to varying meteorological conditions between the two acquisition years, as well as to site management activities.

Field inspections of previously restored areas indicated that significant vegetation changes were observed in only one location, which was correctly identified in the change detection layer (**Figure 3.4.7**). The total area of detected changes amounts to approximately 1 ha.

During the field campaigns, additional reference data on GEST types were collected to support subsequent GEST type mapping within the area of interest.

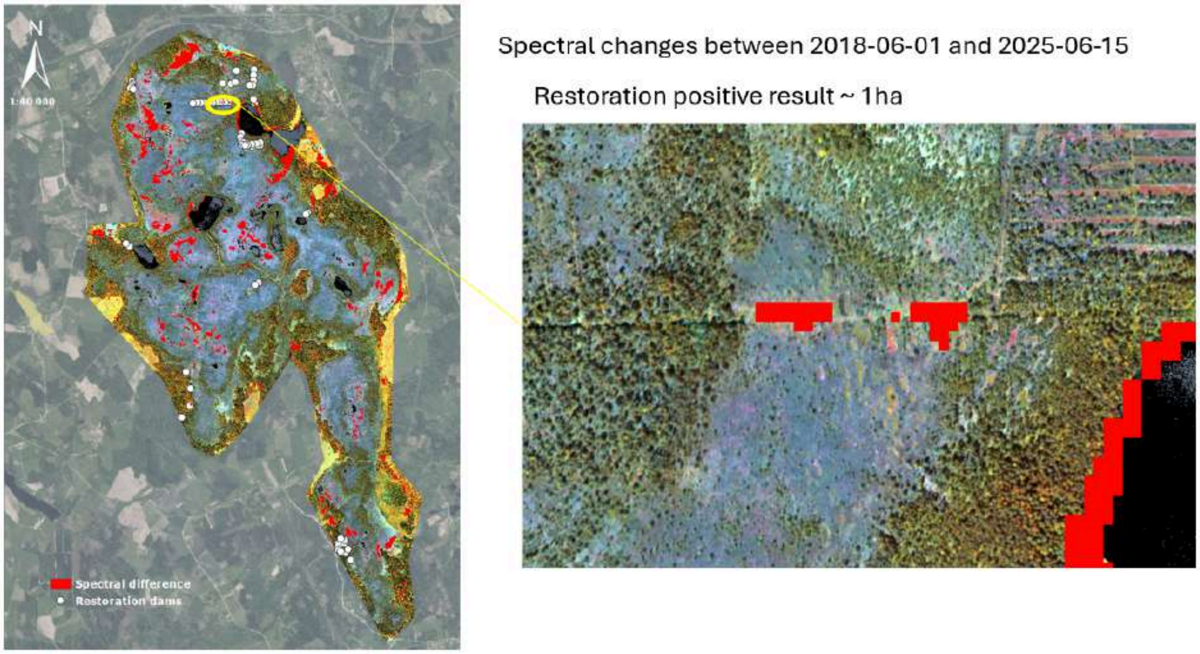

__Figure 3.4.7.__ Sudas-Zviedru Mire: detected changes in land cover between 2018 and 2025 and restoration positive results (~1 ha) visible in these changes.

Remote sensing data for ecosystem modelling – Plant Functional Types

Each GEST type was analysed based on the available data on species composition. Plant species were grouped into Plant Functional Types (PFTs), and the average summarised and normalised PFT distribution within each GEST type is presented in **Figure 3.4.8**.

At present, this analysis has been completed for three pilot areas: Cena Mire, Melnais Lake Mire, and Lielais Pelečāre Mire. Reference data for Sudas–Zviedru Mire are not yet available; therefore, PFT analysis has not been conducted for this site.

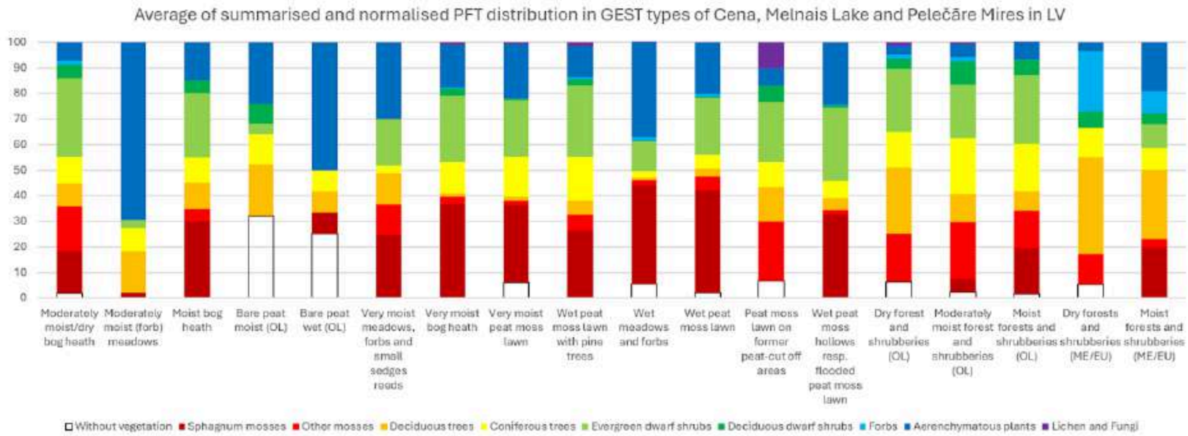

Figure 3.4.8. *Average of summarised and normalised PFT distribution in GEST types.*

Satellite data products for improvement of national GHG inventories

Currently, the main focus has been on testing and demonstrating vegetation intensity mapping and GEST type upscaling using freely available Sentinel satellite data. Such data are typically the primary source for national-scale mapping applications.

Vegetation intensity mapping is commonly performed using the Normalised Difference Vegetation Index (NDVI). National greenhouse gas (GHG) inventory and modelling approaches often require seasonal assessments of vegetation dynamics. An RGB composite representing seasonal NDVI variation for Melnais Lake Mire is presented in **Figure 3.4.9**. The colour gradients highlight areas exhibiting the most pronounced seasonal NDVI changes, which largely correspond to peat extraction sites.

Monthly NDVI profiles for all four pilot mires are shown in **Figure 3.4.10**, demonstrating the potential for more frequent monitoring of vegetation intensity compared to single seasonal assessments. However, consistent monthly NDVI mapping cannot be guaranteed due to frequent cloud cover in the region, which limits the availability of suitable satellite imagery. Despite this limitation, seasonal vegetation intensity maps can be reliably produced.

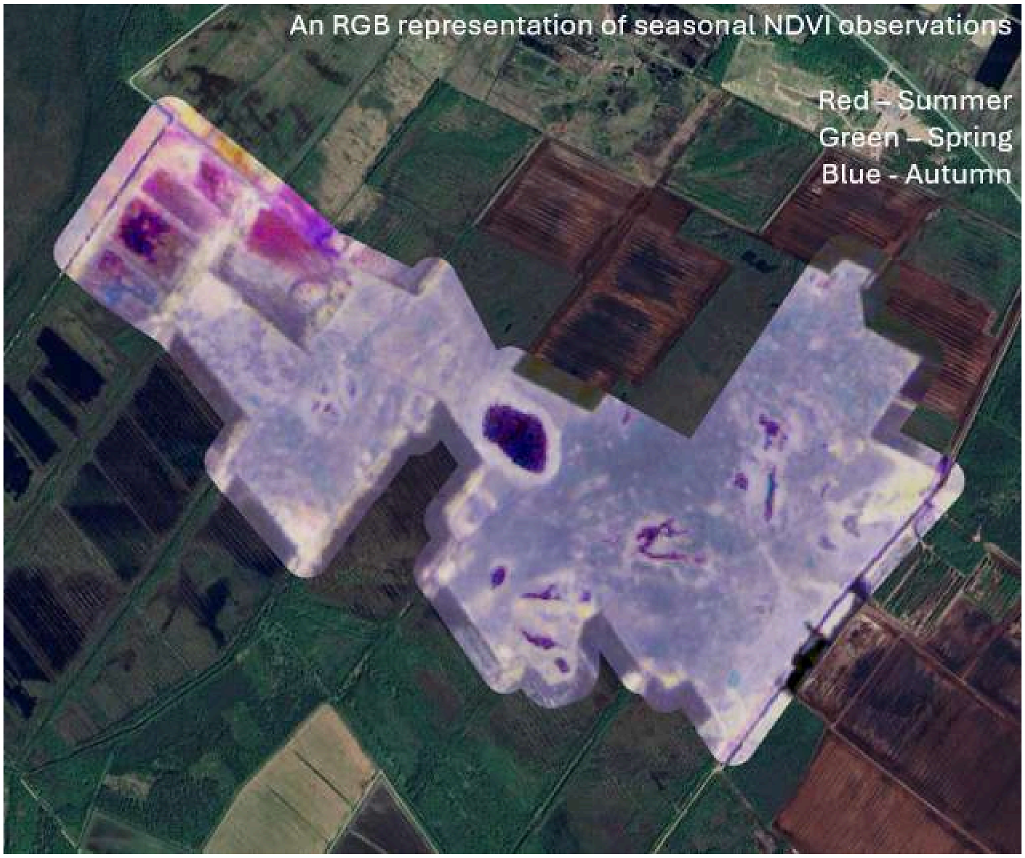

Figure 3.4.9. *Melnais Lake Mire: An RGB representation of a seasonal NDVI.*

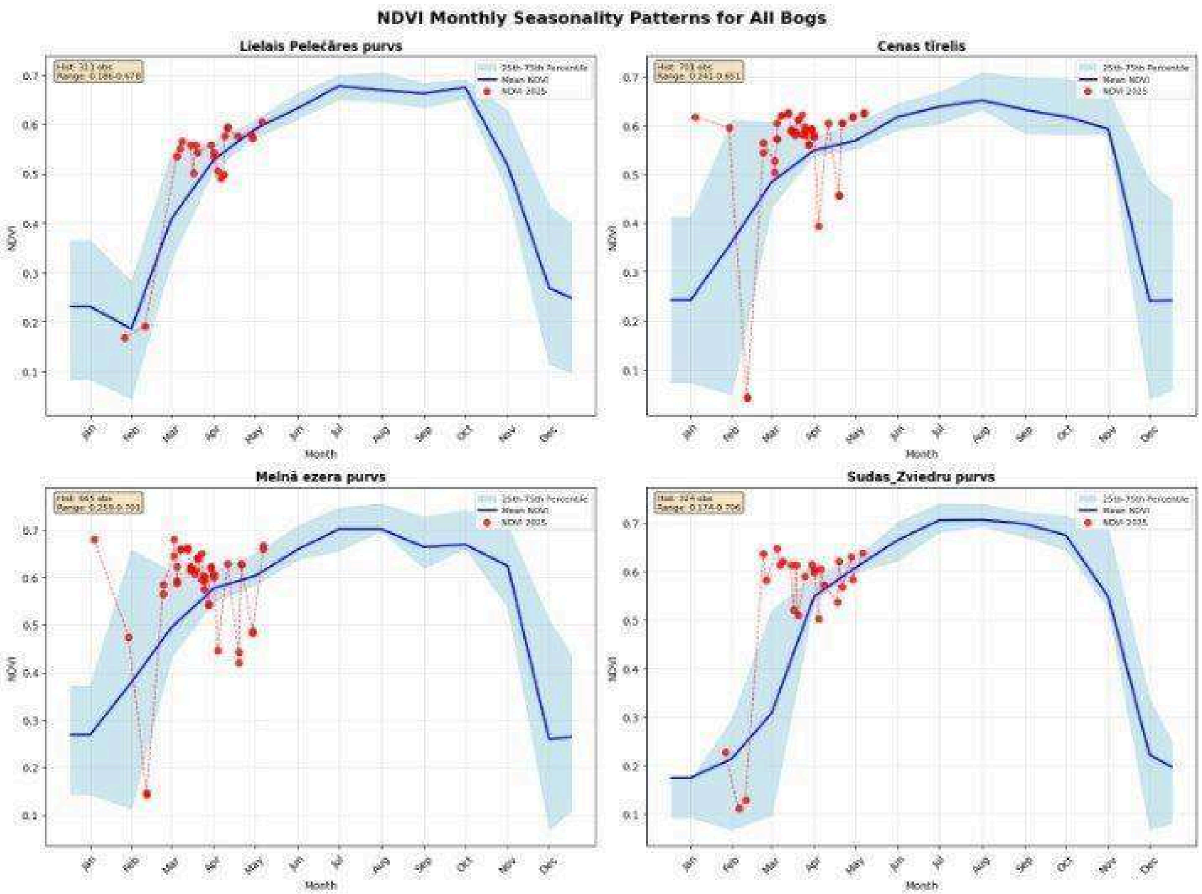

Figure 3.4.10. *Monthly NDVI seasonality patterns for all pilot mires.*

The potential for upscaling high spatial resolution (1 m/pixel) airborne GEST type mapping using lower spatial resolution (10 m/pixel) Sentinel satellite data was assessed for Melnais Lake Mire and Lielais Pelečāre Mire. The airborne-based GEST type map was used as reference data for the preparation of training and validation datasets. Initially, the classification capability of Sentinel-2 data was evaluated using all GEST classes identified from the airborne dataset (13 classes in Melnais Lake Mire). A comparison between the high-resolution airborne GEST classification and the Sentinel-2 data-based classification for Melnais Lake Mire is presented in **Figure 3.4.11**.

The results indicate that Sentinel-2 data perform adequately for GEST types forming relatively large and homogeneous patches, corresponding to at least several Sentinel pixels. However, the classification accuracy decreases in heterogeneous areas where multiple GEST types may occur within a single 10 m pixel. Consequently, the overall classification performance using Sentinel-2 data was substantially lower (see confusion matrix for 13 classes in **Figure 3.4.12**). Class-specific accuracies ranged from 23% to 100%, resulting in an overall accuracy of 40%. Misclassification was most frequently observed between spectrally similar and spatially adjacent GEST classes.

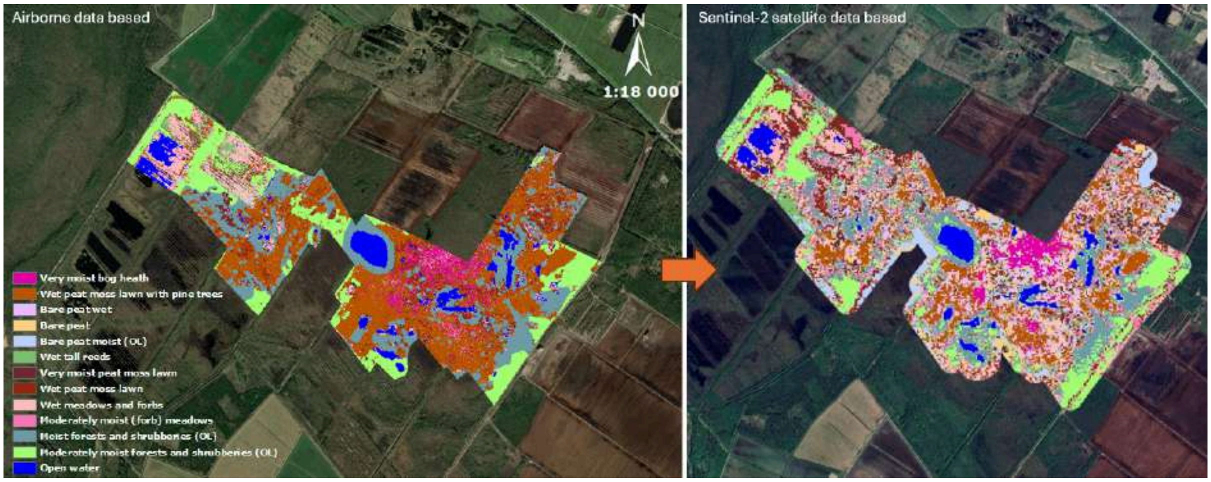

Figure 3.4.11. *Melnais Lake Mire: comparison of GEST type classifications from high resolution airborne data and lower resolution Sentinel satellite data.*

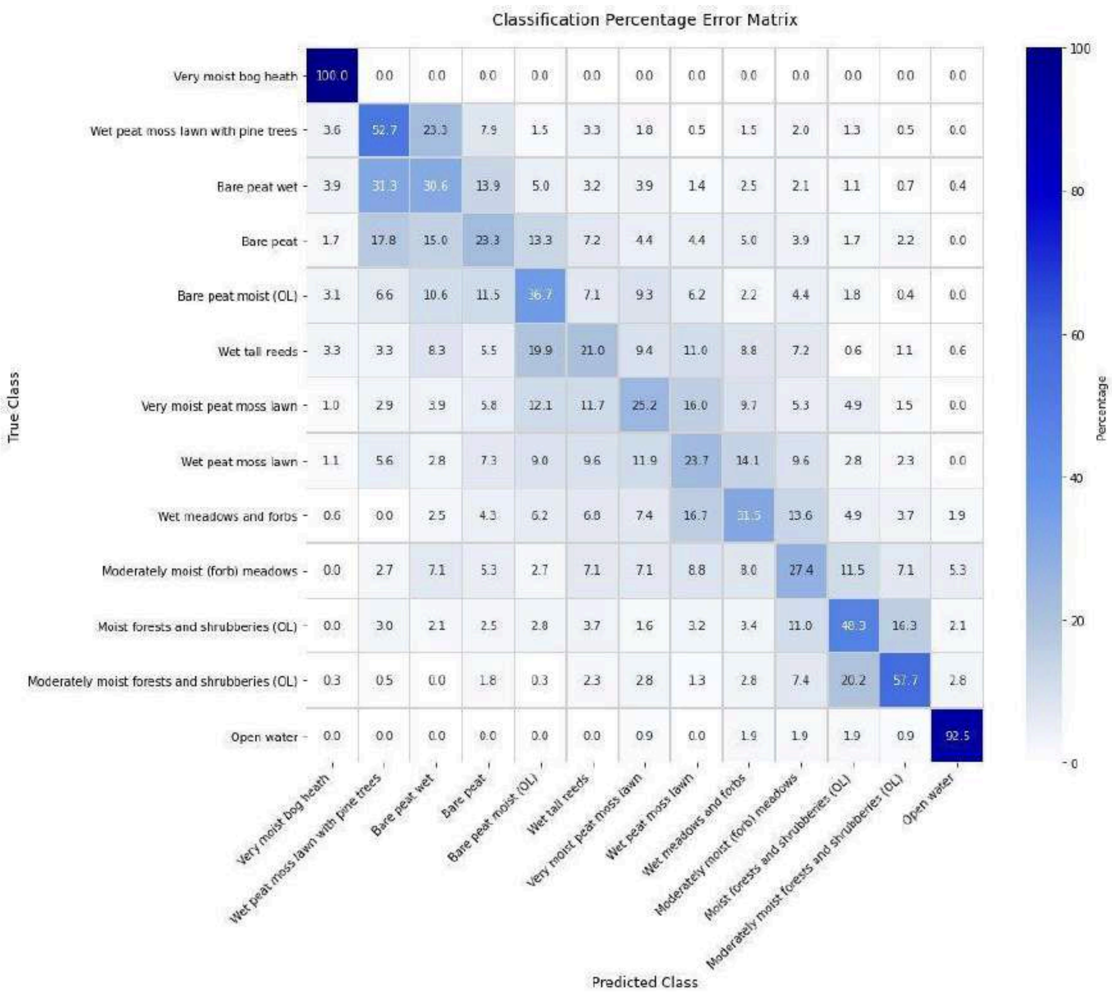

Figure 3.4.12. *Melnais Lake Mire: Sentinel satellite data performance on all 13 GEST classes.*

To improve classification performance, the number of GEST classes was reduced by merging those classes for which misclassification was most frequently observed. In Melnais Lake Mire, simplifying the classification scheme from 13 to 5 aggregated GEST classes increased the overall classification accuracy from 40% to 70% (**Figure 3.4.13**). Class-specific accuracies under the simplified scheme ranged between 50% and 85%.

These results demonstrate that class aggregation substantially enhances the applicability of Sentinel-2 data for GEST-type mapping, particularly in heterogeneous peatland environments.

Figure 3.4.13. *Melnais Lake Mire: Sentinel satellite data performance on 5 aggregated GEST classes.*

A similar assessment of Sentinel-2 GEST type classification capability was conducted for Lielais Pelečāre Mire. Initial classification using all 16 airborne-derived GEST classes resulted in an overall accuracy of 44%, with class-specific accuracies ranging from 20% to 100% (Figure 13). The confusion matrix was analysed to identify systematically misclassified and spectrally similar GEST types, forming the basis for class aggregation. Following the aggregation of classes into 7 broader GEST categories, classification performance improved (**Figure 3.4.14**), achieving an overall accuracy of 61%, with individual class accuracies ranging between 51% and 100%.

These results indicate that further refinement of class aggregation strategies and/or revision of input reference data may contribute to additional performance improvements when applying Sentinel-2 data for GEST type mapping.

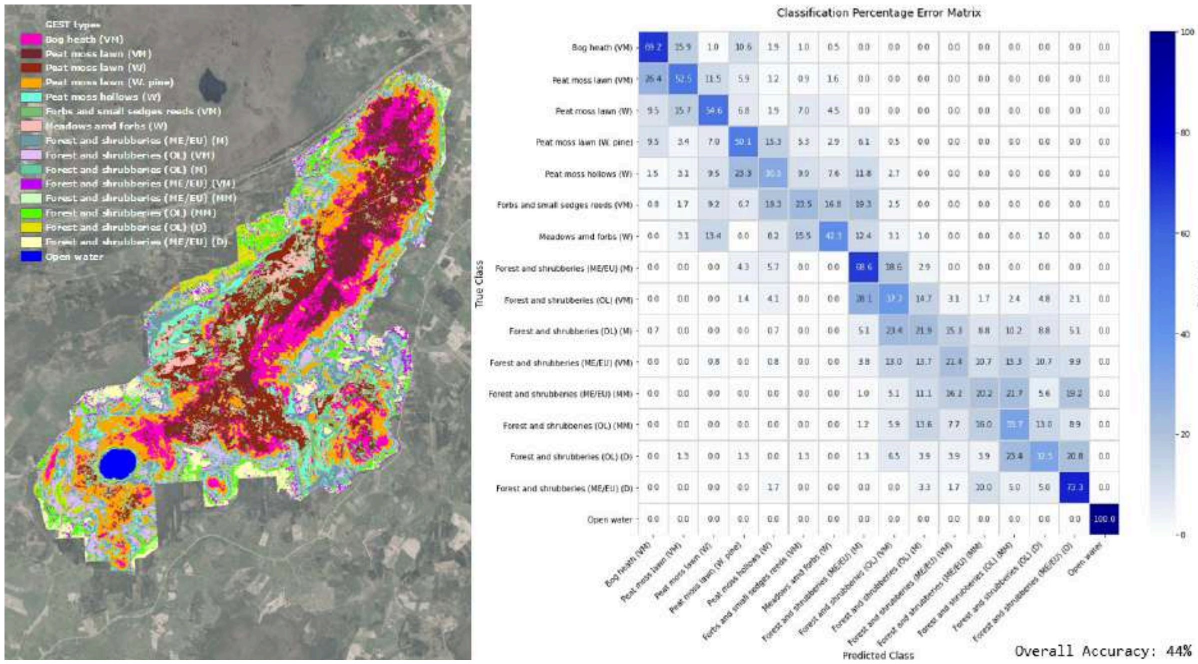

Figure 3.4.14. *Lielais Pelečāre Mire: Sentinel satellite data performance on all 16 GEST classes.*

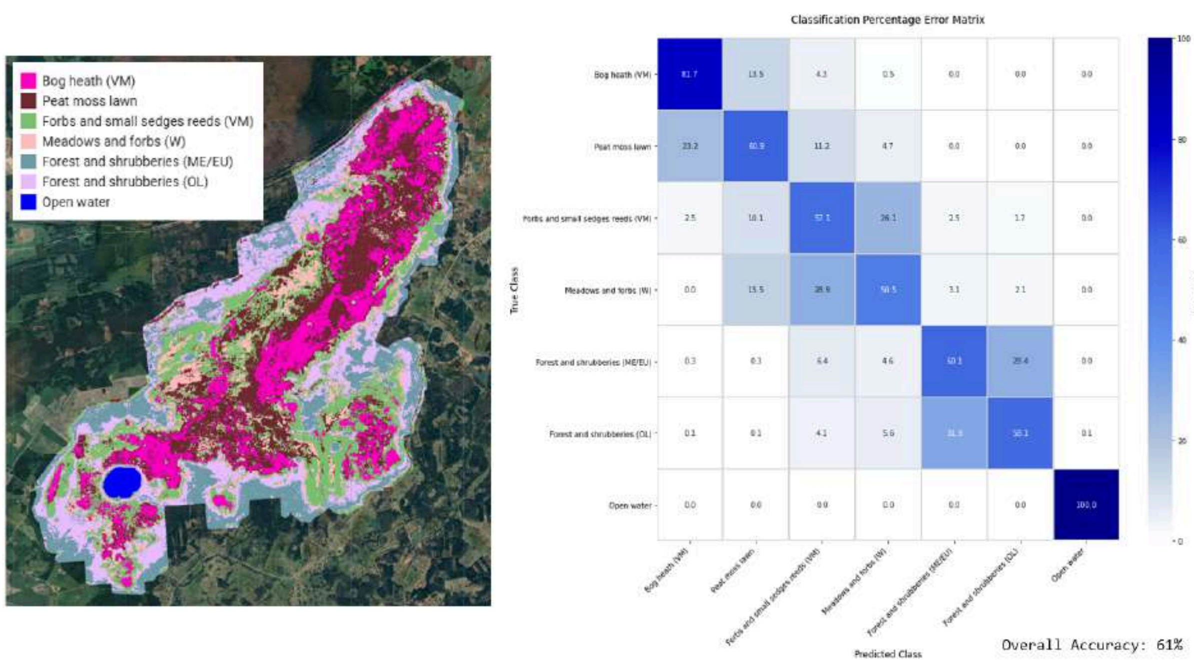

Figure 3.4.15. *Lielais Pelečāre Mire: Sentinel satellite data performance on 7 aggregated GEST classes.*

In addition, a national wetland habitat type classification for Latvia was developed to provide input data for greenhouse gas (GHG) modelling. The applied classification scheme was aligned, where possible, with the approach used by the Finnish project partners, in which land cover classes are primarily defined based on Plant Functional Types (PFTs) that can be reliably distinguished using available remote sensing data.

A habitat-type-based mapping approach was selected because a country-wide and recently updated reference dataset was available, ensuring consistency and robustness of the classification framework. The defined classes were chosen to be reliably separable using Sentinel satellite data. As a result, the national wetland classification scheme comprises eight classes (see legend in **Table 3.4.3**). Examples of habitat-type-based mapping of wetlands are shown in **Figures 3.4.15** and **3.4.16**.

Table 3.4.3. *The legend for habitat type land cover classification of wetlands.*

Colour	Class (Latvian)	Class (English)
	Ūdens	Water
	Skuju koki	Coniferous trees
	Lapu koki	Broadleaf trees
	Aktīvi augstie purvi	Active raised bogs
	Degradēti augstie purvi	Degraded raised bogs
	Pārejas purvi	Transitional mires
	Zāļu purvi	Fens
	Kūdras atradnes	Peat extraction sites

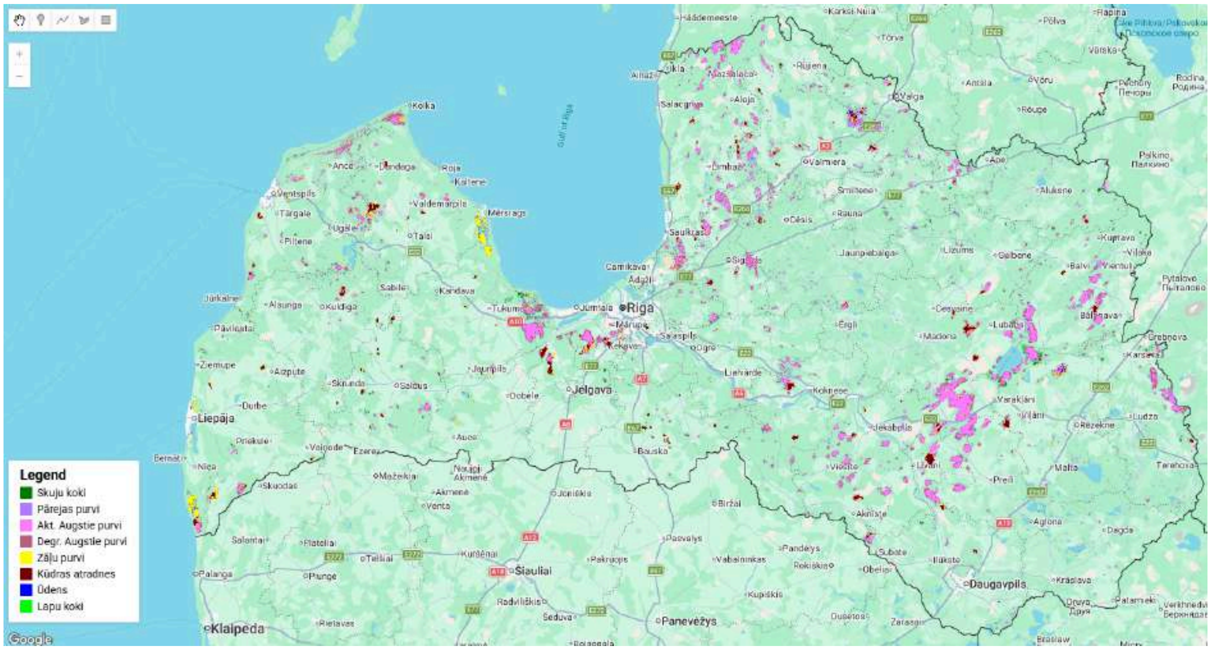

Figure 3.4.15. *Habitat-type-based mapping of wetlands in Latvia.*

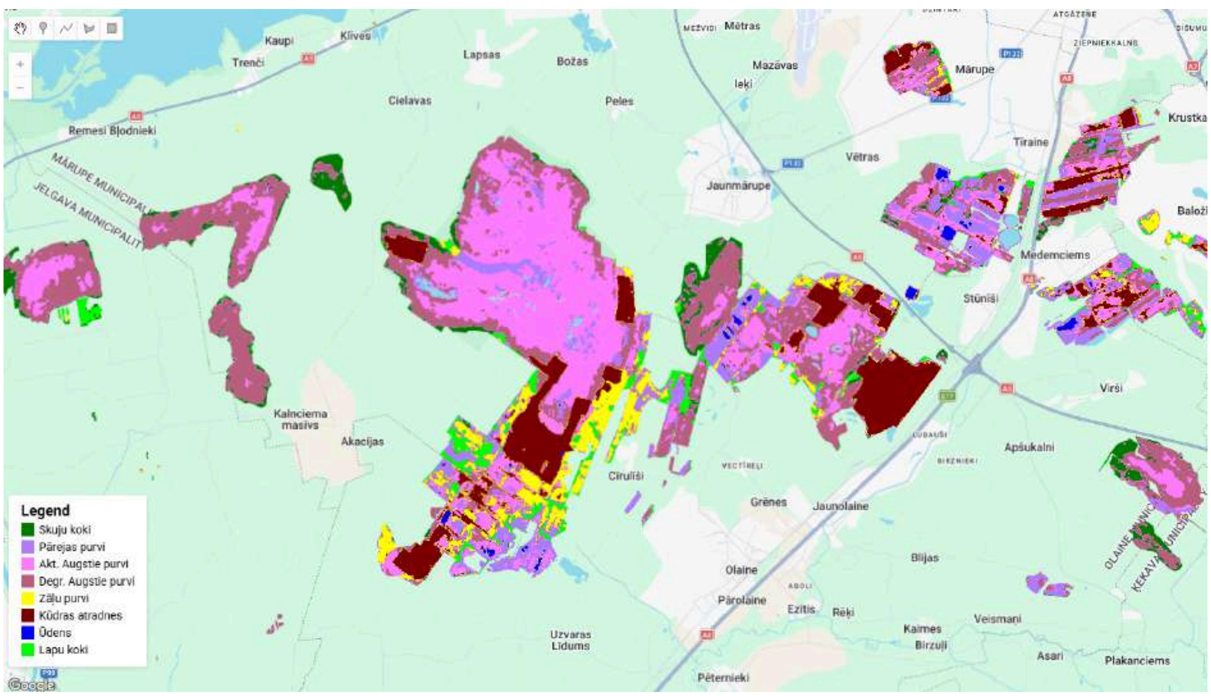

Figure 3.4.16. *Cena Mire and Melnais Lake Mire: Habitat-type-based mapping of wetlands.*

Classification performance results are shown in **Figure 3.4.17**. Single class accuracies range from 62 % to 100 %. The Forest class was subsequently subdivided into Broadleaf trees and Coniferous trees, achieving classification accuracies of 92% and 90%, respectively.

The national wetland extent layer was developed through the integration of multiple available databases, including the habitat database, natural resource database, forest inventory database, and the CORINE Land Cover dataset. This integrated approach has produced the most comprehensive wetland extent dataset currently available at the national level.

Further improvements could be achieved by establishing clearly defined and standardized criteria for delineating wetland boundaries, as well as by specifying primary and secondary data sources. Such methodological clarification would enhance consistency, transparency, and reproducibility of future updates to the dataset.

This approach demonstrates an alternative methodology for developing country-specific GEST-type maps based on freely available Sentinel satellite imagery, supporting scalable and cost-efficient wetland monitoring and GHG modelling at the national level.

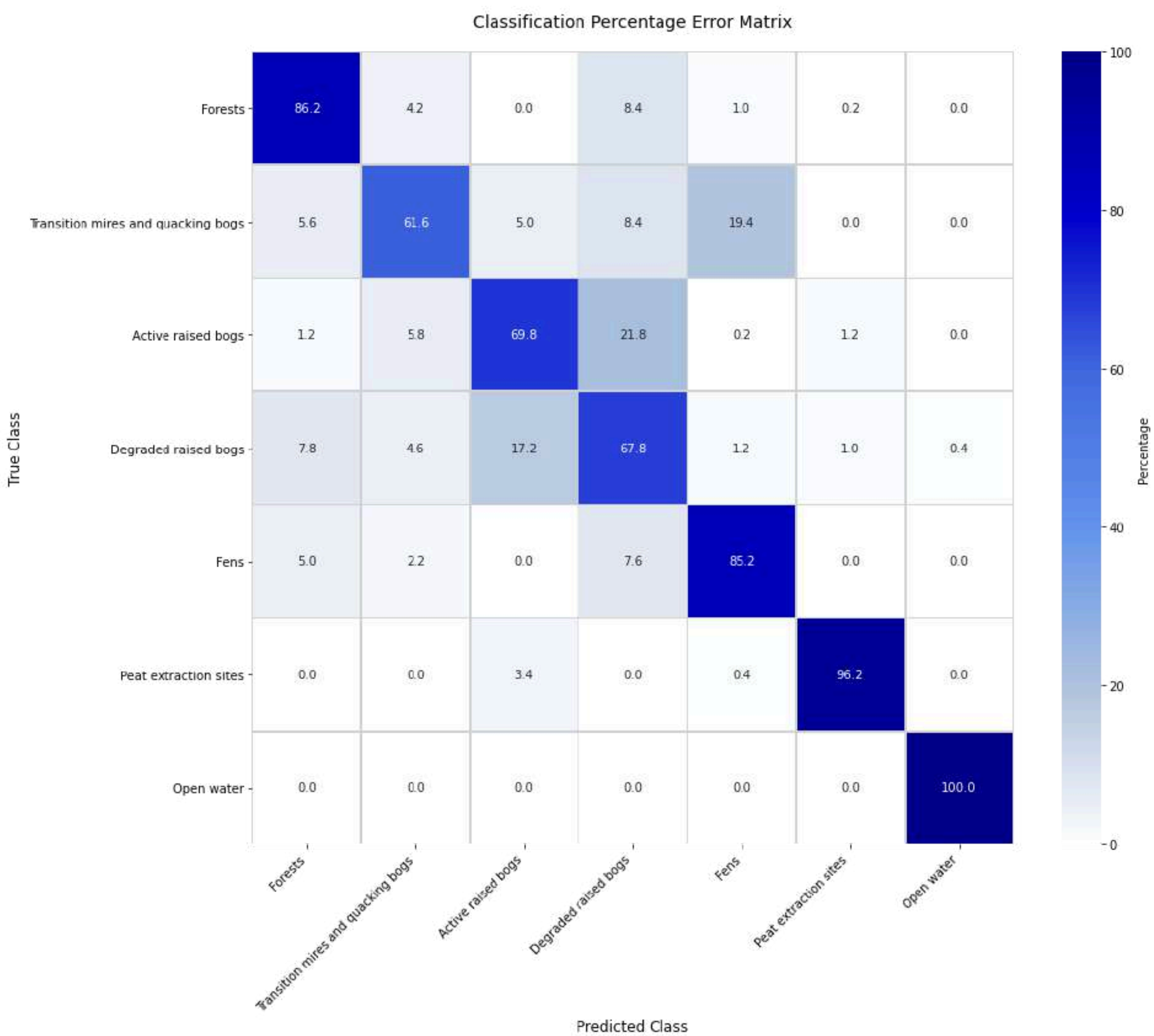

Figure 3.4.17. The classification performance for Habitat-type-based mapping of wetlands.

In 2024 GEST monitoring occurred in accordance with the calibrated remote sensing methodology of the project published in the 1st Monitoring report. The main progress of GEST monitoring was continuation in classification of remote sensing data collected in 2023, besides expeditions of the reference data collection for GEST classification needs of Lielais Pelečāre Mire that was postponed to 2024. The overall progress of the GEST monitoring in 2024 is described for each project site separately below.

3.4.1. Cena Mire

In 2024, based on data collected by aircraft on 2023 September 16 and subsequent reference data collected on 2023 October 17, 19. In the 1st Monitoring report 13 GEST types were described found in Cena Mire. Based on the reference information of the GEST types of GEST classification map was made (**Figure 3.4.18**). Later the GEST map was converted into GHG maps - CO_2, CH_4 and GWP maps (**Figure 3.4.19**).

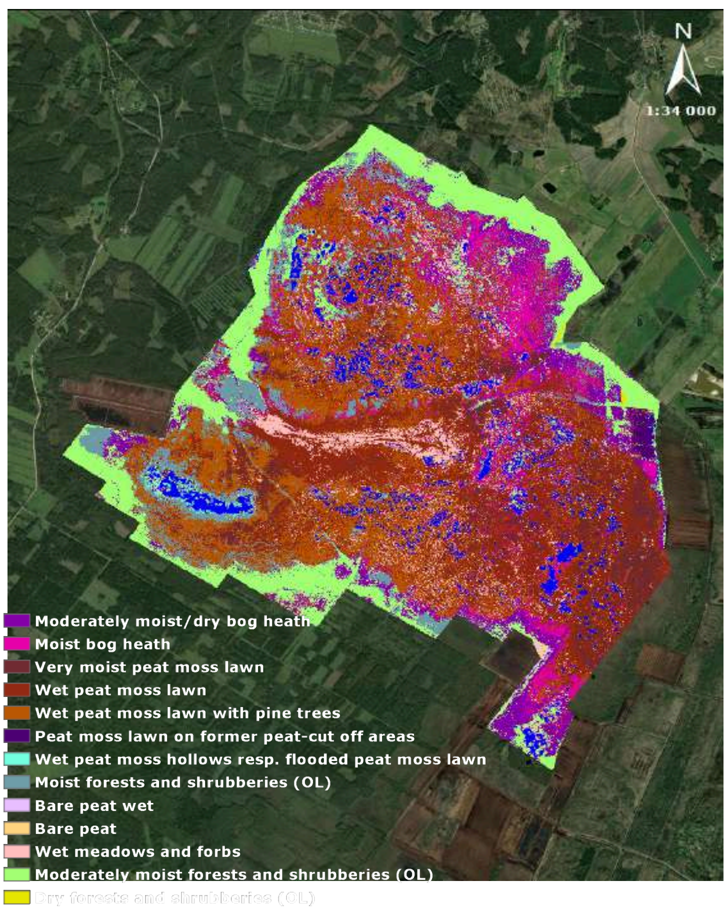

***Figure 3.4.18**. GEST classification map of Cena Mire in 2023. © Institute for Environmental Solutions.*

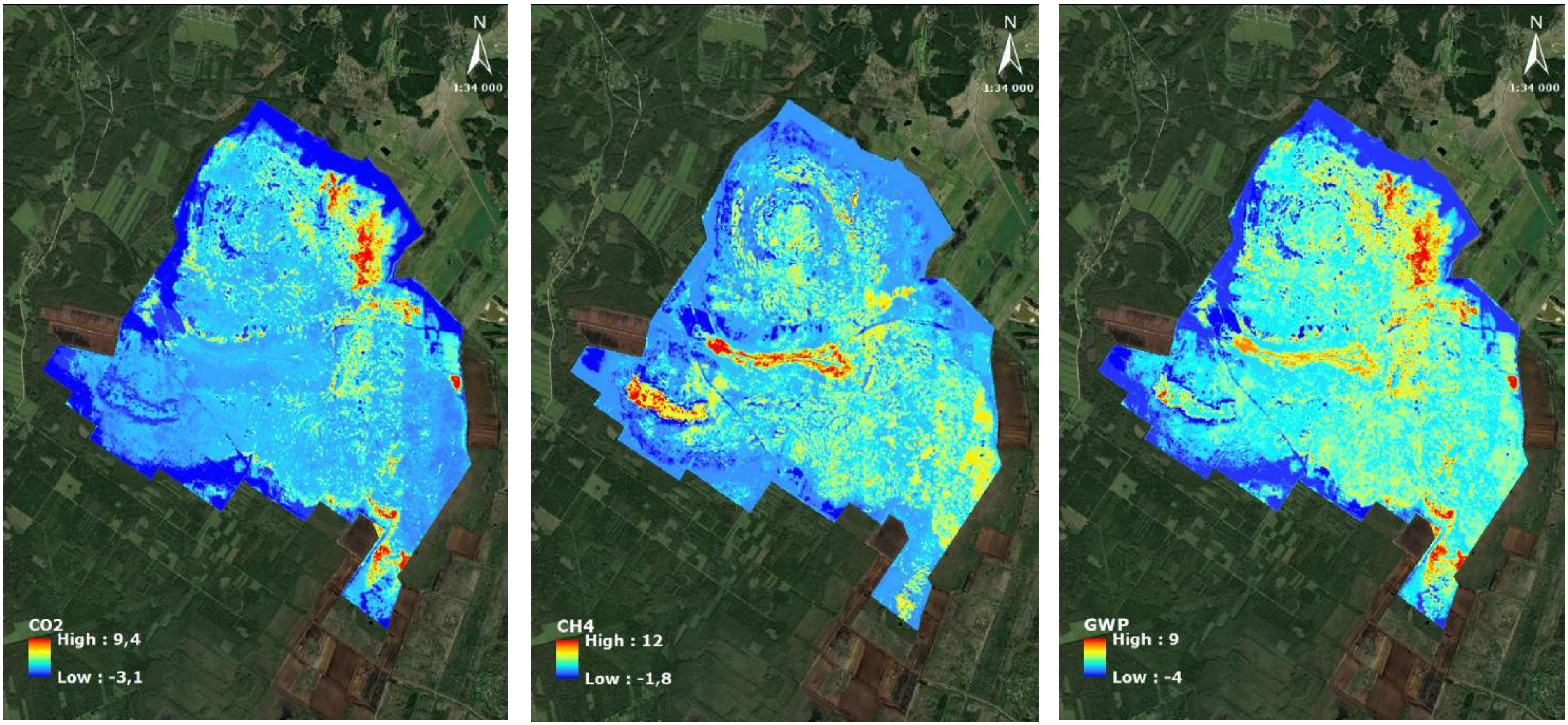

CO_2 emission image (t CO_2 eq./ha/year)

CH_4 emission image (t CO_2 eq./ha/year)

GWP emission image (t CO_2 eq./ha/year)

Figure 3.4.19. *GHG maps of Cena Mire in 2023 including wood biomass data. Abbreviation: GWP – global warming potential. © Institute for Environmental Solutions.*

The conversion of the GEST map into the GHG maps was based on data published in the Handbook for Assessment of Greenhouse Gas Emissions from Peatlands (Jarašius et al. 2022[13]). However, four GEST types missed the required values in the book: 1) Moderately moist/dry bog heath; 2) Dry Forest and shrubberies (OL); 3) Open water/ditches; 4) Wet peat moss lawn with pine trees. As it is noticeable in **Table 3.4.4**, some of those GEST types are very common or even dominant in Cena Mire. Therefore, the produced GHG maps (**Figure 3.4.19**) are quite incomplete to represent GHG emissions of the site. Due to the reason, IES organised a meeting on November 12 with SILAVA asking for advice for gap-filling of the missing GHG values for the particular GEST type. SILAVA accepted IES suggestions for the gap-filling. The refreshed GHG value dataset of GEST types is presented in **Table 3.4.5**.

***Table 3.4.4**. The classified GEST types and their area in Cena Mire*

GEST type	**Area, ha**
Wet peat moss lawn with pine trees	488.82
Wet peat moss lawn	454.80
Moderately moist forest and shrubberies (OL)	332.28
Moist forests and shrubberies (OL)	194.72
Moderately moist/dry bog heath	188.65
Very moist peat moss lawn	183.83
Moist bog heath	173.76
Wet meadows and forbs	139.76
Open water/ditches	110.54
Peat moss lawn on former peat-cut off areas	16.98
Wet peat moss hollows resp. flooded peat moss lawn	7.19
Bare peat wet (OL)	2.48
Bare peat dry (OL)	2.27
Dry forest and shrubberies (OL)	1.53

[13] Jarašius L. *et al*. 2022. Handbook for assessment of greenhouse gas emissions from peatlands. Applications of direct and indirect methods by LIFE Peat Restore. Lithuanian Fund for Nature, Vilnius, 201 p.

Table 3.4.5. *GHG values of GEST types used for the GEST map conversion into GHG maps. Letter colour marks: black – values published in GEST Handbook[1]; purple – gap-filling values extrapolated by IES from other scientific publications describing similar vegetation types. Green colour: GEST types that data with wood biomass is relevant in GHG calculations)*

GEST type	Water level	Data without wood biomass (t CO_2 -eq./ha/year)			Water level	Data with wood biomass (t CO_2 -eq./ha/year)		
		CO_2	CH_4	GWP		CO_2	CH_4	GWP
Open peatland								
Bare peat dry (OL)	2-/3-	7	0.4	7.5	2-/3-	7	0.4	7.5
Moderately moist/dry bog heath	2+/2-	**13.5**	**0.1**	**13.6**	2+/2-	**13.5**	**0.1**	**13.6**
Moderately moist (forb) meadows	2+	20	0	20	2+	20	0	20
Moist reeds and (forbs) meadows	3+	4.6	7.5	12.2	3+	4.6	7.5	12.2
Moist bog heath	3+	9.4	0	9.4	3+	9.4	0	9.4
Bare peat moist (OL)	3+	6.2	0	6.2	3+	6.2	0	6.2
Bare peat wet (OL)	4+	1.5	0.1	1.6	4+	1.5	0.1	1.6
Very moist meadows, forbs and small sedges reeds	4+	-0.5	2.3	1.9	4+	-0.5	2.3	1.9
GEST type	**Water level**	Data without wood biomass (t CO_2 -eq./ha/year)			**Water level**	Data with wood biomass (t CO_2 -eq./ha/year)		
		CO_2	CH_4	GWP		CO_2	CH_4	GWP
Open peatland								
Very moist bog heath	4+	1.7	3	4.6	4+	1.7	3	4.6
Very moist peat moss lawn	4+	-1.1	3.4	2.3	4+	-1.1	3.4	2.3
Very moist tall sedges reeds	4+	0.5	6.9	7.4	4+	0.5	6.9	7.4
Wet peat moss lawn with pine trees	4+	3.9	0.2	4.1	4+	**1.17**	**0.2**	**1.37**
Very moist/Wet calcareous meadows, forbs and small sedges reeds (EU)	4+/5+	2.4	0.5	2.9	4+/5+	2.4	0.5	2.9
Wet meadows and forbs	5+	0	5.8	5.8	5+	0	5.8	5.8
Wet bog heath	5+	3.1	21.6	24.7	5+	3.1	21.6	24.7
Wet tall sedges reeds	5+	-0.1	8.5	8.4	5+	-0.1	8.5	8.4
Wet small sedges reeds mostly with moss layer	5+	-3.5	6.8	3.3	5+	-3.5	6.8	3.3
Wet tall reeds	5+	-2.3	6.3	4	5+	-2.3	6.3	4
Wet peat moss lawn	5+	-0.5	0.3	-0.3	5+	-0.5	0.3	-0.3
Peat moss lawn on former peat-cut off areas	5+	1.5	0.4	1.9	5+	1.5	0.4	1.9
Wet peat moss hollows resp. flooded peat moss lawn	5+	-3.1	12	8.9	5+	-3.1	12	8.9
Open water/ditches	6+	**1.42**	2.8	**4.22**	6+	**1.42**	2.8	**4.22**
Forested peatland								
Dry forest and shrubberies (OL)	2-/3-	26	0	26	2-/3-	**nd**	**nd**	**nd**
Moderately moist forest and shrubberies (OL)	2+	20	0	20	2+	**-3.1**	**-0.11**	**-3.22**
Moist forests and shrubberies (OL)	3+	9.4	0	9.4	3+	**-2.2**	**-1.8**	**-4**
Very moist forest and shrubberies (OL)	4+	1.7	3	4.7	4+	**-2.3**	**1.75**	**-0.55**
Dry forests and shrubberies (ME/EU)	2-/3-	43.4	0	43.4	2-/3-	**nd**	**nd**	**nd**
Moderately moist forest and shrubberies (ME/EU)	2+	20	0	20	2+	**1**	**nd**	**1**

Moist forests and shrubberies (ME/EU)	3+	4.6	7.5	12.2	3+	**21.59-24.98**	**0.004-5.35**	**21.59-30.33**
Very moist forest and shrubberies (ME/EU)	4+	-0.5	2.1	1.6	4+	**-10.72-(-5.97)**	**0.81-4.27**	**-9.91-(-1.7)**
Wet forests and shrubberies (ME/EU)	5+	-3.5	6.8	3.3	5+	**-4.98**	**0.04-11.46**	**-4.85-6.57**

In the following years of the project, the GHG maps of the Cena Mire will be re-produced on the basis of gap-filling values shown in the **Table 3.4.2**. Few GEST types are monitored by chambers in GHG monitoring of the project. When will be accumulated the longest data queue possible during the project years in the GHG monitoring done by SILAVA, a comparison will be made between literature based GHG values of GEST types and the values determined by GHG monitoring. If significant differences will be observed in these data, GHG maps will be updated according to the GHG monitoring results.

3.4.2. Melnais Lake Mire

In 2024, the processing of the reference data collected on 2023 November 2 was carried out to produce a database for GEST classification of Melnais Lake Mire exactly in the same way as is it was done for Cena Mire in 2023. In total 17 different GEST types were classified in the Melnais Lake Mire (**Table 3.4.6**). Four GESTs belong to forest types, and the other 13 to open types.

***Table 3.4.6**. List of classified GEST types in Melnais Lake Mire*

OPEN / FORESTED	GEST type
FORESTED	Dry forest and shrubberies (OL)
FORESTED	Dry forests and shrubberies (ME/EU)
FORESTED	Moderately moist forest and shrubberies (OL)
FORESTED	Moist forests and shrubberies (OL)
OPEN	Bare peat dry
OPEN	Bare peat moist
OPEN	Bare peat wet
OPEN	Moderately moist (forbs) meadows
OPEN	Wet meadows and forbs
OPEN	Open water/ditches
OPEN	Very moist bog heath
OPEN	Wet tall reeds
OPEN	Peat moss lawn on former peat-cut off areas
OPEN	Very moist peat moss lawn
OPEN	Wet peat moss hollows resp. flooded peat moss lawn
OPEN	Wet peat moss lawn
OPEN	Wet peat moss lawn with pine trees

Few examples of classified GEST types observed during the reference data collection in Melnais Lake Mire are shown in Figure **3.4.20.**


Bare peat moist (OL)


Bare peat wet (OL)


Moist forests and shrubberies (OL)


Wet peat moss lawn with pine trees


Wet peat moss lawn


Very moist bog heath

Figure 3.4.20*. Examples of GEST types in Melnais Lake Mire. Images: © L. Strazdiņa.*

The database of GEST reference information was further used to obtain the GEST classification map from the hyperspectral remote sensing data collected for the work on 2023 September 16 (**Figure 3.4.21**).

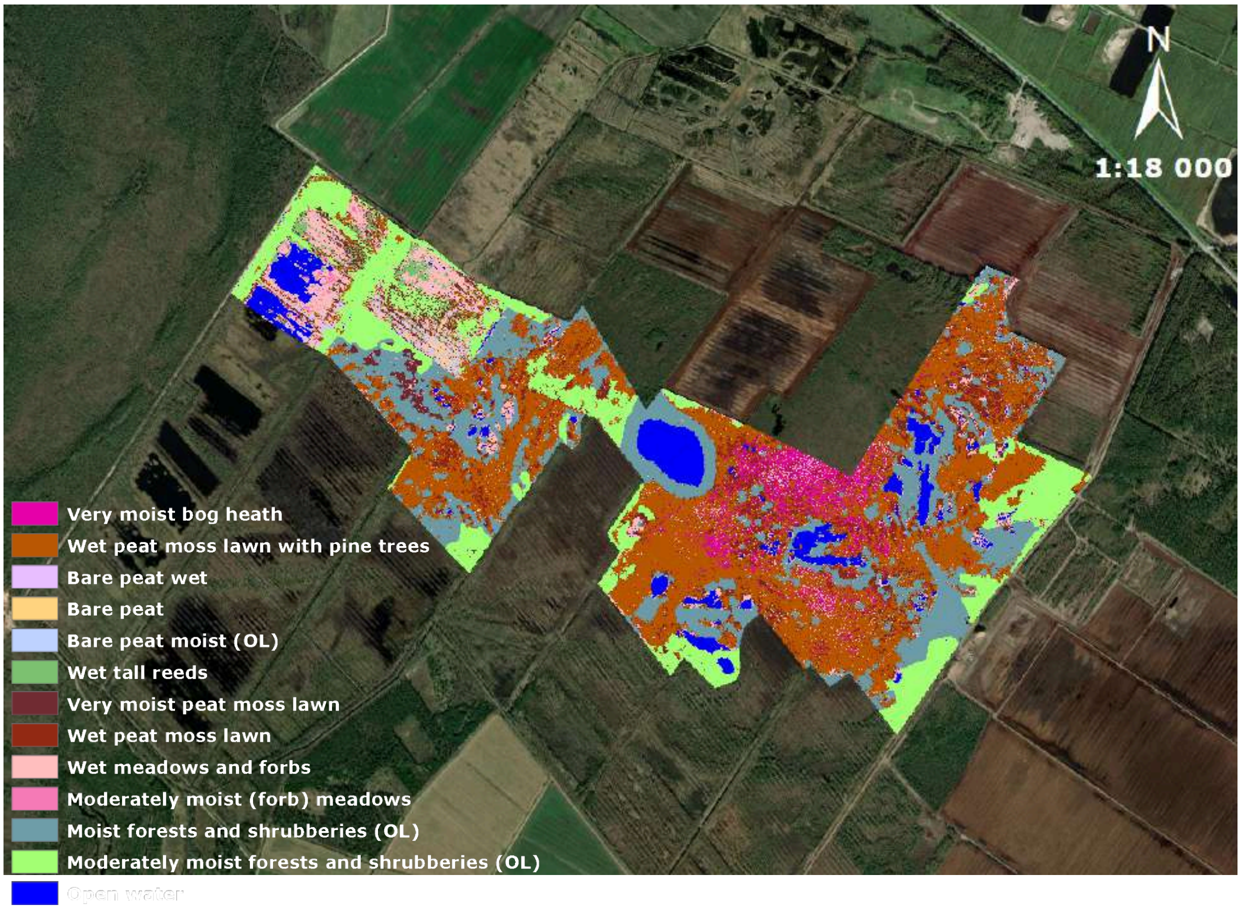

Figure 3.4.21*. GEST classification map of Melnais Lake Mire, 2023. © Institute for Environmental Solutions.*

Further the GEST maps of Melnais Lake Mire were converted into GHG maps – maps of CO_2, CH_4, GWP maps. It was done according to the GHG values presented in Table 2, including IES extrapolated gap-filling values. As a result, two versions of the GHG maps were created – with or without wood biomass data (**Figure 3.4.22, 3.4.23**).

In Melnais Lake Mire GHG monitoring is carried out by SILAVA using climate chambers. For a few GEST types there will be GHG values assessed. During next reporting periods the values will be integrated as well in the GEST monitoring for the Melnais Lake Mire and compared with literature based GHG mapping results.

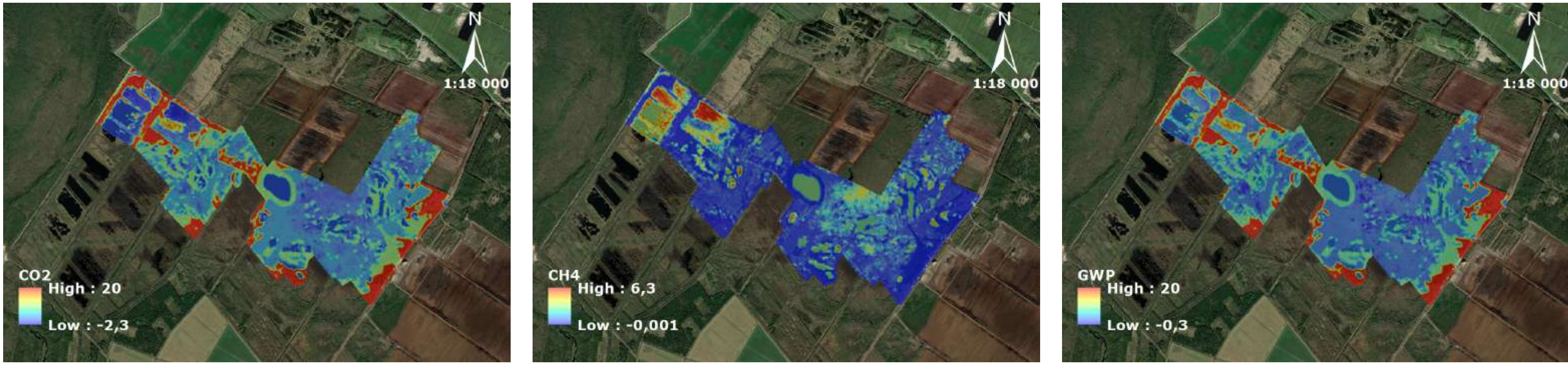

CO_2 emission image (t CO_2 eq./ha/year) CH_4 emission image (t CO_2 eq./ha/year) GWP emission image (t CO_2 eq./ha/year)

***Figure 3.4.22**. GHG maps of Melnais Lake Mire in 2023 without wood biomass data. Abbreviation: GWP – global warming potential. © Institute for Environmental Solutions.*

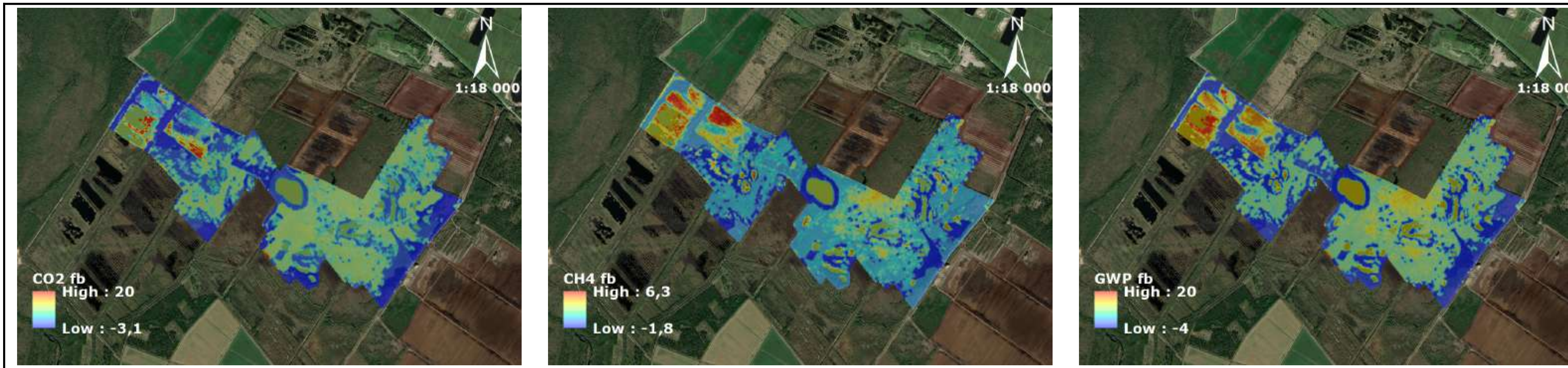

CO_2 emission image (t CO_2 eq./ha/year) CH_4 emission image (t CO_2 eq./ha/year) GWP emission image (t CO_2 eq./ha/year)

***Figure 3.4.23**. GHG maps of Melnais Lake Mire in 2023 including wood biomass data. Abbreviation: GWP – global warming potential. © Institute for Environmental Solutions.*

3.4.3. Lielais Pelečāre Mire

In 2024, May 21, 22, 30, 31 four expeditions of reference data gathering were organised in Lielais Pelečāre Mire. It was necessary for remote sensing data (collected in 2023, August 16) classification into GEST map of the project site. According to collected vegetation data (tree, shrub, herb and bryophyte layer), land usage history, drainage impact, peat characteristics and water table observations, a total of 12 different GESTs were classified in the Lielais Pelečāre Mire (**Table 3.4.7**). Four GESTs belong to forest types, and the other 8 to open types.

Table 3.4.7*. List of classified GEST types in Lielais Pelečāre Mire*

OPEN / FORESTED	GEST type
FORESTED	Dry forest and shrubberies (OL)
FORESTED	Moderately moist forest and shrubberies (OL)
FORESTED	Moist forests and shrubberies (OL)
FORESTED	Moist forests and shrubberies (ME/EU)
OPEN	Very moist meadows, forbs and small sedges reeds
OPEN	Wet meadows and forbs
OPEN	Open water/ditches
OPEN	Very moist bog heath
OPEN	Very moist peat moss lawn
OPEN	Wet peat moss hollows resp. flooded peat moss lawn
OPEN	Wet peat moss lawn
OPEN	Wet peat moss lawn with pine trees

Few examples of classified GEST types observed during the reference data collection in Lielais Pelečāre Mire are shown in Figure **3.4.24**.

Very moist bog heath

Wet meadows and forbs

Wet peat moss lawn

Wet peat moss hollows resp. flooded peat moss lawn

Wet peat moss lawn with pine trees

Moist forests and shrubberies (OL)

Very moist peat moss lawn

Very moist meadows, forbs and small sedges reeds

Figure 3.4.24*. Examples of GEST types in Lielais Pelečāre Mire. Images: © L. Strazdiņa.*

GEST monitoring of Lielais Pelečāre Mire will be continued in the same way as for Cena and Melnais Lake Mire in the next reporting period.

3.5. Annualised net GHG fluxes by interpolation

To illustrate variation in site- and subplot-specific interpolated annual soil C and GHG fluxes, sites were categorised into three broad groups representing mire management states: near-natural, degraded, and rewetted (**Table 3.5.1**).

Table 3.5.1. *Categorisation of the study sites. RB – raised bog, DIZ – drainage impact zone, RE – restoration effect*

Mire	Site	Plot	Category	Habitat
Sudas-Zviedru	LPC_1	A	Near-natural	Near-natural RB
	LPC_1	B	Rewetted	Rewetted degraded RB with direct RE
	LPC_1	C	Rewetted	Rewetted overgrown RB with cumulative RE
Lielais Pelečāre	LPC_2	A	Near-natural	Near-natural RB
	LPC_2	B	Degraded	Drained RB with dense tree layer in the strong DIZ
	LPC_2	C	Degraded	Drained RB with dense tree layer in the weak DIZ
Melnais Lake	LPC_3	A	Near-natural	Near-natural RB
	LPC_3	B	Rewetted	Rewetted degraded RB with direct RE
	LPC_3	C	Degraded	Degraded bog woodland
Cenas	LPC_4	A	Near-natural	Near-natural RB
	LPC_4	B	Rewetted	Restored RB along ditch with direct RE
	LPC_4	C	Degraded	Drained RB with dense tree layer with cumulative RE
	LPC_5	A	Near-natural	Near-natural RB
	LPC_5	B	Degraded	Peat field along drainage ditch in the strong DIZ
	LPC_5	C	Degraded	Dry peat field in the strong DIZ
Lielais Pelečāre	LPC_6	A	Near-natural	Natural RB
	LPC_6	B	Near-natural	Natural RB
	LPC_6	C	Near-natural	Natural RB
	LPC_7	A	Near-natural	Near-natural RB
	LPC_7	B	Near-natural	Natural RB
	LPC_7	C	Near-natural	Near-natural RB

Annualised soil CO_2 efflux, C inputs, and consequently estimated soil C balance did not differ significantly between habitat categories due to high flux variability. On average, annual soil C inputs were similar across all categories. In near-natural mires, inputs were estimated at 4.38 t C ha^{-1} yr^{-1} ; in degraded areas, values ranged from 3.94 to 5.93 t C ha^{-1} yr^{-1} across peat fields and woodlands; and in rewetted sites, inputs were 4.35 t C ha^{-1} yr^{-1} . In contrast, soil heterotrophic respiration showed an increasing trend across categories (near-natural → rewetted → peat field → woodland), rising from a mean of 2.68 to 4.71 t C ha^{-1} yr^{-1} (**Figure 3.5.1**).

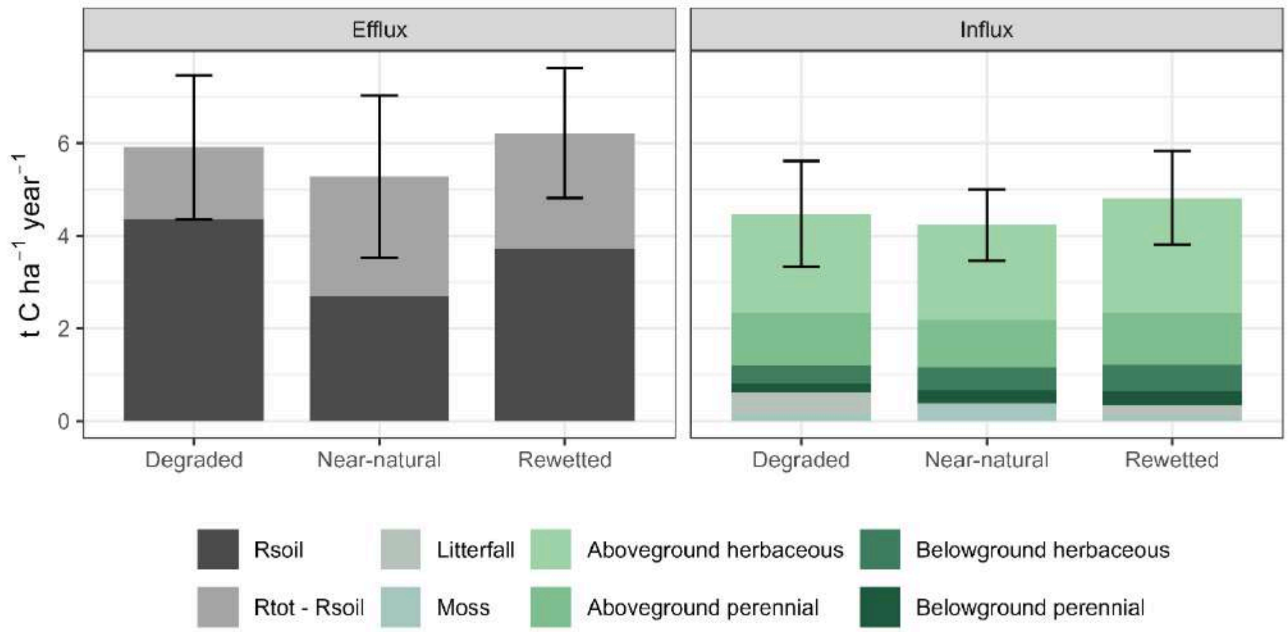

***Figure 3.5.1**. Annual soil CO_2-C efflux and influx (Rsoil – soil respiration, Rtot – soil and ground vegetation respiration)*

Consequently, mean values indicated that degraded soils were close to C flux equilibrium, suggesting relatively stable soil C stocks, whereas near-natural and rewetted soils showed potential for C sequestration, albeit with considerable uncertainty.

Notably, one rewetted site with an insufficient increase in water table can be reclassified as degraded. Following this adjustment, further stratification of degraded sites into dry peat fields and woodlands revealed distinct patterns. Near-natural sites showed a soil C sequestration potential of 1.69 ± 1.26 t C ha^{-1} yr^{-1}. In rewetted sites, this potential was lower, averaging 0.99 ± 0.91 t C ha^{-1} yr^{-1}. In contrast, dry peat fields showed minimal sequestration (0.23 ± 0.95 t C ha^{-1} yr^{-1}), while woodlands exhibited higher values (1.23 ± 1.20 t C ha^{-1} yr^{-1}) (**Figure 3.5.2**).

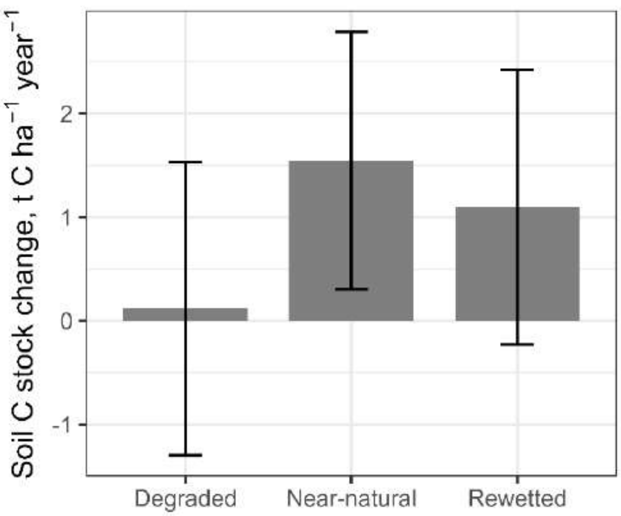

***Figure 3.5.2**. Estimated soil carbon balance*

When CH_4 and N_2O emissions were included and expressed as CO_2 equivalents using 100-year global warming potentials (IPCC AR5), all habitat types acted as net GHG sources. Near-natural habitats were close to GHG neutrality on average, while degraded habitats showed slightly higher emissions and rewetted habitats exhibited the highest net GHG emissions (**Figure 3.5.3**). Following the classification adjustment described above, mean net GHG emissions in rewetted sites increased further to 2.35 t CO_2-C eq. ha^{-1} yr^{-1}, considerably exceeding the near-neutral balance observed in near-natural mires. In contrast, degraded sites showed lower emissions, with dry peat fields estimated at 0.33 t CO_2-C eq. ha^{-1} yr^{-1} and woodlands acting as a net sink (−0.86 t CO_2-C eq. ha^{-1} yr^{-1}). The lower net emissions in degraded sites were primarily driven by reduced CH_4 fluxes and, in the case of woodlands, higher soil C sequestration associated with greater litter inputs.

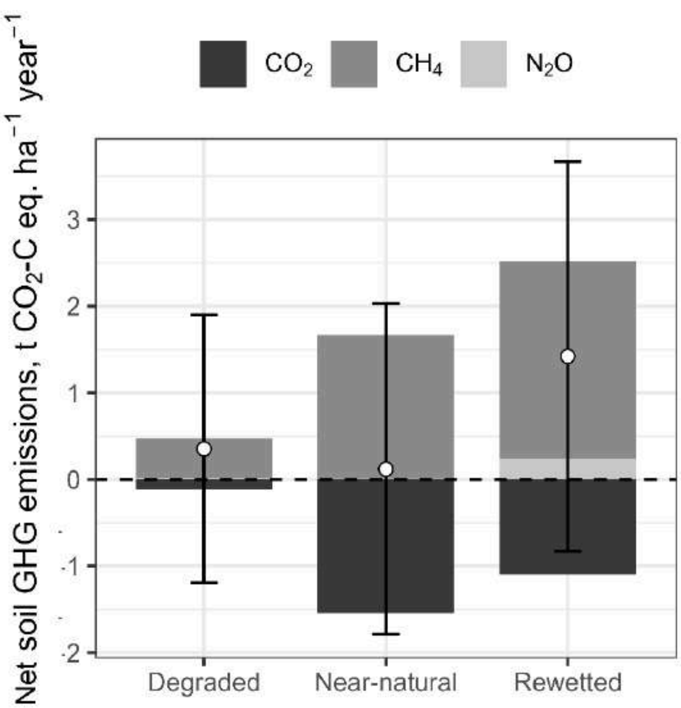

***Figure 3.5.3**. Net soil GHG emissions*

These patterns could largely be associated with water table dynamics. In most degraded subplots, the water table was variable, but generally averaged around 20 cm below the surface, limiting organic matter decomposition while simultaneously creating conditions conducive to CH_4 emissions. Near-natural sites with water table levels generally between 0 and 20 cm below the surface showed potential for soil C removals sufficient to offset CH_4 emissions. In contrast, despite relatively stable raised groundwater levels, rewetted sites exhibited the highest GHG emissions due to elevated CH_4 and N_2O fluxes, probably reflecting recent disturbance effects. One rewetted plot, distinct from the others due to a developed tree stand, showed no increase in N_2O and CH_4 emissions, as water table observations indicated that rewetting had not resulted in a consistently elevated water table.

Overall, the results suggest that both near-natural and rewetted sites show potential for preserving or increasing peatland carbon stocks. However, when CH_4 emissions are included in the GHG balance, rewetting in our sites did not result in net GHG emission reductions. Near-natural plots generally showed lower CH_4 emissions despite elevated groundwater levels. At the same time, observed outliers in near-natural plots indicate that substantially increased CH_4 emissions may occur not only following rewetting but can also persist as long-term emission hotspots.

3.6. Modelling of restoration measures

Restoration measures were simulated by implementing peat dams within the drainage ditches. In the model, drainage ditches are represented by lowering the top bottom surface of the highly permeable upper layer below the ground surface. This created effective channel geometries allowing rapid lateral drainage.

Restoration dams were implemented by locally restoring the bottom surface elevation of the highly permeable layer to the surrounding ground surface. This effectively interrupts channel flow and reduces drainage efficiency. The hydraulic properties of dam cells are identical to the surrounding peat material. Therefore, dams act as hydraulic flow restrictions rather than impermeable barriers.

The spatial distribution of dams follows the ditches along the sloping margins of the raised bogs. Multiple dams were placed along drainage channels at approximately regular elevation intervals. This configuration creates a terraced structure reducing drainage gradually rather than forming large impoundments.

Two simulation scenarios were considered:

- drained scenario — with drainage ditches and no restoration measures
- restored scenario — with dams implemented along drainage channels

All other model parameters, boundary conditions, and meteorological forcing were identical between scenarios. This paired-simulation design allows direct attribution of differences in groundwater dynamics to restoration measures.

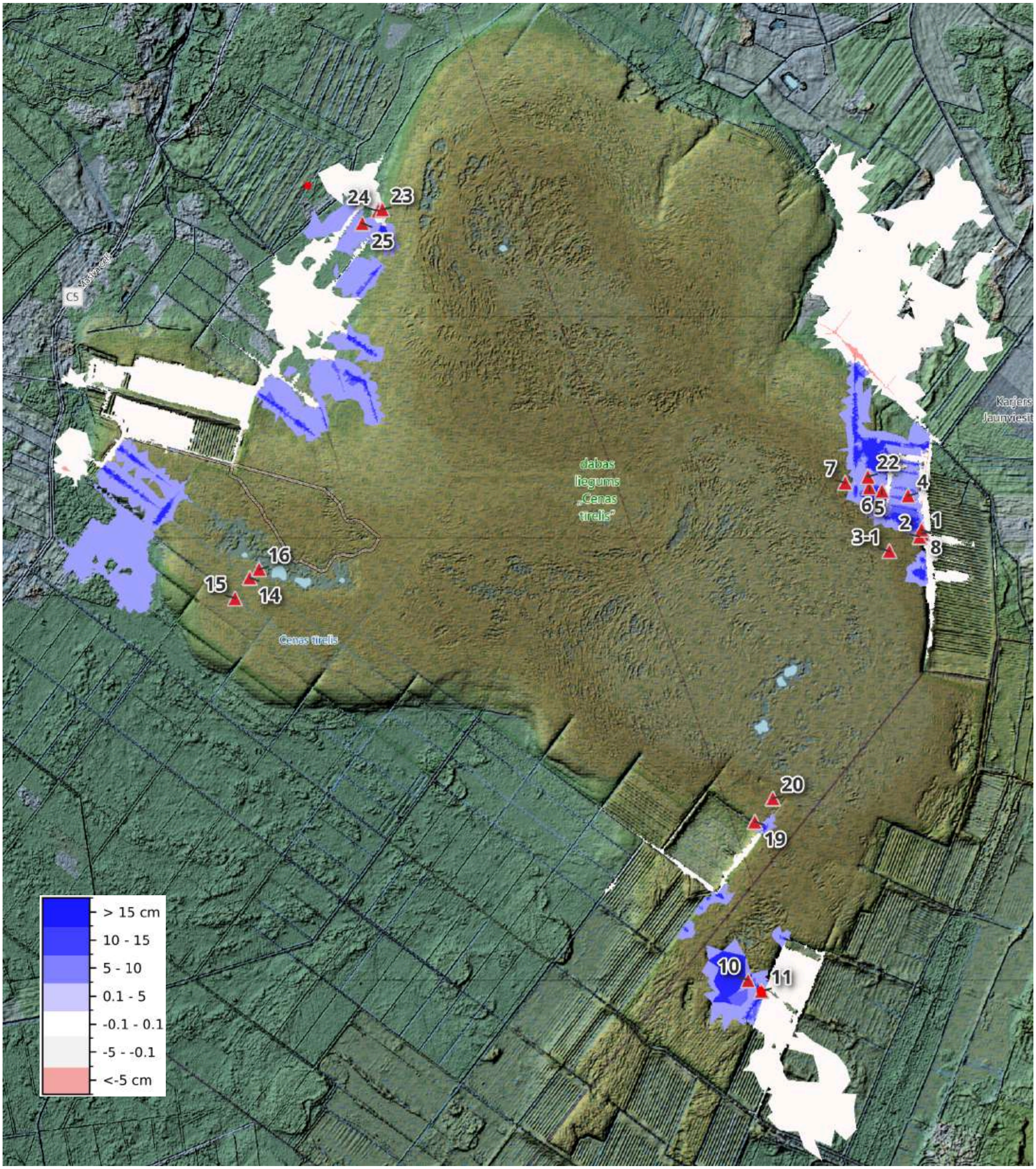

Figure 3.6.1. *Impact of restoration measures in Cena Mire. Mean water table difference ("restored scenario" minus "drained scenario") over 3 years*.

The restoration effect was evaluated as the difference in simulated water table between restored and drained scenarios. Analysis focused on spatial distribution of water table change and temporal evolution of groundwater levels.

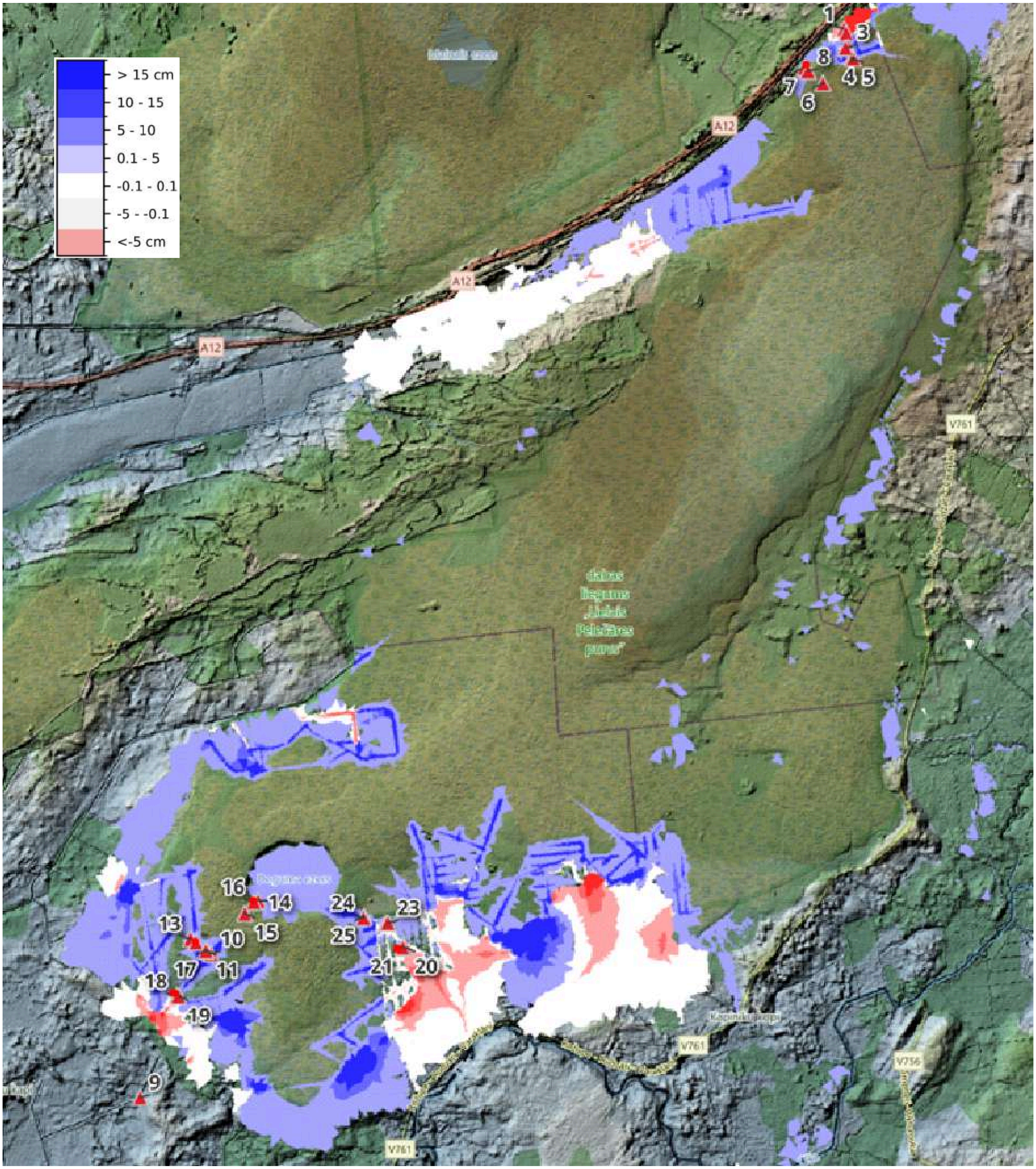

Figure 3.6.2. *Impact of restoration measures in Lielais Pelečare Mire. Mean water table difference ("restored scenario" minus "drained scenario") over 3 years*.

Dams are located mainly along sloping marginal areas; therefore, the expected restoration effect is spatially localized. The central dome of the mires is weakly connected to the drainage system and therefore shows limited response to ditch blocking. The restoration strategy is therefore expected to stabilize groundwater levels in degraded peripheral zones while leaving the hydrological regime of the central dome largely unchanged.

The modest magnitude of water table rise is expected because restoration measures were applied in already relatively wet peatlands. Observed groundwater fluctuations are small, and drainage intensity is moderate. Therefore, ditch blocking results in localized stabilization rather than large-scale water table rise.

We measure impact of restoration measures by comparing yearly average water levels between baseline and restoration scenarios. The spatial extent of the impact of restoration measures is calculated up to 1 mm of water level change.

The simulated spatial extent of impact of restoration measures in Cenas Mire is about 1.5 km^2 (**Figure 3.6.2**.) while in Lielais Pelečāre Mire – 12 km^2. The largest water table rise occurs within drainage channels, here water level increases due to interruption of channel drainage. Note, that water table may lower due to restoration downstream the peat dams – see red zones in **Figures 3.6.1** and **3.6.2**.

In areas adjacent to drainage ditches, the simulated water table rise is limited to a few centimeters. This localized response reflects lateral redistribution of water within the upper peat layer.

Further away from drainage channels, the restoration effect becomes spatially widespread but very small. Water table changes extend over large areas of the peatland but remain in the order of millimeters. These changes approach the level of numerical uncertainty and indicate weak hydraulic connectivity between peripheral drainage systems and the central dome.

Overall, restoration in both Cenas and Pelecare mires results in localized hydrological stabilization near drainage features, while the central dome remains largely unaffected. Thus, restoration primarily stabilizes groundwater levels in degraded marginal areas.

4. References

Bārdule, A., Butlers, A., Spalva, G., Ivanovs, J., Meļņiks, R. N., Līcīte, I., Lazdiņš, A., 2023. The Surface-to-Atmosphere GHG Fluxes in Rewetted and Permanently Flooded Former Peat Extraction Areas Compared to Pristine Peatland in Hemiboreal Latvia. *Water*, *15*(10), 1954. https://doi.org/10.3390/w15101954

Butlers, A., Lazdiņš, A., Kalēja, S., Purviņa, D., Spalva, G., Saule, G., Bārdule, A., 2023. CH4 and N2O Emissions of Undrained and Drained Nutrient-Rich Organic Forest Soil. *Forests*, *14*(7), Article 7. https://doi.org/10.3390/f14071390

Hutchinson, G. L., Livingston, G. P., 1993. Use of chamber systems to measure trace gas fluxes. *ASA Special Publication (USA)*. http://agris.fao.org/agris-search/search.do?recordID=US9423815

Indriksons, A., 2008. Gruntsūdens līmeņa monitorings LIFE projekta "Purvi" vietās. Grām.: Pakalne M. (red.). Purvu aizsardzība un apsaimniekošana īpaši aizsargājamās dabas teritorijās Latvijā. Jelgavas tipogrāfija, Rīga, 142 – 150.

Jakovels, D., Filipovs, J., Brauns, A., Taskovs, J. Erins, G., 2016. Land cover mapping in Latvia using hyperspectral airborne and simulated Sentinel-2 data. In Fourth International Conference on Remote Sensing and Geoinformation of the Environment (RSCy2016), Vol. 9688, pp. 553-563, SPIE.

Jarašius, L., Etzold, J., Truus, L., Purre, H.-A., Sendžikaitė, J., Strazdiņa, L., Zableckis, N., Pakalne, M., Bociąg, K., Ilomets, M., Herrmann, A., Kirschey, T., Pajula, R., Pawlaczyk, P., Chlost, I., Cieśliński, R., Gos, K., Libauers, K., Sinkevičius, Ž., Jurema, L., 2022. Handbook for assessment of greenhouse gas emissions from peatlands. Applications of direct and indirect methods by LIFE Peat Restore. Lithuanian Fund for Nature, Vilnius, 201 p.

Landgrebe, D. A., 2003. Signal theory methods in multispectral remote sensing, Vol. 24. John Wiley & Sons.

Loftfield, N., Flessa, H., Augustin, J., Beese, F., 1997. Automated Gas Chromatographic System for Rapid Analysis of the Atmospheric Trace Gases Methane, Carbon Dioxide, and Nitrous Oxide. *Journal of Environment Quality*, *26*(2), 560. https://doi.org/10.2134/jeq1997.00472425002600020030x

Räsänen, A., Virtanen, T., 2019. Data and resolution requirements in mapping vegetation in spatially heterogeneous landscapes. Remote Sensing of Environment, 230, 111207.

Ukonmaanaho, L., Pitman, R., Bastrup-Birk, A., Breda, N., Rautio, P., 2016. Part XIII Sampling and Analysis of Litterfall. In UNECE ICP Forests Programme Co-ordinating Centre: Manual on methods and criteria for harmonized sampling, assessment, monitoring and analysis of the effects of air pollution on forests (p. 14). Thünen Institute for Forests Ecosystems. http://www.icp-forests.org/manual.htm

Abdalla, M., Hastings, A., Truu, J., Espenberg, M., Mander, Ü., & Smith, P. (2016). Emissions of methane from northern peatlands: A review of management impacts and implications for future management options. *Ecology and Evolution*, *6*(19), 7080–7102. https://doi.org/10.1002/ece3.2469

Albert-Saiz, M., Lamentowicz, M., Rastogi, A., & Juszczak, R. (2025). Unveiling water table tipping points in peatland ecosystems: Implications for ecological restoration. *CATENA*, *257*, 109149. https://doi.org/10.1016/j.catena.2025.109149

Bārdule, A., Butlers, A., Spalva, G., Ivanovs, J., Meļņiks, R. N., Līcīte, I., & Lazdiņš, A. (2023). The Surface-to-Atmosphere GHG Fluxes in Rewetted and Permanently Flooded Former Peat Extraction Areas Compared to Pristine Peatland in Hemiboreal Latvia. *Water*, *15*(10), 1954. https://doi.org/10.3390/w15101954

Butlers, A., Lazdiņš, A., Kalēja, S., Purviņa, D., Spalva, G., Saule, G., & Bārdule, A. (2023). CH4 and N2O Emissions of Undrained and Drained Nutrient-Rich Organic Forest Soil. *Forests*, *14*(7), 1390. https://doi.org/10.3390/f14071390

Darusman, T., Murdiyarso, D., Impron, & Anas, I. (2023). Effect of rewetting degraded peatlands on carbon fluxes: A meta-analysis. *Mitigation and Adaptation Strategies for Global Change*, *28*(3), 10. https://doi.org/10.1007/s11027-023-10046-9

Goodrich, J. P., Campbell, D. I., Roulet, N. T., Clearwater, M. J., & Schipper, L. A. (2015). Overriding control of methane flux temporal variability by water table dynamics in a Southern Hemisphere, raised bog. *Journal of Geophysical Research: Biogeosciences*, *120*(5), 819–831. https://doi.org/10.1002/2014JG002844

Hutchinson, G. L., & Livingston, G. P. (1993). Use of chamber systems to measure trace gas fluxes. *ASA Special Publication (USA)*. http://agris.fao.org/agris-search/search.do?recordID=US9423815

Jauhiainen, J., Heikkinen, J., Clarke, N., He, H., Dalsgaard, L., Minkkinen, K., Ojanen, P., Vesterdal, L., Alm, J., Butlers, A., Callesen, I., Jordan, S., Lohila, A., Mander, Ü., Óskarsson, H., Sigurdsson, B. D., Søgaard, G., Soosaar, K., Kasimir, Å., … Laiho, R. (2023). Reviews and syntheses: Greenhouse gas emissions from drained organic forest soils – synthesizing data for site-specific emission factors for boreal and cool temperate regions. *Biogeosciences*, *20*(23), 4819–4839. https://doi.org/10.5194/bg-20-4819-2023

Kim, D.-G., Vargas, R., Bond-Lamberty, B., & Turetsky, M. R. (2012). Effects of soil rewetting and thawing on soil gas fluxes: A review of current literature and suggestions for future research. *Biogeosciences*, *9*(7), 2459–2483. https://doi.org/10.5194/bg-9-2459-2012

Liu, H., Wrage-Mönnig, N., & Lennartz, B. (2020). Rewetting strategies to reduce nitrous oxide emissions from European peatlands. *Communications Earth & Environment*, *1*(1), 17. https://doi.org/10.1038/s43247-020-00017-2

Loftfield, N., Flessa, H., Augustin, J., & Beese, F. (1997). Automated Gas Chromatographic System for Rapid Analysis of the Atmospheric Trace Gases Methane, Carbon Dioxide, and Nitrous Oxide. *Journal of Environment Quality*, *26*(2), 560. https://doi.org/10.2134/jeq1997.00472425002600020030x

Ojanen, P., Minkkinen, K., Lohila, A., Badorek, T., & Penttilä, T. (2012). Chamber measured soil respiration: A useful tool for estimating the carbon balance of peatland forest soils? *Forest Ecology and Management*, *277*, 132–140. https://doi.org/10.1016/j.foreco.2012.04.027

Ukonmaanaho, L., Pitman, R., Bastrup-Birk, A., Breda, N., & Rautio, P. (2016). Part XIII Sampling and Analysis of Litterfall. In *UNECE ICP Forests Programme Co-ordinating Centre: Manual on methods and criteria for harmonized sampling, assessment, monitoring and analysis of the effects of air pollution on forests* (p. 14). Thünen Institute for Forests Ecosystems. http://www.icp-forests.org/manual.htm

Urbanová, Z., Picek, T., & Bárta, J. (2011). Effect of peat re-wetting on carbon and nutrient fluxes, greenhouse gas production and diversity of methanogenic archaeal community. *Ecological Engineering, Biogeochemical Aspects of Ecosystem Restoration and Rehabilitation*, *37*(7), 1017–1026. https://doi.org/10.1016/j.ecoleng.2010.07.012

Muukkonen, P.: Forest inventory-based large-scale forest biomass and carbon budget assessment: new enhanced methods and use of remote sensing for verification, https://doi.org/10.14214/df.30, 2006.

Bragazza, L., Buttler, A., Siegenthaler, A. and Mitchell, E.A.D. (2009). Plant Litter Decomposition and Nutrient Release in Peatlands. In Carbon Cycling in Northern Peatlands (eds A.J. Baird, L.R. Belyea, X. Comas, A.S. Reeve and L.D. Slater). https://doi.org/10.1029/2008GM000815

Appendices

Appendix 6.1. *Cover of habitats of EU importance in the project sites in Latvia. Source: Nature Conservation Agency, 2023.*

Habitat Code	Habitat type	Cover, ha			
		Cenas Mire	**Melnais Lake Mire**	**Lielais Pelecares Mire**	**Sudas-Zviedru Mire**
2180	Wooded dunes of the Atlantic, Continental and Boreal region	0.8	-	-	-
3150	Natural eutrophic lakes with Magnopotamion or Hydrocharition - type vegetation	-	-	-	61.21
3160	Natural dystrophic lakes and ponds	67.53	18.79	55.45	52.26
3260	Water courses of plain to montane levels with the Ranunculion fluitantis and Callitricho-Batrachion vegetation	-	-	-	0.66
7120	Degraded raised bogs still capable of natural regeneration	50.34	88.68	25.56	58.79
7140	Transition mires and quaking bogs	17.12	-	10.63	53.51
7150	Depressions on peat substrates of the Rhynchosporion	-	-	168.1	29.44
7160	Fennoscandian mineral-rich springs and springfens	-	-	-	0.14
7110*	Active raised bogs	1769.19	186.29	3809.36	2089.39
9010*	Western Taïga	27.8	3.97	26.54	167.68
9020*	Fennoscandian hemiboreal natural old broad-leaved deciduous forests (Quercus. Tilia. Acer. Fraxinus or Ulmus) rich in epiphytes	-	-	14.42	5.76
9050	Fennoscandian herb-rich forests with Picea abies	-	-	-	12.49
9080*	Fennoscandian deciduous swamp woods	-	-	0.86	2.35
9160	Sub-Atlantic and medio-European oak or oak-hornbeam forests of the Carpinion betuli	-	-	24.58	7.09
91D0*	Bog woodland	85.05	-	1041.62	307.34
91E0*	Alluvial forests with Alnus glutinosa and Fraxinus excelsior (Alno-Padion. Alnion incanae. Salicion albae)	-	-	-	0.65
	In total:	**2017.83**	**297.73**	**5177.12**	**2848.76**

Appendix 6.2. *Distribution of habitats of EU importance and location of monitoring plots in project sites in Latvia. Source: Nature Conservation Agency, 2023. Images: © L. Strazdiņa*

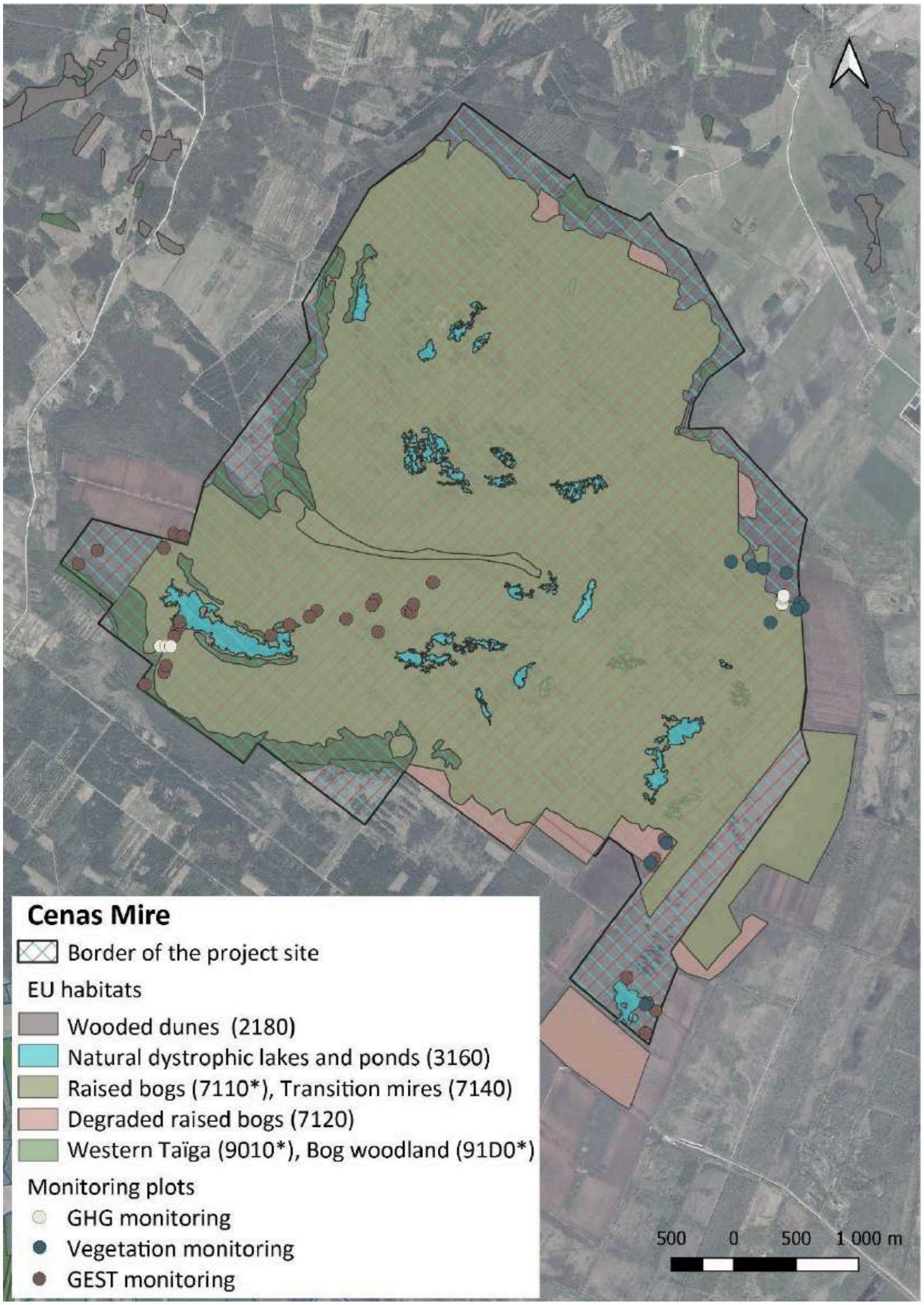

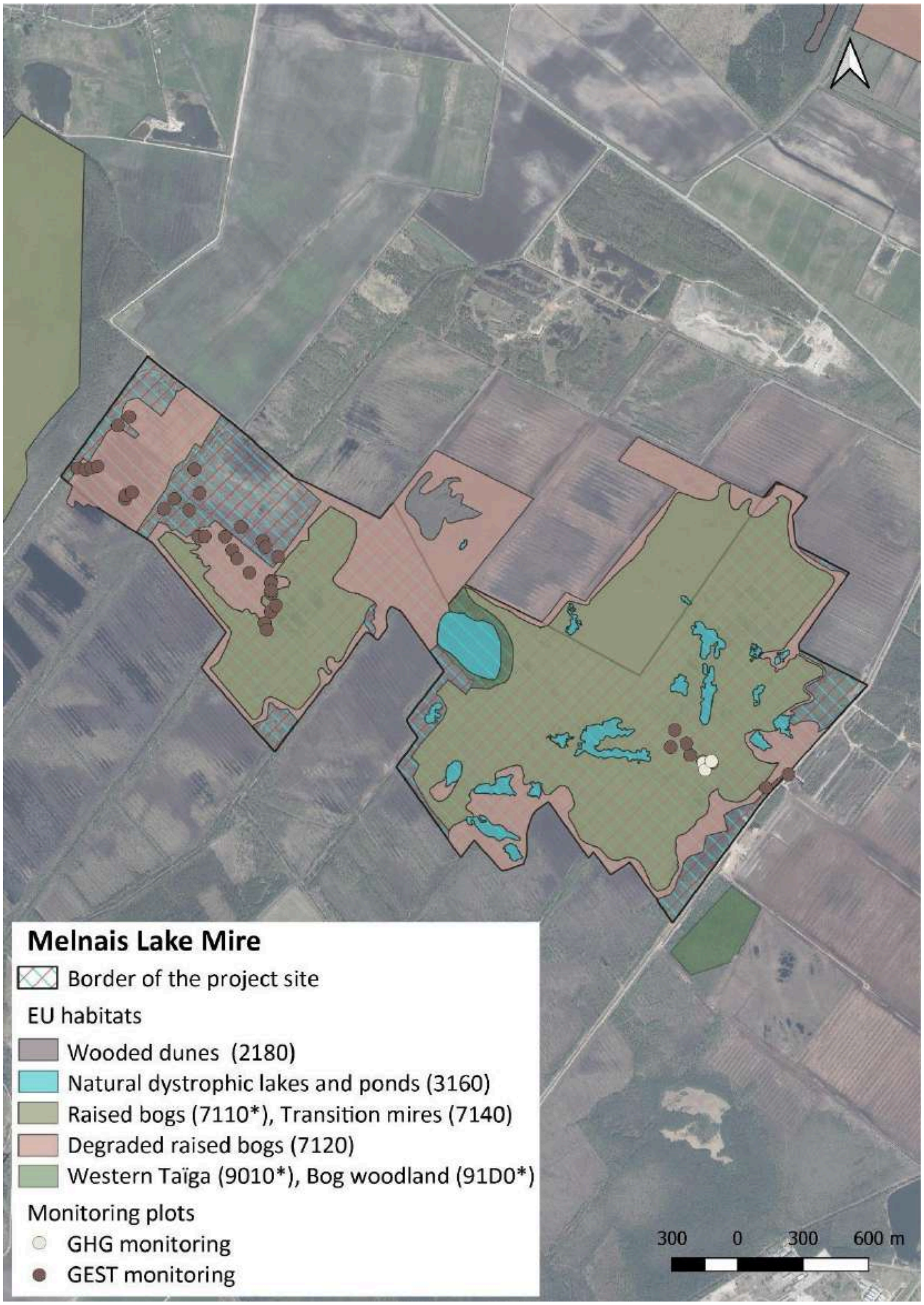
Melnais Lake Mire
Border of the project site
EU habitats
Wooded dunes (2180)
Natural dystrophic lakes and ponds (3160)
Raised bogs (7110*), Transition mires (7140)
Degraded raised bogs (7120)
Western Taïga (9010*), Bog woodland (91D0*)
Monitoring plots
GHG monitoring
GEST monitoring
300 0 300 600 m

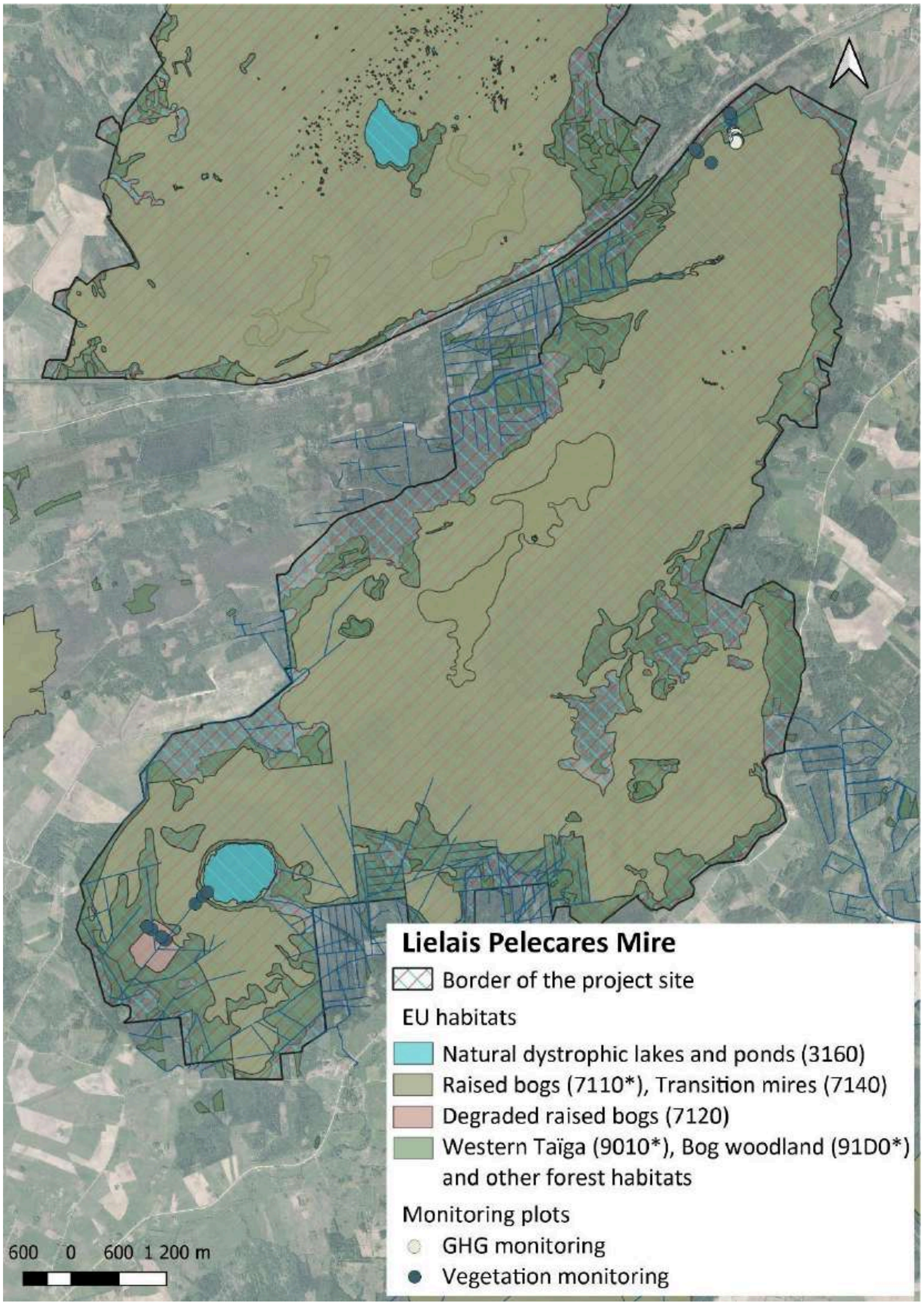
Lielais Pelecares Mire
Border of the project site
EU habitats
Natural dystrophic lakes and ponds (3160)
Raised bogs (7110*), Transition mires (7140)
Degraded raised bogs (7120)
Western Taïga (9010*), Bog woodland (91D0*) and other forest habitats
Monitoring plots
GHG monitoring
Vegetation monitoring
600 0 600 1 200 m

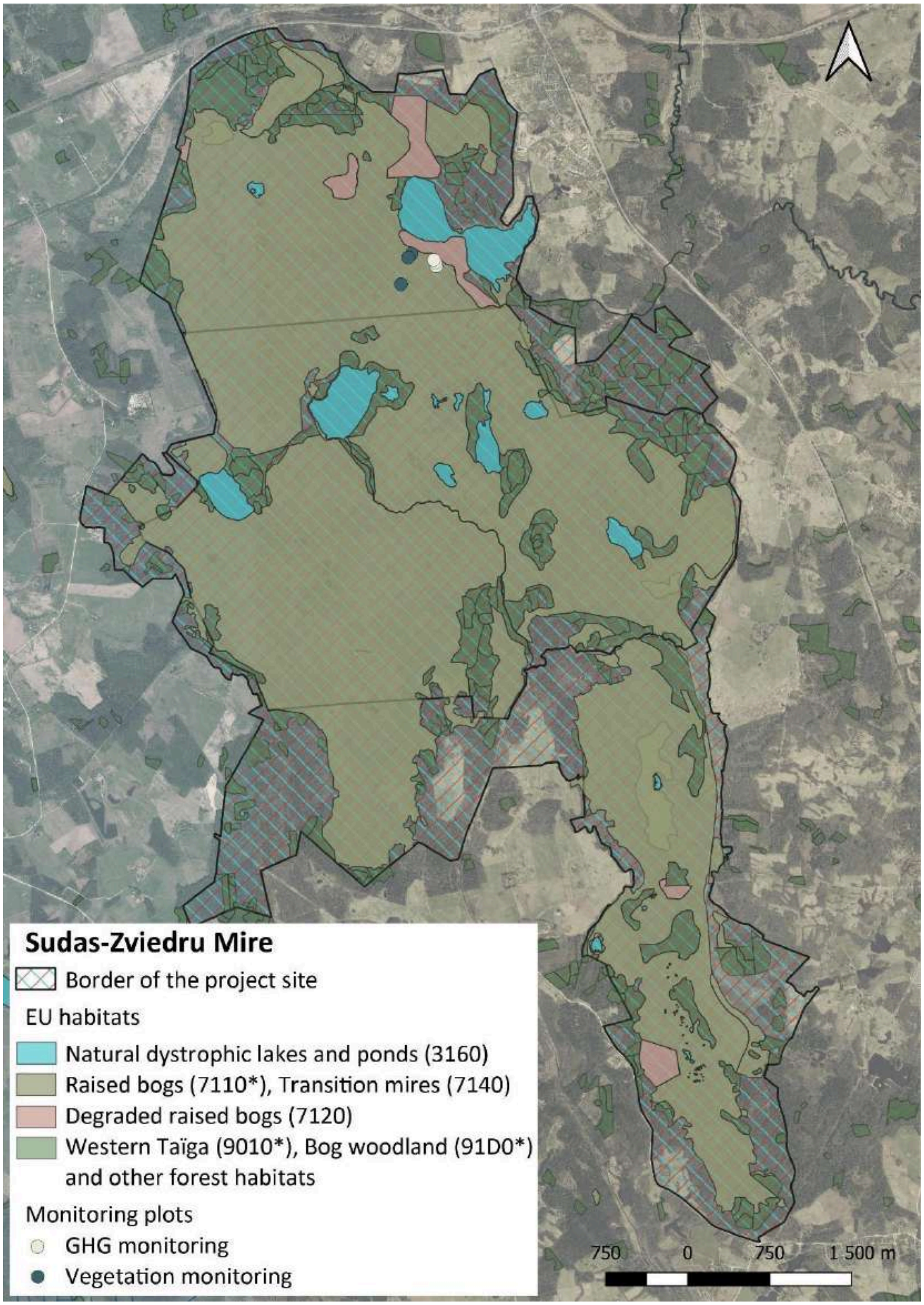
Sudas-Zviedru Mire
Border of the project site
EU habitats
Natural dystrophic lakes and ponds (3160)
Raised bogs (7110*), Transition mires (7140)
Degraded raised bogs (7120)
Western Taïga (9010*), Bog woodland (91D0*) and other forest habitats
Monitoring plots
GHG monitoring
Vegetation monitoring
750
0
750
1 500 m

Appendix 6.3. *Parameters of hydrological regime monitoring automatic measurement points in Cena Mire.*

ID	Type*	Lat / Lon	Well head hight m a.s.l. LAS 2000.5 / relative hight	Type of probe Installation date	Construction	Aim of the monitoring
Cena1	MW	56.853095 / 23.888816	11.26 / 0.64	Levelogger 5 Junior 2024-05-07	Well filter interval: 1.36-3.36 m	Monitoring the water level gradient from the contour ditch to the undisturbed raised bog
Cena2	MW	56.852887 / 23.888461	12.15 / 0.32	Levelogger 5 Junior 2024-05-07	Well filter interval: 0.68 -2.68	
Cena3-1	MW	56.851967 / 23.884983	13.12 / 0.66	Levelogger 5 Junior 2023-06-08	Well filter interval: 0.34-2.34 m	
Cena3-2	MW	56.85197 / 23.884984	13.12 / 0.66	Levelogger 5 Junior 2024-05-07	Well filter interval: 0.34-2.34 m	Investigate the impact of mire surface movement on the borehole without anchoring
Cena3-3	MW	56.851965 / 23.884992	13.10 / 0.66	Levelogger 5 Junior 2024-05-07	Well filter interval: 4.34-5.34 m	Piezometric water level comparison in the upper part (acrotelm) and base (catotelm) of the raised bog
Cena4	MW	56.855515 / 23.887163	11.03 / 0.48	Levelogger 5 Junior 2023-06-08	Well filter interval: 0.52-2.52 m	Water level observations in the peatland area with hydrological regime restoration measures
Cena5	MW	56.855852 / 23.884118	11.12 / 0.23	Levelogger 5 Junior 2023-06-08	Well filter interval: 0.77-2.77 m	
Cena6	MW	56.856034 / 23.882628	11.66 / 0.29	Levelogger 5 Junior 2023-06-08	Well filter interval: 0.71-2.71 m	
Cena7	MW	56.856342 / 23.879809	12.80 / 0.18	Levelogger 5 Junior 2023-06-08	Well filter interval: 0.82-2.82 m	
Cena22	MW	56.856748 / 23.882486	13.23 / 0.20	Levelogger 5 Junior 2024-05-07	Well filter interval: 0.80-2.80 m	
Cena8	Q	56.853344 / 23.888705	10.12 / 0.58	Levelogger 5 Junior 2023-06-08	Rectangular spillway, 0.13 m wide, discontinued, no data available	Dithc discharge monitoring
Cena10	MW	56.824516 / 23.8686	12.11 / 0.93	Levelogger 5 Junior 2024-05-07	Well filter interval: 1.07-2.07 m, anchored into mineral subsoil	Monitoring water level fluctuations in the mire lake and ditch that is draining it, in the area where restoration measures are planned

ID	Type*	Lat / Lon	Well head hight m a.s.l. LAS 2000.5 / relative hight	Type of probe Installation date	Construction	Aim of the monitoring
Cena11	Q	56.823796 / 23.870205	9.39 / 0.60	Levelogger 5 LTC	Water level monitoring in a ditch	
Cena14	MW	58.536282 / 23.801378	12.87 / 0.47	Levelogger 5 Junior 2024-05-27	Well filter interval: 0.53-2.53 m	Water level monitoring in the raised bog where hydrological regime restoration measures were carried out in 2007 near Skaists Lake
Cena15	MW	56.848839 / 23.808701	12.74 / 0.44	Levelogger 5 Junior 2024-05-27	Well filter interval: 0.56 – 2.56 m	
Cena16	MW	56.850719 / 23.811501	12.88 / 0.48	NA	Well filter interval: 0.52 – 1.52, anchored into mineral subsoil, Skaists Lake	
Cena18	MW	56.834618 / 23.869317	12.41 / 0.28	NA	Well filter interval: 0.72 – 2.72 m	Water level monitoring in the raised bog where hydrological regime restoration measures were carried out in 2007 in the S part of the Cena Mire NR
Cena19	MW	56.834647 / 23.869363	12.99 / 0.71	NA	Well filter interval: 0.29 – 2.29	
Cena20	MW	56.836139 / 23.87148	13.53 / 0.59	Levelogger 5 Junior 2024-05-07	Well filter interval: 0.41 – 2.41 m	
Cena21	MW	56.836138 / 23.87148	13.67 / 0.58	Levelogger 5 Junior 2024-05-07	Well filter interval: 0.42 – 2.42 m	
Cena23	MW	56.87376 / 23.825739	12.86 / 0.37	Levelogger 5 Junior 2024-05-27	Well filter interval: 0.63 – 1.63 m	Water level monitoring in the transition zone between raised bog and drained forest for assessing the impact of restoration measures on adjacent areas
Cena24	MW	56.873682 / 23.825327	9.65 / 0.55	Levelogger 5 Junior 2024-05-27	Well filter interval: 0.45 – 1.45 m	
Cena25	MW	56.872862 / 23.823469	8.86 / 0.18	Levelogger 5 Junior 2024-05-27	Well filter interval: 0.00 – 0.82 m	

* MW – monitoring well; Q – discharge monitoring

Appendix 6.4. *Summary data of hydrological monitoring points in Lielais Pelečāre Mire.*

ID	Type*	Lat / Lon	Well head-hight m a.s.l. LAS 2000.5 / relative hight	Type of probe Installation date	Construction	Aim of the monitoring
Pelecare_a1_mezs	SW	56.55436 / 26.60368	111.04 (soil surface)	Meter Teros 21 water potential probe and Teros 11 volumetric water content probe 2023-10-04	Teros 21: 0.1 m and 0.6 m Teros 11: 0.1, 0.3 and 0.6 m deep	The drained portion of the Deigļu Mire (part of Lielais Pelečāres Mire), selected as a detailed monitoring plot for the impact of the restoration measures. The objective of water level observations is to assess the overall impact of restoration measures. Monitoring includes a profile of monitoring points in a section of raised bog least affected by drainage.
Pelecare_a2_purvs	SW	56.55248 / 26.60430	111.22 (soil surface)	Meter Teros 21 water potential probe and Teros 11 volumetric water content probe 2023-10-04	Teros 21: 0.1 m and 0.6 m Teros 11: 0.1, 0.3 and 0.6 m deep	
Pelecare1	MW	56.5543 / 26.6037	110.95 / 0.48	Levelogger 5 Junior 2023-06-20	Filter depth: 1.62-3.62 m	
Pelecare2	MW	56.5539 / 26.6040	109.64 / 0.21	Levelogger 5 Junior 2023-06-20	Filter depth: 0.79-1.79 m	
Pelecare3	MW	56.5524 / 26.6043	111.64 / 0.69	Levelogger 5 Junior 2023-06-20	Filter depth: 0.31-2.31 m	
Pelecare4	MW	56.5515 / 26.6050	111.63 / 0.67	Levelogger 5 Junior 2023-06-20	Filter depth: 0.33-2.33 m	
Pelecare5	MW	56.5513 / 26.6052	111.84 / 0.55	Levelogger 5 Junior 2023-06-20	Filter depth: 0.45-2.45 m	
Pelecare6	MW	56.5489 / 26.5995	112.14 / 0.47	Levelogger 5 Junior 2023-06-20	Filter depth: 0.53-2.53 m	
Pelecare7	MW	56.5506 / 26.5963	109.87 / 0.28	Levelogger 5 Junior 2023-06-20	Filter depth: 0.72-1.72 m	
Pelecare8	MW	56.5502 / 26.5969	111.18 / 0.45	Levelogger 5 Junior 2024-04-23	Filter depth: 0.55-2.55 m	
Pelecare26	MW	56.55237 / 26.60392	111.19 / 0.53	NA	Filter depth: 0.47-1.47 m	
Pelecare9	Q	56.4492 / 26.4684	99.37 / NA	Levelogger 5 Junior 2023-06-20	Filter depth: 0-1 m	The monitoring site includes heavily drained portion of the Malnupeite River catchment and Deguma Lake, that has lesser drainage impact. Given the considerable peat thickness affected by drainage, changes of the water composition (quality) can be expected. The objective of monitoring is to assess the success of hydrological regime restoration in the significantly degraded and forested portion of the mire,
Pelecare10	MW	56.4634 / 26.4821	104.92 / 0.21	Levelogger 5 Junior 2023-06-20	Filter depth: 0.79-2.79 m	
Pelecare11	MW	56.4638 / 26.4814	105.86 / 0.73	Levelogger 5 Junior 2023-06-20	Filter depth: 0.27-2.27 m	
Pelecare12	MW	56.4646 / 26.4795	106.04 / 0.47	Levelogger 5 Junior 2023-06-20	Filter depth: 0.53-2.53 m	
Pelecare13	MW	56.4650 / 26.4786	106.52 / 0.41	Levelogger 5 Junior 2023-06-20	Filter depth: 0.59-2.59 m	
Pelecare14 (Deguma Lake)	MW	56.4686 / 26.4911	105.75 / 0.48	Levelogger 5 Junior 2023-06-20	Filter depth: 0.52-2.52 m	
Pelecare15	MW	56.4674 / 26.4886	107.75	Levelogger 5 Junior 2024-04-23		
Pelecare16	MW	56.4683 / 26.4903	106.80 / 0.51	Levelogger 5 Junior 2023-06-20	Filter depth: 0.49-2.49 m	

ID	Type*	Lat / Lon	Well head-hight m a.s.l. LAS 2000.5 / relative hight	Type of probe Installation date	Construction	Aim of the monitoring
Pelecare17	MW	56.46375 / 26.48132	105.64 / 0.42	Levelogger 5 Junior 2024-04-23	Filter depth: 0.58-2.58 m	as well as in the less affected raised bog dome area including the relatively large Deguma Lake.
Pelecare18	MW	56.45932 / 26.47571	105.30 / 0.50	Levelogger 5 Junior 2024-04-23	Filter depth: 0.5-1.5 m	
Pelecare19	MW	56.45928 / 26.47601	108.73 / 0.37	Levelogger 5 Junior 2024-04-23	Filter depth: 0.63-1.63 m	
Pelecare20	MW	56.46333 / 26.51757	107.65 / 0.87	Levelogger 5 Junior 2024-04-23	Filter depth: 0.13-1.13 m	The ditch Azara Grovs and drainage network connected to it encompass both the nature reserve (NR) territory and the State Forest Service (LVM) lands outside the NR, where forest on drained peat soils is found. The aim of the water level monitoring is to evaluate the restoration success by comparing similar sites with and without restoration measures.
Pelecare21	MW	56.46336 / 26.51723	107.53 / 0.67	Levelogger 5 Junior 2024-04-23	Filter depth: 0.33-1.33 m	
Pelecare22	MW	56.46586 / 26.51413	104.43 / 0.51	Levelogger 5 Junior 2024-04-23	Filter depth: 0.49-1.49 m	
Pelecare23	MW	56.46590 / 26.51454	104.78 / 0.48	Levelogger 5 Junior 2024-04-23	Filter depth: 0.52-1.52 m	
Pelecare24	MW	56.46650 / 26.51017	105.11 / 0.77	Levelogger 5 Junior 2024-04-23	Filter depth: -0.27-1.73 m	
Pelecare25	MW	56.46664 / 26.51040	105.13 / 0.78	Levelogger 5 Junior 2024-04-23	Filter depth: -0.28-1.72 m	

* SW – soil water monitoring point; MW – monitoring well; Q – discharge monitoring site

Appendix 6.5. *Summary data of hydrological monitoring points in Sudas-Zviedru Mire.*

ID	Type*	Lat / Lon	Well head-hight m a.s.l. LAS 2000.5 / relative hight	Type of probe Installation date	Construction	Aim of the monitoring
Suda1	MW	57.16235 / 25.01733	118.259 / 0.63	Leveloger5 Junior 2024-06-11	Filter depth 0.37 -1.37 m	Profile radial to the slope of the bog dome across blocked ditches, to examine the gradient from healthy raised bog to degrade bog with forest cover
Suda2	MW	57.16298 / 25.01852	117.228 / 0.52	Leveloger5 Junior 2024-06-11	Filter depth -0.48 -2.48 m	
Suda3	MW	57.1628 / 25.01863	116.935 / 0.37	Leveloger5 Junior 2024-06-11	Filter depth -0.63 -2.63 m	
Suda4	MW	57.16274 / 25.01866	117.244 / 0.35	Leveloger5 Junior 2024-06-11	Filter depth -0.65 -2.65 m	
Suda7	MW	57.16231 / 25.0187	117.951 / 0.37	Leveloger5 Junior 2024-06-11	Filter depth -0.63 -2.63 m	Profile along the axis of a ditch to examine dynamics the water level gradient across a dam and in flooded segment of the ditch
Suda5	MW	57.16248 / 25.01874	117.317 / 0.44	Leveloger5 Junior 2024-06-11	Filter depth -0.56 -2.56 m	
Suda6	MW	57.16247 / 25.01864	117.702 / 0.54	Leveloger5 Junior 2024-06-11	Filter depth -0.46 -2.46 m	

* MW – monitoring well

Appendix 6.6. *Summary data of hydrological monitoring points in Melnais Lake Mire.*

ID	Type*	Lat / Lon	Well head-hight m a.s.l. LAS 2000.5 / relative hight	Type of probe Installation date	Construction	Aim of the monitoring
Melnais1	MW	56.83686 / 23.98986	13.69 / 0.4	Leveloger5 Junior 2024-05-30	Filter depth -0.60 -2.60 m	Examine the water level dynamics in a strip of dens pine forest in the raised bog
Melnais2	MW	56.83678 / 23.98865	13.94 / 0.46	Leveloger5 Junior 2024-05-30	Filter depth -0.54 -2.54 m	A profile perpendicular to blocked ditch to examine water level gradient near the ditch
Melnais3	MW	56.83705 / 23.98869	13.97 / 0.43	Leveloger5 Junior 2024-05-30	Filter depth -0.57 -2.57 m	
Melnais4	MW	56.83692 / 23.98733	13.84 / 0.36	Leveloger5 Junior 2024-05-30	Filter depth -0.64 -2.64 m	A profile perpendicular to blocked ditch to examine water level gradient near the ditch
Melnais5	MW	56.83718 / 23.9874	14.17 / 0.46	Leveloger5 Junior 2024-05-30	Filter depth -0.54 -2.54 m	
Melnais6	MW	56.83647 / 23.99187	13.06 / 0.52	Leveloger5 Junior 2024-05-30	Filter depth -0.48 -1.48 m	A profile perpendicular to unsuccessful blocked ditch to examine water level gradient near the ditch
Melnais7	MW	56.83675 / 23.99196	14.29 / 0.64	Leveloger5 Junior 2024-05-30	Filter depth -0.36 -2.36 m	

* MW – monitoring well

Appendix 6.7. *Summary data of vegetation, GHG and GEST monitoring points in project sites.*

Plot name	Comments	Date	Coordinates
CM1	Peat field along ditch	22.08.2023	56.853386, 23.888896
CM2	Peat field along ditch	22.08.2023	56.853090, 23.889289
CM3	Impacted raised bog	22.08.2023	56.852883, 23.888502
CM4	Natural, active raised bog	22.08.2023	56.851952, 23.885061
CM5	Peat field	22.08.2023	56.855533, 23.887116
CM6	Drained raised bog along ditch	22.08.2023	56.855851, 23.884141
CM7	Impacted raised bog	22.08.2023	56.856014, 23.882665
CM8	Natural, active raised bog	22.08.2023	56.856324, 23.879880
CM9	Restored peat field with trees	17.10.2023	56.834659, 23.869344
CM10	Restored peat field	17.10.2023	56.836074, 23.871436
CM11	Drained raised bog along ditch	17.10.2023	56.824436, 23.868726
CM GHG 1-3	Near-natural raised bog	22.08.2023	56.853273, 23.886614
CM GHG 4-6	Peat field along drainage ditch	22.08.2023	56.853726, 23.886711
CM GHG 7	Dry peat field	22.08.2023	56.853878, 23.886777
CM GHG 10-12	Near-natural raised bog	17.10.2023	56.85024482, 23.80636698
CM GHG 13-15	Restored raised bog along ditch	17.10.2023	56.85008141, 23.80575113
CM GHG 16-18	Drained raised bog with dense tree level	17.10.2023	56.85017528, 23.80492508
Cena 1	Moderately moist/dry bog heath	17.10.2023	56.834638, 23.869352
Cena 2	Moist bog heath	17.10.2023	56.836039, 23.871523
Cena 3	Moist bog heath	17.10.2023	56.8363523, 23.8711842
Cena 4	Dry forest and shrubberies (OL)	17.10.2023	56.8344698, 23.8695558
Cena 5	Wet meadows and forbs	17.10.2023	56.824519, 23.868922
Cena 6	Wet meadows and forbs	17.10.2023	56.8245814, 23.8689807
Cena 7	Dry forest and shrubberies (OL)	17.10.2023	56.82637936, 23.86618683
Cena 8	Wet meadows and forbs	17.10.2023	56.82401213, 23.87008753
Cena 9		17.10.2023	56.8223757, 23.8687601
Cena 10	Moderately moist forest and shrubberies (OL)	17.10.2023	56.84741392, 23.80267463
Cena 11	Open water/ditches	17.10.2023	56.84830575, 23.80543272
Cena 12	Moist forests and shrubberies (OL)	17.10.2023	56.8488333, 23.80542164
Cena 13	Moist forests and shrubberies (OL)	17.10.2023	56.85082086, 23.80660195
Cena 14	Wet peat moss hollows resp. flooded peat moss lawn	17.10.2023	56.85133077, 23.80705896
Cena 15	Wet peat moss hollows resp. flooded peat moss lawn	17.10.2023	56.8516829, 23.8075365
Cena 16	Wet peat moss hollows resp. flooded peat moss lawn	17.10.2023	56.8519144, 23.8074872
Cena 17	Wet peat moss hollows resp. flooded peat moss lawn	17.10.2023	56.85182283, 23.80762653
Cena 18	Wet peat moss lawn	19.10.2023	56.85320014, 23.83215685
Cena 19	Wet peat moss lawn	19.10.2023	56.8535187, 23.8331735
Cena 20	Wet peat moss lawn	19.10.2023	56.85605784, 23.84295525
Cena 21	Wet peat moss lawn	19.10.2023	56.854768, 23.840716
Cena 22	Wet peat moss lawn with pine trees	19.10.2023	56.85322957, 23.83819603
Cena 23	Wet meadows and forbs	19.10.2023	56.85270925, 23.83745568
Cena 24	Wet meadows and forbs	19.10.2023	56.85264650, 23.83791090
Cena 25	Moist forests and shrubberies (OL)	19.10.2023	56.85116025, 23.83361897
Cena 26	Wet peat moss lawn with pine trees	19.10.2023	56.85218585, 23.82932086
Cena 27	Very moist peat moss lawn	19.10.2023	56.85226881, 23.82450318
Cena 28	Moist forests and shrubberies (OL)	19.10.2023	56.85173110, 23.82187277
Cena 29	Moist forests and shrubberies (OL)	19.10.2023	56.8509298, 23.8194702
Cena 30	Bare peat wet	19.10.2023	56.8582709, 23.8066641
Cena 31	Moderately moist/dry bog heath	19.10.2023	56.858168, 23.802378

Plot name	Comments	Date	Coordinates
Cena 32	Moist forests and shrubberies (OL)	19.10.2023	56.85786318, 23.79527779
Cena 33	Moderately moist forest and shrubberies (OL)	19.10.2023	56.85616756, 23.7941930
MP GHG 1-3	Near-natural raised bog	02.11.2023	56.83702901, 23.98912981
MP GHG 4-6	Restored raised bog along drainage ditch	02.11.2023	56.83673032, 23.98926006
MP GHG 7-9	Drained raised bog with dense tree level	02.11.2023	56.83708759, 23.98972926
Melnais 1		02.11.2023	56.84922436, 23.94222253
Melnais 2		02.11.2023	56.84909677, 23.94279974
Melnais 3		02.11.2023	56.84914538, 23.94316302
Melnais 4		02.11.2023	56.84921344, 23.94366542
Melnais 5		02.11.2023	56.84802554, 23.94578550
Melnais 6		02.11.2023	56.84809560, 23.94613376
Melnais 7		02.11.2023	56.84789070, 23.94580028
Melnais 8		02.11.2023	56.84746759, 23.94872531
Melnais 10		02.11.2023	56.84766832, 23.95017148
Melnais 11		02.11.2023	56.84634404, 23.95125298
Melnais 12		02.11.2023	56.84633233, 23.95185218
Melnais 13		02.11.2023	56.84636535, 23.95326559
Melnais 15		02.11.2023	56.84556047, 23.95423035
Melnais 16		02.11.2023	56.84485431, 23.95510741
Melnais 17		02.11.2023	56.84444105, 23.95668284
Melnais 18		02.11.2023	56.84450052, 23.95670793
Melnais 19		02.11.2023	56.84413314, 23.95685522
Melnais 21		02.11.2023	56.84348948, 23.95696519
Melnais 26		02.11.2023	56.84544407, 23.95710973
Melnais 27		02.11.2023	56.84589941, 23.95635171
Melnais 30		02.11.2023	56.84874957, 23.95050136
Melnais 33		02.11.2023	56.83708759, 23.98972926
Melnais 34		02.11.2023	56.83702901, 23.98912981
Melnais 37		02.11.2023	56.83772569, 23.98670962
Melnais 38		02.11.2023	56.8335960, 23.98700026
Melnais 39		02.11.2023	56.83606504, 23.99414192
PM1	Bog woodland	17.08.2023	56.554451, 26.603734
PM2	Bog woodland	17.08.2023	56.553834, 26.604048
PM3	Impacted raised bog margin	17.08.2023	56.552468, 26.604359
PM4	Drained bog along ditch	17.08.2023	56.551442, 26.604957
PM5	Near natural raised bog	17.08.2023	56.551300, 26.605113
PM6	Natural, active raised bog	17.08.2023	56.548955, 26.599563
PM7	Natural bog margin	17.08.2023	56.550194, 26.596978
PM8	Bog woodland	17.08.2023	56.550577, 26.596307
PM10	Drained bog along ditch	18.08.2023	56.463422, 26.482182
PM11	Drained raised bog	18.08.2023	56.463760, 26.481407
PM12	Drained raised bog	18.08.2023	56.464678, 26.479470
PM13	Impacted raised bog with trees	18.08.2023	56.465033, 26.478486
PM15	Natural, active raised bog	18.08.2023	56.467399, 26.488595
PM16	Woodland around lake	18.08.2023	56.468257, 26.490226
PM17	Transition mire	18.08.2023	56.468654, 26.491079
PM GHG 1-3	Near natural raised bog	17.08.2023	56.551057, 26.604783
PM_GHG_1'_1	Near-natural raised bog	17.08.2023	56.551128, 26.604788
PM_GHG_1'_2	Near-natural raised bog	17.08.2023	56.551121, 26.604756
PM_GHG_1'_3	Near-natural raised bog	17.08.2023	56.551186, 26.604778

Plot name	Comments	Date	Coordinates
PM GHG 4-6	Drained raised bog along ditch	17.08.2023	56.551595, 26.604743
PM_GHG_4'_1	Drained raised bog along ditch	17.08.2023	56.551613, 26.604804
PM_GHG_4'_2	Drained raised bog along ditch	17.08.2023	56.551551, 26.604802
PM_GHG_4'_3	Drained raised bog along ditch	17.08.2023	56.551545, 26.604708
PM GHG 7-9	Impacted raised bog margin	17.08.2023	56.552159, 26.604630
PM_GHG_7'_1	Impacted raised bog margin	17.08.2023	56.552073, 26.604759
PM_GHG_7'_2	Impacted raised bog margin	17.08.2023	56.552045, 26.604818
PM_GHG_7'_3	Impacted raised bog margin	17.08.2023	56.552002, 26.604753
SZ1_1-5	Restored raised bog along drainage ditch	26.07.2023	57.163416, 25.015646
SZ2_1-3	Impacted raised bog	26.07.2023	57.163084, 25.015113
SZ3_1-3	Natural, active raised bog	26.07.2023	57.160901, 25.013935
SZ GHG 1-3	Near-natural raised bog	26.07.2023	57.162342, 25.019327
SZ GHG 4-6	Restored raised bog along ditch	26.07.2023	57.162627, 25.019203
SZ GHG 7-9	Drained raised bog with dense tree level	26.07.2023	57.162848, 25.018991
SZ 1	Moderately moist forest and shrubberies (OL)	14.10.2025	57.165551, 25.022721
SZ 2	Wet peat moss hollows resp. flooded peat moss lawn	14.10.2025	57.169347, 25.018935
SZ 3	Moist forests and shrubberies (OL)	14.10.2025	57.169625, 25.018314
SZ 4	Very moist bog heath	14.10.2025	57.170215, 25.018036
SZ 5	Wet meadows and forbs	14.10.2025	57.171097, 25.018232
SZ 6	Very moist bog heath	14.10.2025	57.171161, 25.017976
SZ 7	Moderately moist/dry bog heath	14.10.2025	57.172487, 25.015721
SZ 8	Wet small sedges reeds mostly with moss layer	14.10.2025	57.172504, 25.015043
SZ 9	Wet peat moss lawn with pine trees	14.10.2025	57.172577, 25.009854
SZ 10	Very moist bog heath	14.10.2025	57.172894, 25.008520
SZ 11	Moderately moist forest and shrubberies (OL)	14.10.2025	57.166383, 25.009228
SZ 12	Wet meadows and forbs	22.10.2025	57.095913, 25.054801
SZ 13	Very moist peat moss lawn	22.10.2025	57.095869, 25.054771
SZ 14	Very moist bog heath	22.10.2025	57.095985, 25.054826
SZ 15	Very moist bog heath	22.10.2025	57.095914, 25.058023
SZ 16	Very moist peat moss lawn	22.10.2025	57.095880, 25.059847
SZ 17	Very moist bog heath	22.10.2025	57.096010, 25.060038
SZ 18	Wet meadows and forbs	22.10.2025	57.096035, 25.059849
SZ 19	Very moist peat moss lawn	22.10.2025	57.034213, 25.062003
SZ 20	Wet tall sedges reeds	22.10.2025	57.093645, 25.062981
SZ 21	Moderately moist forest and shrubberies (OL)	22.10.2025	57.094186, 25.063272
SZ 22	Very moist peat moss lawn	22.10.2025	57.095577, 25.064636
SZ 23	Very moist forests and shrubberies (OL)	22.10.2025	57.097759, 25.059485
SZ 24	Dry forest and shrubberies (OL)	22.10.2025	57.143041, 24.992937
SZ 25	Moist forests and shrubberies (OL)	22.10.2025	57.143428, 24.993609
SZ 26	Wet peat moss lawn with pine trees	22.10.2025	57.143893, 24.993947
SZ 27	Wet small sedges reeds mostly with moss layer	22.10.2025	57.144954, 24.995041
SZ 28	Wet peat moss lawn	22.10.2025	57.144865, 24.995032
SZ 29	Very moist bog heath	22.10.2025	57.143501, 24.996243
SZ 30	Very moist bog heath	22.10.2025	57.141832, 24.997948
SZ 31	Wet meadows and forbs	22.10.2025	57.140623, 24.996979
SZ 32	Wet peat moss lawn	22.10.2025	57.139883, 24.997149
SZ 33	Very moist bog heath	22.10.2025	57.138181, 24.992933
SZ 34	Very moist forests and shrubberies (OL)	22.10.2025	57.138271, 24.992145
SZ 35	Very moist bog heath	22.10.2025	57.139112, 24.990525
SZ 36	Wet meadows and forbs	22.10.2025	57.140122, 24.988705

Appendix 6.8. *The list of vascular plant, bryophyte and lichen species recorded in project sites in vegetation monitoring plots, GHG monitoring plots and GEST points in 2023.*

	Cenas Mire			Melnais Lake Mire		Lielais Pelečāres Mire		Sudas-Zviedru Mire	
	Vegetation monitoring	GHG	GEST	GHG	GEST	Vegetation monitoring	GHG	Vegetation monitoring	GHG
TREES AND SHRUBS									
Betula pendula	x		x		x	x		x	
Betula pubescens	x			x	x		x	x	
Frangula alnus					x	x			
Picea abies			x		x			x	
Pinus sylvestris	x	x	x	x	x	x	x	x	x
Prunus padus					x				
Salix sp.					x				
Sorbus acuparia					x				
DWARF SHRUBS									
Andromeda polifolia	x	x	x	x	x	x	x	x	x
Calluna vulgaris	x	x	x	x	x	x	x	x	x
Chamaedaphne calyculata	x		x			x	x		
Empetrum nigrum	x	x	x	x	x	x			x
Ledum palustre	x	x	x	x	x	x	x		x
Oxycoccus microcarpa	x					x			
Oxycoccus palustris	x	x	x	x	x	x	x	x	x
Rubus chamaemorus	x	x	x		x	x	x	x	x
Rubus idaeus					x				
Vaccinium myrtillus			x		x	x	x		
Vaccinium uliginosum		x	x		x	x	x	x	
Vaccinium vitis-idaea		x	x	x	x	x	x		x
HERBACEOUS PLANTS									
Carex rostratum			x						
Carex sp.					x				
Deschampsia caespitosa					x				
Drosera anglica	x							x	
Drosera rotundifolia	x	x	x	x	x	x	x	x	x
Dryopteris filix-mas					x				
Epilobium sp.					x				
Eriophorum angustifolium					x				
Eriophorum vaginatum	x	x	x	x	x	x	x	x	x
Juncus sp.					x				
Luzula pilosa						x			
Lycopodium annotinum			x		x				
Melampyrum pratense						x			
Molinia caerulea					x				
Phragmites australis	x				x				
Rhynchospora alba	x		x		x	x	x	x	x
Scheuchzeria palustris			x		x	x	x		
BRYOPHYTES									
Aulacomnium palustre	x	x	x	x	x	x			
Brachythecium rutabulum	x				x				

	Cenas Mire			Melnais Lake Mire		Lielais Pelečāres Mire		Sudas-Zviedru Mire	
	Vegetation monitoring	GHG	GEST	GHG	GEST	Vegetation monitoring	GHG	Vegetation monitoring	GHG
Campylopus introflexus					x				
Dicranum bergeri					x		x	x	
Dicranum bonjeanii									x
Dicranum polysetum	x	x	x		x	x	x	x	
Dicranum scoparium	x	x	x		x	x		x	
Hylocomium splendens			x		x				
Hypnum cupressiforme	x								
Mylia anomala	x								
Plagiomnium affine					x				
Pleurozium schreberi	x	x	x	x	x	x	x	x	
Pohlia nutans					x				
Polytrichum commune			x		x		x		
Polytrichum juniperinum	x	x	x		x			x	
Polytrichum strictum			x			x	x	x	x
Sphagnum angustifolium	x		x	x	x	x	x	x	x
Sphagnum capillifolium	x	x	x		x	x	x	x	
Sphagnum contortum						x			
Sphagnum cuspidatum	x	x	x	x	x	x	x	x	
Sphagnum fallax					x				
Sphagnum flexuosum	x	x	x	x	x	x			
Sphagnum fuscum	x	x	x		x	x	x	x	
Sphagnum girgensohnii			x			x			
Sphagnum medium	x	x	x	x	x	x	x	x	x
Sphagnum recurvum			x						
Sphagnum rubellum	x	x	x	x	x	x	x	x	x
Sphagnum tenellum	x							x	
LICHENS									
Cladonia stellaris					x		x	x	
Cladonia stygia							x	x	
Cladonia sp.					x				

Appendix 6.9. *The list of vascular plant, bryophyte and lichen species recorded in project sites in GHG monitoring plots and GEST points in 2025.*

	Melnais Lake Mire	Sudas-Zviedru Mire	
	GHG	GHG	GEST
TREES AND SHRUBS			
Betula pendula			X
Betula pubescens	x	x	X
Frangula alnus			X
Juniperus commune			X
Picea abies			X
Pinus sylvestris	x	x	X
Populus tremula			X
Quercus robur			X
Sorbus acuparia			X
DWARF SHRUBS			
Andromeda polifolia	x	x	X
Calluna vulgaris	x	x	X
Empetrum nigrum	x	x	X
Ledum palustre	x	x	X
Oxycoccus microcarpa		x	
Oxycoccus palustris	x	x	X
Rubus chamaemorus		x	X
Vaccinium myrtillus			X
Vaccinium uliginosum			X
Vaccinium vitis-idaea	x	x	X
HERBACEOUS PLANTS			
Carex lasiocarpa			X
Carex limosa			X
Carex nigra			X
Comarum palustre			X
Drosera rotundifolia	x	x	X
Equisetum fluviatile			X
Eriophorum vaginatum	x	x	X
Menyanthes trifoliata			X
Molinia caerulea			X
Peucedanum palustre			X
Pteridium aquilinum			X
Rhynchospora alba		x	X
Scheuchzeria palustris			X
BRYOPHYTES			
Aulacomnium palustre	x		
Dicranum polysetum			X
Dicranum scoparium			X
Hylocomium splendens			X
Pleurozium schreberi	x		X
Polytrichum commune			X
Polytrichum strictum		x	X
Sphagnum angustifolium	x	x	X
Sphagnum capillifolium	x	X	
Sphagnum cuspidatum	x	x	X

	Melnais Lake Mire	Sudas-Zviedru Mire	
	GHG	GHG	GEST
Sphagnum divinum	x		X
Sphagnum flexuosum	x	x	X
Sphagnum fuscum			X
Sphagnum girgensohnii			X
Sphagnum medium	x	x	X
Sphagnum palustre			X
Sphagnum riparium			X
Sphagnum rubellum	x	x	X
Sphagnum russowii	x		
Sphagnum tenellum	x		
LICHENS			
Cladonia sp.			X

__Appendix 6.10.__ Photos of the greenhouse gas emission monitoring study sites and subplots representing different habitat types

Subplot A (near-natural raised bog).

Subplot B (rewetted degraded raised bog with direct restoration effect)

Subplot C (rewetted overgrown raised bog with cumulative restoration effect)

Figure 6.10.1. *Study site LPC_1 (Sudas-Zviedru Mire). Images: © G. Saule*

Subplot A (near-natural raised bog)

Subplot B (drained raised bog with dense tree layer in the strong drainage impact zone)

Subplot C (drained raised bog with dense tree layer in the weak drainage impact zone)

Figure 6.10.2. *Study site LPC_2 (Lielais Pelečāre Mire). Images: © G. Saule*

Subplot A (near-natural raised bog)

Subplot B (rewetted degraded raised bog with direct restoration effect)

Subplot C (degraded bog woodland)

Figure 6.10.3. *Study site LPC_3 (Melnais Lake Mire). Images: © G. Saule*

Subplot A (near-natural raised bog)

Subplot B (restored raised bog along ditch with direct restoration effect)

Subplot C (drained raised bog with dense tree layer with cumulative restoration effect)

Figure 6.10.4. *Study site LPC_4 (Cenas Mire). Images: © G. Saule*



Subplot A (near-natural raised bog)

Subplot B (peat field along drainage ditch in the strong drainage impact zone)

Subplot C (dry peat field in the strong drainage impact zone)

Figure 6.10.5. *Study site LPC_5 (Cena Mire). Images: © G. Saule*



Subplot A (natural raised bog)

Subplot B (natural raised bog)

Subplot C (natural raised bog)

Figure 6.10.6. *Study site LPC_6 (Lielais Pelečāres Mire). Images: © G. Saule*



Subplot A (near-natural raised bog)

Subplot B (natural raised bog)

Subplot C (near-natural raised bog)

Figure 6.10.7. *Study site LPC_7 (Lielais Pelečāre Mire). Images: © G. Saule*